BNL-94271-2010
Formal Report

Proceedings of RIKEN BNL Research Center Workshop Volume 98

Saturation, the Color Glass Condensate and the Glasma: What Have We Learned from RHIC?

May 10-12, 2010

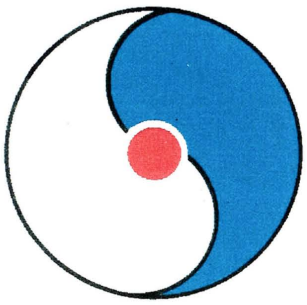

Organizers:

J. Dunlop, L. McLerran, D. Morrison and R. Venugopalan

RIKEN BNL Research Center

Building 510A, Brookhaven National Laboratory, Upton, NY 11973-5000, USA

DISCLAIMER

This work was prepared as an account of work sponsored by an agency of the United States Government. Neither the United States Government nor any agency thereof, nor any of their employees, nor any of their contractors, subcontractors or their employees, makes any warranty, express or implied, or assumes any legal liability or responsibility for the accuracy, completeness, or any third party's use or the results of such use of any information, apparatus, product, or process disclosed, or represents that its use would not infringe privately owned rights. Reference herein to any specific commercial product, process, or service by trade name, trademark, manufacturer, or otherwise, does not necessarily constitute or imply its endorsement, recommendation, or favoring by the United States Government or any agency thereof or its contractors or subcontractors. The views and opinions of authors expressed herein do not necessarily state or reflect those of the United States Government or any agency thereof.

Notice: This manuscript has been authored by employees of Brookhaven Science Associates, LLC under Contract No. DE-AC02-98CH10886 with the U.S. Department of Energy. The publisher by accepting the manuscript for publication acknowledges that the United States Government retains a non-exclusive, paid-up, irrevocable, world-wide license to publish or reproduce the published form of this manuscript, or allow others to do so, for United States Government purposes.

Preface to the Series

The RIKEN BNL Research Center (RBRC) was established in April 1997 at Brookhaven National Laboratory. It is funded by the "Rikagaku Kenkyusho" (RIKEN, The Institute of Physical and Chemical Research) of Japan. The Memorandum of Understanding between RIKEN and BNL, initiated in 1997, has been renewed in 2002 and again in 2007. The Center is dedicated to the study of strong interactions, including spin physics, lattice QCD, and RHIC physics through the nurturing of a new generation of young physicists.

The RBRC has both a theory and experimental component. The RBRC Theory Group and the RBRC Experimental Group consists of a total of 25-30 researchers. Positions include the following: full time RBRC Fellow, half-time RHIC Physics Fellow, and full-time, post-doctoral Research Associate. The RHIC Physics Fellows hold joint appointments with RBRC and other institutions and have tenure track positions at their respective universities or BNL. To date, RBRC has ~50 graduates of which 14 theorists and 6 experimenters have attained tenure positions at major institutions worldwide.

Beginning in 2001 a new RIKEN Spin Program (RSP) category was implemented at RBRC. These appointments are joint positions of RBRC and RIKEN and include the following positions in theory and experiment: RSP Researchers, RSP Research Associates, and Young Researchers, who are mentored by senior RBRC Scientists. A number of RIKEN Jr. Research Associates and Visiting Scientists also contribute to the physics program at the Center.

RBRC has an active workshop program on strong interaction physics with each workshop focused on a specific physics problem. In most cases all the talks are made available on the RBRC website. In addition, highlights to each speaker's presentation are collected to form proceedings which can therefore be made available within a short time after the workshop. To date there are ninety seven proceeding volumes available.

A 10 teraflops RBRC QCDOC computer funded by RIKEN, Japan, was unveiled at a dedication ceremony at BNL on May 26, 2005. This supercomputer was designed and built by individuals from Columbia University, IBM, BNL, RBRC, and the University of Edinburgh, with the U.S. D.O.E. Office of Science providing infrastructure support at BNL. Physics results were reported at the RBRC QCDOC Symposium following the dedication. QCDSP, a 0.6 teraflops parallel processor, dedicated to lattice QCD, was begun at the Center on February 19, 1998, was completed on August 28, 1998, and was decommissioned in 2006. It was awarded the Gordon Bell Prize for price performance in 1998.

N. P. Samios, Director
March 2010

*Work performed under the auspices of U.S.D.O.E. Contract No. DE-AC02-98CH10886.

CONTENTS

Preface to the Series
Introduction i
Introduction to the Physics of Saturation
Yuri Kovchegov 1
Color Glass Condensate and Glasma
Francois Gelis 7
Parton Saturation at Strong Coupling: What have we Learned from RHIC and AdS/CFT?
Edmond Iancu 13
HERA Results and DGLAP Evolution: Theory and Phenomenology
Stefano Forte 19
The New HERA F_2 Data and the Determination of the Infrared Behaviour of the BFKL Amplitude
Henri Kowalski 25
Summary of RBRC Workshop: P- and CP-odd Effects in Hot and Dense Matter
Harmen Warringa 31
Extended Longitudinal Scaling: Direct Evidence of Saturation
Wit Busza 37
Multiplicity Fluctuations and Negative Binomial Distributions
Tomoaki Nakamura for PHENIX 43
V_2 Cumulant Measurements and Eccentricity Fluctuations for the STAR Collaboration
Paul Sorenson for STAR 49
Limiting Fragmentation in Hadronic Collisions
Anna Stasto 55
Initial Conditions and Global Event Properties
Adrian Dumitru 61
Anomalous Transport Processes in Turbulent Nonabelian Plasmas
Berndt Mueller 67
Hydrodynamics: Fluctuating Initial Conditions and Two Particle Correlations
Frederique Grassi 73
The Ridge(s) in STAR
Lanny Ray for STAR 79
Studying the Medium Response by Two Particle Correlations
John Chen for PHENIX 85
Long Range Correlations in Phobos
Wei Li for PHOBOS 91
Initial Geometry Fluctuations and Triangular Flow
Burak Alver for PHOBOS 97
Three-Particle Pseudorapidity Correlations in STAR
Pawan Netrakanti for STAR 103
The "Ridges" and Large Jet v_2 are Explained by Magnetic Plasma Near Tc
Edward Shuryak 109
Long Range Correlations and Hydrodynamic Expansion
Sean Gavin 115
Forward-Backward Multiplicity Correlations at STAR
Mike Skoby for STAR 121
Multiplicity Distributions and Long Range Rapidity Correlations
Tuomas Lappi 127
Long Range Correlations; Event Simulation and Parton Percolation
Carlos Pajares 133

Dependence of Single Particle Distributions on Rapidity and Centrality
Ramiro Debbe from BRAHMS Summarizing Results from all RHIC experiments 141
Leading Twist Nuclear Shadowing, Onset of Black Disk Regime and Post Selection Effect for the Leading Hadron Production
Mark Strikman 149
Single Particle Distributions, Leading Twist and Beyond
Javier Albacete 155
Two Particle Correlations at Forward Rapidity in STAR
Ermes Braidot for STAR 161
Signatures of Color Glass Condensate: Forward Azimuthal Angle Di-Hadron Correlations in PHENIX
Beau Meredith for PHENIX 167
Forward di-Hadron Correlations in d+Au Collisions
Cyrille Marquet 173
Two Particle Correlations: Saturation and Issues with Universality
Bowen Xiao 179
Charmonium Production in pp, pA and AA Collisions
Boris Kopeliovich 185
J/ψ and Charm at RHIC
Alexandre Lebedev for PHENIX 191
J/ψ and Charm at STAR
Chris Perkins for STAR 197
Understanding J/ ψ Production in pp, dA and AA Collisions
Jian Wei Qiu 203
Charmonium and Open Charm Production and Saturation
Kirill Tuchin 209
Photons and Dileptons
Jason Kamin for PHENIX 215
Future Directions in CGC Studies at RHIC
Les Bland for STAR 221
Decadal Planning in PHENIX
Jamie Nagle for PHENIX 227
FOCAL a Forward Calorimeter for Phenix
Rich Seto for PHENIX 233
Small x Physics with ALICE
Tapan Nayak for ALICE 241
Small-x Physics with CMS at LHC
Magdalena Malek for CMS 247
Low-x Measurements with ATLAS
Brian Cole for ATLAS 253
The EIC, Saturation, and the CGC
Thomas Ullrich 259
Using Heavy Ions (Pb+Pb) to Search for New Forms of QCD Matter at LHC
Miklos Gyulassy 265
The Status of Saturation, CGC and Glasma
Jean Paul Blaizot 271
List of Registered Participants 277
Agenda 279
Additional RIKEN BNL Research Center Proceeding Volumes 283
Contact Information

INTRODUCTION

The workshop "Saturation, the Color Glass Condensate and the Glasma: What Have We Learned from RHIC?" had as its goal to assess the evidence concerning the possible existence of exotic forms of matter that might affect the earliest stages of RHIC collisions. The Color Glass Condensate (CGC) is a very high energy density state of gluonic matter in the wavefunction of a hadron. This part of the wavefunction might be seen in high energy collision processes. It is argued in the workshop that the CGC might explain many features of electron-hadron collisions, and the initial conditions for high energy nucleus-nucleus collisions.

The Glasma is formed by the collision of two Color Glass Condensates in the earliest stages of hadron-hadron interactions. The Glasma is an ensemble of highly coherent longitudinal color electric and color magnetic fields. In the workshop, it was argued that the Glasma may explain multiplicity distributions in nucleus-nucleus collisions, forward charm particle production in dA collisions, and various two particle correlation results such as the ridge in nucleus-nucleus collisions. There was much excitement about forward-backward angular correlations in the deuteron fragmentation region of dAu collisions presented by the STAR and PHENIX collaborations.

The talks of the meeting were summarized in the talk of Jean-Paul Blaizot who strongly argued for the CGC and Glasma interpretation of the RHIC results. The proceedings of this meeting will be published in a special edition of Nuclear Physics A. The meeting was very well attended, and successfully brought together theorists and experimentalists in an attempt to reach consensus about what we have learned in the RHIC experiments.

Introduction to the Physics of Saturation

Yuri V. Kovchegov

Department of Physics, The Ohio State University
Columbus, OH 43017

In my talk I briefly describe major developments in the physics of saturation/Color Glass Condensate (CGC) in recent decades.

I begin by emphasizing the main postulate of the saturation physics, stating that the high energy hadronic and nuclear wave functions have an intrinsic momentum scale associated with them, the so-called saturation scale Q_s. The scale grows with energy and the atomic number of the nucleus, as explained in the first attached slide.

High energy hadronic and nuclear wave functions at high energy can be described by classical gluon fields, since the saturation scale in such wave functions is large making the strong coupling constant small. Classical gluon field description is the main result of the McLerran–Venugopalan model, as shown in the second slide.

The classical gluon fields can also be used to describe particle production in high energy proton-nucleus and nucleus-nucleus collisions (see slide three).

At higher energies quantum corrections to classical fields become important, bringing in rapidity/energy dependence in the wave functions and corresponding cross sections. These corrections are taken into account by the Balitsky–Kovchegov (BK) and Jalilian-Marian–Iancu–McLerran–Weigert–Leonidov–Kovner (JIMWLK) evolution equations. The physical mechanism behind the BK equation is outlined in slide four.

Our current understanding of high energy QCD is summarized in slide five in the Bjorken-x and Q^2-plane. There one can see the saturation region where non-linear BK and JIMWLK evolution equations become important, while perturbative weak-coupling approaches still apply. Studying and understanding this new interesting regime of QCD is the main goal of saturation/CGC physics.

What sets the scale of running QCD coupling in high energy collisions?

- Saturation physics is based on the existence of a large internal mometum scale Q_S which grows with both energy s and nuclear atomic number A

$$\boxed{Q_S^2 \sim A^{1/3}\ s^{\lambda}}$$

such that $\boxed{\alpha_S = \alpha_S(Q_S) << 1}$

and we can calculate total cross sections, particle spectra and multiplicities, etc from first principles.

McLerran-Venugopalan Model

- The wave function of a single nucleus has many small-x quarks and gluons in it.
- In the transverse plane the nucleus is densely packed with gluons and quarks.

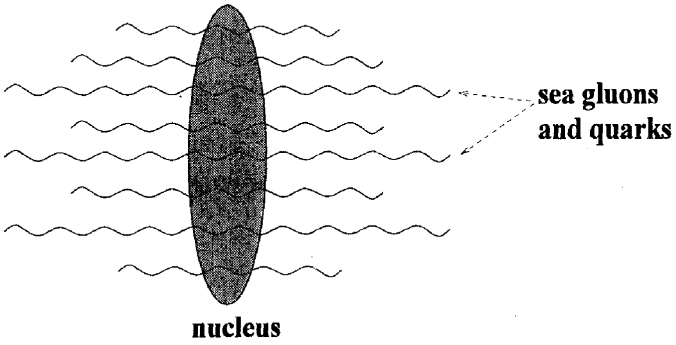

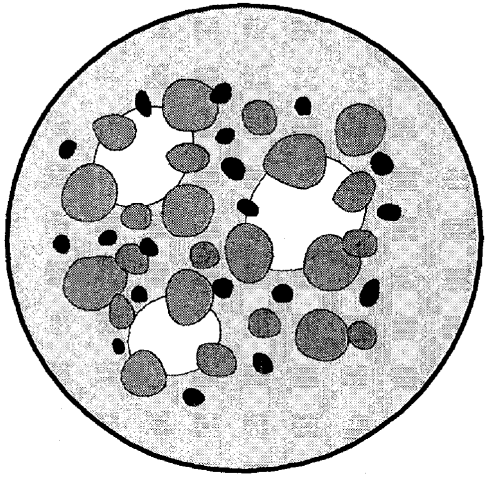

Large occupation number ⇨ Classical Field

Classical Gluon Production in Proton-Nucleus Collisions (pA)

To find the gluon production cross section in pA one has to solve the same classical Yang-Mills equations

$$D_\nu F^{\mu\nu} = J^\mu$$

for two sources – proton and nucleus.

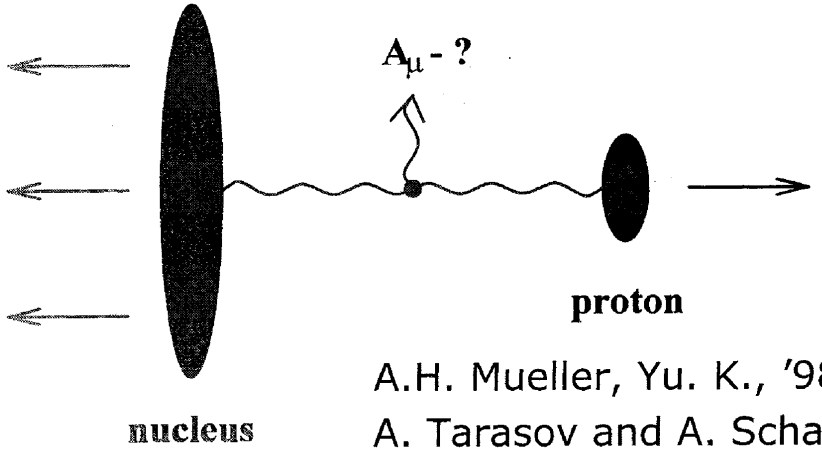

A.H. Mueller, Yu. K., '98; B. Kopeliovich, A. Tarasov and A. Schafer, '98; A. Dumitru, L. McLerran '01.

Nonlinear Equation

At very high energy parton recombination becomes important. Partons not only split into more partons, but also recombine. Recombination reduces the number of partons in the wave function.

new parton is emitted as energy increases
it could be emitted off anyone of the N partons

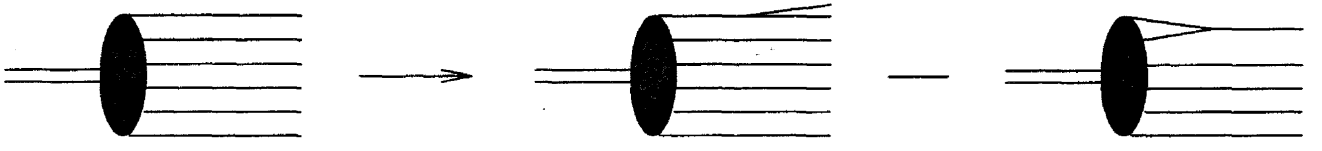

N partons **any two partons can recombine into one**

$$\frac{\partial N(x,k^2)}{\partial \ln(1/x)} = \alpha_s K_{BFKL} \otimes N(x,k^2) - \alpha_s [N(x,k^2)]^2$$

Number of parton pairs ~ N^2

Yu. K. '99 (large N_c QCD)
I. Balitsky '96 (effective lagrangian)

Map of High Energy QCD

Saturation physics allows us to study regions of high parton density in the small coupling regime, where calculations are still under control!

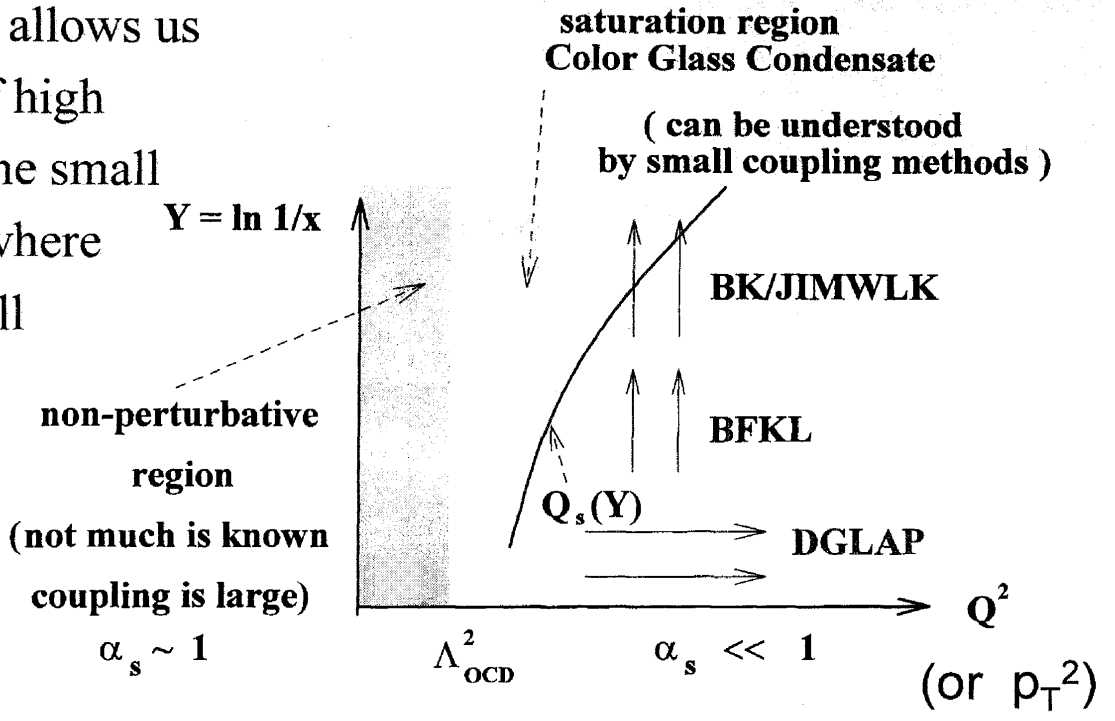

Transition to saturation region is characterized by the saturation scale

$$Q_S^2 \sim A^{1/3}\left(\frac{1}{x}\right)^{\lambda}$$

Color Glass Condensate and Glasma

François Gelis
IPhT, CEA/Saclay

Abstract

I discuss the main features of the Color Glass Condensate and of the Glasma in heavy ion collisions. I show how the glasma classical fields naturally imply long range rapidity correlations among final state particles. Finally, I discuss the difficulties in understanding how the hydrodynamical flow develops from these classical field configurations.

Correlations in η and $\vec{x}_\perp$ at Leading Log

- The factorization valid for $\left\langle T^{\mu\nu} \right\rangle$ can be extended to multi-point correlations :

$$\left\langle T^{\mu_1\nu_1}(\tau,\eta_1,\vec{\boldsymbol{x}}_{1\perp}) \cdots T^{\mu_n\nu_n}(\tau,\eta_n,\vec{\boldsymbol{x}}_{n\perp}) \right\rangle_{\text{LLog}} =$$
$$= \int \left[D\rho_1\, D\rho_2\right]\, W_1\left[\rho_1\right]\, W_2\left[\rho_2\right]$$
$$\times\, T^{\mu_1\nu_1}_{\text{LO}}(\tau,\vec{\boldsymbol{x}}_{1\perp}) \cdots T^{\mu_n\nu_n}_{\text{LO}}(\tau,\vec{\boldsymbol{x}}_{n\perp})$$

- Note: at Leading Log accuracy, all the rapidity correlations come from the evolution of the distributions $W[\rho_{1,2}]$
  ▷ they are a property of the pre-collision initial state

- This formula predicts long range ($\Delta\eta \sim \alpha_s^{-1}$) rapidity correlations for points located at the same impact parameter

Glasma flux tubes

- The initial chromo-$\vec{E}$ and $\vec{B}$ fields form longitudinal "flux tubes" extending between the projectiles:

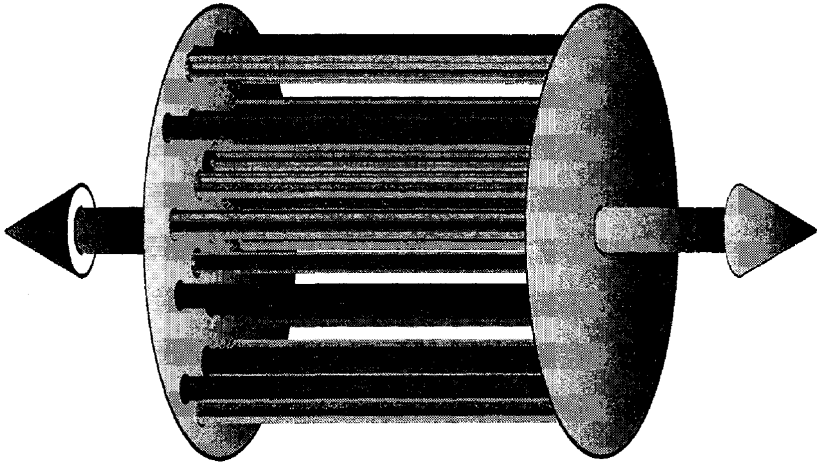

- Correlation length in the transverse plane: $\Delta r_\perp \sim Q_s^{-1}$
- Correlation length in rapidity: $\Delta\eta \sim \alpha_s^{-1}$
- The flux tubes fill up the entire volume

Importance of initial rapidity correlations

Early physics can survive in long range rapidity correlations

$$t_{\text{correlation}} \leq t_{\text{freeze out}} \; e^{-\frac{1}{2}|\eta_A - \eta_B|}$$

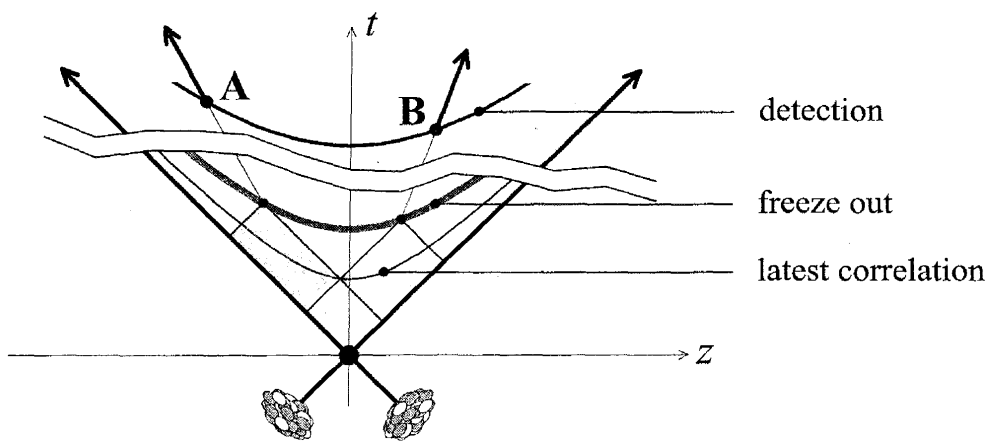

$T^{\mu\nu}$ of the Glasma

- Glasma:

$$\left\langle T^{\mu\nu}(0^+,\eta,\vec{\boldsymbol{x}})\right\rangle = \begin{pmatrix} \epsilon & & & \\ & \epsilon & & \\ & & \epsilon & \\ & & & -\epsilon \end{pmatrix}$$

- Ideal hydro:

$$T^{\mu\nu}_{\text{ideal}}(0^+,\eta,\vec{\boldsymbol{x}}) = \begin{pmatrix} \epsilon & & & \\ & p & & \\ & & p & \\ & & & p \end{pmatrix}$$

- If a smooth matching from the Glasma to Hydro is possible, one should be able to recover the fluid behavior from classical fields

Hydro behavior in a toy model (1+0 dim)

Classical field evolution with fluctuations

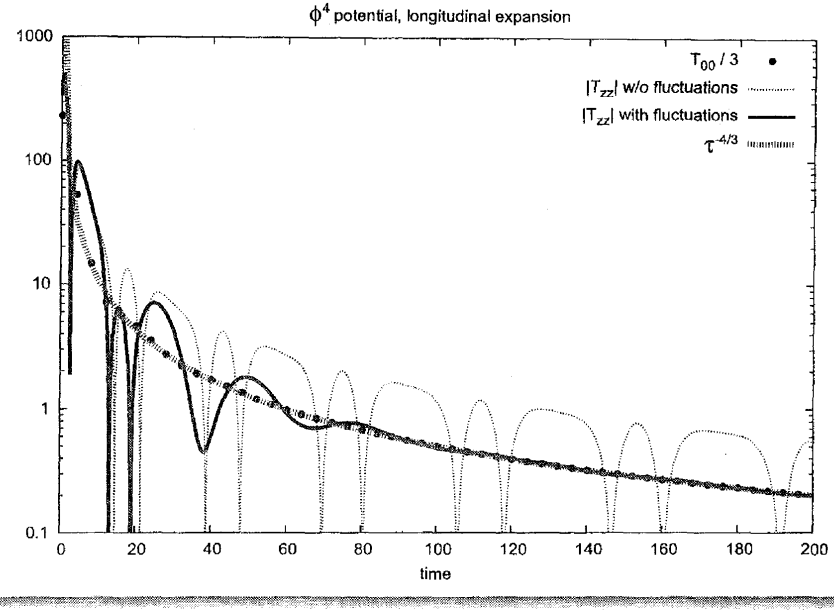

- Without fluctuations, p oscillates forever
- With fluctuations, p relaxes quickly to $\epsilon/3$
- ϵ and p decrease as $1/\tau^{4/3}$

  $\triangleright$ same behavior as in ideal hydro with EoS $\epsilon = 3p$...

Parton saturation at strong coupling : What have we learnt from RHIC and AdS/CFT ?

Edmond Iancu
Institut de Physique Théorique, Saclay & CNRS

May 10th, 2010

The AdS/CFT correspondance *(Maldacena, 1997)*

- A 'duality' (equivalence) between 2 very different theories
- A gauge theory ($\mathcal{N}=4$ SYM) in $D=3+1$ at strong coupling
  - SU(N_c), conformal invariance, fixed coupling, no confinement
- A string theory in $D=9+1$ ($AdS_5 \times S^5$) at weak coupling
  - AdS_5 : Our physical world ($D=4$) $\times$ a 'radial' dimension χ
- Strong 't Hooft coupling : $\lambda \equiv g^2 N_c \gg 1 \quad \& \quad g^2 \ll 1$
  - semiclassical limit of the string theory (gravity)
- $\mathcal{N}=4$ SYM at finite temperature $\Longrightarrow$ Black Hole in AdS_5
  - a Black Hole has entropy and thermal (Hawking) radiation

DIS off the Black Hole *(Hatta, E.I., Mueller, 07)*

- Virtual photon in 4D $\longleftrightarrow$ Maxwell wave A_μ in AdS_5 BH
- DIS cross section $\longleftrightarrow$ absorption of the wave by BH

- Physical world: $\chi = 0$

  Black Hole horizon: $\chi = 1/T$

- Maxwell equations in AdS_5 BH

$$\partial_m\left(\sqrt{-g}g^{mn}g^{pq}F_{nq}\right) = 0$$

$$F_{mn} = \partial_m A_n - \partial_n A_m$$

- No explicit coupling

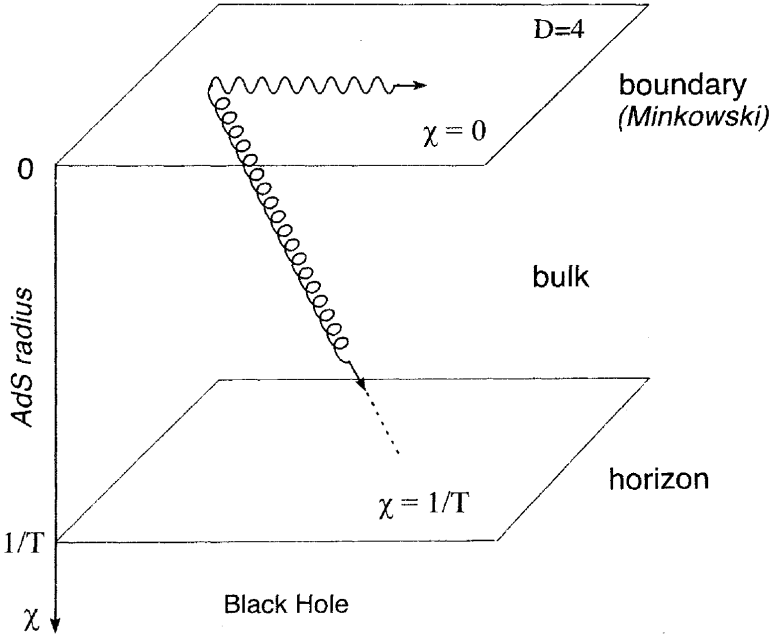

Saturation line

- Gravitational interactions are proportional to the energy density in the wave (ω) and in the plasma (T)

$$\text{DIS kinematics}: \quad x \equiv \frac{Q^2}{2\omega T} \quad \text{and} \quad Q \gg T$$

- Large ωT is tantamount to small Bjorken's x
- Critical ('saturation') value $x_s(Q) \simeq \frac{T}{Q} \ll 1$
  - $x > x_s \simeq T/Q$: $F_2(x, Q^2) \approx 0$: no partons !
  - $x < x_s \simeq T/Q$: $F_2(x, Q^2) \sim x\, N_c^2 Q^2$
- Consistent with the energy–momentum sum rule:

$$\int \mathrm{d}x\, F_2(x, Q^2) \simeq \Big[x F_2(x, Q^2) \Big]_{x=x_s} \sim N_c^2 T^2$$

Parton evolution at strong coupling

- All partons branch down to the smallest value of x consistent with energy conservation $\Longrightarrow$ no pointlike constituents

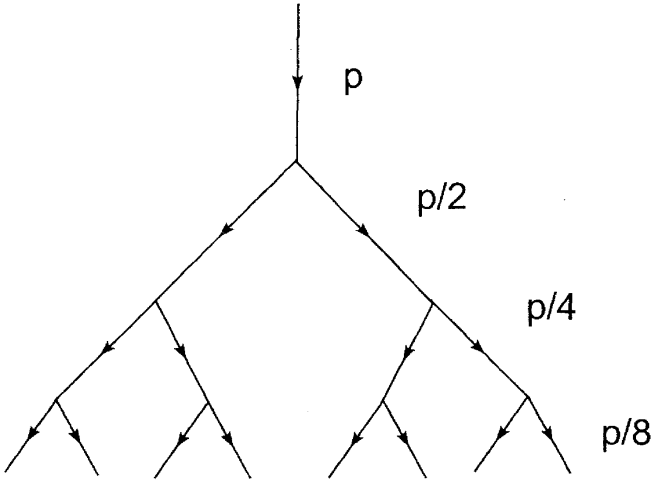

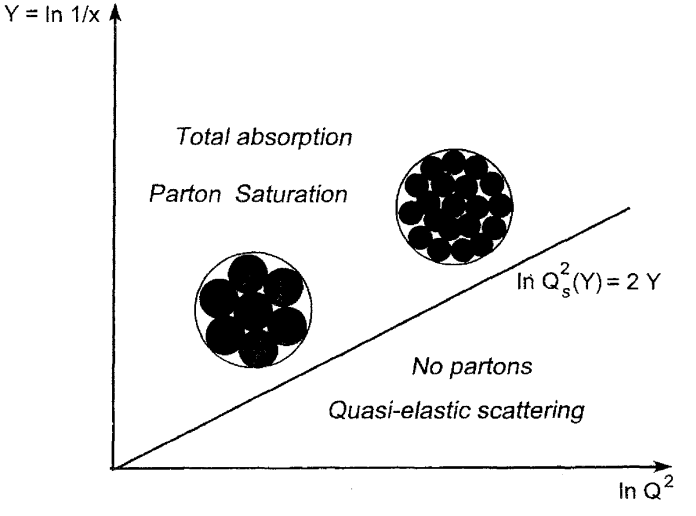

- The energy of the plasma is carried mostly by the partons along the saturation line: $x_s \simeq T/Q \ll 1$

Parton saturation: weak vs. strong coupling

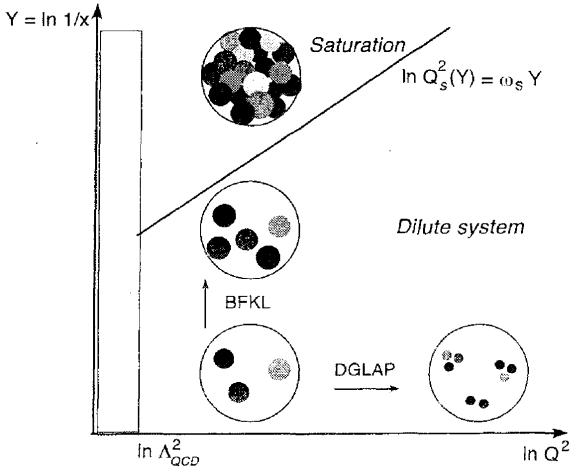

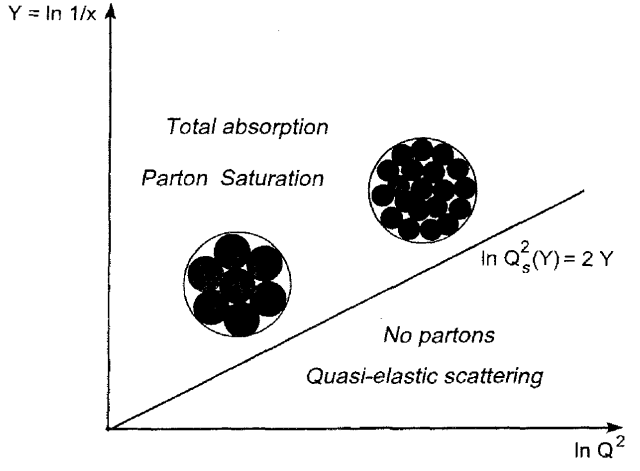

- Weak coupling : $Q_s^2(x) \propto 1/x^{0.3}$
  - $Q > Q_s(x)$: 'leading–twist' pdf
  - $Q < Q_s(x)$: $n \sim 1/\alpha_s$ (CGC)
- Strong coupling : $Q_s^2(x) \propto 1/x$
  - $Q > Q_s(x)$: no partons
  - $Q < Q_s(x)$: $n \sim 1$

HERA results and DGLAP evolution: theory and phenomenology

Stefano Forte

Dipartimento di Fisica, Università di Milano and
INFN, Sezione di Milano,
Via Celoria 16, I-20133 Milano, Italy

Abstract:

I review the current status of the application of linear perturbative QCD evolution to HERA and Tevatron data and its future use at the LHC. First, I review recent results on small x resummation of DGLAP equations and its impact on deep–inelastic scattering: I show that in the HERA region resummation has a moderate but visible effect, comparable in size to that of next-to-next-to-leading (NNLO) fixed–order corrections, but with the opposite sign. I then review recent NLO global parton (PDF) determinations: I show that DIS and hadronic (Tevatron) data are beautifully consistent with each other, thereby showing that in this kinematic region there is no evidence in the data for deviations from NLO DGLAP theory, within its expected accuracy. Finally, I discuss possible evidence for deviations from NLO DGLAP: after showing that geometric scaling does not provide such evidence, I show that the behaviour of NLO global fits in their lowest x and Q^2 range does provide some evidence in this direction, consistent with expectations based on perturbative resummation (but perhaps also with saturation). Recent precise combined HERA data strengthen this conclusion, and suggest that resummation may be necessary for phenomenology whose accuracy is better than NLO. In summary, I show that resummation effects are likely to affect HERA phenomenology and perhaps have already been seen, but their size is comparable to that of NNLO corrections (but with the opposite sign).

SMALL x RESUMMATION: WHERE DO WE STAND?

- SMALL x TERMS IN DGLAP RESUMMED TO ALL ORDERS AT THE LEADING AND SUBLEADING LEVEL (BFKL 75-76, Fadin-Lipatov 98)
- SMALL x CORRECTIONS TO HARD CROSS SECTIONS KNOWN AT THE LEADING NONTRIVIAL LEVEL FOR HQ PHOTO– & ELECTROPRODUCTION (Catani, Ciafaloni, Hautmann, 91; DIS (Catani, Hautmann, 94); HQ HADROPRODUCTION (Ball, K.Ellis, 01); GG→HIGGS (Marzani, Ball, Del Duca, s.f., Vicini, 08); DRELL-YAN (Marzani, Ball, 09); ISOLATED PHOTON (Diana, 10)
- TWO ALTERNATIVE APPROACHES TO DGLAP RESUMMATION:
  - SMALL x RESUMMATION OF DGLAP (Altarelli, Ball, s.f., ABF
  - INCLUSION INTO BFKL OF FIXED-ORDER DGLAP & SUBSEQUENT NUMERICAL DECONVOLUTION OF RESUMMED DGLAP SPLITTING FUNCTION (Ciafaloni, Colferai, Salam, CCS)
- STABLE PERTURBATIVE EXPANSION OF THE RESUMMED DGLAP SPLITTING FUNCTION UP TO NLO WITH $n_f = 0$ (CCS+Stasto 02, ABF 06):
  - DGLAP-BFKL MATCHING THROUGH SUITABLE DOUBLE BFKL+GLAP EXPANSION (Ball, s.f. 95, ABF 2000)
  - COLLINEAR/ANTICOLLINEAR GLUON EMISSION SYMMETRY (Salam 99)
  - RUNNING COUPLING (CCS 99, ABF 01)
- EXTENSION TO HARD COEFFICIENT FUNCTIONS OF SMALL x RUNNING COUPLING RESUMMATION (Ball 08)
- EXTENSION TO $n_f \neq 0$ AND SCHEME–INDEPENDENT MATCHING OF DIS COEFFICIENT FUNCTIONS AND DGLAP EVOLUTION (ABF 09)
- DIS RESUMMED PHENOMENOLOGY (ABF+Rojo 2010+ in progress)

THE EFFECT ON PHYSICAL OBSERVABLES

KEEP F_2 & F_L FIXED AT $Q_0 = 2$ GeV

COMPUTE $K(Q) \equiv F_2^{\rm new}(x,Q^2)/F_2^{\rm NLO}(x,Q^2)$; $F_L^{\rm new}(x,Q^2)/F_L^{\rm NLO}(x,Q^2)$

NNLO, RESUMMED $Q_0\overline{\rm MS}$, RESUMMED $\overline{\rm MS}$; $x = 10^{-2}$, 10^{-4}, 10^{-6}

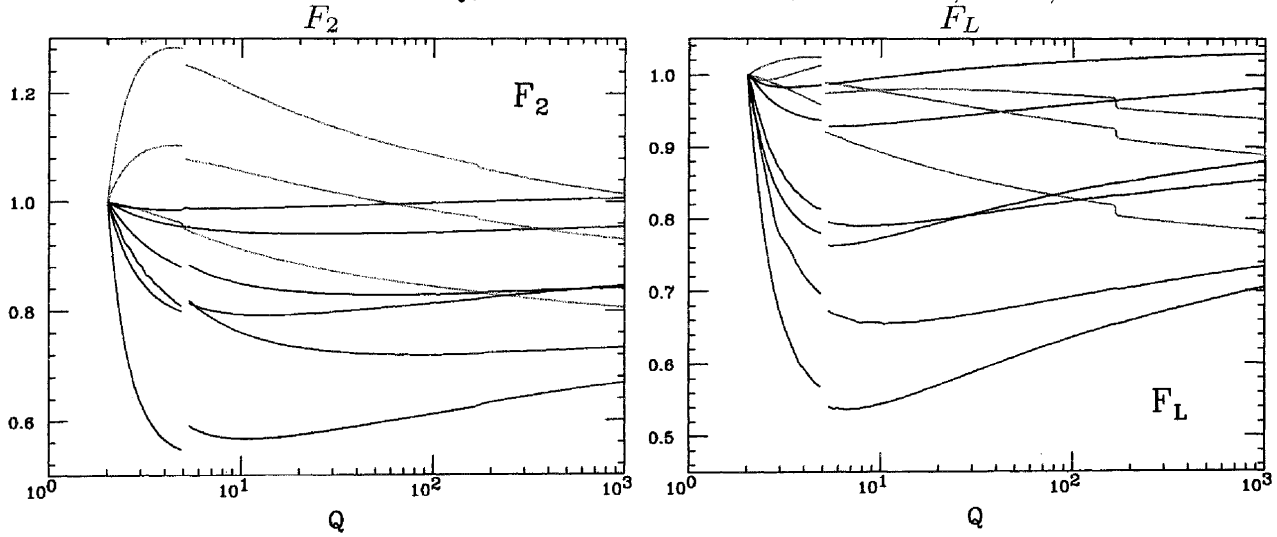

(ABF, 08)

- EFFECT OF RESUMMATION COMPARABLE TO NNLO
- RESUMMED SUPPRESSION DUE TO DIP IN EVOLUTION & PDF SUPPR. LOW SCALE
- SCHEME DEPENDENCE SMALLER THAN FOR PDFS
- EVOLUTION WASHES OUT THE DIFFERENCES

COMPATIBILITY:
DIS VS. HADRONIC DATA AGAIN

A SENSITIVE TEST: IS THE IMPACT OF A DATASET INDEP. OF THE DATA IT IS ADDED TO?

ADDING JET DATA. . .

. . . TO DIS DATA

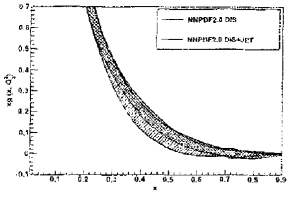

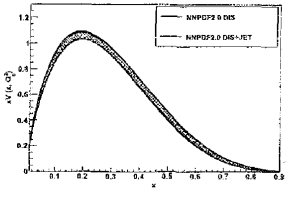

. . . TO DIS+DY DATA

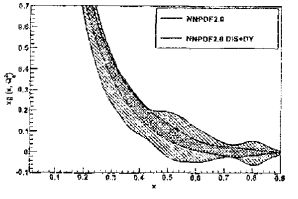

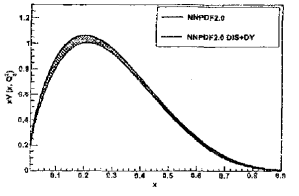

ADDING DRELL-YAN DATA. . .

. . . TO DIS DATA

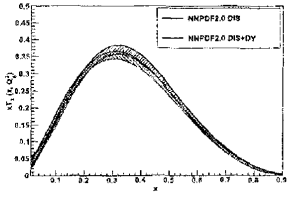

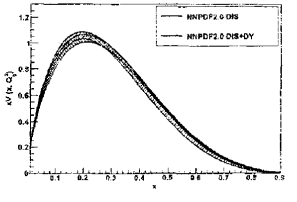

. . . TO DIS+JET DATA

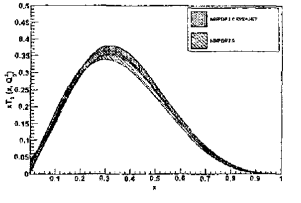

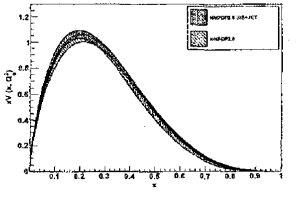

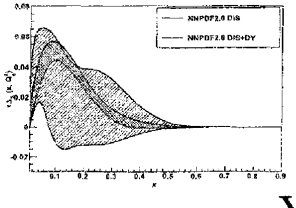

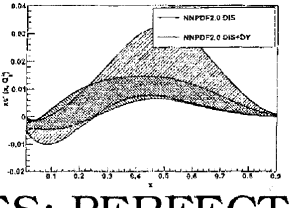

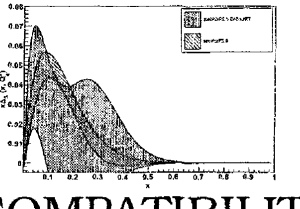

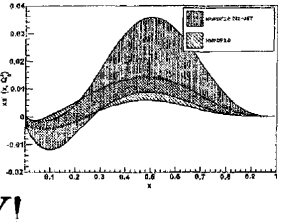

YES: PERFECT COMPATIBILITY!

WHAT ABOUT GEOMETRIC SCALING?

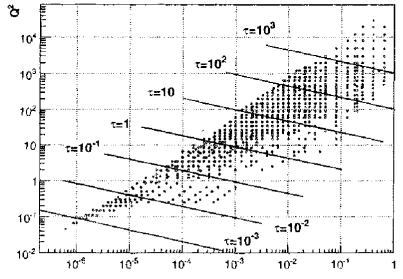

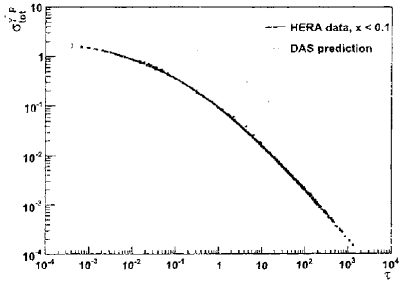

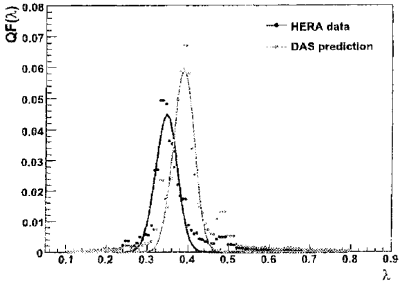

- STRUCTURE FUNCTION DATA SCALE W.R. TO $\tau = \frac{Q^2}{Q_0}^2 (x/x_0)^\lambda$
  (Stašto, Golec-Biernat, Kwieciński, 2001)
- EVIDENCE FOR NONLINEAR EVOLUTION? (RECOMBINATION, SATURATION,. . .)
- DOES DGLAP FAIL?? FOR $Q^2 \gtrsim 10$ GEV^2
- BUT DOUBLE–LOG SOLUTION TO LO (LINEAR) DGLAP ("DAS") ALSO SCALES!
  CAN ALSO BE SHOWN ANALYTICALLY
  (Caola, s.f., 2008)
- CAN DETERMINE OPTIMAL SCALING FROM "QUALITY FACTOR" ANALYSIS
  (Gélis et al., 2007)
  $\Rightarrow$ OBSERVED λ AGREES WITH "DAS": DGLAP PREDICTS GEOMETRIC SCALING
  A FINER TEST NEEDED TO REVAL DEVIATIONS FROM DGLAP!

NEW (COMBINED) HERA DATA

BACKWARD EV. VS DATA

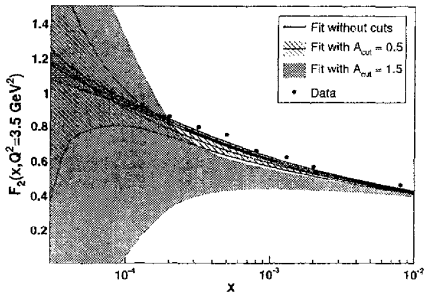

DAT/TH DIST: NO CUT

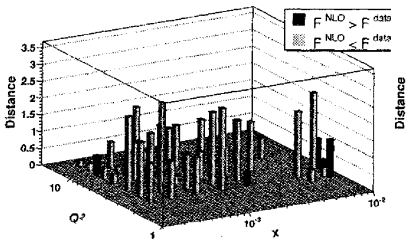

DAT/TH DIST: CUT

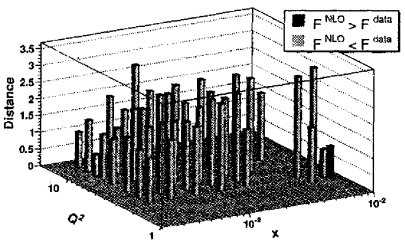

- DATA AT LOW x AND Q^2 SHOW LESS EVOLUTION THAN PREDICTED BY NLO DGLAP
- BACKWARD EVOLVED FIT LIES SYSTEMATICALLY BELOW DATA
- WITH MORE PRECISE DATA, THE FIT NO LONGER MANAGES TO COMPENSATE BY READJUSTING THE PDFS: EVEN FULL FIT LIES BELOW DATA

DETERIORATION IN FIT QUALITY:

χ^2 VS τ SLICES

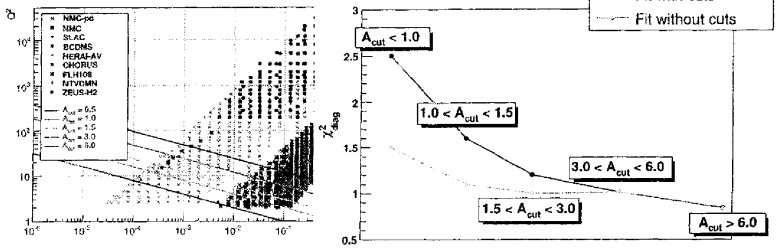

- QUALITY OF [illegible] DETERIORATES IN LOW τ REGIONS
- QUALITY OF CUT FIT INCREASINGLY POOR AS τ DECREASES

The New HERA F_2 data and the Determination of the Infrared Behaviour of the BFKL Amplitude

talk by Henri Kowalski,
based
on the H1 and ZEUS Combination paper, JHEP 1001:109,2010
and
the paper with L.N. Lipatov, D.A. Ross and G. Watt
arXiv 1005.0355

Workshop on Saturation, the Color Glass Condensate and Glasma

BNL, 10th of May 2010

Combining ZEUS and H1 F_2 data

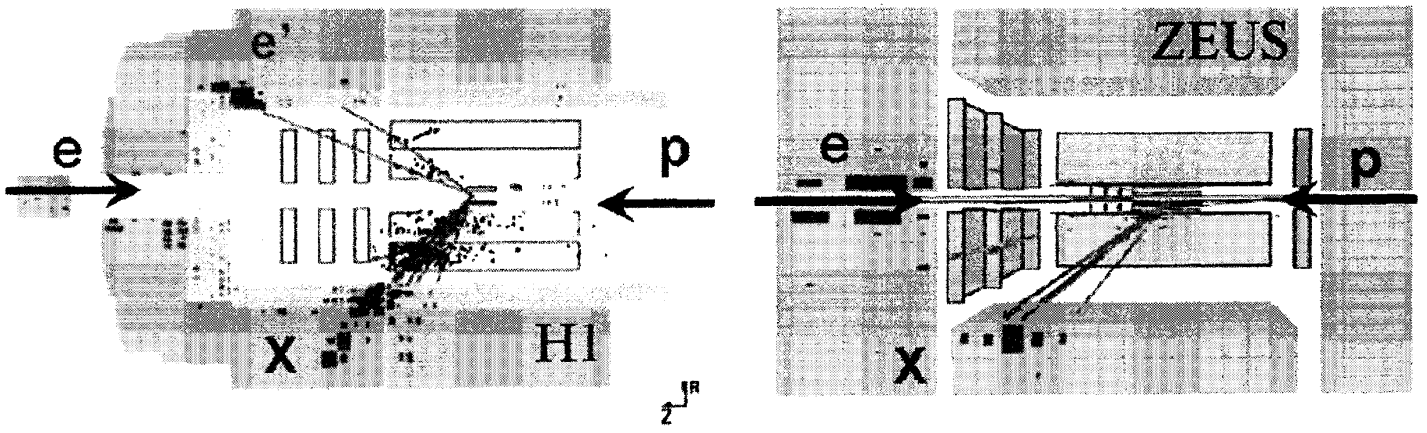

H1 and ZEUS collected similar amount of data: 100 pb^{-1}

➥ improved statistical precision by ~ $1/\sqrt{2}$

Improved systematic precision

H1 and ZEUS detectors and data analysis are quite different.

➥ The H1 and ZEUS cross-sections have different sensitivities to similar sources of correlated systematic uncertainties

Combination Method

Swim H1 and ZEUS data to the same grid points:

$$\sigma_{\mathrm{H1}}\left(x_{\mathrm{H1}}, Q^2_{\mathrm{H1}}\right) \rightarrow \sigma_{\mathrm{H1}}(x,Q^2) \quad ; \quad \sigma_{\mathrm{ZEUS}}\left(x_{\mathrm{ZEUS}}, Q^2_{\mathrm{ZEUS}}\right) \rightarrow \sigma_{\mathrm{ZEUS}}(x,Q^2)$$

New measurements are obtained by building the χ^2 estimate:

Combination at point i
*[Estimate of 1 **true cross section**]*

Measurement at point i

$$\chi^2_{\exp}(\boldsymbol{m},\boldsymbol{b}) = \sum_i \frac{\left[m^i - \sum_j \gamma^i_j m^i b_j - \mu^i\right]^2}{\delta^2_{i,\mathrm{stat}}\,\mu^i\left(m^i - \sum_j \gamma^i_j m^i b_j\right) + \left(\delta_{i,\mathrm{uncor}}\, m^i\right)^2} + \sum_j b_j^2$$

***Sensitivity** of the cross section to the j^{th} source of **correlated** uncertainty.*

γ^i_j defined as the relative change of the measurement for a 1 sigma shift of the error source

*Shift of the j^{th} source of **correlated** uncertainty*

$\delta_{i,\mathrm{stat}}/\delta_{i,\mathrm{uncor}}$ *Relative stat. / syst. error on the measurement*

- **1402** measurements with **110** correlated sources of uncertainty combined to **741** cross sections.
- χ^2 / dof = 636.5 / 656 ; No tension in Pulls ; $|b_j| < 2$ ⇒ **H1 and ZEUS Agree!**

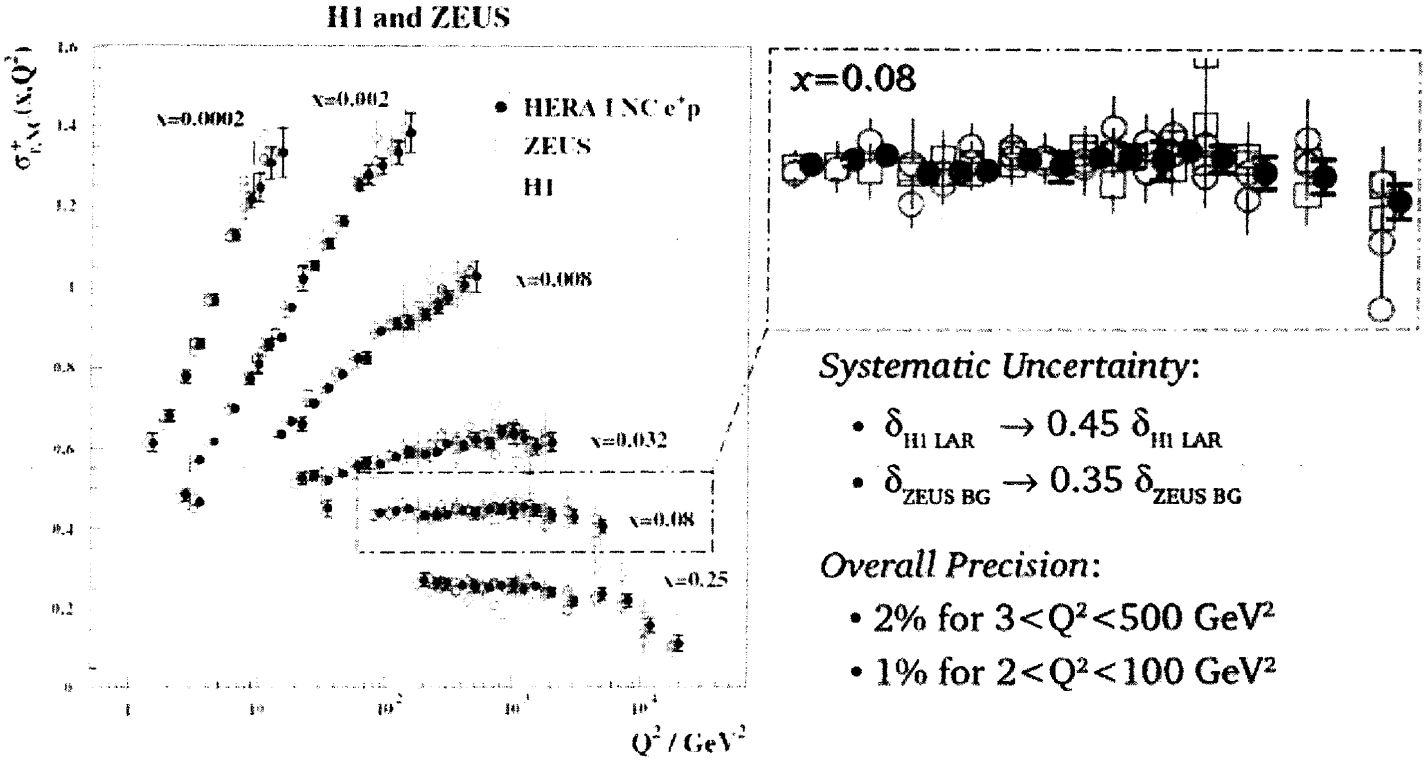

Systematic Uncertainty:

- $\delta_{\text{H1 LAR}} \rightarrow 0.45\ \delta_{\text{H1 LAR}}$
- $\delta_{\text{ZEUS BG}} \rightarrow 0.35\ \delta_{\text{ZEUS BG}}$

Overall Precision:

- 2% for $3<Q^2<500$ GeV^2
- 1% for $2<Q^2<100$ GeV^2

Study of the gluon-gluon amplitude (above the saturation region)

One of the major results from HERA is that, at low x, F_2 is dominated by the gluon density. The study of the gluon dynamics is very interesting because of its importance to other physics reactions, like Higgs production at LHC, but also because it is a fundamental quantity, which is comparable to black body radiation in QED.

The dynamics of the gluon distribution at low x is determined by the amplitude for the scattering of a gluon on a gluon, described by the BFKL eq.

$$\frac{\partial}{\partial \ln s}\mathcal{A}(s,\mathrm{k},\mathrm{k}') = \delta(k^2-k'^2) + \int dq^2 \mathcal{K}(\mathrm{k},\mathrm{q})\mathcal{A}(s,\mathrm{q},\mathrm{k}'),$$

which can be solved in terms of the eigenfunctions of the kernel

$$\int dk'^2 \mathcal{K}(\mathrm{k},\mathrm{k}') f_\omega(\mathrm{k}') = \omega f_\omega(\mathrm{k}).$$

in LO $\quad f_\omega(\mathrm{k}) = \left(k^2\right)^{i\nu-1/2}$ with $\quad \omega = \alpha_s \chi_0(\nu)$ for fixed $\quad \alpha_s$

The BFKL eq., with the fixed α_s predicts that the rate of rise λ is only slowly varying with Q^2, $\lambda \sim 0.3$ (in NLO). Therefore, the prevailing opinion was that the BFKL analysis was not applicable to HERA data.

The rate of rise λ

$F_2 \sim (1/x)^{\lambda}$

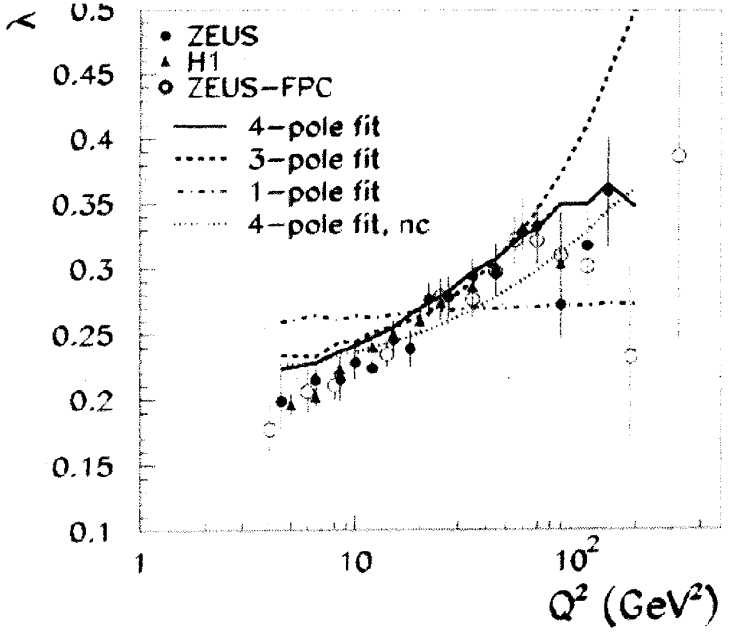

First hints that λ can be substantially varying with Q^2 in BFKL was given in PL 668 (2008) 51 by EKR

Lipatov 86 & EKR 2008: BFKL solutions with the running α_s are substantially different from solutions with the fixed α_s.

Summary of RIKEN BNL workshop

P- and CP-odd effects in hot and dense matter

April 26-30, 2010

Caveats
- 39 Talks + Th. + Exp. Discussion
  Impossible to summarize all in 15 min / 5 slides.
  Focus on relevance to glasma + experimental results.
  I am very sorry if I do not talk about your results.
- It's a personal summary
  Not necessarily the viewpoint of any workshop participant, or any other workshop organizer.

Talks online at: http://quark.phy.bnl.gov/~kharzeev/cpodd

Harmen Warringa, Goethe Universität, Frankfurt

What was part of the workshop about?

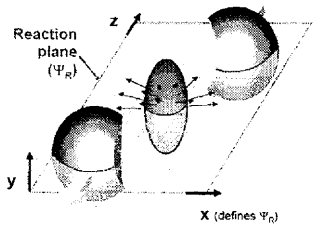

P- and CP-odd effects might occur in hot matter

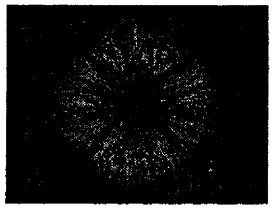

How to observe these effects in data?

QCD: Topological charge fluctations

- Quantum tunneling: Instanton, Caloron (finite T. instanton)

Talks by Edvard Shuryak and Pierre van Baal

- Thermal activation: Sphaleron

Talks by Guy Moore, Valery Rubakov and Edvard Shuryak

- In Glasma *Talk by Larry McLerran*

Topological charge + axial anomaly -> chirality = P- and CP-odd effect

Possible way to observe P- and CP-odd effects: The Chiral Magnetic Effect

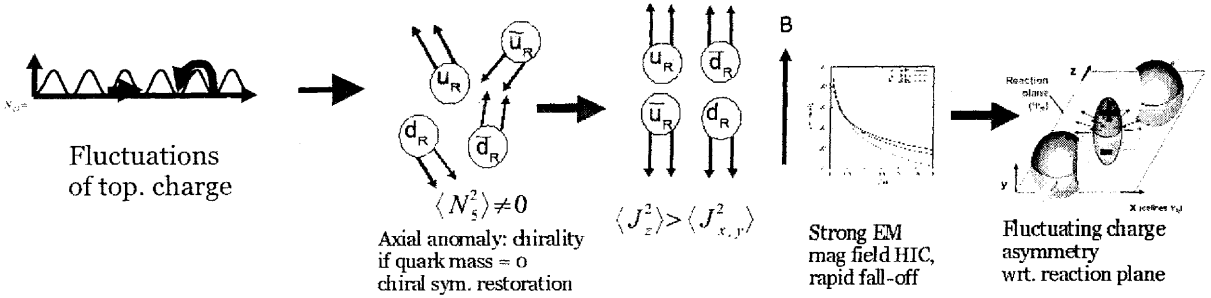

Talk by Harmen Warringa

Charge asym. from topology + magnetic field

Confirmation from Lattice QCD

Density of the electric charge vs. magnetic field, 3D time slices

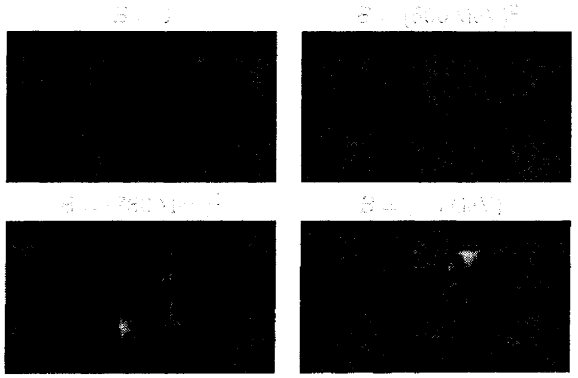

Talk by Mikhail Polikarpov

Classical instanton (-like solution) Put it all together. It works...

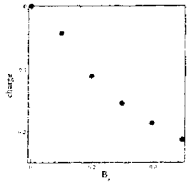

Charge in top (z-)half of lattice from near-zero-modes. Dividing in x, y, or t gives zero, effect flips sign under $B_3 \to -B_3$

Talk by Tom Blum

Confirmation from analytic studies

- Large axial chemical potential μ_5 for some reason
- Leads to a vector current: charge separation
- π^+ and π^- would have anticorrelation in momenta
- Some experimental signal?
- Can be explained by $j \sim \mu_5 B$ Kharzeev, Fukushima, Warringa, McLerran...
- Chiral rotation effect: $j \sim \mu_5 \omega$ *Talk by Dam Son*

Chiral magnetic spiral: *Talk by Gerald Dunne*

Problems with boundary terms in AdS/CFT
Talks by Ho-Ung Yee and Anton Rebhan

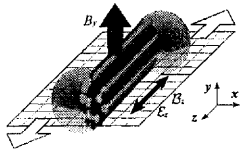

Induced current over chirality vs. mag field

Homogeneous color flux tube + perp. EM mag. field

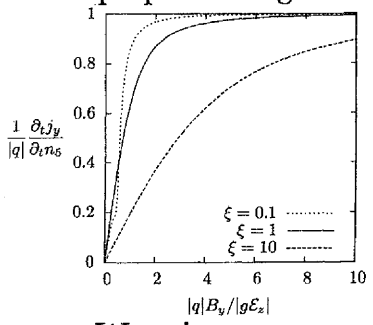

Talk by Harmen Warringa

Charge correlations STAR

Also data at 62 GeV

Red points:

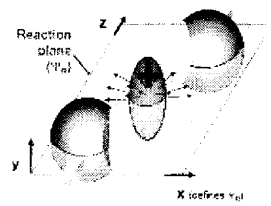

Blue points:

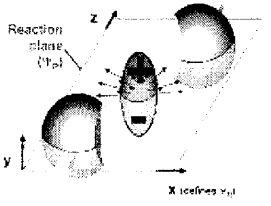

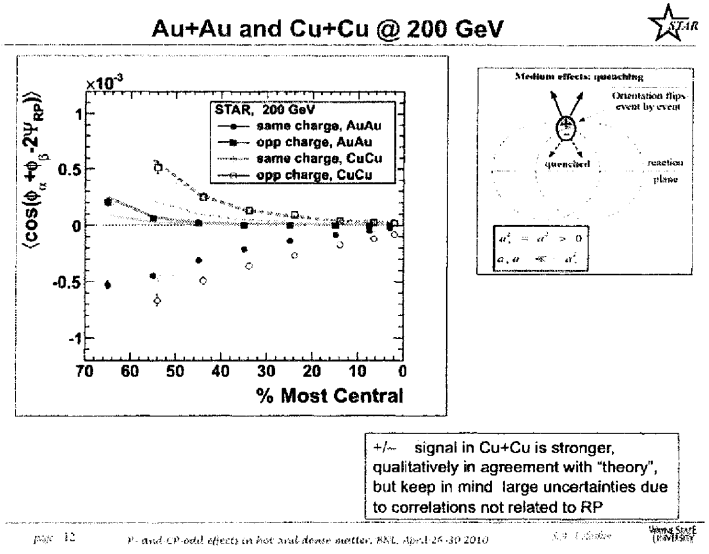

min. bias, $|\eta|<1.0$

$0.15<p_t<2$ GeV/c

Data cannot be explained by

HIJING
HIJING+v2,
MeVSIM,
UrQMD

Talk by Sergei Voloshin

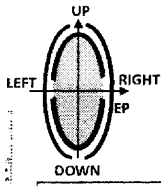

$$A_{\pm,UD} = \frac{N_{\pm,up} - N_{\pm,down}}{N_{\pm,up} + N_{\pm,down}}$$

$$A_{\pm,LR} = \frac{N_{\pm,left} - N_{\pm,right}}{N_{\pm,left} + N_{\pm,right}}$$

Charge Asym. Correl. Results

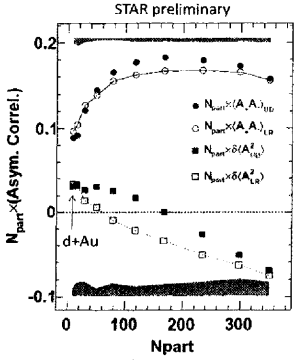

- Oppo-sign aligned; $\langle A_+A_-\rangle_{UD} > \langle A_+A_-\rangle_{LR}$
  LPV expects: $\langle A_+A_-\rangle_{UD} < \langle A_+A_-\rangle_{LR}$
  Contradicts LPV expectations.

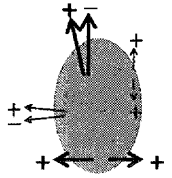

- Same-sign back-to-back in central, unexpected from *only* LPV.
  Data: $\langle A^2\rangle_{UD} > \langle A^2\rangle_{LR}$
  LPV expects: $\langle A^2\rangle_{UD} > \langle A^2\rangle_{LR}$

Important to understand backgrounds (*Talk by Jinfeng Liao*) and relate different observables

Talk by Fuqiang Wang

Charge correlations PHENIX

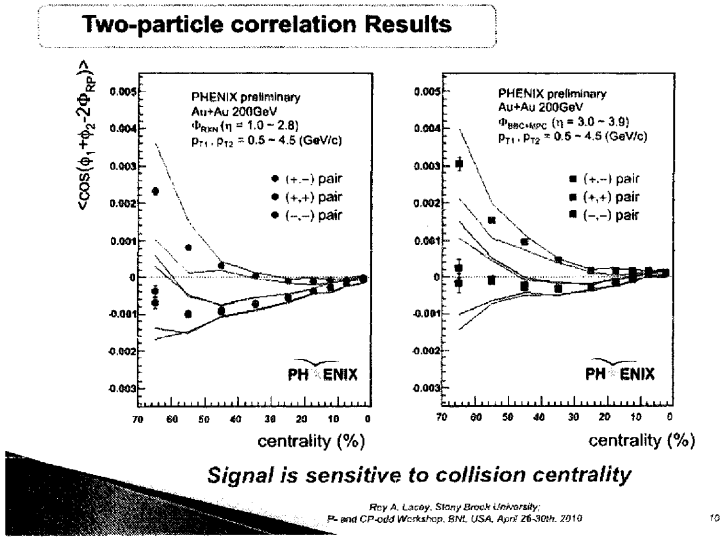

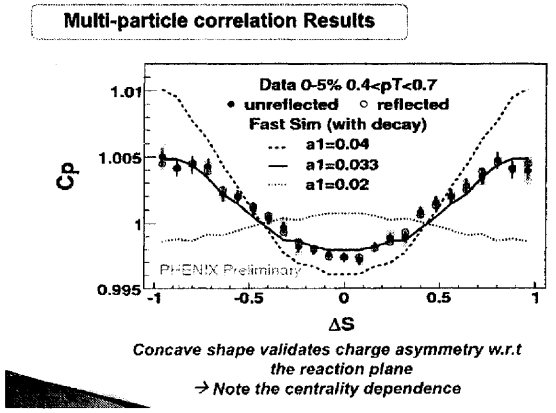

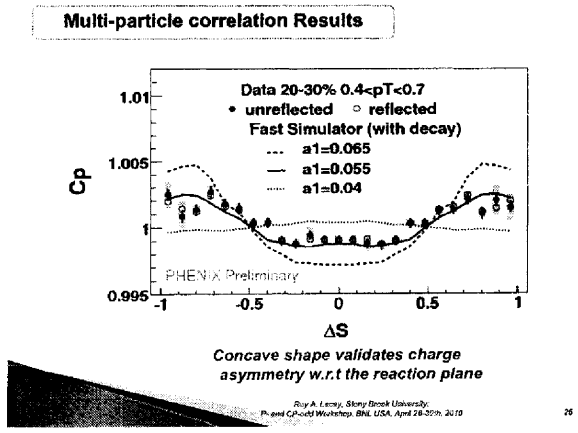

Two-particle correlations consistent with STAR data

Cp: multi-particle correlation.
Cp is insensitive to jets and flow.

Talks by Roy Lacey

My personal conclusions

- Topological charge fluctuations in the presence of external magnetic field lead to P- and CP-odd effects which cause electric charge fluctuations perpendicular to reaction plane. The magnitude is however uncertain.

- The magnetic field is only large at initial time, if the above mechanism is realized the glasma is key to its understanding.

- There are also alternative mechanisms for charge fluctuations (*Talk by B. Mueller*). Need to quantify them all and come with detailed predictions, e.g. dependence on energy, species, centrality, rapidity, particle ID, etc.

- Both STAR and PHENIX have observed charge correlations in azimuthal angle. Evidence for fluctuating charge asymmetries. Need to understand backgrounds and make all observations consistent.

- In order to explain the source of the observed asymmetries, detailed quantitative predictions from theory are required, with help of additional results from experiment.

Talks online: http://quark.phy.bnl.gov/~kharzeev/cpodd

EXTENDED LONGITUDINAL SCALING: DIRECT EVIDENCE OF SATURATION

Wit Busza (MIT)

In 1969 Benecke, Chou, Yang and Yen proposed the hypothesis of limiting fragmentation. It was based on the "two-fireball model" to explain cosmic ray physics and the "..intuitive picture of a high-energy collision process as two extended objects going through each other, breaking into fragments...". The expectations were that it would apply to the "fragmentation region" – i.e. within a unit or so of the rapidity of the projectile or target particle. It is a surprising feature of all the global high energy multiparticle production data that "limiting fragmentation" seems to apply to almost the entire longitudinal phase space. It is in fact the dominant longitudinal feature in high energy multiparticle production and for that reason, when applied to the whole phase space, has been renamed by PHOBOS as "extended longitudinal scaling". In this talk I briefly review the existing extensive data on extended longitudinal scaling in pp, pA and AA collisions and point out that this phenomenon is a direct manifestation of some kind of saturation that takes place in the multiparticle production process. Recent LHC data relevant to extended longitudinal scaling are shown and discussed.

Direct manifestation of the saturation of particle production

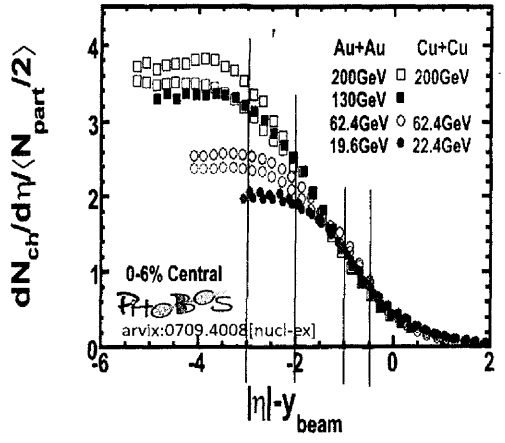

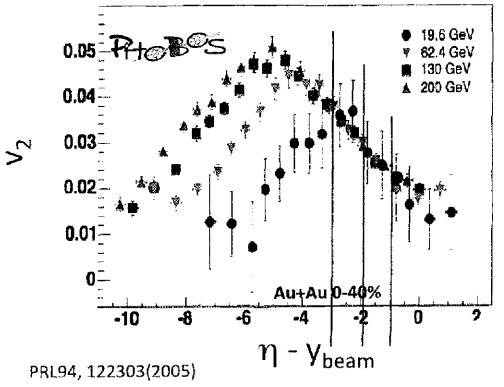

PRL94, 122303(2005)

Taking y≈η

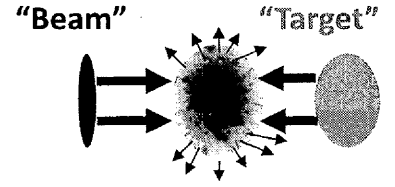

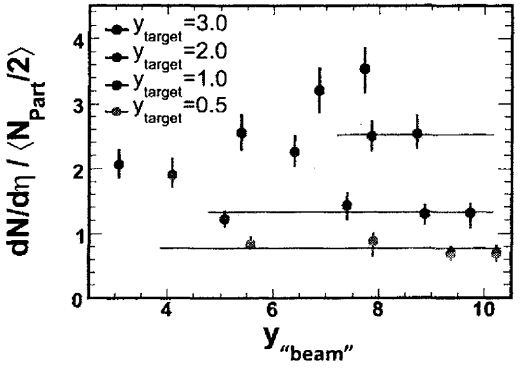

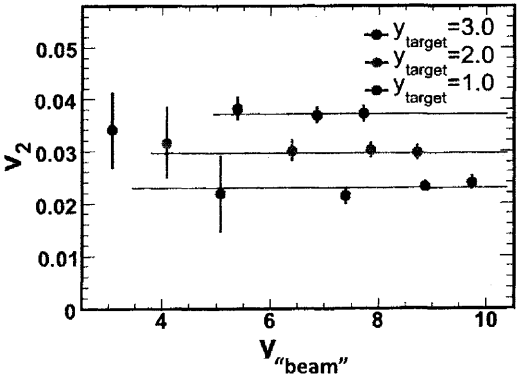

Wit Busza

Glasma workshop BNL May 2010

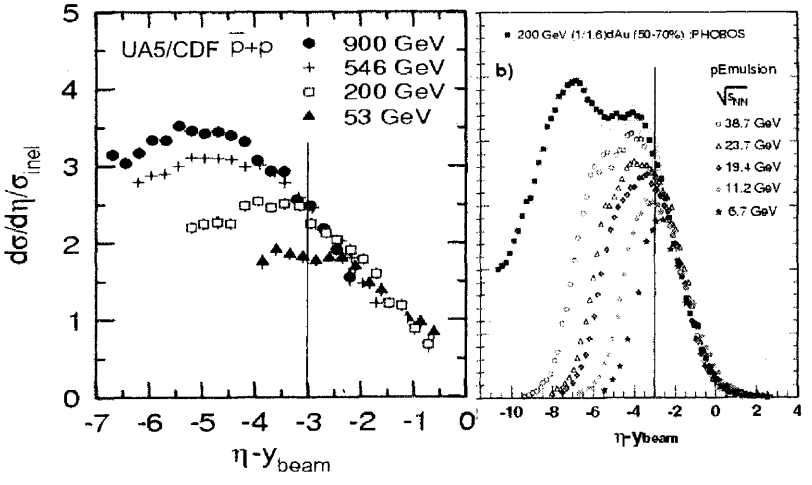

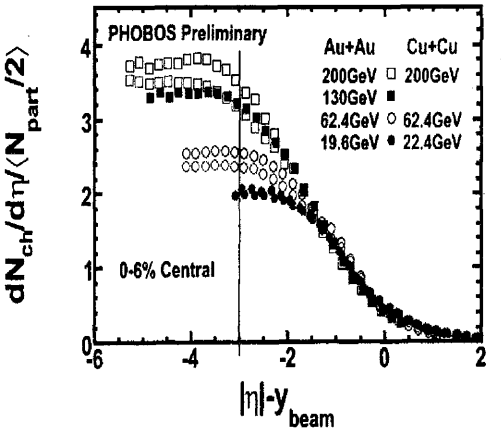

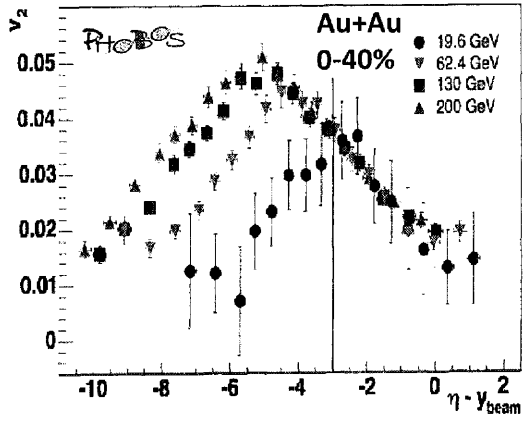

Direct evidence of saturation in pp, pA and AA

p+p($\bar{p}$) Non-Single-Diffractive

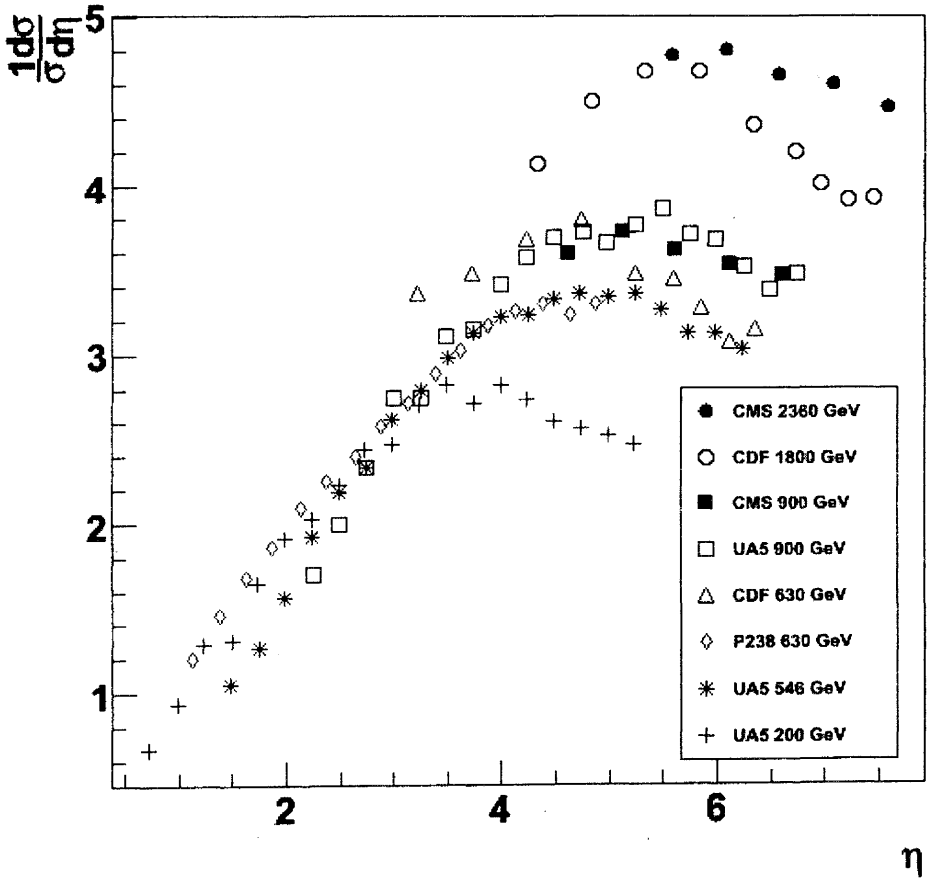

Extrapolation of PHOBOS data to LHC energies will almost certainly fail (at least for dn/dη)

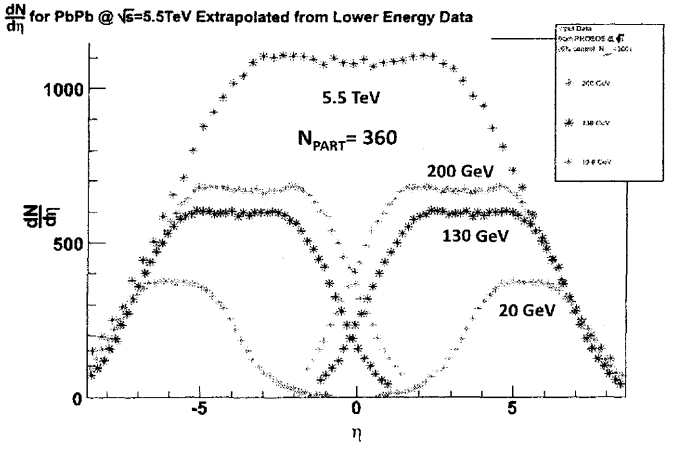

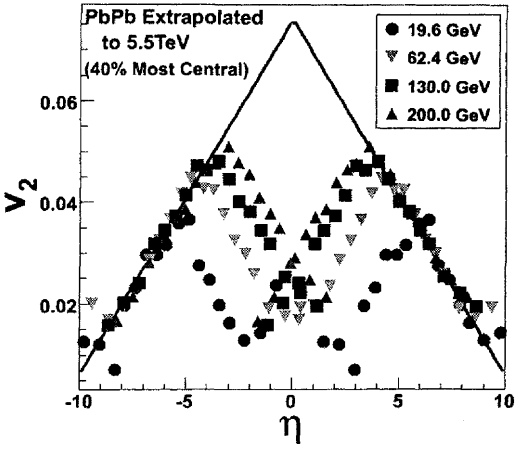

Total charged multiplicity in central (N_{part} = 386) PbPb collisions at $\sqrt{s}$ = 5.5 TeV = 15000 ± 1000

Mid-rapidity dN/dη in central (N_{part} = 386) PbPb collisions at $\sqrt{s}$ = 5.5 TeV = 1200 ± 100

Total charged multiplicity in inelastic pp collisions at $\sqrt{s}$ = 14 TeV (10 TeV) = 60 ± 10 (56 ± 9)

AuAu Data from PHOBOS, Nucl. Phys. A757 (2005) 28

Extrapolation: WB J. Phys. G35, 044040 (2008).

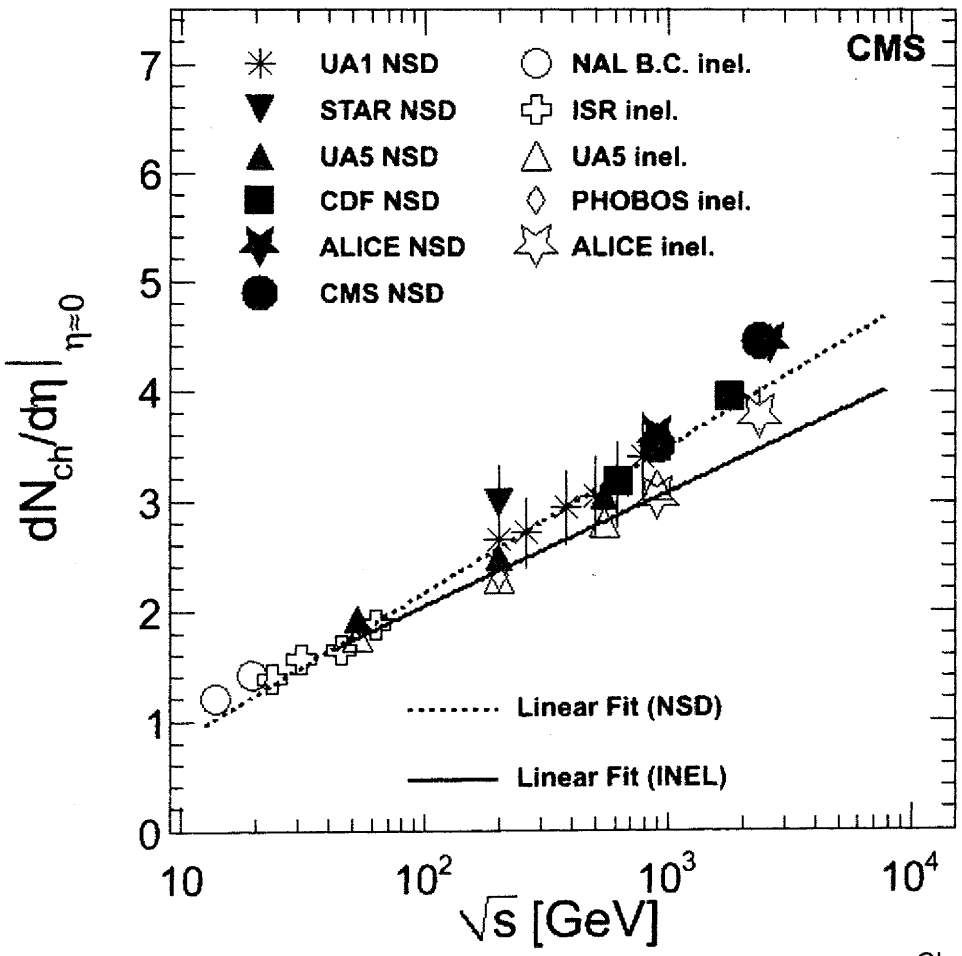

Data points from CMS
JHEP 02 (2010)041

Multiplicity fluctuations and Negative binomial distributions

Contents

- Multiplicity distributions for Au+Au 200GeV/62.4GeV, Cu+Cu 200GeV/62.4GeV and NBD fit.
- Comparison of Clan model parameters with past experiments.
- Density correlations in heavy-ion collisions.
- Centrality dependence of density correlations.

Tomoaki Nakamura
(RIKEN)
for the PHENIX collaboration

Multiplicity and NBD in Au+Au, Cu+Cu at RHIC energy

200 GeV Au+Au

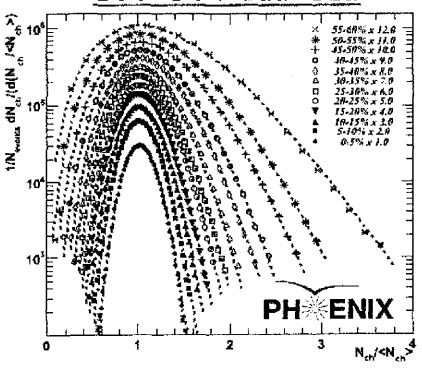

62.4 GeV Au+Au

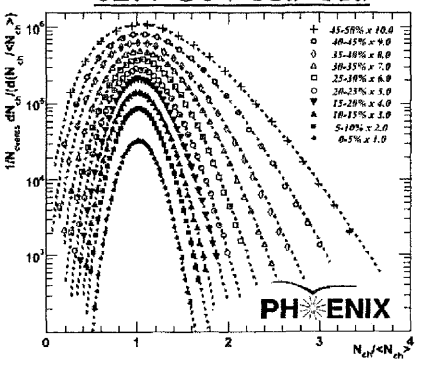

NBD:

$$P(n) = \frac{\Gamma(n+k)}{\Gamma(n+1)\Gamma(k)} \frac{(\mu/k)^n}{(1+\mu/k)^{n+k}}$$

μ:	mean of the distribution
k^{-1}:	deviation from Poissonian width
k:	multiplicity of B. E. emission source

200 GeV Cu+Cu

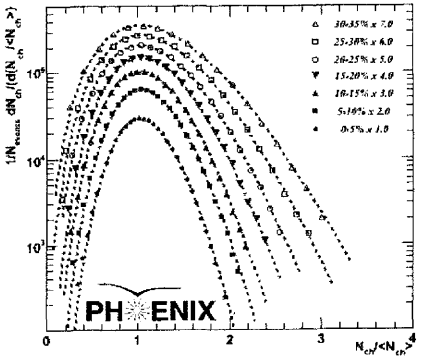

62.4 GeV Cu+Cu

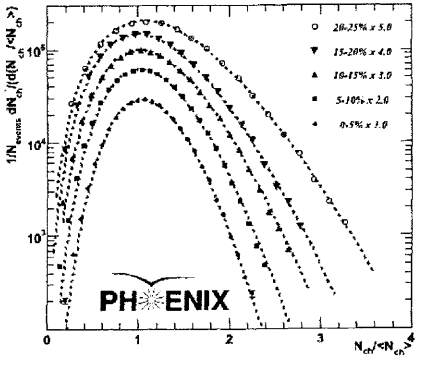

22.5 GeV Cu+Cu

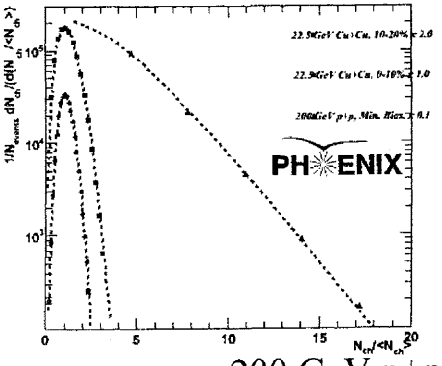

200 GeV p+p

Clan model varying collision systems and δη

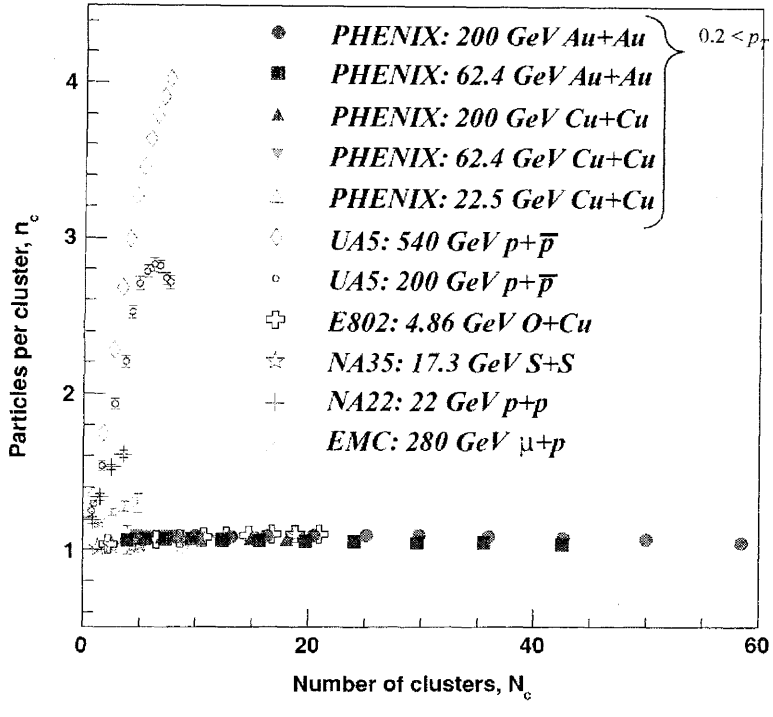

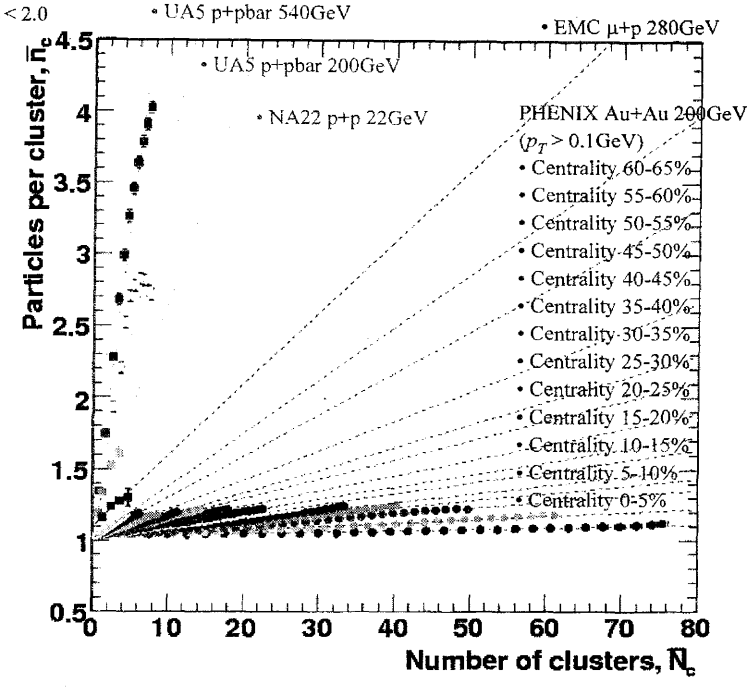

PHENIX: Phys. Rev. C78, 044902

PHENIX: Phys. Rev. C76, 034903

Clan model parameters A. Giovannini et al.: Z. Phys. C30, 391

$$\overline{N}_c = k \ln(1 + \mu / k)$$

$$\overline{n}_c = (\mu / k) / \ln(1 + \mu / k)$$

A+A collisions exhibit weak clustering characteristics, independent of collision energy.

Extraction of the density correlations

$$k^{-1}(\delta\eta) = F_2 - 1 = \frac{\int_0^{\delta\eta}\int_0^{\delta\eta} C_2(\eta_1,\eta_2)d\eta_1 d\eta_2}{\delta\eta^2 \overline{\rho}_1^{\,2}} = \frac{2\alpha\xi^2(\delta\eta/\xi - 1 + e^{-\delta\eta/\xi})}{\delta\eta^2} + \beta$$

Au+Au 200 GeV

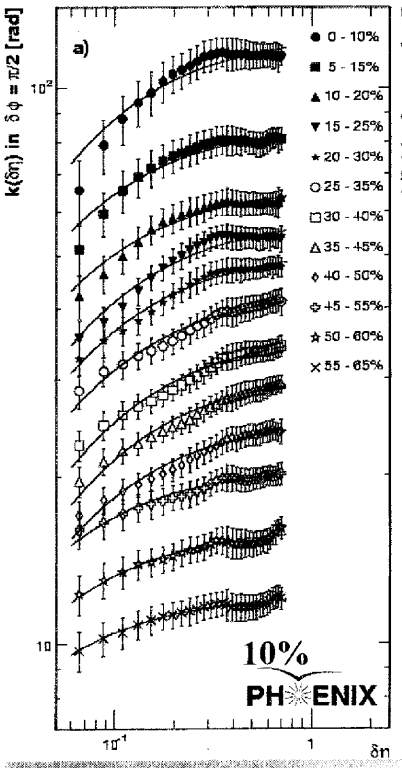

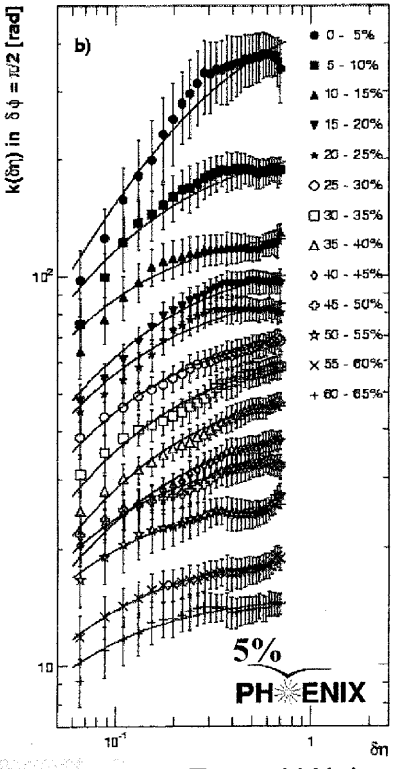

Au+Au 62.4 GeV

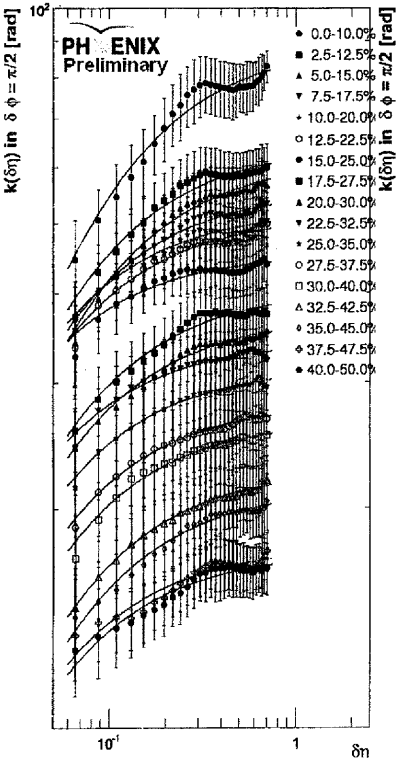

Cu+Cu 200 GeV

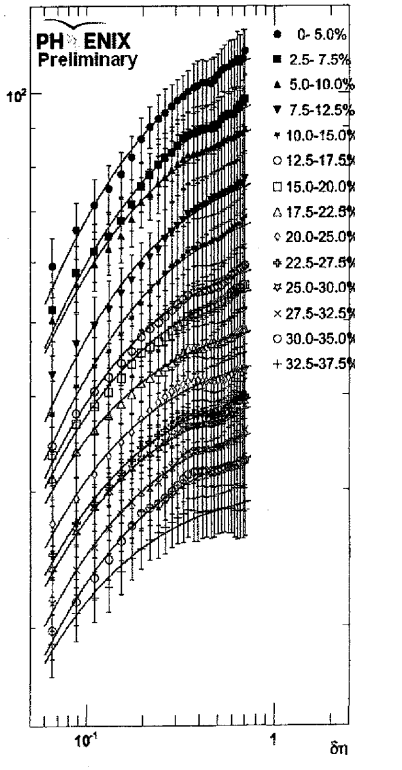

Centrality dependence of density correlations

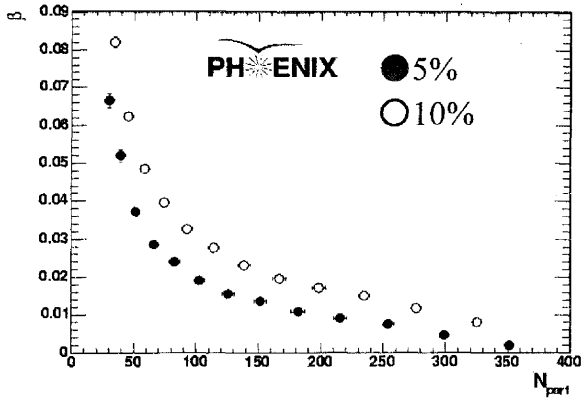

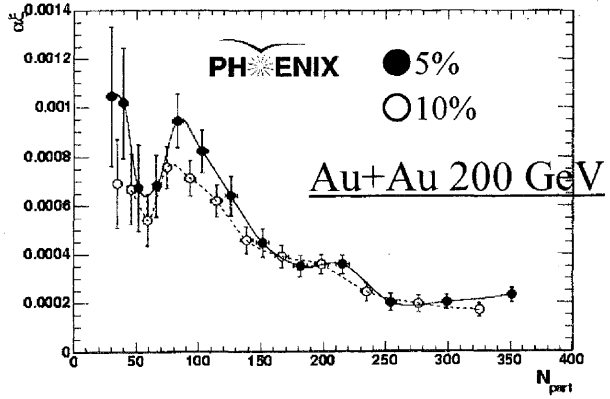

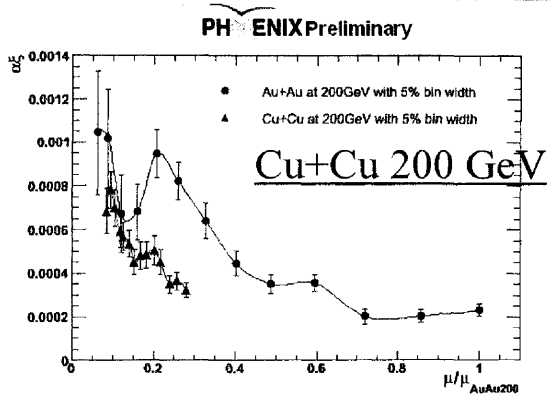

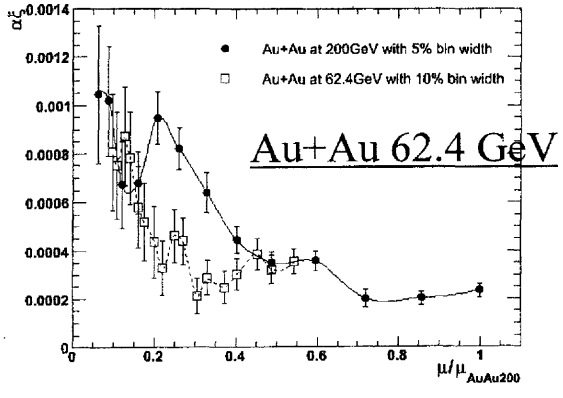

α: correlation strength
ξ: correlation length
β: rapidity independent correlation

$$\alpha\xi = \chi_{k=0} T / \bar{\rho}_1^{\,2} \propto \bar{\rho}_1^{\,-2} \frac{T}{|T - T_C|}$$

Summary

- **The multiplicity fluctuations** have been measured for all available datasets. It may be related the isothermal compressibility in grand canonical ensemble but no critical behavior was seen as a function of the centrality.
- **The longitudinal density correlations** have been measured via the functional form for pseudorapidity density fluctuations derived in the Ginzburg-Landau thermodynaical theory. The functional form can reasonably fit NBD k parameters as a function of pseudorapidity window sizes $\delta\eta$ not only for Au+Au 200 GeV but also for Cu+Cu 200 GeV and Au+Au 62.4 GeV.
- **The $\alpha\xi$ product** in the correlation function, which is monotonically related to susceptibility $\chi_{k=0}$ of the system, have been measured as a function of the number of participant nucleons N_{part}. No critical behavior was seen without any physical assumptions at the present precision.
- **A possible indication** of a local maximum is seen at $N_{part} \sim 90$ [$\varepsilon_{Bj}\tau \sim 2.4\text{GeV}/(\text{fm}^{-2}\text{c})$] as compared to the power law baseline only for the Au+Au 200GeV dataset. This might be a hint to search for the critical behavior at the QCD phase transition.
- **PHENIX** carries on to survey the multiplicity fluctuations for further different collision systems (5, 7, 39 GeV). Now we are taking the data at RHIC Run10.

v_2 Cumulant Measurements and Eccentricity Fluctuations for the STAR Collaboration

Paul Sorensen
for the STAR Collaboration

BROOKHAVEN NATIONAL LABORATORY

The 2- and 4-particle v_2 cumulants have been measured for Au+Au and Cu+Cu collisions at 62.4 and 200 GeV

We used the difference $v_2^2\{2\}-v_2^2\{4\}$ to test models of the initial eccentricity (the difference is a measurement not an error)

MCG models predict larger eccentricity fluctuations in central Au+Au collisions leaving little room for non-flow effects while the fKLN-CGC model is well within the range allowed by σ_{tot}

Above $dN/d\eta$~200, v_2 scales with fKLN-CGC eccentricity but not MCG-N eccentricity

STAR Data at 2 Energies and 2 Systems

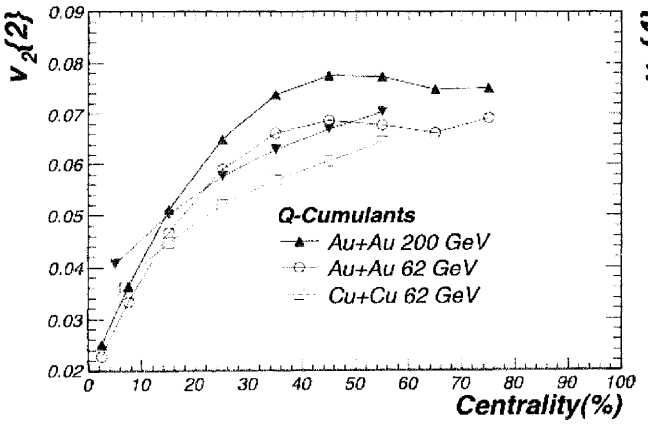

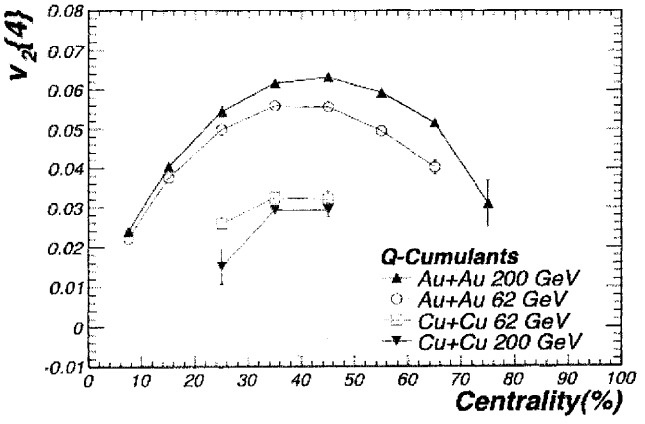

$v_2\{2\}$ and $v_2\{4\}$ have been measured by STAR for Au+Au and Cu+Cu collisions at 62.4 and 200 GeV

Direct Q-cumulant calculation is used Priv. Com.: Voloshin, Bilandzic, Snellings

We will study $\sigma_{tot}^2 = v_2\{2\}^2 - v_2\{4\}^2$

The total width $\sigma_{tot}^2 = v_2\{2\}^2 - v_2\{4\}^2$

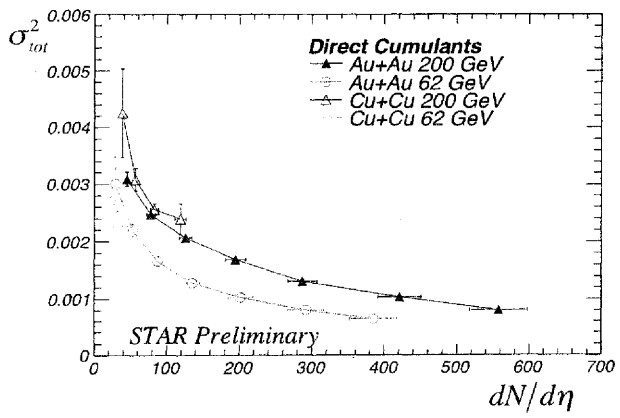

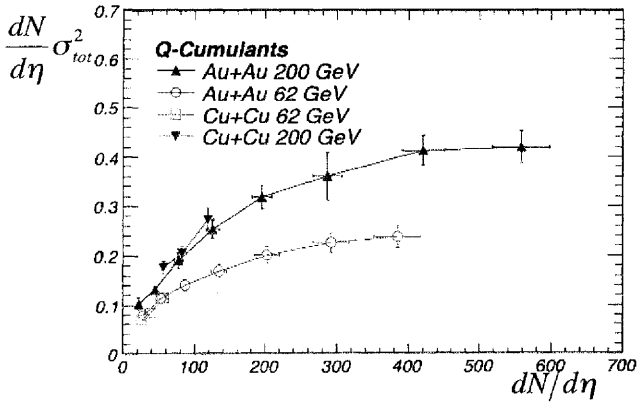

Width falls with multiplicity but deviates from the 1/N expected for dilution of correlations with increased combinatorics

Width scales smoothly from Cu+Cu to Au+Au when plotted vs dN/dη

Width scaled by dN/dη increases with centrality (violating a simple linear superposition model for correlations).

Comparison of models to σ_{tot}

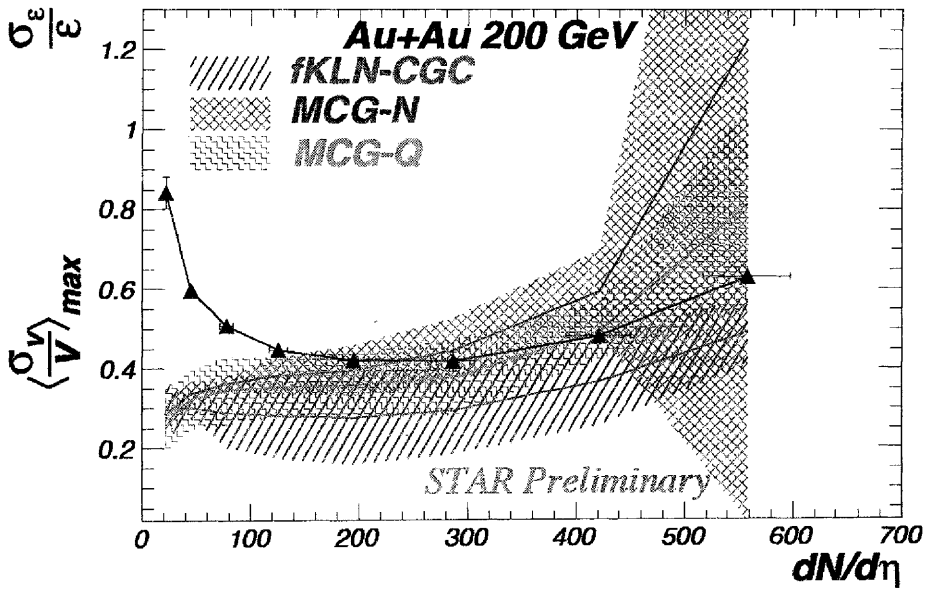

For central 200 GeV Au+Au collisions, the width expected from MCG-N eccentricity fluctuations nearly exceeds the total width of data

MCG-Q and fKLN-CGC remain smaller and consistent with $\delta_2>0$

The remaining width

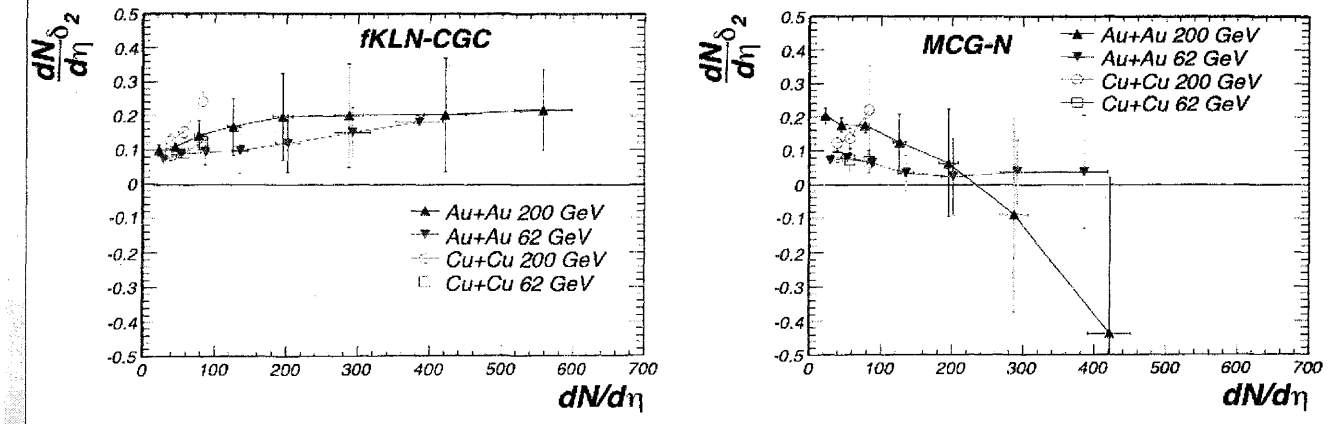

errors dominated by model calculations

fKLN-CGC $\sigma_\varepsilon/\varepsilon$ leaves room for increasing δ_2 with centrality:

σ_ε and ε calculations can be supplemented with predictions for δ_2 to check for consistency

v_2/ε Scaling

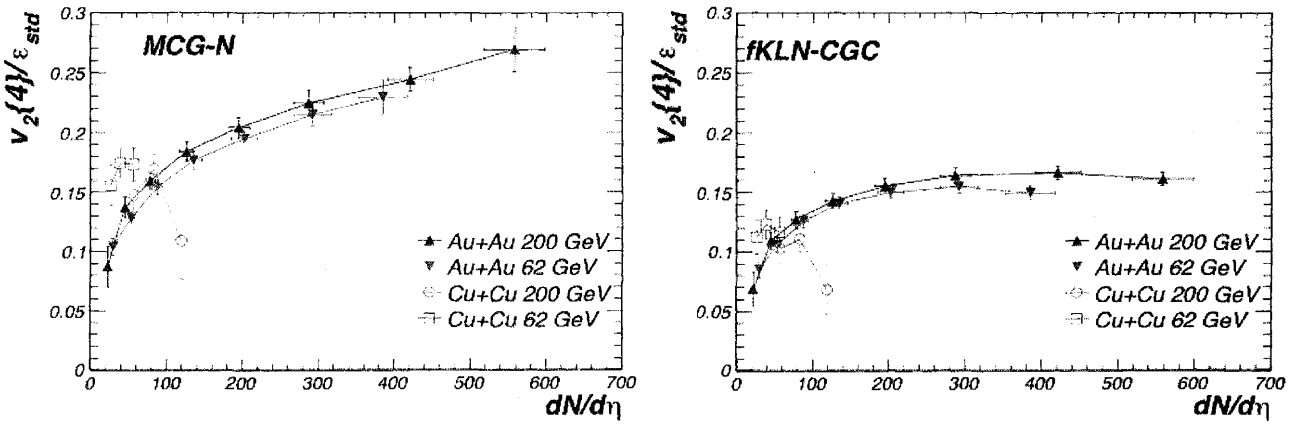

For the MCG-N model, v_2/ε rises continuously

No indication of a saturation at a hydro-limit

For the fKLN-CGC model, v_2/ε rises then saturates

For $dN_{ch}/d\eta > 250$, v_2 scales with ε

Limiting fragmentation in hadronic collisions

Anna Stasto
Penn State University & RBRC & INP Kraków

May 11, 2010

I discuss the limiting fragmentation phenomenon in the collisions of two hadrons at high energy. After a brief motivation and discussion of the original idea by Benecke et al, I present a microscopic derivation of the limiting fragmentation within the Color Glass Condensate model. The theoretical calculations are shown to describe the experimental data on rapidity distributions from RHIC quite well both in proton-proton collisions and in nucleus - nucleus collisions. I present the extrapolations for the LHC and discuss the limitations and possible issues at higher energies.

Hypothesis of limiting fragmentation

Benecke, Chou, Yang, Yen:

- For very high energy collisions in the lab system (target at rest) or a projectile system (projectile at rest) some of the outgoing particles approach *limiting distributions*.
- The limiting distributions represent the broken-up fragments of the target. The fragments of the projectile move with increasing velocity as $\sqrt{s} \to \infty$ (in the lab frame) and do not contribute to the limiting fragmentation. To study these fragments one has to go to the projectile system.
- In the laboratory frame the incoming particle is a Lorentz contracted system which passes through the target. The excitation of the target may cause a break up of the target.

Qualitative analysis

When $x_1 \gg x_2$ (or $x_2 \gg x_1$) we have separation of integrals in k_T space:

$$\frac{dN}{dy} \sim \int \frac{d^2 p_T}{p_T^2} \phi_B(x_2, |p_T|) \int d^2 k_T \, \phi_A(x_1, |k_T|)$$

- Integral over projectile density constant: $\int \frac{d^2 p_T}{p_T^2} \phi_B(x_2, |p_T|) = const.$
- Integral over target density:

$$\boxed{\int^{Q_s(x_2)} d^2 k_T \, \phi_A(x_1, |k_T|) = x_1 f(x_1, Q_s(x_2))}$$

Integrated parton density at large values of x_1:

$$\boxed{x_1 f(x_1, Q_s(x_2)) = x_1 f(x_1)}$$

shows x_1 (Bjorken) scaling.

Proton-antiproton and AuAu(central) collisions

Gelis, Venugopalan, A.S.

proton-proton:

Gold-Gold central:

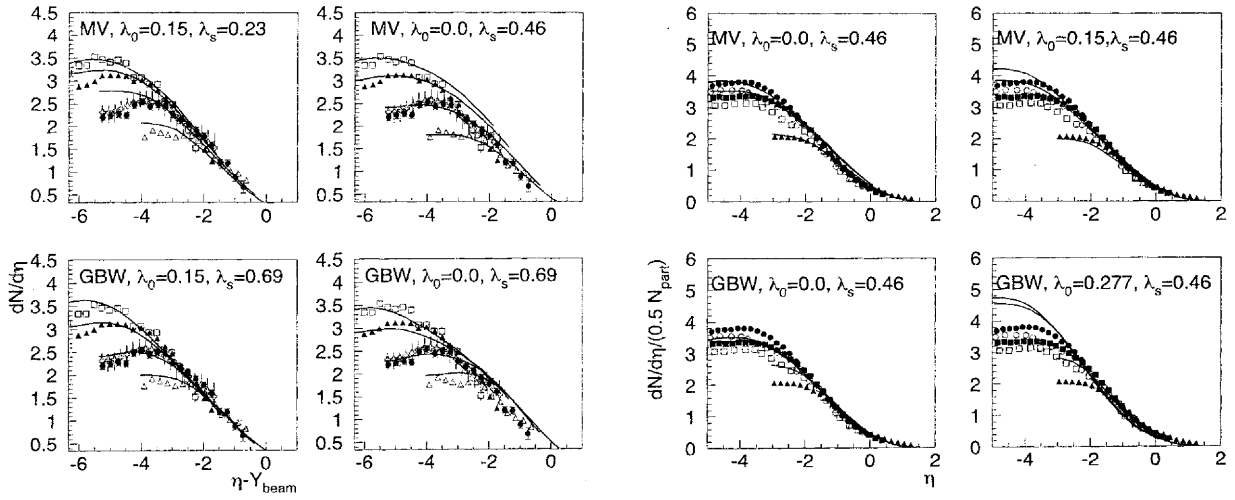

- Small violations of limiting fragmentation scaling due to the fact that in some models we do not have approximately scaling of $x_1 f(x_1)$.
- Additional uncertaintes due to $y \leftrightarrow \eta$ change and fragmentation functions.

Extrapolation to LHC

pp collisions:

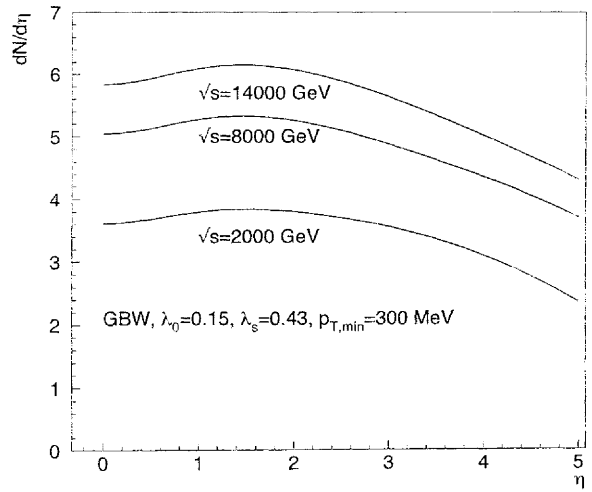

AuAu central collisions:

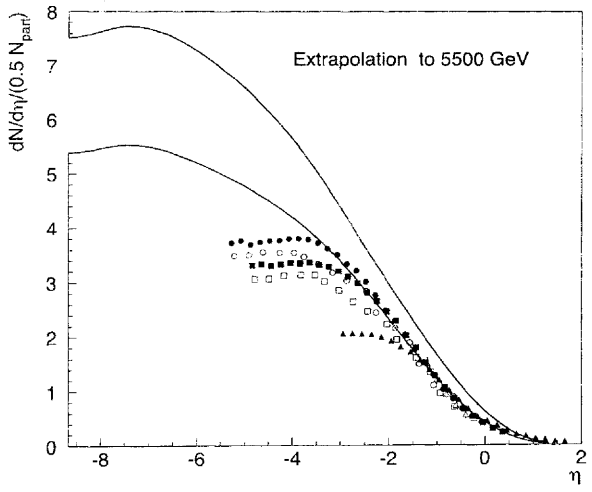

Still there are many parameters: a lot of uncertainty in the predictions. Some models give violations of limiting fragmentation. For example McLerran-Venugopalan input $\phi_A(x_1, k_T)$ at large x_1 has too large tail in k_T.

Limiting fragmentation scaling is related to x_1 scaling at large x_1.

Conclusions:

- Factorization of parton distributions in target and projectile at large rapidities.
- The multiplicity distribution is directly proportional to the parton density in the target (i.e. gluon and quark density at large x) which is independent of the scales in the process, and consequently of the total c.m.s energy in the process.
- These models imply that the limiting fragmentation arises because the rapidity distribution of the produced particles is determined early in the scattering process, essentially by the form of the initial states.
- Caution: model has a lot of assumptions (factorization, extrapolation into soft region, parton-hadron duality, relatively large number of free parameters)
- Outlook: do we have limiting fragmentation at $7\ \mathrm{TeV}$ at LHC? Where does it break down?

Initial Conditions and Global Event Properties

Adrian Dumitru

RIKEN-BNL and Baruch College/CUNY

- non-trivial QCD dynamics determines initial conditions for hydro:
  - v_2/ε versus centrality (deviation from conform.)
  - R^Q_{AA}
- initial state also seen via "topological structures" / flux tubes / long-range correl. which survive hydro evolution
  - confirmation from pp @ LHC would improve our understanding

Inclusive gluon production

K_t-factorization:

$$\frac{dN}{d^2r_t dy} \sim \int \frac{d^2p_t}{p_t^2} \int d^2k_t \; \alpha_s \, \phi_A(x_1, k_t^2) \; \phi_B(x_2, (p_t - k_t)^2)$$

Kharzeev, Levin, Nardi model:

$$\phi(x, k_t^2; \vec{r}_t) \sim \frac{1}{\alpha_s(Q_s^2)} \frac{Q_s^2(x, \vec{r}_t)}{max(Q_s^2, k_T^2)}$$

$$Q_s^2 \sim \rho_{\mathrm{part}} \, x^{-\lambda}$$

Fluctuations of nucleons ("light-cone sources")

important for

- central / peripheral Au+Au
- smaller systems (Cu+Cu)
- fluctuations of v_2

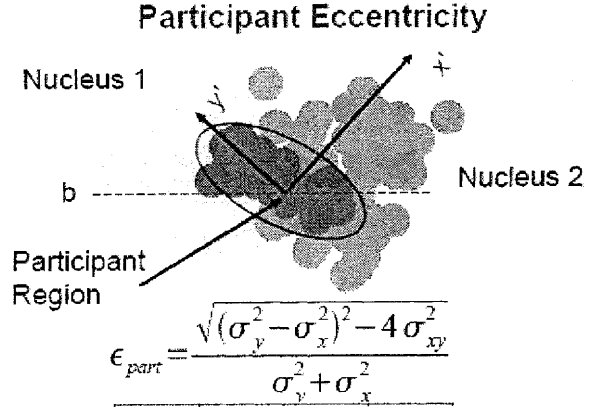

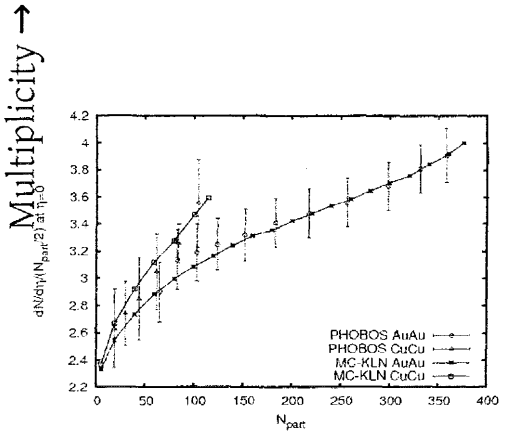

Centrality →

Very good fit, both Au+Au and Cu+Cu pretty much down to pp (too good, actually...)

Drescher and Nara: nucl-th/0611017

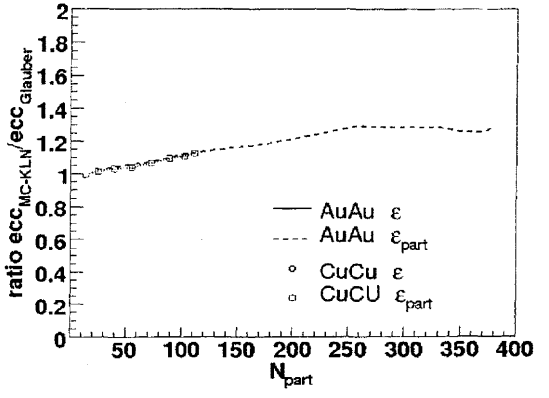

ε ~ 25-30% higher, comp. to dissip. correction

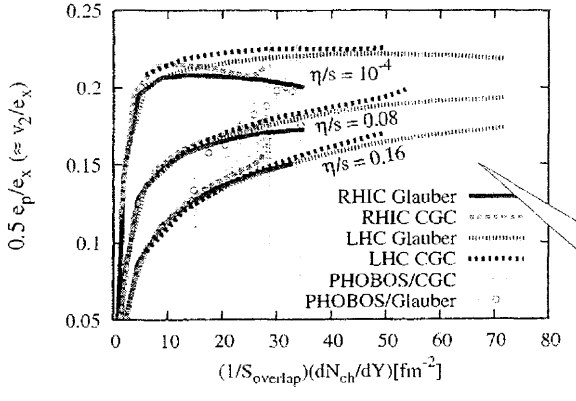

broken by λ/R, T_{fo}/T_i, T_c/T_i, ...

should be flat in conformal limit !

Luzum, Romatschke: arXiv:0901.4588

Noronha, Gyulassy, Torrieri arXiv:0906.4099

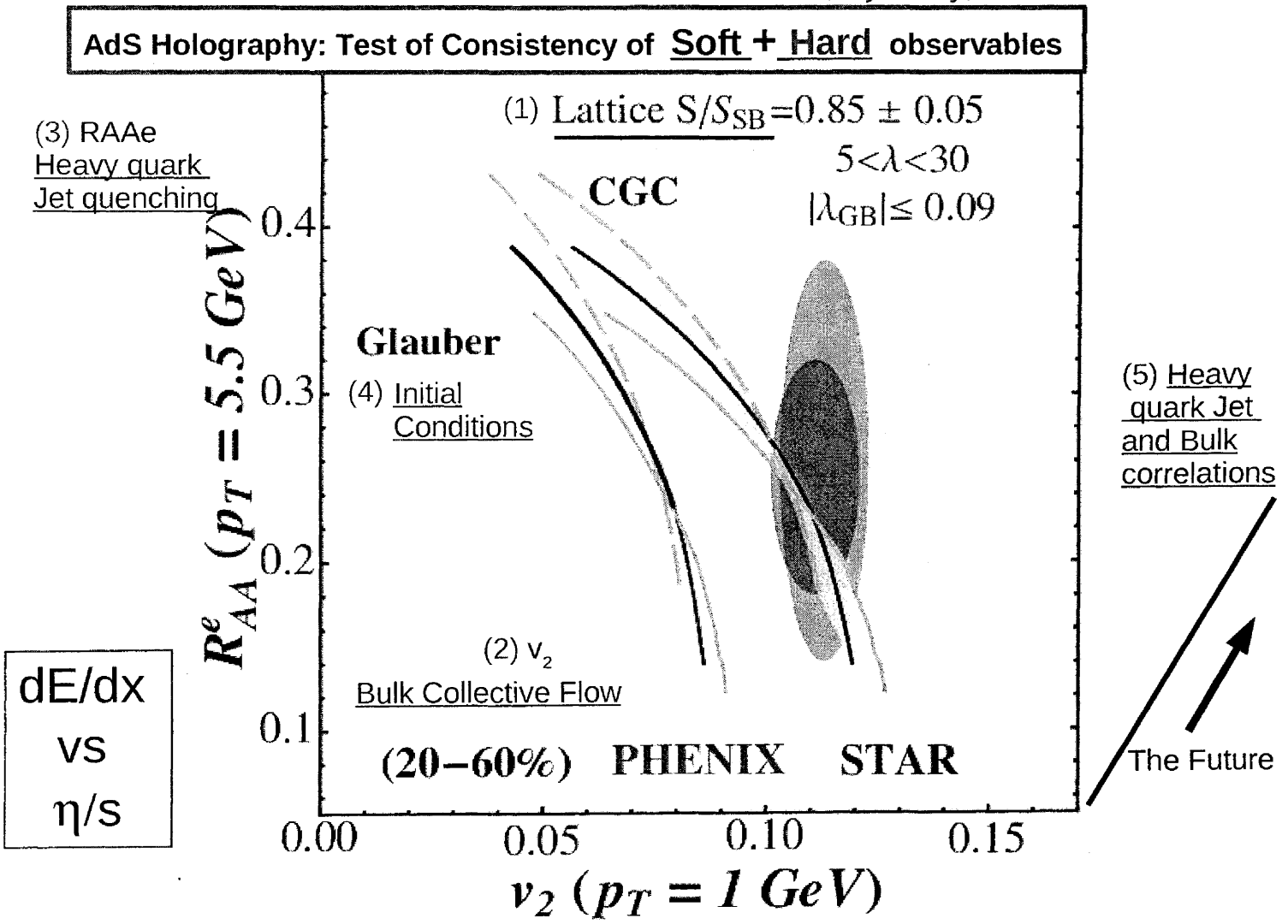

exciting discovery by STAR: long-range rapidity correlations at RHIC !

STAR (arXiv:0909.0191)

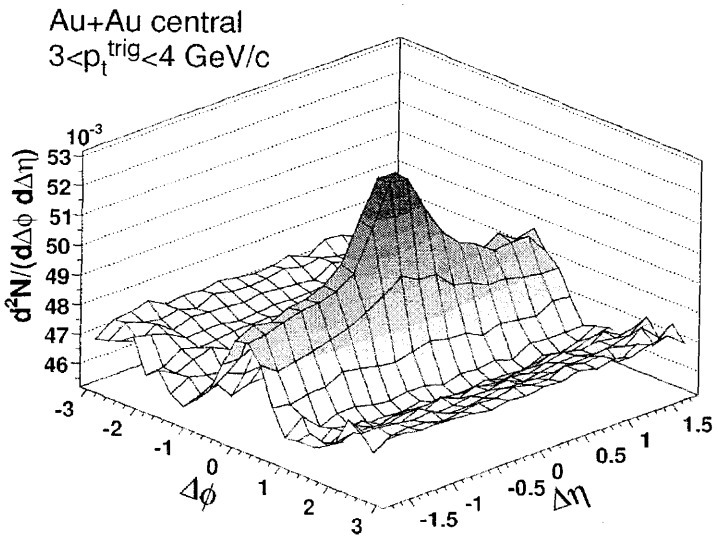

EPOS string model

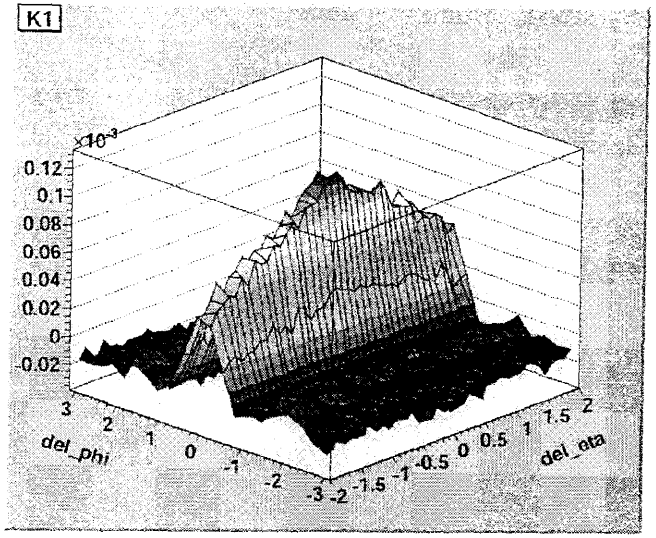

K. Werner et al, arXiv:1004.0805

But, two-particle production diagrams Nc-suppressed:

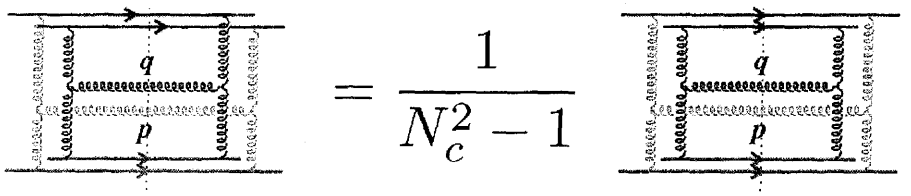

$$= \frac{1}{N_c^2 - 1}$$

A.D., Gelis, McLerran, Venugopalan: 0804.3858

genuine B-JIMWLK terms from THIS diagram:

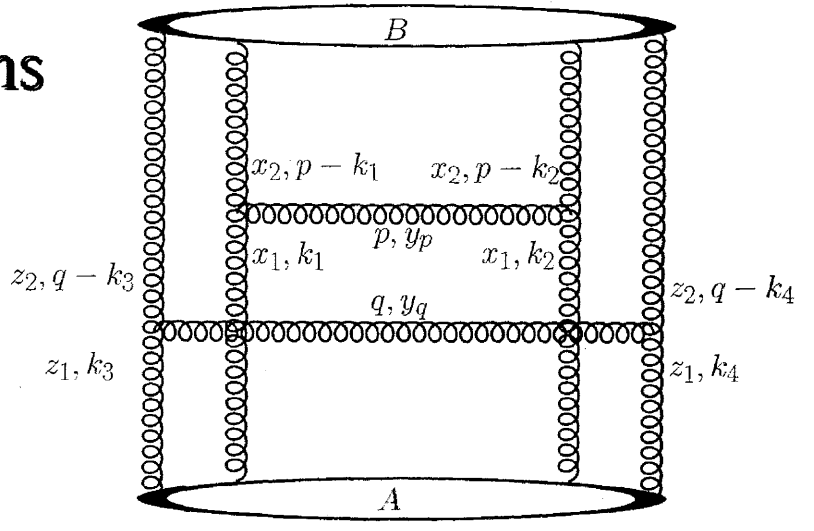

B-JIMWLK four-point function (in Gaussian approximation), incl. "Nc corrections":

$$\left\langle \rho^a \rho^b \rho^c \rho^d \right\rangle = \delta^{ab}\delta^{cd} \left\langle \rho^2 \right\rangle^2 + \frac{1}{N_c} f^{abe} f^{cde} \mathcal{F}(k_i) \left\langle \rho^2 \right\rangle^2 + \cdots$$

A.D., J. Jalilian-Marian, arXiv:1001.4820

★ **ridge in pp (or very periph. AA) @ LHC ?!**

Anomalous Transport Processes in Turbulent Nonabelian Plasmas

Masayuki Asakawa,[1] Steffen A. Bass,[2] and Berndt Müller[2,3]

[1]*Department of Physics, Osaka University, Toyonaka 560-0043, Japan*
[2]*Department of Physics, Duke University, Durham, NC 27708, USA*
[3]*Center for Theoretical & Mathematical Sciences, Duke University, Durham, NC 27708, USA*

Turbulent color fields, which can arise in the early and late stages of relativistic heavy ion collisions, may contribute significantly to the transport processes in the matter created in these collisions. We review the theory of these *anomalous* transport processes and discuss their possible phenomenology in the glasma and quasi-stationary expanding quark-gluon plasma.

The theory of perturbative saturation of strong glue fields (the "color glass condensate") in fast moving nuclei provides compelling reasons to believe that the pre-equilibrium stage of nuclear collisions at high energy is governed by the nonlinear dynamics of color fields at moderate coupling $\alpha_s(Q_s^2)$, where $Q_s \sim 1 - 2$ GeV is the nuclear saturation scale [1]. Recent improved simulations of lattice QCD have also shown strong evidence that QCD matter at thermal equilibrium (the quark-gluon plasma) has a quasiparticle structure at temperatures as low as 250 MeV [2]. This suggests that the matter created in heavy ion collisions at top RHIC energy is not as strongly coupled as many aspects of the phenomenology of these reactions (the near maximal elliptic flow and the strong jet quenching) indicate [3].

It is thus worthwhile asking the questions whether the extreme opaqueness of the quark-gluon plasma observed in the RHIC experiments can be explained without invoking a super-strong coupling? In this lecture, we argue that the answer may lie in the peculiar transport properties of turbulent (nonabelian) plasmas.

- The term *plasma turbulence* describes a random, non-thermal pattern of excitation of coherent field modes in a plasma with a power spectrum similar to the that of vorticities in a turbulent fluid: the phenomenon is often caused by plasma instabilities.
- Strong color fields in the early *glasma* are known to exhibit chromo-electric (Sauter-type) and chromo-magnetic (Nielsen-Olesen-type) instabilities that create turbulent color fields.
- Weibel-type instabilities arise naturally in expanding near-equilibrium plasmas with an anisotropic momentum distribution and have been shown to exhibit a power-law spectrum.

As we have shown [4, 5], soft color fields generate anomalous transport coefficients which may dominate the transport properties of the plasma at weak and moderately weak coupling. The two most relevant transport coefficients are the shear viscosity η and the jet quenching parameter $\hat{q}$. The latter is proportional to the mean squared momentum per unit length imparted by the turbulent fields on an energetic parton; the former is inversely proportional to the same quantity (for partons of "average" momentum). In a quasi-thermal medium, this results in the relationship $\eta/s \approx T^3/\hat{q}$ [6].

For an expanding equilibrated quark-gluon plasma, the anomalous shear viscosity can be shown to dominate over the collisional shear viscosity in the weak coupling limit, for a fixed velocity gradient. The absolute values are not known, because the momentum diffusion constant

$$D_{ij}(\mathbf{v};\mathbf{r},t) = \int_{-\infty}^{t} dt' \, \langle F_i(\mathbf{r}(t'),t') F_j(\mathbf{r},t) \rangle \qquad (1)$$

has not been numerically evaluated as a function of the momentum anisotropy of the turbulent plasma. In the *glasma* phase, the jet quenching parameter is of order

$$\hat{q}(\tau) \approx \frac{Q_s^3}{Q_s \tau} \approx \frac{10 \text{ GeV}^2/\text{fm}}{Q_s \tau}, \qquad (2)$$

which is in reasonable agreement with experimentally deduced values of $\hat{q}$ extrapolated to early times. More accurate determinations of the momentum diffusion constant in the glasma phase by numerical simulations of the nonlinear color field dynamics [7, 8] would be of interest.

[1] L. McLerran, arXiv:0812.4989 [hep-ph].
[2] M. Cheng *et al.*, Phys. Rev. D **81**, 054504 (2010) [arXiv:0911.2215].
[3] M. Gyulassy and L. McLerran, Nucl. Phys. A **750**, 30 (2005) [arXiv:nucl-th/0405013].
[4] M. Asakawa, S. A. Bass and B. Müller, Phys. Rev. Lett. **96**, 252301 (2006) [arXiv:hep-ph/0603092].
[5] M. Asakawa, S. A. Bass and B. Müller, Prog. Theor. Phys. **116**, 725 (2007) [arXiv:hep-ph/0608270].
[6] A. Majumder, B. Müller and X. N. Wang, Phys. Rev. Lett. **99**, 192301 (2007) [arXiv:hep-ph/0703082].
[7] A. Krasnitz, Y. Nara and R. Venugopalan, Phys. Rev. Lett. **87**, 192302 (2001) [arXiv:hep-ph/0108092].
[8] T. Lappi, Phys. Rev. C **67**, 054903 (2003) [arXiv:hep-ph/0303076].

Anomalous viscosity

Classical expression for shear viscosity:

$$\eta \approx \tfrac{1}{3} n \bar{p} \lambda_f$$

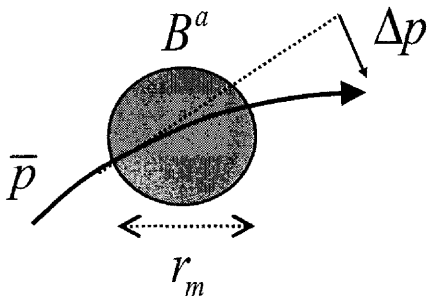

Momentum change in one coherent domain:

$$\Delta p \approx g Q^a B^a r_m$$

Anomalous mean free path in medium:

$$\lambda_f^{(A)} \approx r_m \left\langle \frac{\bar{p}^2}{(\Delta p)^2} \right\rangle \approx \frac{\bar{p}^2}{g^2 Q^2 \langle B^2 \rangle r_m}$$

Anomalous viscosity due to random color fields:

$$\eta_A \approx \frac{n\bar{p}^3}{3 g^2 Q^2 \langle B^2 \rangle r_m} \approx \frac{\frac{9}{4} s T^3}{g^2 Q^2 \langle B^2 \rangle r_m}$$

Anomalous q-hat

Jet quenching parameter:

$$\hat{q} = \frac{\left\langle \Delta p_T^2 (L) \right\rangle}{L}$$

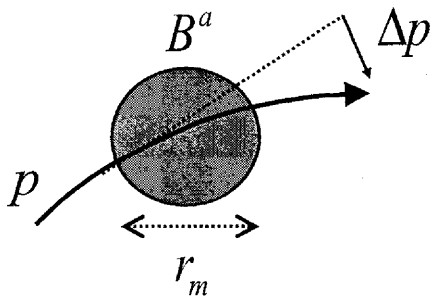

Momentum change in one coherent domain:

$$\Delta p_T = g Q^a B_\perp^a r_m$$

Anomalous jet quenching parameter:

$$\hat{q}_A = \frac{\left\langle \Delta p_T^2 \right\rangle}{r_m} = g^2 Q^2 \left\langle B_\perp^2 \right\rangle r_m$$

Relation to anomalous shear viscosity:

$$\frac{\eta_A}{s} \approx \frac{T^3}{\hat{q}_A}$$

Special case of general relation between η/s and q^ (A. Majumder, BM & Wang, PRL 99, 192301 ('07).

Turbulence ⇔ p-Diffusion

Vlasov-Boltzmann transport of thermal partons:

$$\left[\frac{\partial}{\partial t}+\frac{p}{E_p}\cdot\nabla_r+F\cdot\nabla_p\right]f(r,p,t)=C[f]$$

with Lorentz force

$$F=gQ^a\left(E^a+\mathrm{v}\times B^a\right)$$

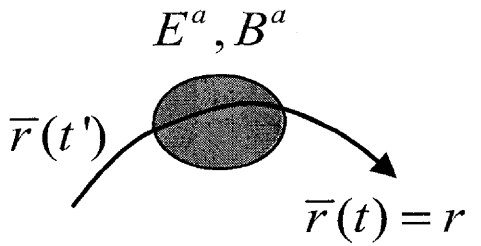

Assuming E, B random $\Rightarrow$ Fokker-Planck eq:

$$\left[\frac{\partial}{\partial t}+\frac{p}{E_p}\cdot\nabla_r-\nabla_p\cdot D(p)\cdot\nabla_p\right]\bar{f}(r,p,t)=C\left[\bar{f}\right]$$

with diffusion coefficient

$$D_{ij}(p)=\int_{-\infty}^{t}dt'\left\langle F_i\left(\bar{r}(t'),t'\right)F_j\left(r,t\right)\right\rangle.$$

Diffusion is dominated by chromo-magnetic fields:

$$\int dt'\left\langle B(t')B(t)\right\rangle\equiv\left\langle B^2\right\rangle\tau_m$$

Weibel regime

Take moments of $\left[\frac{\partial}{\partial t}+\frac{p}{E_p}\cdot\nabla_r-\nabla_p\cdot D(p)\cdot\nabla_p\right]\bar{f}(r,p,t)=C\left[\bar{f}\right]$ with p_z^2

$$\frac{1}{\eta}=O(1)\frac{N_c}{N_c^2-1}\frac{g^2\left\langle B^2\right\rangle\tau_m}{sT^3}+O\left(10^{-2}\right)\frac{g^4\ln g^{-1}}{T^3}\equiv\frac{1}{\eta_A}+\frac{1}{\eta_C}$$

Self-consistency ⟹ $\frac{\eta_A}{s}\sim\left(\frac{T}{g^3|\nabla u|}\right)^{1/2}$ compare with $\frac{\eta_C}{s}\sim\frac{1}{g^4\ln g^{-1}}$

Anomalous shear viscosity dominates over *collisional shear viscosity* at fixed ∇u in the limit $g \to 0$.

Glasma regime

In the *glasma*, most of the energy density is in the form of *color fields*:

Anomalous transport dominates over Boltzmann (collision) transport.

$$\eta_A \approx \frac{N_c^2-1}{15\pi^2 C_2 g^2 \left\langle \mathcal{E}^2+\mathcal{B}^2 \right\rangle \tau_m} \int_0^\infty dp\, p^5 f(p) \approx \frac{\left(N_c^2-1\right)Q_s^2}{C_2 g^2 \tau_m} \cdot \frac{\varepsilon_{\text{part}}}{\varepsilon_{\text{field}}}$$

Anomalous jet quenching:

$$\hat{q}_A \approx \frac{C_2 g^2 \left\langle \mathcal{E}^2+\mathcal{B}^2 \right\rangle \tau_m}{N_c^2-1} \approx \frac{g^2 \varepsilon_{\text{field}}}{Q_s} \approx \frac{Q_s^3}{(Q_s\tau)} \approx \frac{10\ \text{GeV}^2/\text{fm}}{Q_s\tau}$$

In line with estimates of q^ ~ 2 - 4 GeV^2/fm from fits to data.

Hydrodynamics: Fluctuating Initial Conditions and Two Particle Correlations

R.P.G.Andrade[1], F.Grassi[1], Y.Hama[1], W.L.Qian[1]

[1] Instituto de Física, Universidade de São Paulo, Brazil

Saturation-CGC-Glasma Workshop

Summary

- Hydrodynamics with tubular initial conditions predicts two-particle correlations in qualitative agreement with data.
- Near-side and away-side structures are related to "two horn" emission from each tube.
- Possible test: 2+1 correlation in $\Delta\phi_2$-$\Delta\eta_2$ with the restriction $\Delta\phi_1 \sim 2$.

Hydrodynamics with fluctuating initial conditions: differences between models and references on two particle correlations

- SPheRIO group: NeXus initial conditions+ ideal (SPH) hydro
  Phys. Rev. Lett. 103, 242301 (2009), arXiv:0911.0811 and 0912.0703
- H.Petersen/M.Bleicher et al.: UrQMD initial conditions+ ideal (grid) hydro
  only midrapidity variables at RHIC (private communication)
- EPOS initial conditions+ ideal (grid) hydro
  K.Werner et al. ArXiv:1004.0805

NeXSPheRIO: dihadron $\Delta\eta - \Delta\phi$ correlations

- Initial conditions have tubular structures,
- two particle correlations exhibit *near* and *away-side* ridges,
- double check: use of two different methods for v_2 subtraction (ZYAM+ event plane alignment).

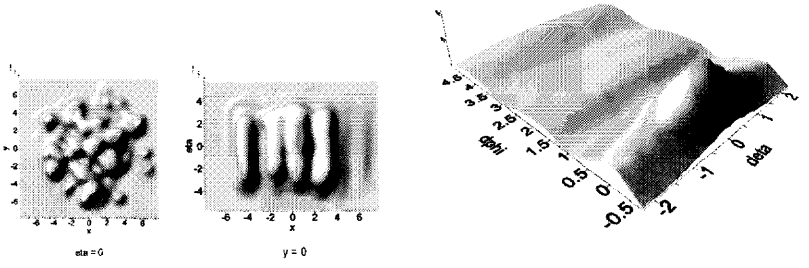

NeXSPheRIO central collisions Au+Au at 200 GeV A (2.5 GeV $\times$ 1.5 GeV).

One tube model

MAIN RESULT: single particle angular distribution has TWO PEAKS separated by $\Delta phi \sim 2$

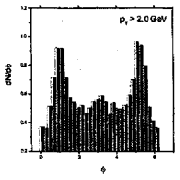

CONSEQUENCE: two particle angular distribution has three peaks

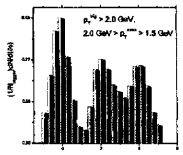

Three particle correlations in $\Delta\phi_1 = \phi_1 - \phi_t$ and $\Delta\phi_2 = \phi_2 - \phi_t$ (in progress)

Data by STAR (PRL 102(2009) 052302) and PHENIX (NPA783 (2007) 519).

- Theory: one tube prediction is clean "no off diagonal peaks" (left fig.)
- Practice: "off diagonal peaks" present
  - ▷ one tube RAW result (center fig.) (correlation peak/bkgd)
  - ▷ in NeXSPheRIO result w/subtraction (right fig.)

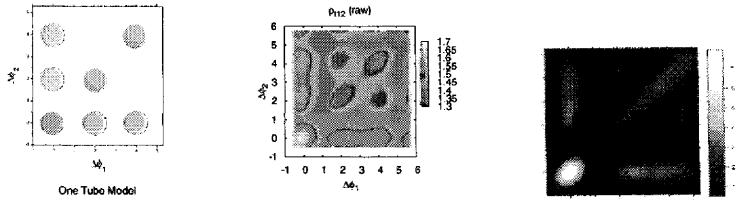

Other models: Mach cone (Renk & Ruppert PRC76 (2007) 014908), AMPT (G.L.Ma et al. PLB647 (2006) 122), etc, have similar "off diagonal" predictions.

Lanny Ray
The University of Texas at Austin
Austin, Texas

The Ridge(s) in STAR

Saturation, the CGC and Glasma Workshop, BNL May 10-12, 2010

Extended two-particle correlations on relative pseudorapidity (η) and at small relative azimuthal angle (ϕ), the so-called *ridge*, have been observed by the STAR experiment in Au-Au and Cu-Cu collisions at 62 and 200 GeV using tagged ("trigger") – associated particle pairs and using all particle pairs, i.e. no trigger particle. A unified view of the various correlation analyses is afforded by considering where the selected particles are in 2D transverse momentum space. The 2D relative η,ϕ correlations using all particles with $p_t > 0.15$ GeV/c show that the same-side amplitude and η elongation display an unexpected centrality trend which exceeds binary scaling expectations and which appears to begin at a common initial state condition based on the initial overlap density and effective cross section. An equally significant away-side ridge exists which follows the same-side ridge amplitude and which exceeds that expected from global p_t conservation. Analysis of the p_t dependence indicates that the η elongated ridge diminishes above about 4 GeV/c, above which the pQCD expected jet correlation peak becomes apparent. At the higher p_t range studied the ratio of jet-to-ridge yields is approximately independent of collision energy (62 and 200 GeV). A summary of the experimental constraints which theorists must keep in mind before offering explanations for these phenomena and some further theoretical implications of these data will be discussed.

200 GeV Au-Au data

Analyzed 1.2M minbias 200 GeV Au+Au events;
included all tracks with $p_t > 0.15$ GeV/c, $|\eta| < 1$, full φ

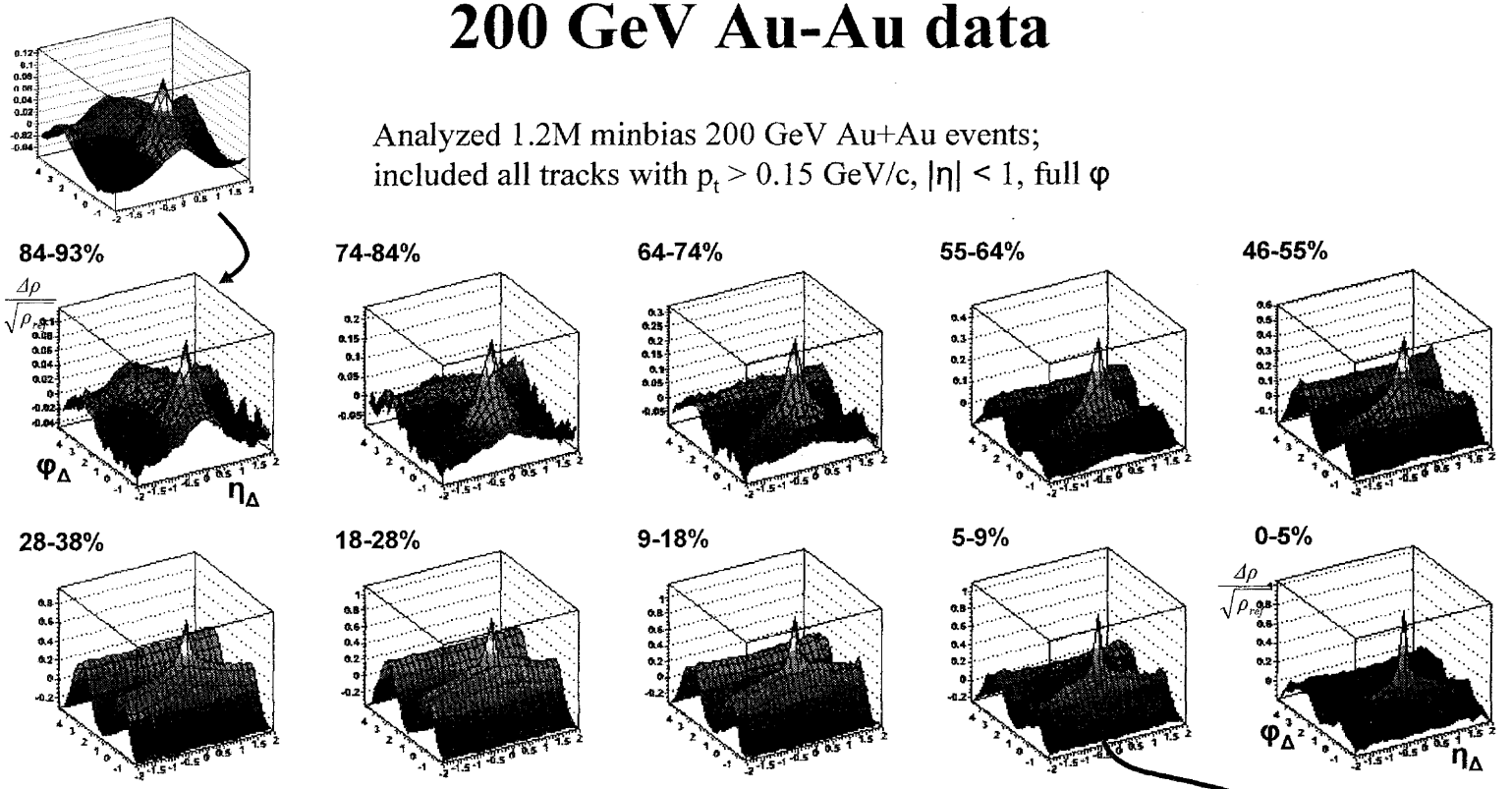

STAR Preliminary

We observe the evolution of several correlation structures including the same-side low p_t ridge

Similar analysis was done for minbias Au-Au at 62 GeV and Cu-Cu at 62 and 200 GeV

From M. Daugherity's Ph.D Thesis (2008)

Fits to 62 & 200 GeV Au-Au data

$$\frac{\Delta\rho}{\sqrt{\rho_{ref}}}$$

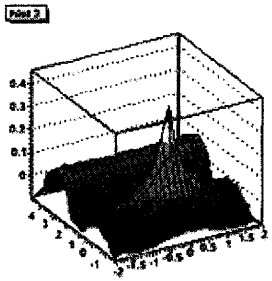

SS Peak Amplitude

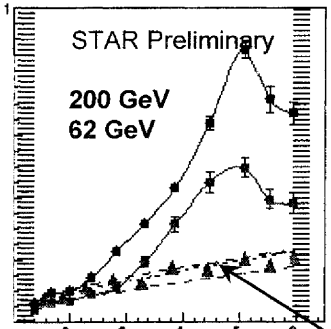

Peak η Width

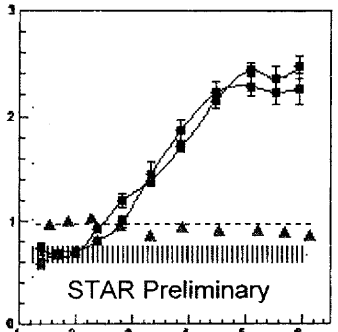

Peak φ Width

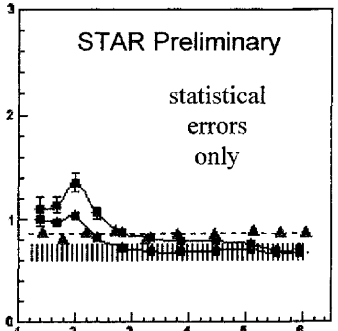

$$\nu \equiv \frac{\langle N_{bin} \rangle_{200GeV}}{\langle N_{part}/2 \rangle}$$

Up to 1/3 of multiplicity in central Au-Au associated with jet angular correlations

Dipole Amplitude

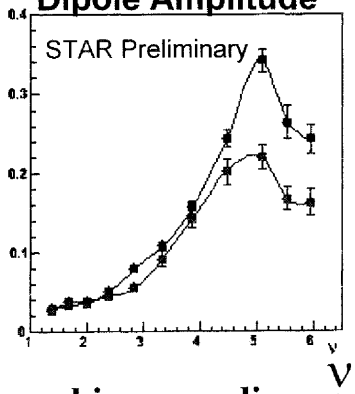

Binary scaling: Kharzeev and Nardi

$$\text{Amplitude} = A_{AA} \propto \frac{N_{bin}}{N_{chrg}}$$

HIJING 1.382 default parameters, 200 GeV, quench off

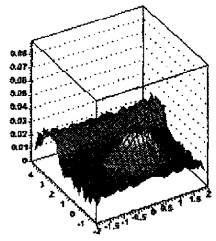

pQCD HIJING jets

Deviations from binary scaling represent new physics unique to heavy ion collisions; the departure from N-N superposition is referred to as a *transition* in the trends.

2D fit parameter evolution

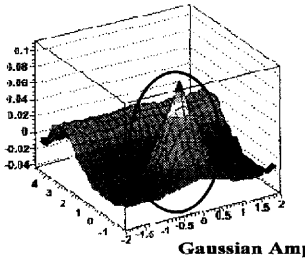

same-side jet peak parameters

200 GeV

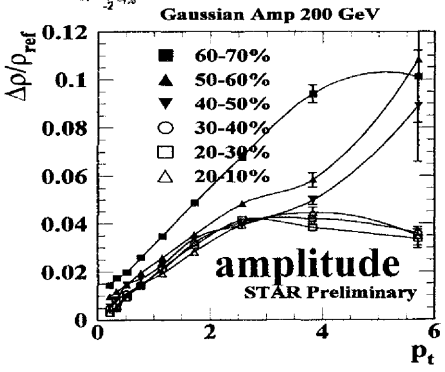

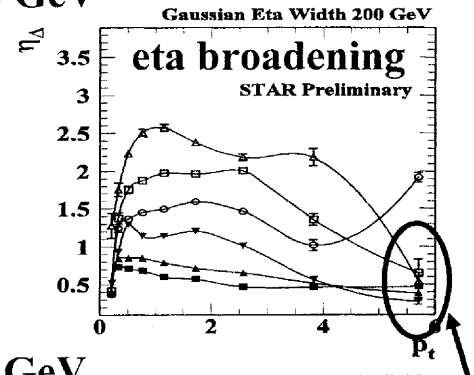

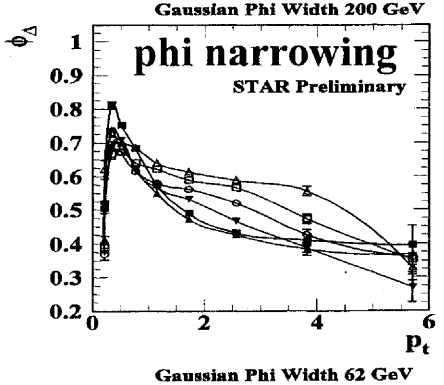

62 GeV

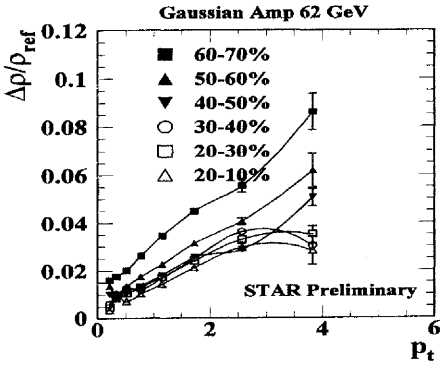

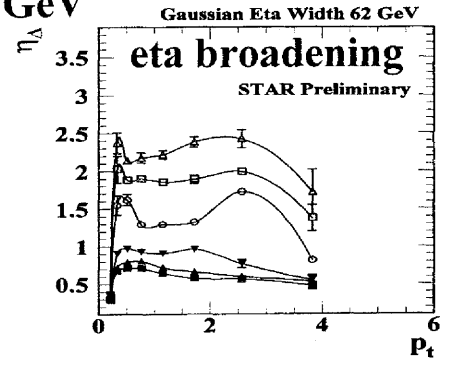

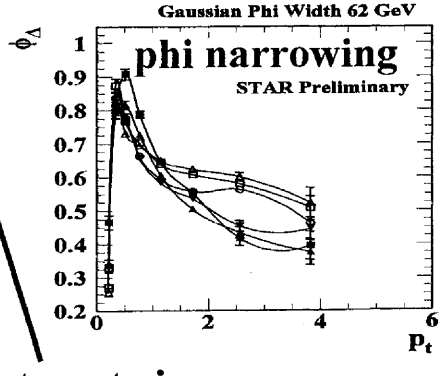

angular correlations: marginal on p_t or y_t

unexpected width evolution with centrality, p_t

return to in-vacuum jets above 4 GeV/c

Jet/Ridge 62 vs. 200 GeV in Au-Au, Cu-Cu

3.0 GeV/c < $p_T^{trigger}$ 6.0 GeV/c; 1.5 GeV/c < $p_T^{associated}$ < $p_T^{trigger}$

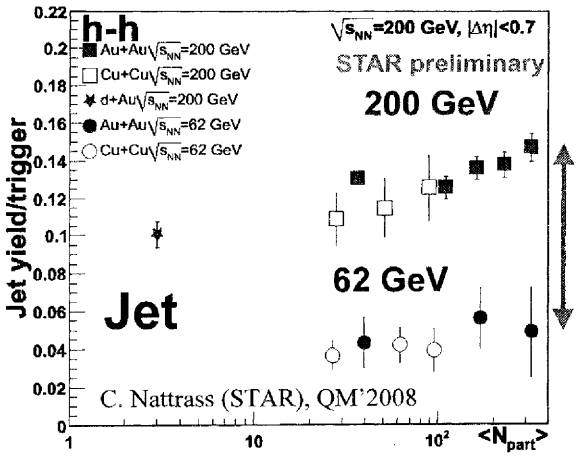

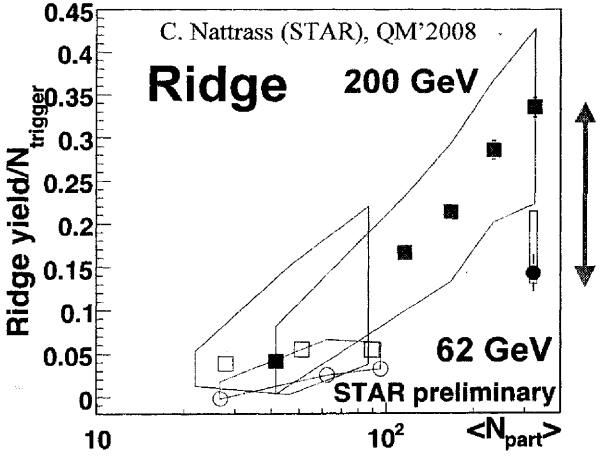

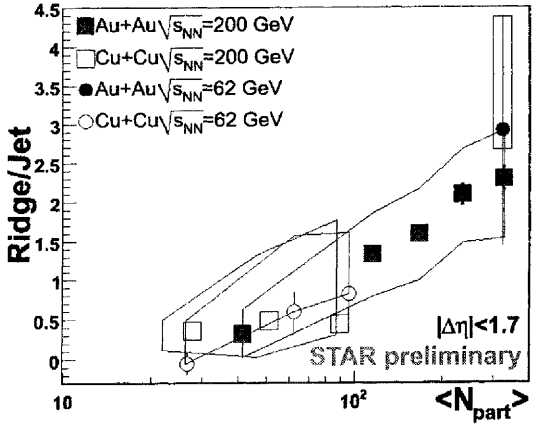

- Jet yield smaller at 62 GeV, consistent with pQCD
- Ridge/Jet ratio comparable in 62 and 200 GeV
  - ridge properties related to jet/pQCD?
- Are we seeing vacuum fragmentation after energy loss on the same-side in central Au-Au with the lost energy deposited in the ridge?

Theoretical models of same-side ridge - initial fluctuations + radial flow

- ***Voloshin***, Nucl. Phys. A**749**, 287c (2005); ***Shuryak***, Phys. Rev. C**76**, 047901 (2007) – beam-jet fragments pushed out by radial flow.
- ***Dumitru, Gelis, McLerran, Venugopalan***, arXiv:0804.3858[hep-ph] - glasma flux tubes pushed out by radial flow.

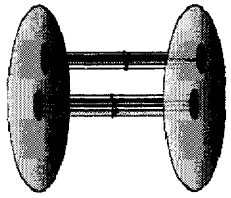

- ***S. Gavin***, Phys. Rev. Lett. **97**, 162302 (2006) – initial state energy fluctuations spread along η by shear viscosity; pushed out by radial flow.

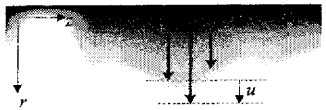

$u(z,t) \approx v_r - \langle v_r \rangle$

These fail to predict the growth of the away-side ridge.

Two-particle (yt1,yt2) correlations on <u>both</u> the same and away-sides?

Studying the Medium Response by Two Particle Correlations

John Chin-Hao Chen (for PHENIX Collaboration)
Department of Physics and Astronomy
Stony Brook University

We present two dimensional $\Delta\eta$-$\Delta\phi$ inclusive photon-charged hadron correlations measured by the PHENIX experiment. Jet-like correlations are modified in central Au+Au compared to p+p, in both the trigger jet and opposing jet. The trigger jet is elongated in pseudo-rapidity (the ``ridge''), while the opposing jet shows a double peak structure ("head" and ``shoulder''). We decompose the structures by fitting the $\Delta\eta$ and $\Delta\phi$ correlations to disentangle contributions from the medium and the punch-through and trigger jets. The ridge exists for associated particle pT below 3 GeV/c; it is broad in rapidity and narrow in $\Delta\phi$. The yield of the ridge closely resembles the shoulder in the centrality dependence of particle yield and spectra.

STONY BROOK UNIVERSITY PHENIX

2-D $\Delta\eta-\Delta\phi$ correlations

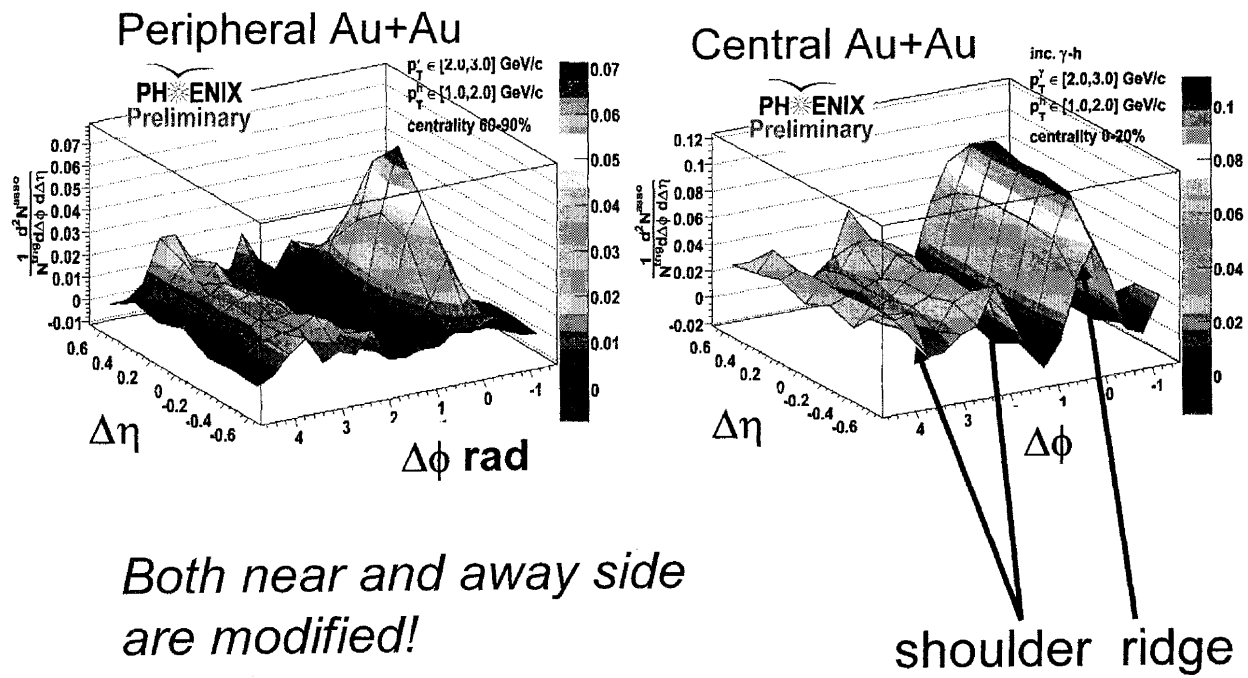

Both near and away side are modified!

Is Ridge similar to bulk?

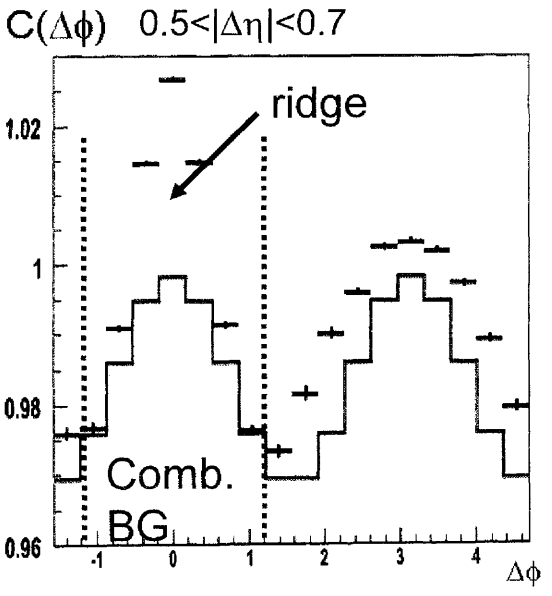

Ratio
= ridge /(Comb. BG. in nearside)

Ridge/background ratio

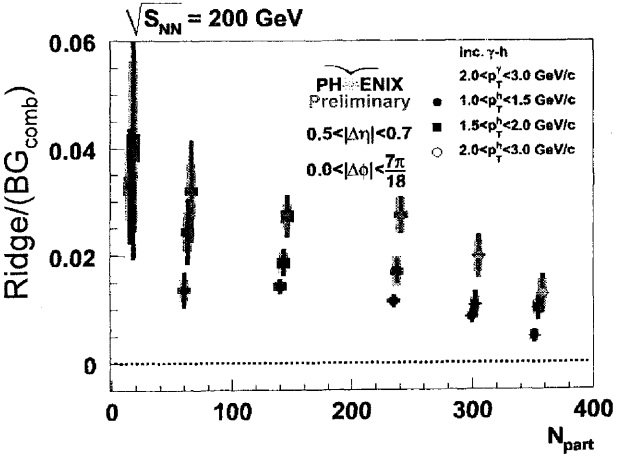

N_{part} ↑ , ratio ↓

Y_{ridge} changes from 3% to 1% of the bulk when increase N_{part}

Shoulder & ridge p_T spectra vs. p+p

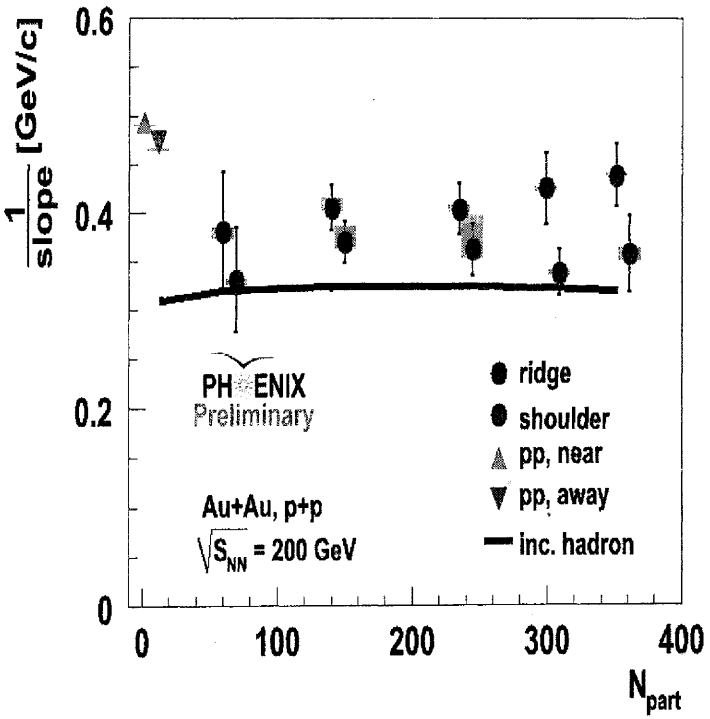

- Both are softer than hard scattering.
- Ridge harder than shoulder?
- Shoulder not quite as soft as inclusive hadrons

Where does the momentum go?

$$p_T \text{ ratio } (\Delta\eta) = \frac{p_T \text{ carried by awayside component per } \Delta\eta}{p_T \text{ carried by nearside component per } \Delta\eta}$$

awayside: head, shoulder, total awayside

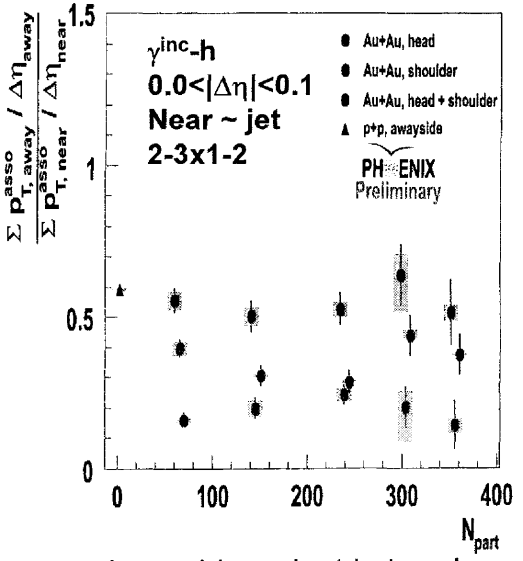

Awayside p_T lost in head is recovered in shoulder

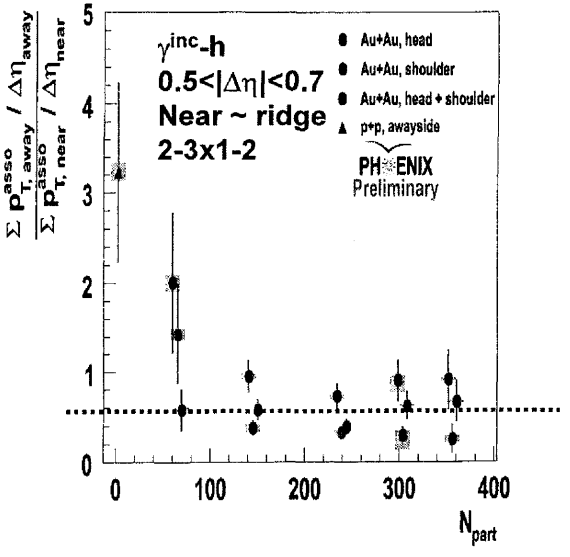

The p_T carried by ridge scales with the p_T carried by shoulder

Summary

- Ridge and shoulder are:
  - Similar in yields
  - Similar in inverse slope (ridge is harder)
  - Softer than hard scattering
  - Harder than inclusive hadron
  - Different in reaction plane dependence
- The momentum sum of head and shoulder scales with nearside in central $\Delta\eta$ region
- The pT carried by ridge scales with the pT carried by shoulder

Long-range correlations in PHOBOS

Wei Li (for the PHOBOS collaboration)
Massachusetts Institute of Technology

The PHOBOS detector at RHIC has a uniquely-large angular coverage for charged particles, which allows for the study of correlations over a very wide pseudorapidity interval. These studies can address critical issues in all different stages of the system evolution: initial state, jet interactions with thermalized medium and final-state hadronization. The inclusive two-particle correlations in A+A collisions suggest that particles are produced in very large clusters at the hadronization stage, which are wider in pseudorapidity than the limit expected for isotropic decays. In the analysis of correlations with a high-p_T trigger particle (p_T > 2.5 GeV/c), a ridge extending at least 4 units of pseudorapidity was found. The ridge and broad away-side features observed in data could be explained by the concept of triangular flow induced by the triangular anisotropy of the fluctuating initial nuclear overlap geometry. Furthermore, an analysis method using two-particle correlations is introduced to measure non-flow correlations, relying on the assumption that non-flow correlations are most prominent at short ranges ($|\eta|<2$). It provides a better constraint on the measured upper limit of the relative event-by-event elliptic flow fluctuation.

Inclusive two-particle correlations

PHOBOS

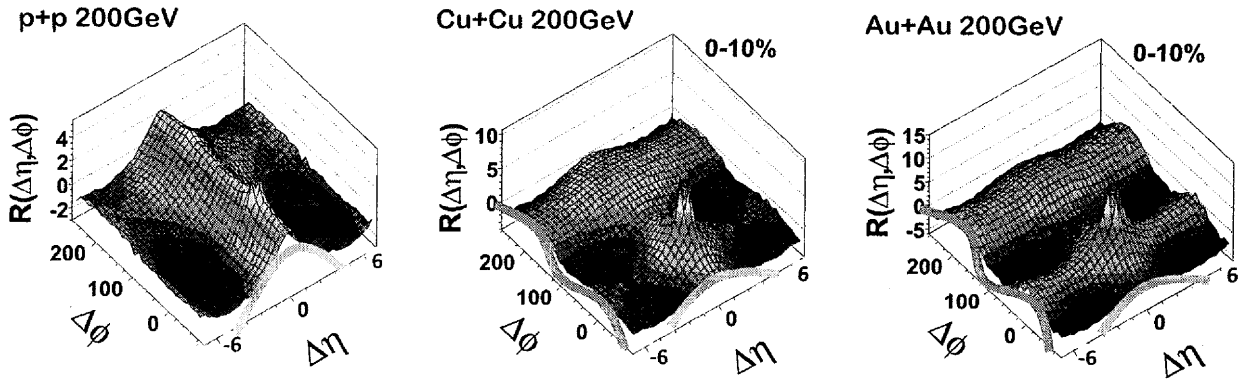

Phys. Rev. C75(2007)054913
Phys. Rev. C81(2010)024904

$$R(\Delta\eta,\Delta\varphi) = < (N-1)\left(\frac{S_N(\Delta\eta,\Delta\varphi)}{B_N(\Delta\eta,\Delta\varphi)} - 1\right) >_{evt}$$

Similar structure in p+p, Cu+Cu and Au+Au collisions,
in A+A collisions a clear trace of elliptic flow is visible

Clusters in HI collisions

- Cluster size is large: (up to 6 charged particles – much more than predicted from known resonances)
- Cluster width exceeds that for isotropic decay at rest (~0.9)
- Cluster size and width very similar at the same centrality, defined as the same fraction of cross section.

The geometry of the interaction area determines the properties of hadronization?

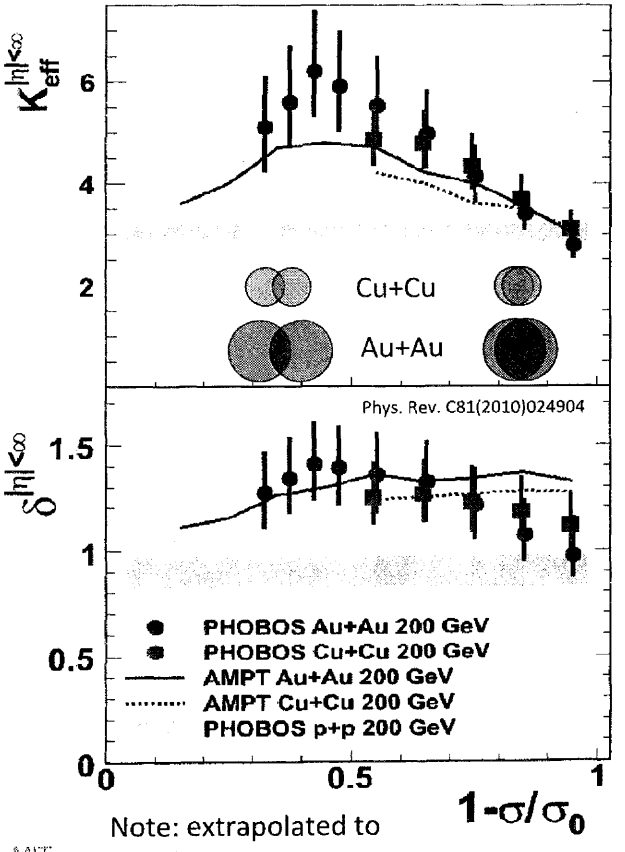

Note: extrapolated to full phase space

Separate non-flow correlations

- Flow is long range in η, correlating all particle via impact parameter b
- Non-flow is dominated by short-range correlations (small $\Delta\eta$)

Study $v_2^2(\eta_1,\eta_2) \equiv < \cos(2\Delta\phi) > (\eta_1,\eta_2)$

$$v_2^2(\eta_1,\eta_2) - v_2^{fit}(\eta_1) \times v_2^{fit}(\eta_2) = \delta(\eta_1,\eta_2)$$

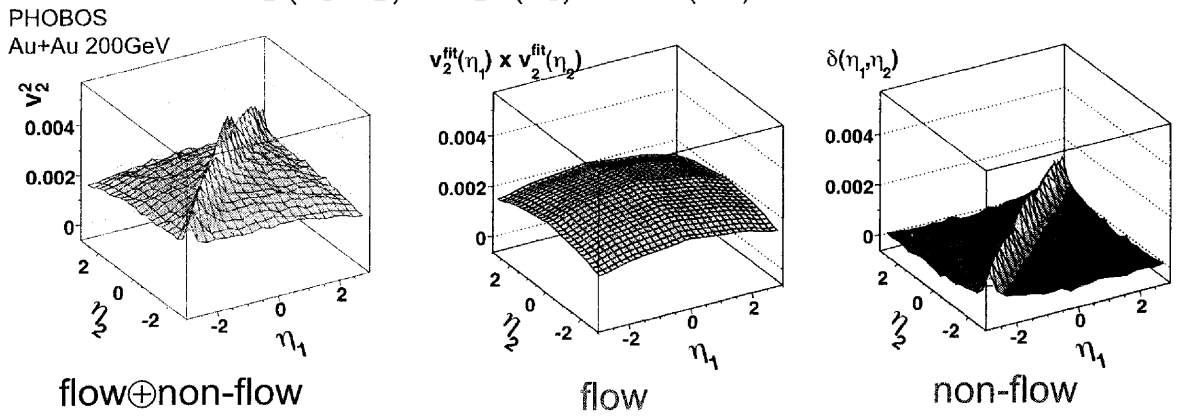

flow⊕non-flow　　flow　　non-flow

PRC 81, 034915 (2010)

High p_T triggered correlations

$$\frac{1}{N_{trig}} \cdot \frac{d^2N_{ch}}{d\Delta\phi\, d\Delta\eta}$$

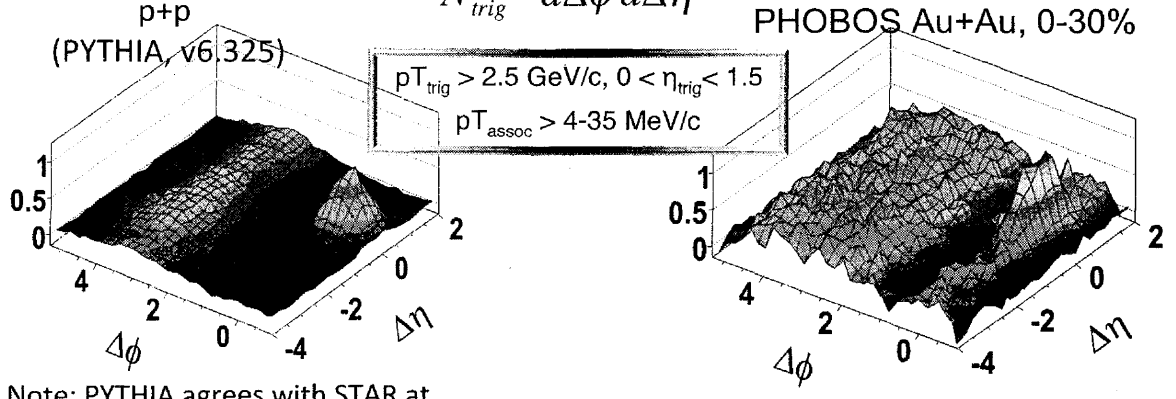

Note: PYTHIA agrees with STAR at midrapidity for a similar set of p_T cuts

PRL 104, 062301 (2010)

$$\frac{1}{N_{trig}} \cdot \frac{d^2N_{ch}}{d\Delta\phi\, d\Delta\eta} = B(\Delta\eta)\left\{\frac{s(\Delta\phi,\Delta\eta)}{b(\Delta\phi,\Delta\eta)} - a(\Delta\eta)\left[1 + 2V_2(\Delta\eta)\cos(2\Delta\phi)\right]\right\}$$

Normalization | Raw | Scale factor | Elliptic flow

Ridge and triangular flow

Triangular eccentricity

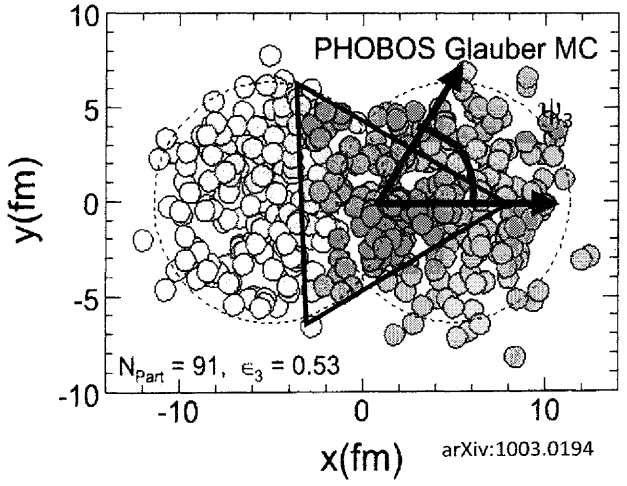

$$v_3 = \left\langle \cos\left(3(\phi - \psi_3)\right) \right\rangle$$

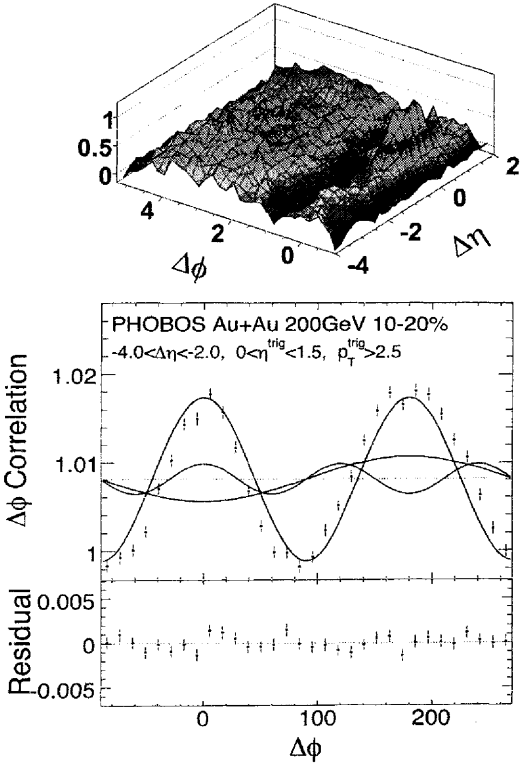

Long range correlations are well described by 3 Fourier Components

Initial geometry fluctuations and triangular flow

Burak Alver, Gunther Roland
Massachusetts Institute of Technology
arXiv: 1003.0194, PRC (in press)

We introduce the concepts of participant triangularity and triangular flow in heavy-ion collisions, analogous to the definitions of participant eccentricity and elliptic flow. The participant triangularity characterizes the triangular anisotropy of the initial nuclear overlap geometry and arises from event-by-event fluctuations in the participant-nucleon collision points. In studies using a multi-phase transport model (AMPT), a triangular flow signal is observed that is proportional to the participant triangularity and corresponds to a large third Fourier coefficient in two-particle azimuthal correlation functions. Using two-particle azimuthal correlations at large pseudorapidity separations measured by the PHOBOS and STAR experiments, we show that this Fourier component is also present in data. Ratios of the second and third Fourier coefficients in data exhibit similar trends as a function of centrality and transverse momentum as in AMPT calculations. These findings suggest a significant contribution of triangular flow to the ridge and broad away-side features observed in data. Triangular flow provides a new handle on the initial collision geometry and collective expansion dynamics in heavy-ion collisions.

Participant triangularity

Triangular anisotropy in initial geometry can be quantified by "participant triangularity" analogous to participant eccentricity.

$$\varepsilon = \frac{\sqrt{\left\langle \left(r^2\cos(2\phi)\right)\right\rangle^2 + \left\langle \left(r^2\sin(2\phi)\right)\right\rangle^2}}{\left\langle r^2\right\rangle}$$

$$\varepsilon_3 = \frac{\sqrt{\left\langle \left(r^2\cos(3\phi)\right)\right\rangle^2 + \left\langle \left(r^2\sin(3\phi)\right)\right\rangle^2}}{\left\langle r^2\right\rangle}$$

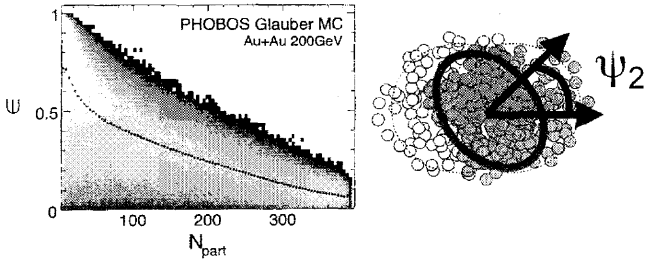

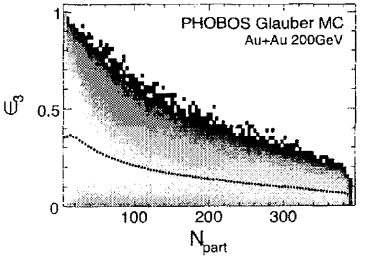

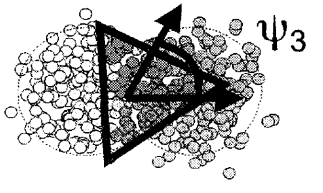

$$v_2 = \left\langle \cos\left(2(\phi - \psi_2)\right)\right\rangle$$

$$v_3 = \left\langle \cos\left(3(\phi - \psi_3)\right)\right\rangle$$

Correlations at large Δη

STAR inclusive
1.2<Δη<1.9

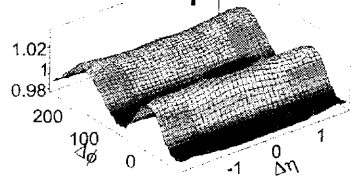

arXiv:0806.0513

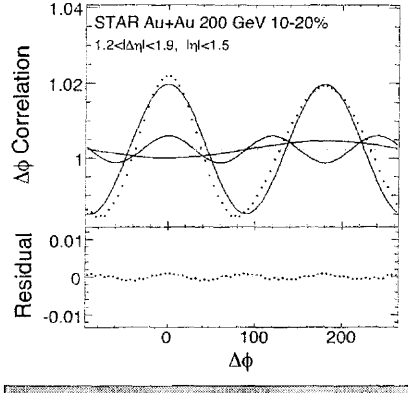

PHOBOS inclusive
2<Δη<4

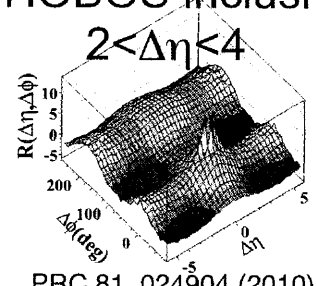

PRC 81, 024904 (2010)

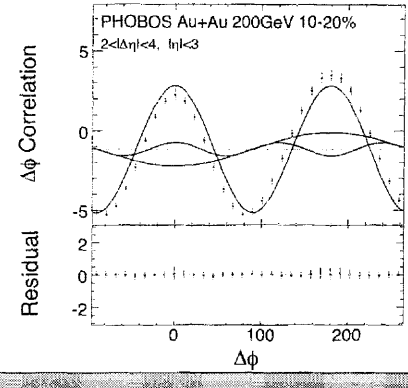

PHOBOS p_T^{trig}>2GeV
2<Δη<4

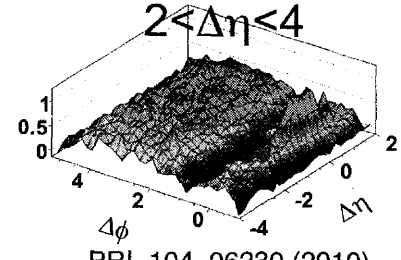

PRL 104, 06230 (2010)

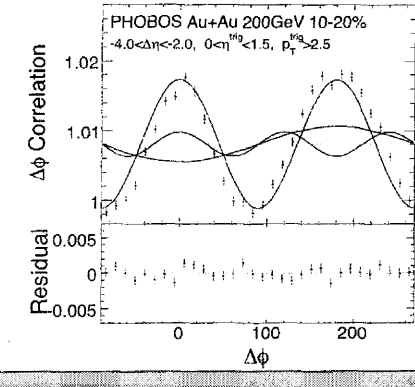

Long range correlations are well described by 3 Fourier Components.

Triangular flow in AMPT

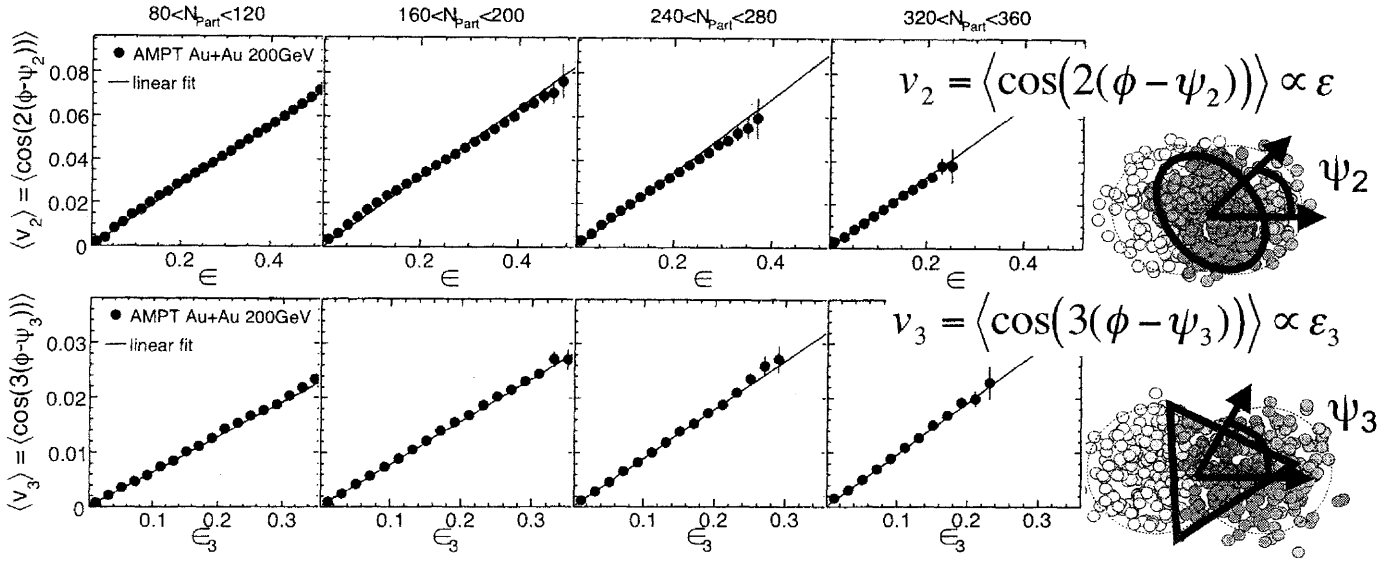

Triangularity leads to triangular flow in AMPT.

Flow and correlations in AMPT

$$\frac{dN}{d\Delta\phi} = \frac{N}{2\pi}\left(1 + \sum 2V_{n\Delta}\cos(n\Delta\phi)\right) \qquad V_{n\Delta}^{flow} \sim \int v_n(\eta) \times v_n(\eta + \Delta\eta)\, d\eta$$

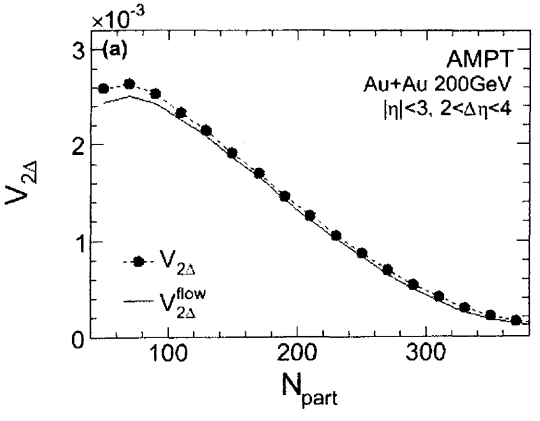

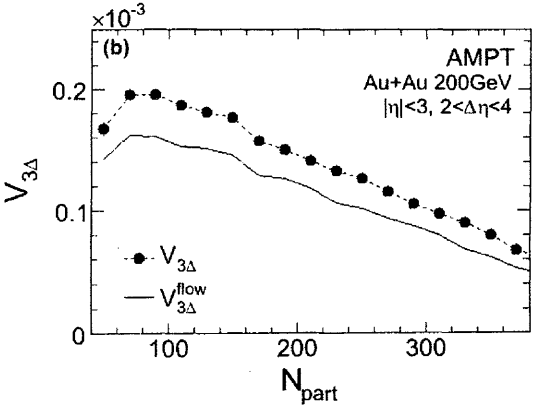

$$V_{3\Delta} = \left\langle \cos(3(\phi_1 - \phi_2)) \right\rangle$$

$$V_{3\Delta}^{flow} = \left\langle \cos(3(\phi_1 - \psi_3)) \right\rangle \left\langle \cos(3(\phi_2 - \psi_3)) \right\rangle$$

Elliptic and triangular flow have the dominant contribution in azimuthal correlations in AMPT.

Triangular flow in data

PHOBOS

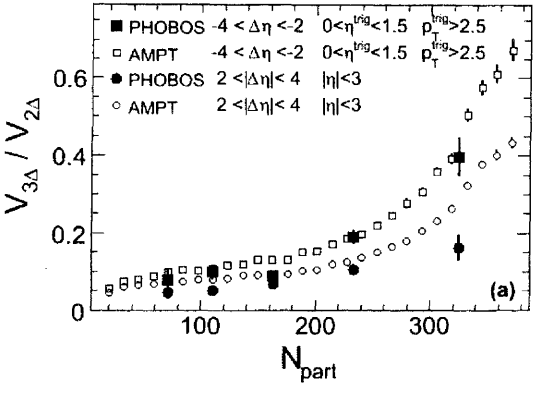

STAR

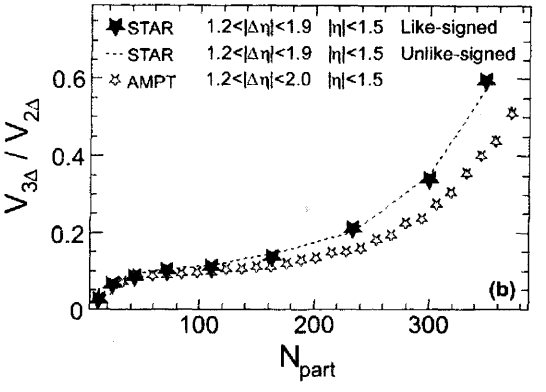

The ratio of Fourier components of azimuthal correlations qualitatively agree between data and AMPT suggesting similar origin: elliptic and triangular flow.

STAR arXiv:0806.0513

PHOBOS PRC 81, 024904 (2010)

PHOBOS PRL 104, 06230 (2010)

Three-particle pseudorapidity correlations in STAR

Pawan Kumar Netrakanti
Purdue University
(For STAR Collaboration)

We report the first three-particle correlation measurements in pseudorapidity($\Delta\eta$) between a high transverse momentum (p_T) trigger particle ($3<p_T^{Trig}$GeV/c) and two lower p_T associated particles ($1<p_T^{Assoc}<3$ GeV/c) within azimuth $|\Delta\phi|<0.7$ in $\sqrt{s_{NN}}$ = 200 GeV d+Au and Au+Au collisions. Charge ordering Properties are exploited to separate the jet-like component and the ridge (long-range $\Delta\eta$ correlations). We found that the same-sign associated pairs correlated to the same-sign trigger particle are dominated by ridge particles.
The results indicate that the correlation of ridge particles are uniform not only with respect to the trigger particle but also between themselves event-by-event. In addition, the production of the ridge appears to be uncorrelated to the presence of the narrow jet-like component.

Ref: B.I. Abelev (STAR Collaboration) **arXiv: 0912.3977**

Theoretical model expectations

1)In medium radiation + longitudinal flow push

N.Armesto et.al Phys.Rev.Lett. 93(2004) 242301

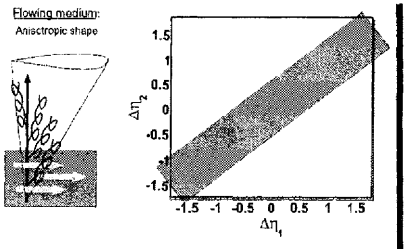

2)Turbulent color fields

A.Majumder et.al Phys. Rev. Lett. 99(2004)042301

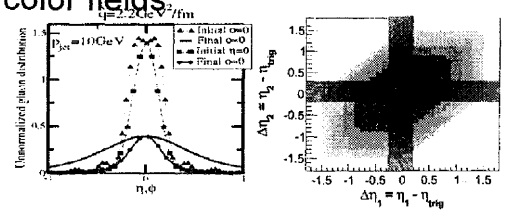

3) Recombination between thermal and shower partons R.C. Hwa & C.B. Chiu Phys. Rev. C 72 (2005) 034903

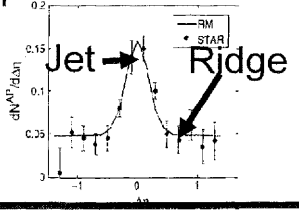

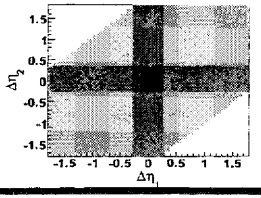

4) Momentum Kick C.Y. Wong hep-ph:0712.3282

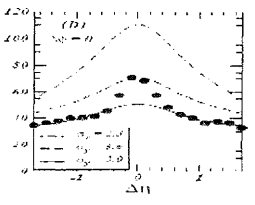

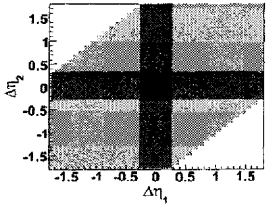

5) Transverse flow boost

S.A.Voloshin, Phys.Lett.B. 632(2006)490

E.Shuryak, hep-ph:0706.3531

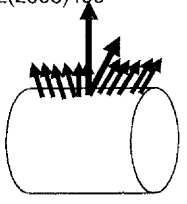

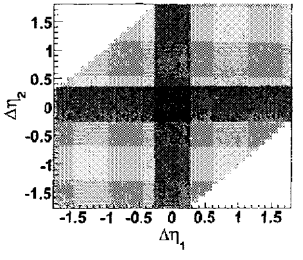

6) Glasma Flux tube

A. Dumitru et. al Nucl. Phys. A 810, 91 (2008)

K. Dusling et. al Nucl. Phys. A 828, 161 (2009)

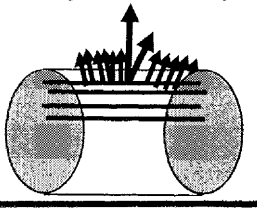

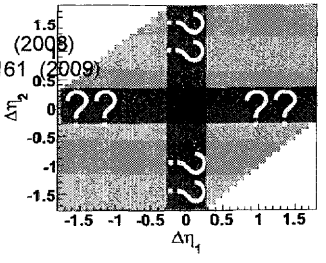

Can we distinguish between these physics interpretations?

→ 3-particle correlation in η

3-particle $\Delta\eta$-$\Delta\eta$ correlations

$3<p_T^{trig}<10$ GeV/c $1<p_T^{assoc}<3$ GeV/c $|\Delta\phi|<0.7$

Same-sign triplets **$(A^{\pm}A^{\pm}T^{\pm})$**

Ridge : 4* $A^{\pm}A^{\pm}T^{\pm}$

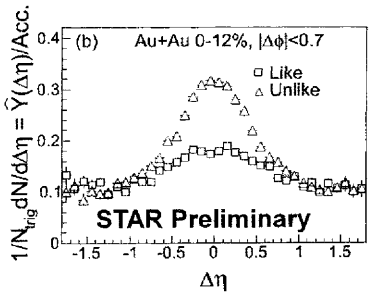

Same-sign associated pair and opposite sign trigger particle **$(A^{\pm}A^{\pm}T^{\mp})$**

Jet-like: Total - Ridge

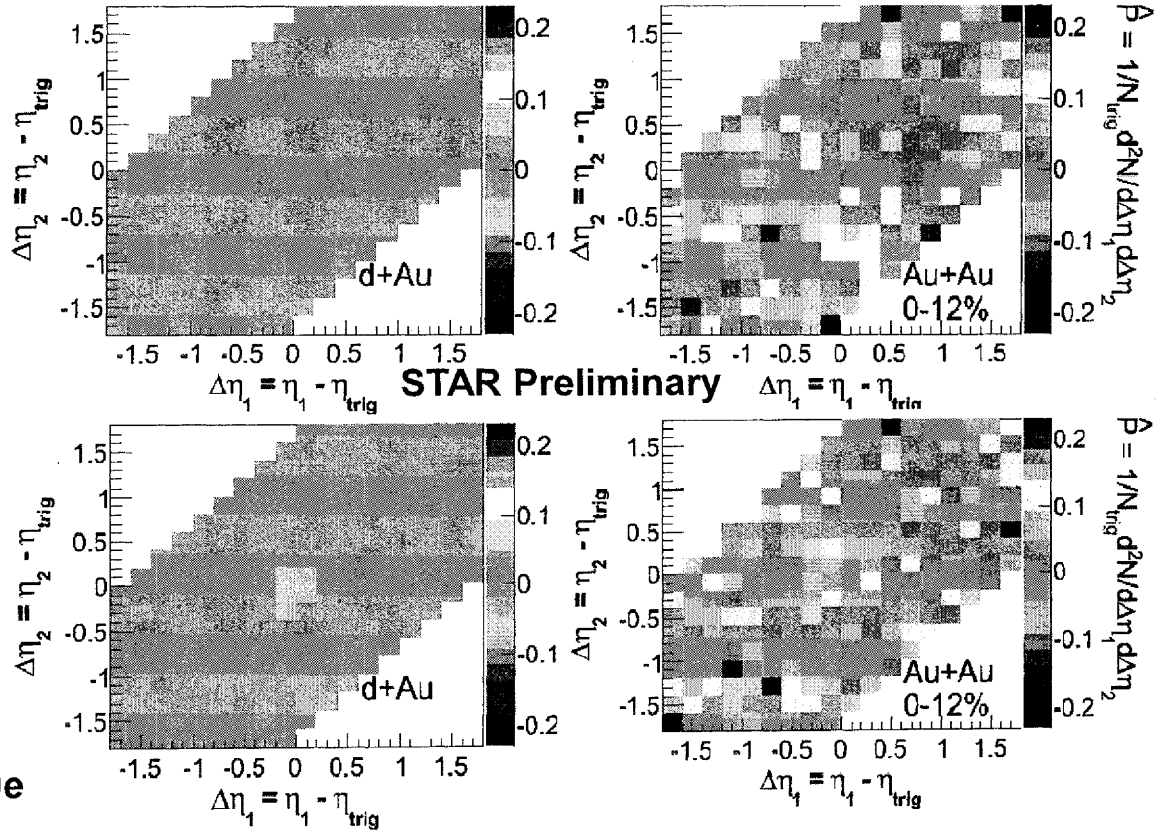

Like-sign triplets : Dominated by ridge

Average pair densities

Au+Au 0-12%

$3<p_T^{trig}<10$ GeV/c
$1<p_T^{assoc}<3$ GeV/c
$|\Delta\phi|<0.7$

Ridge

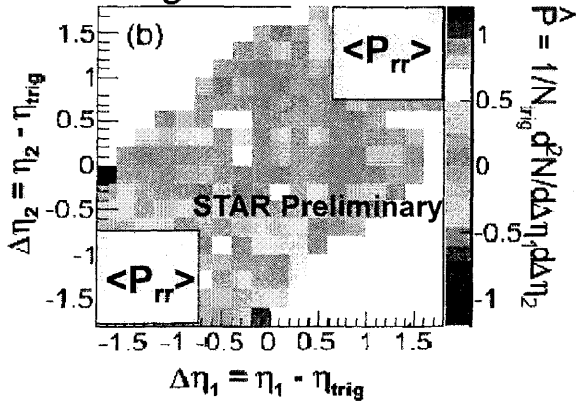

Jet-like

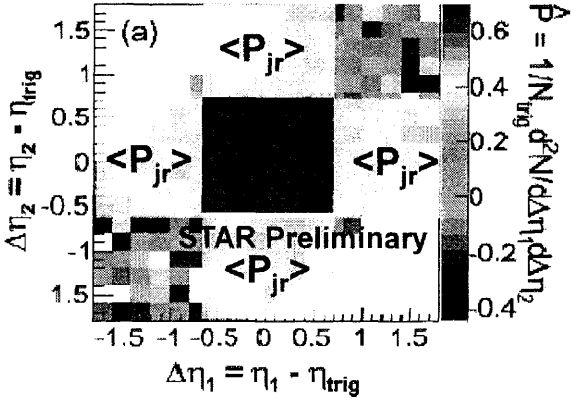

$\langle P_{rr} \rangle$: **0.114 ± 0.039**

$\langle P_{jj} \rangle$: **0.077 ± 0.026**

Jet-ridge cross pairs

$\langle P_{jr} \rangle$: **-0.004 ± 0.025**

Ridge production appears to be uncorrelated with the presence of jet.

Radial and Angular dependence

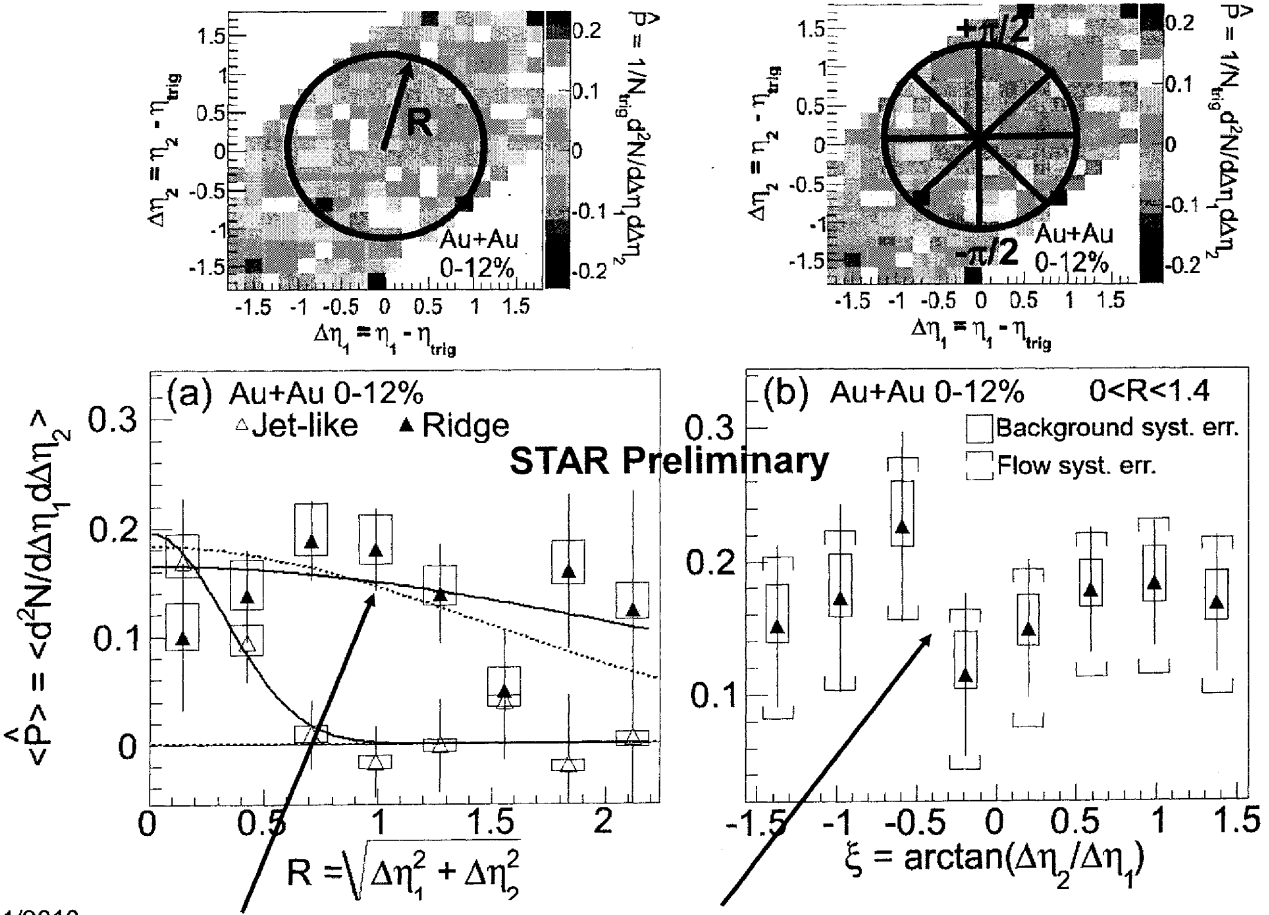

Ridge is broad. No prominent substructures in ridge.

Data and Models

1)In medium radiation + longitudinal flow push

Model : Diagonal excess

Data: Uniform

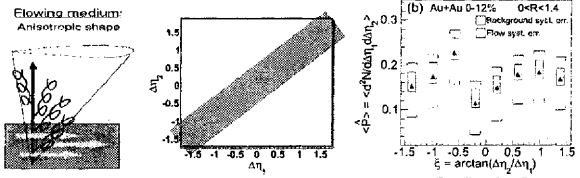

2)Turbulent color fields

Model: uniform ridge, jet-ridge cross pairs.

Data:Broad Ridge, no jet-ridge cross pairs

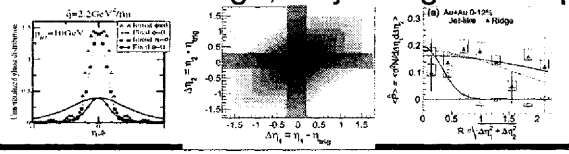

3) Recombination Model

Model: jet-ridge cross pairs.

Data : $\langle P_{jr} \rangle \sim 0$

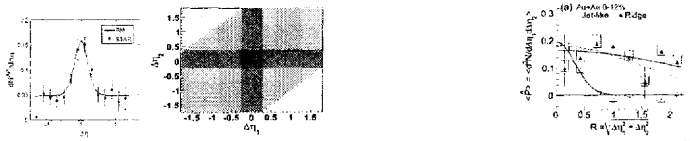

4) Momentum Kick

Model : Jet-ridge cross pairs

Data $\langle P_{jr} \rangle \sim 0$

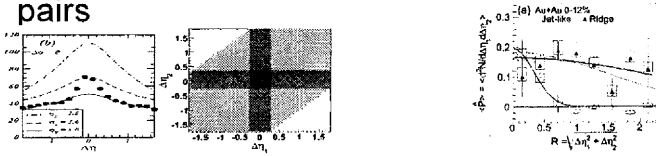

5) Transverse flow boost

Model: Uniform, Jet-ridge cross pairs

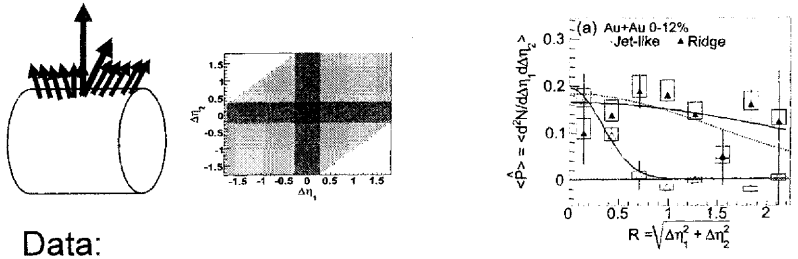

Data:

Uniform. No jet-ridge cross pairs

6) Glasma Flux tube

Model: Uniform. Jet-ridge cross pairs ????

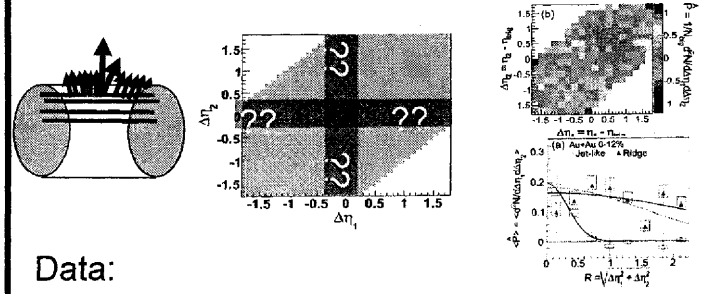

Data:

Uniform. No jet-ridge cross term

5/11/2010

The ``ridges" and large jet v_2 are explained by magnetic plasma near Tc

(RBRC workshop, BNL, May 11th 2010)

Edward Shuryak

Stony Brook

- the ridges: not just radial flow but necessarily (quite robust) flux tubes!
- ``tomography" (v2) of the jet quenching shows that it happens mostly near Tc
- "magnetic" (color monopole) plasma near Tc is the key explaination. It stems from the deconfinement!

Three main observations from jet correlations may be explained by:

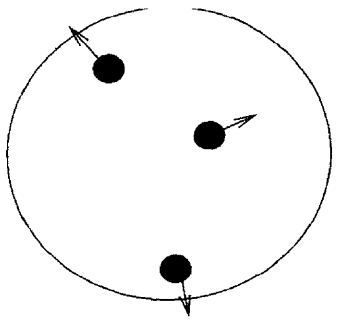

- ``cone" on the away side => hydro flow

(H.Stoecker,J.Casalderrey+ES, 2005)

- ``Hard ridge" => forward-backward bremmstrahlung cones kicked out by hydro radial flow **(4 jets!)**

(Shuryak 0706.3531, PRC76)

- ``Soft ridge" => initial stage fluctuation of the color changes, also carried by flow

(Dumitru,Gelis,McLerran,Venugopalan, 0804.3858, Gavin et al 0806.4718)

PHYSICAL REVIEW C **80**, 054908 (2009)

Fate of the initial state perturbations in heavy ion collisions

Edward Shuryak
Department of Physics and Astronomy, State University of New York, Stony Brook, New York 11794, USA
(Received 20 July 2009; revised manuscript received 14 October 2009; published 13 November 2009)

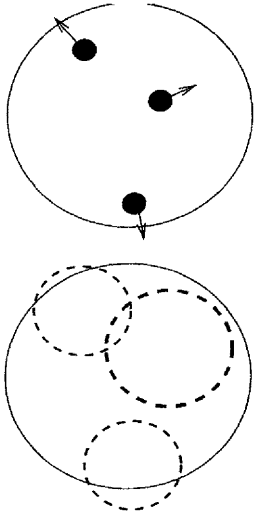

Naively, ``spots" should excite a wave and get expanded to a spherical (or conical, or cylindrical) wave

Like in the case of stone thrown into the pond, nothing is left at the original position: **so how can they be observed?**

Its size =>the sound horizon => is comparable to fireball size 6-8 fm/c

And thus large angular size

$$R_h = \int_0^{\tau_f} d\tau c_s(\tau)$$

If one wants to get large radial flow, one has to wait the time needed for it to develop. The sound speed during this time creates large rings.

Can we restrict its size (at freezeout) from the data?

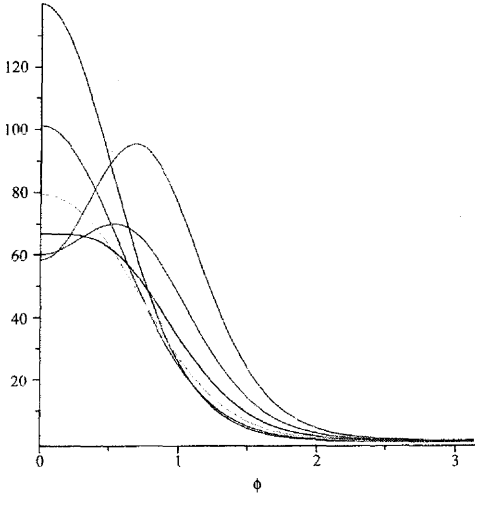

FIG. 5. (Color online) Dependence of the visible distribution in the azimuthal angle on the width of the (semi)circle at the time of freeze-out. Six curves, from the most narrow to the widest ones, correspond to the radius of the circle of 1, 2, 3, 4, 5, and 6 fm, respectively. The original spot position is selected to be at the edge of the nuclei. The distribution is calculated for a particle of $p_t = 1$ GeV and fixed freeze-out $T_f = 165$ MeV.

- This is how azimuthal distribution would look like:
- comparing with data, we concllude

$$R(\tau_{\text{freeze-out}}) < 3\,\text{fm} \text{ or so.}$$

Predictions for energy dependence: ridges

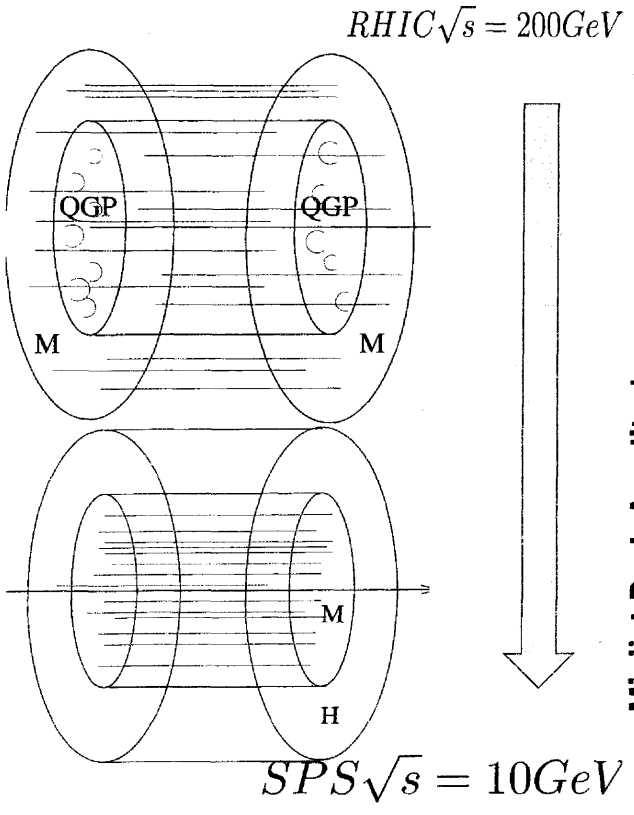

As energy decreases, M phase
Goes inside the fireball =>
Much smaller radial flow =>
Disappearance of the ridge at fixed matter density

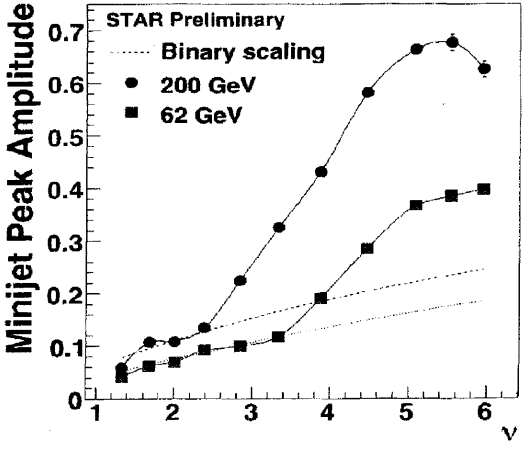

L.Ray

Liao,ES: Resolution of the old puzzle of large v2(large pt):
Phys.Rev.Lett.102:202302,2009.
two different quenching in QGP and M phases (zero in H)
λ=quenching(QGP)/quenching(M)
λ=0.2−0.4 =>

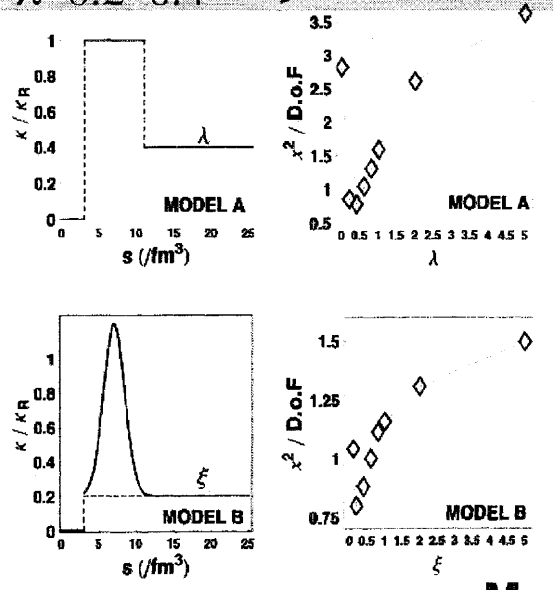

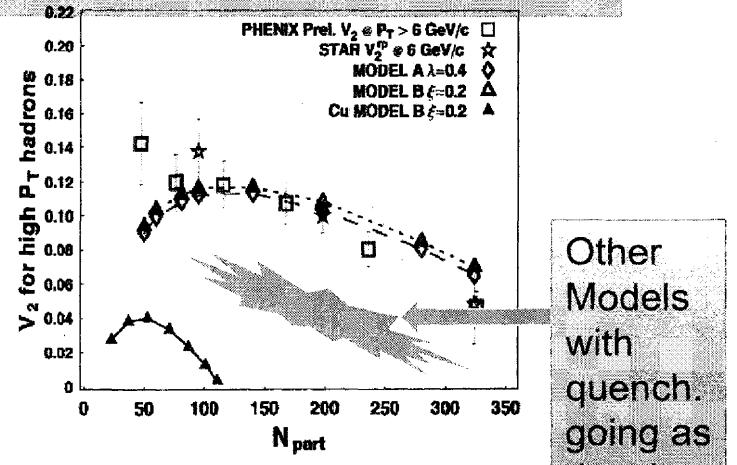

Other Models with quench. going as density

FIG. 3: (color online) Comparison between v_2 experimental data and v_2 calculated from our models, see text.

- **M-region (near Tc) quenched jets stronger**
- **Because light monopoles are there**

Long Range Correlations and Hydrodynamic Expansion

Sean Gavin

Wayne State University

I. Correlations: PHOBOS Data, Flux Tubes and Causality

II. Ridge: Transverse Flow, Blast Wave

III. Glasma Flux Tubes

IV. STAR data: Au+Au and Cu+Cu

V. Questions:

A. STAR Rapidity Dependence?

B. How Robust is the Ridge?

Transverse Flow ⇒ Near-Side ϕ Peak

bulk correlations – longitudinal string fragmentation

string position $\vec{r}$

transverse boost thermalization and flow

$\vec{v}_t \sim \lambda \vec{r}$

flow ⇒ narrow opening angle

$\Delta\phi \sim v_{th}/v_t \sim (\lambda r)^{-1}$

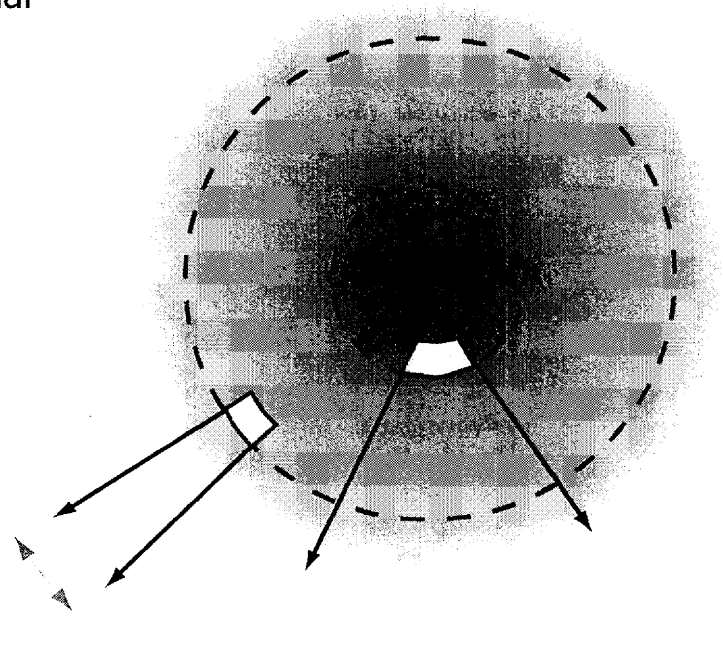

Voloshin; Pruneau, Gavin, Voloshin; Gavin, Moschelli, McLerran; Shuryak; Mocsy & Sorenson

Flux Tubes in Glasma

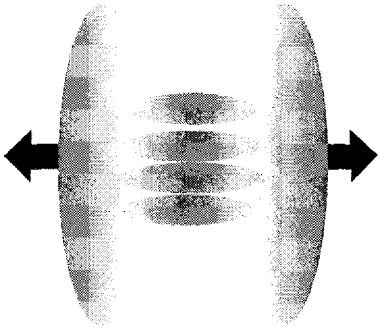

N_{FT} flux tubes

gluon rapidity density $$\frac{dN}{dy} = \frac{\text{gluons}}{\text{tube}} \times \langle N_{FT} \rangle \propto \alpha_s^{-1}(Q_s) \langle N_{FT} \rangle$$

fluctuations in the number of flux tubes $$\mathcal{R} = \frac{Var(N) - \langle N \rangle}{\langle N \rangle^2} \propto \frac{1}{\langle N_{FT} \rangle}$$

long range glasma fluctuations

$$\mathcal{R} \frac{dN}{dy} \propto \alpha_s^{-1}(Q_s)$$

Dumitru, Gelis, McLerran & Venugopalan;
SG, McLerran & Moschelli

Glasma + Blast Wave ⇒ Ridge Height

pair correlation function -- Cooper Frye freeze out

$$\Delta\rho \equiv \text{pairs} - (\text{singles})^2 \quad \propto \quad \iint_{\text{freezeout surface}} f(p_1,x_1) f(p_2,x_2) c(x_1,x_2)$$

- blast wave $\rightarrow f(p,x)$
- scale factor to fit 200 GeV only
- Glasma energy dependence

$$\mathcal{R}\, dN/dy \propto \alpha_s^{-1}(Q_s)$$

STAR Data, J.Phys. G35 (2008) 104090

SG, McLerran, Moschelli et al. PRC 79 (2009) 051902

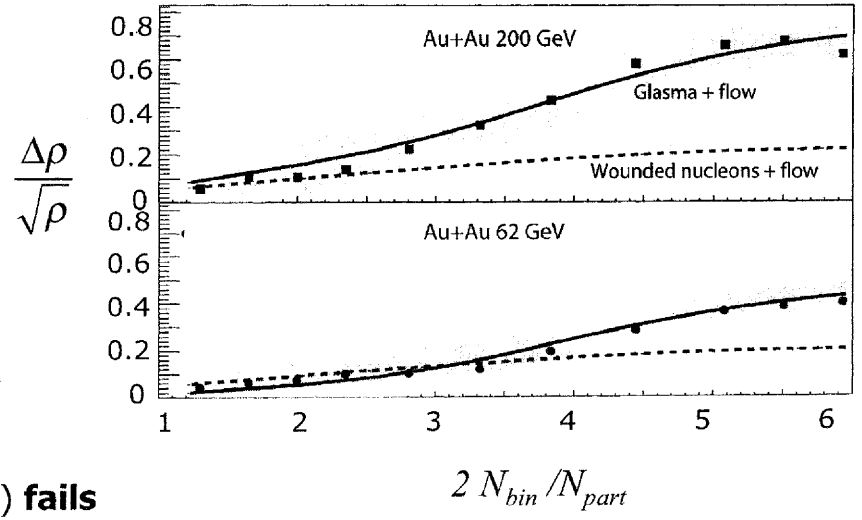

Glasma Q_s dependence: 200 GeV Au+Au ⇒ 62 GeV, Cu+Cu

wounded nucleon model (dashed) **fails**

Peak Amplitude of the Soft Ridge

STAR data, preliminary
Moschelli & SG

Ridge amplitude vs. Centrality, all p_t

→ L. Ray's talk

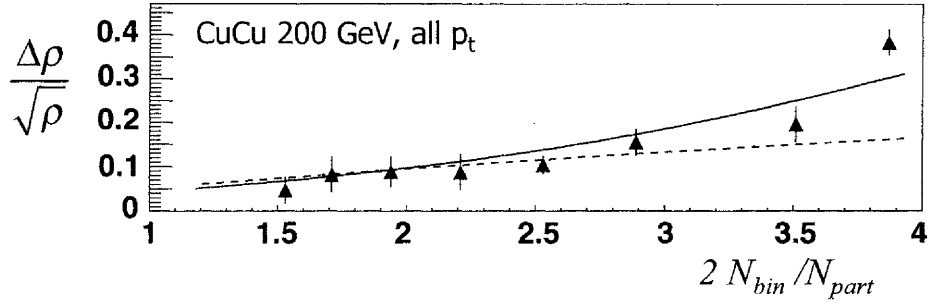

Ridge amplitude for $p_{t1}, p_{t2} > p_{t\,\min}$

Amplitude decreases for higher $p_{t\,\min}$

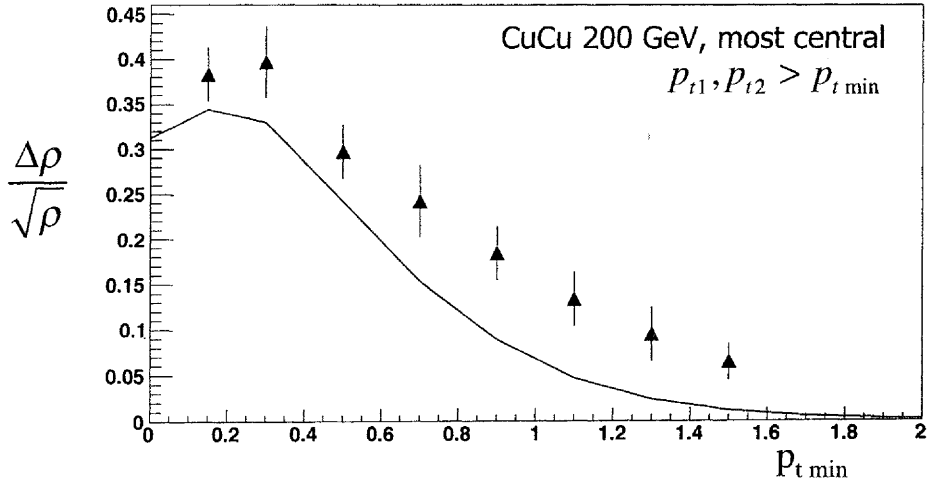

bands: uncertainty of blast wave parameters and Q_s extrapolated from AuAu

Ridge: from Soft to Hard

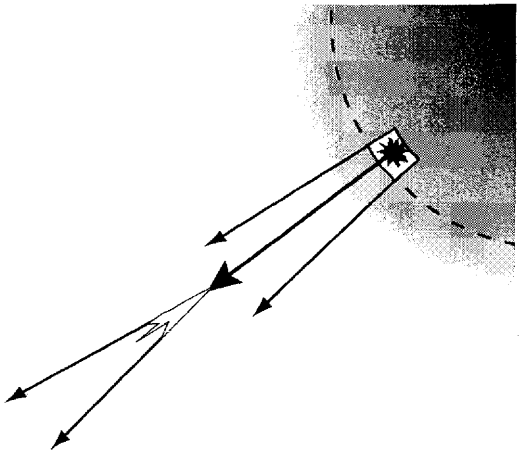

STAR $\Delta\rho$ with low p_t cutoff

- Hard: Jets + quenching
- Bulk: Glasma + flow
- Bulk - Hard correlations

Jet quenching $\Rightarrow$ near side bias
Shuryak, Phys Rev C76, 047901,2007

hard ridge:

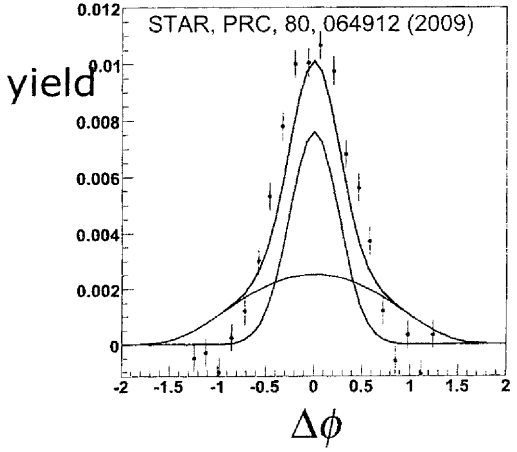

G. Moschelli & SG, Nucl. Phys. A836 (2010) 43

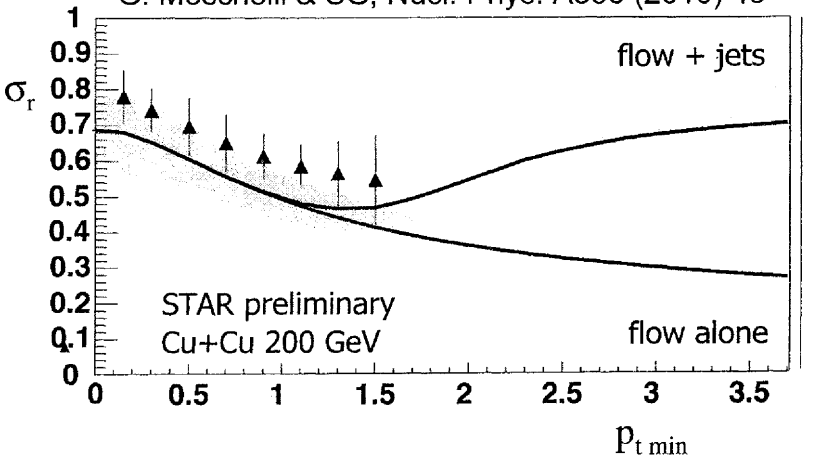

Forward-Backward Multiplicity Correlations at STAR

Michael Skoby
Purdue University
for the STAR Collaboration

Long-Range Forward-Backward multiplicity correlations (LRC) may be a signal for multiple partonic interactions in dense matter. Strong LRC have been measured at STAR in 200 GeV central Au+Au collisions, and were shown to decrease with decreasing centrality. The forward-backward correlation is studied with respect to its particle species dependence (pions, kaons, protons), and is measured as a function of rapidity. The Color Glass Condensate model, which describes sources as longitudinal flux tubes, predicts that the correlation will grow with centrality. Fluctuations in the number of gluons at early times will produce a LRC larger for pions than baryons. Pions and (anti)protons are identified at STAR by measuring their average energy loss. Preliminary results of the measured correlation are presented for pions, kaons, and protons.

Introduction

- Long-range (rapidity separation > 1) multiplicity correlations (LRC) are predicted in high-energy nucleon-nucleon collisions by the Dual Parton Model (DPM) and in nucleus-nucleus collisions by DPM and the Color Glass Condensate (CGC) picture
- Strong LRC using inclusive charged particles have been recently measured in the STAR TPC (B. I. Abelev *et al.* (STAR Collaboration), Phys. Rev. Lett. **103**, 172301 (2009).)
- Multiplicity correlations across different rapidity regions indicate the occurrence of partonic interactions

Forward-Backward Multiplicity Correlations

- As seen previously in hadron-hadron experiments, the average multiplicity of particles in the backward region can be related to the multiplicity in the forward region

$$\langle N_B \rangle (N_F) = a + bN_F$$

- Appling a linear regression one can obtain the correlation strength *b*

$$b = \frac{< N_f N_b > - < N_f >< N_b >}{< N_f^2 > - < N_f >^2} = \frac{D_{bf}^2}{D_{ff}^2}$$

Centrality Dependence of LRC

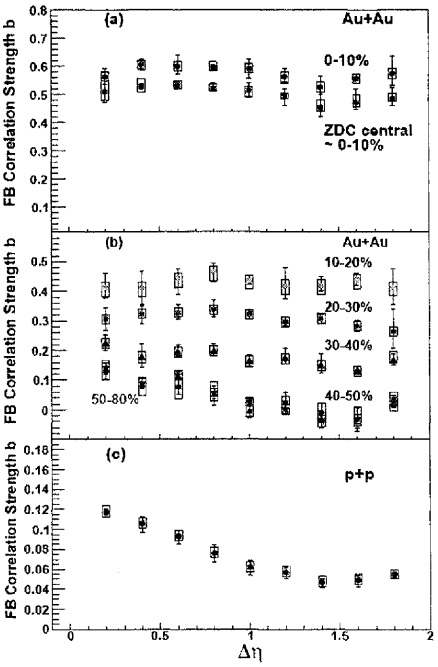

B. I. Abelev *et al.* (STAR Collaboration), Phys. Rev. Lett. **103**, 172301 (2009).

- LRC $\Delta\eta>1$, short-range $\Delta\eta<1$
- Strong LRC in central collisions
- Au+Au and pp at 200 GeV
- All charged hadrons
- $0.15 > p_T > 1.2$ GeV/c

b is flat in central Au+Au but decreases with $\Delta\eta$ in p+p collisions

FB Correlation Strength b

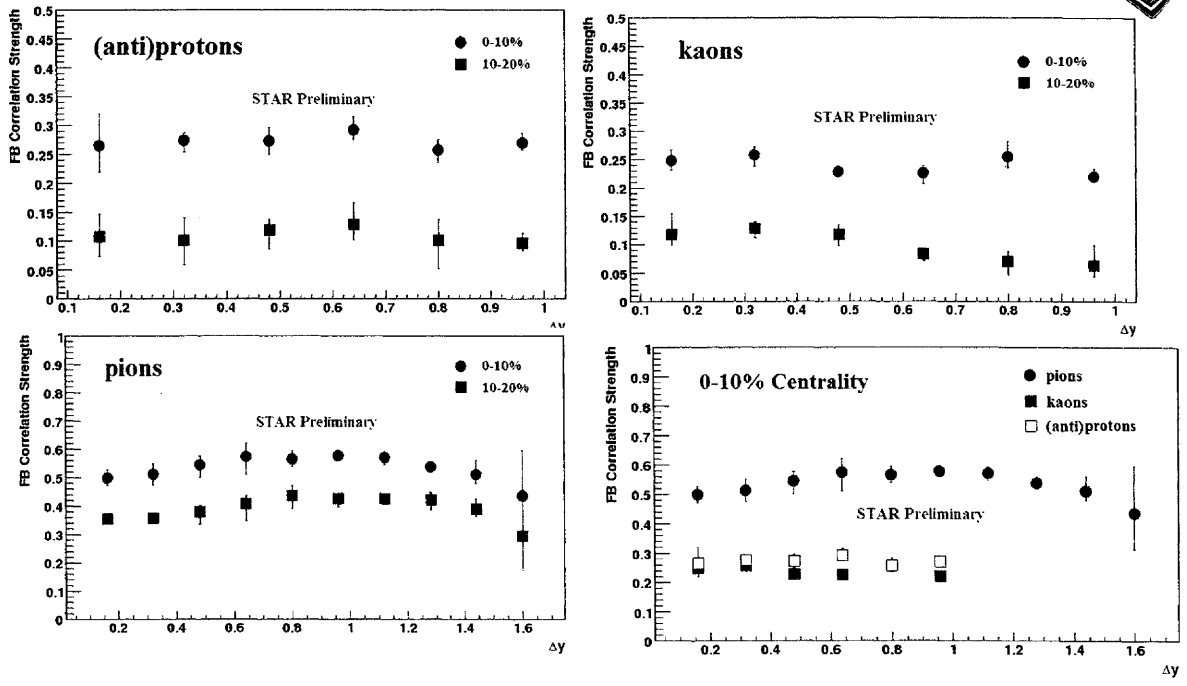

Conclusions

- Strong LRC for inclusive charged hadrons in central Au+Au collisions indicate the occurrence of multiple partonic interactions, and decrease with decreasing centrality
- Preliminary measurements show a strong, uniform LRC across Δy for pions in central Au+Au collisions at 200 GeV, which decreases from central to peripheral collisions
- The small short-range correlation for kaons and (anti)protons, compared to pions, suggests the LRC will also be small for these species
- CGC predicts that the LRC seen for pions is primarily due to the fluctuation in the number of gluons, and can only be created at early times
- The baryon correlation should not grow with increasing centrality in CGC, but we see an increase in the (anti)proton correlation from 10-20% to 0-10%.
- Future measurements of correlations at high p_T for inclusive charged hadrons may not have such a large correlation for central collisions as contributions from baryons at higher p_T increase in the CGC picture

Multiplicity distributions and long range rapidity correlations

T. Lappi
University of Jyväskylä, Finland

We review the recent progress in computing multigluon correlations in the glasma. We argue that multigluon correlations are in some sense easier to compute in the strong field limit than in dilute systems [1].

The CGC naturally produces a negative binomial multiplicity distribution for gluons [2]. This is consistent with the earlier experimental observations with the exception that we expect the "k" parameter in the distribution to increase with $\sqrt{s}$ at higher energies, while it decreases at lower energy. We also recall the recent results for two gluon correlations computed numerically to all orders in the color sources [3] and for large rapidity separations [4].

The STAR collaboration has reported interesting backward-forward multiplicity correlation results that point to strong long range rapidity correlations in central AA. Looking in detail at how the STAR analysis is done, the measured observable is in fact a 3-particle correlation, not a 2-particle one. This is usually not taken into account in the literature and significantly complicates the interpretation of the data [5].

References

[1] F. Gelis, T. Lappi and R. Venugopalan, *Phys. Rev.* **D79** (2008) 094017 [arXiv:0810.4829 [hep-ph]].

[2] F. Gelis, T. Lappi and L. McLerran, *Nucl. Phys.* **A828** (2009) 149 [arXiv:0905.3234 [hep-ph]].

[3] T. Lappi, S. Srednyak and R. Venugopalan, *JHEP* **01** (2010) 066 [arXiv:0911.2068 [hep-ph]].

[4] K. Dusling, F. Gelis, T. Lappi and R. Venugopalan, *Nucl.Phys.* **A836** (2010) 159 [arXiv:arXiv:0911.2720 [hep-ph]].

[5] T. Lappi and L. McLerran, *Nucl. Phys.* **A832** (2010) 330 [arXiv:0909.0428 [hep-ph]].

Multiparticle correlations, power counting

Basic power counting: $\frac{dN}{d^3\boldsymbol{p}} \sim \frac{1}{\alpha_s}$

Fixed sources: correlations loop/quantum effects, suppressed by α_s

$$\text{E.g. Poisson} \quad \overbrace{\langle N^2 \rangle}^{1/\alpha_s^2+\cdots} - \overbrace{\langle N \rangle^2}^{1/\alpha_s^2+\cdots} = \overbrace{\langle N \rangle}^{1/\alpha_s+\cdots}$$

But in CGC must average over sources:

$$\left\langle \frac{dN}{d^3\boldsymbol{p}_1} \cdots \frac{dN}{d^3\boldsymbol{p}_n} \right\rangle_{\text{conn.}} = \left[\int_{[\rho]} \underbrace{W[\rho_1(y)]\, W[\rho_2(y)]}_{\text{source}} \frac{dN}{d^3\boldsymbol{p}_1} \cdots \frac{dN}{d^3\boldsymbol{p}_n} \right]_{\text{conn.}} \sim \frac{1}{\alpha_s^n}$$

LLog corrections factorize into evolution of **source** .

$$\text{E.g. neg. bin} \quad \overbrace{\langle N^2 \rangle}^{1/\alpha_s^2} - \overbrace{\langle N \rangle^2}^{1/\alpha_s^2} = \frac{1}{k} \overbrace{\langle N \rangle^2}^{1/\alpha_s^2} + \overbrace{\langle N \rangle}^{1/\alpha_s}$$

Dominant correlations come from sources

i.e. enhanced by $\ln 1/x \sim 1/\alpha_s$

Negative binomial

Moment $m_q \equiv \langle N^q \rangle$ – disc.

$$
\begin{aligned}
m_q &= (q-1)!\, k \left(\frac{\bar{n}}{k}\right)^q \\
k &\approx \frac{(N_c{}^2 - 1) Q_s^2 S_\perp}{2\pi} \\
\bar{n} &= f_N \frac{1}{\alpha_s} Q_s^2 S_\perp
\end{aligned}
$$

GLuon **I**ntensification **T**hrough **T**enacious **E**mission of **R**adiation.

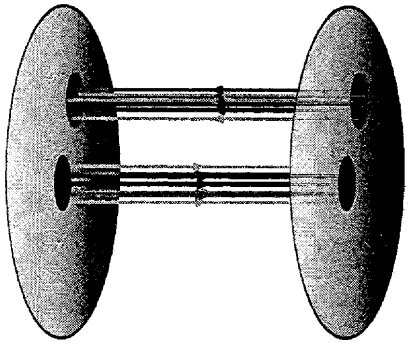

This is a neg. bin.

- Old exp. observation
- Note $k \sim \sqrt{s}^{\lambda}$

$Q_s^2 S_\perp = N_{FT}$, # of flux tubes
$k \approx N_{FT}(N_c{}^2 - 1)$ = emitters
Each emitter produces particles with Bose-Einstein distribution

(Negative binomial is sum of k independent BE's)

Boost invariant correlation: full numerical calculation

T.L., Srednyak, Venugopalan, -09

$$\kappa_2(\mathbf{p}_T, \mathbf{q}_T) = \overbrace{S_\perp Q_s^2}^{\#\text{ of independent regions}} \times \frac{\left\langle \frac{d^2 N_2}{dy_p\, d^2\mathbf{p}_T\, dy_q\, d^2\mathbf{q}_T} \right\rangle}{\left\langle \frac{dN}{dy_p\, d^2\mathbf{p}_T} \right\rangle \left\langle \frac{dN}{dy_q d^2\mathbf{q}_T} \right\rangle} - 1$$

Dilute limit: $\kappa_2(\mathbf{p}_T, \mathbf{q}_T) \sim 1/(N_c{}^2 - 1)$ constant up to logs.

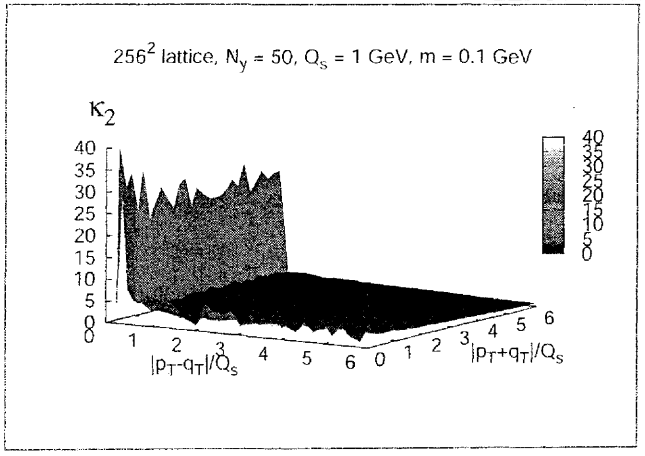

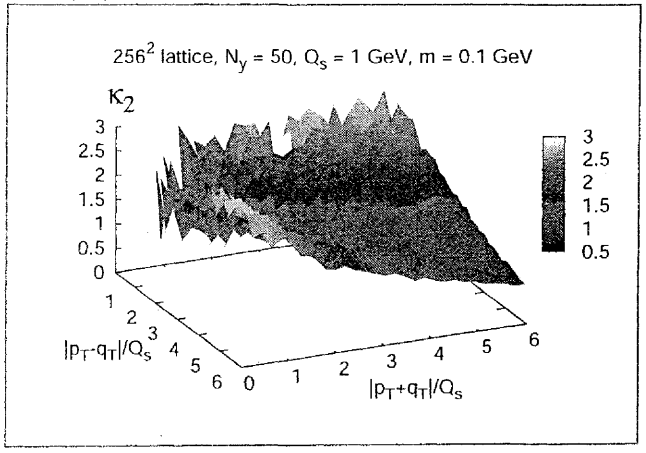

Ridge estimate: $\kappa_2 \approx 1 \ldots 1.5$ Multiplicity distribution: $\kappa_2 \approx 4$

(Note: different momenta)

First calculation of rapidity dependence

k_T-factorized approximation Dusling, Gelis, T.L., Venugopalan, -09

$$C(\mathbf{p},\mathbf{q}) \sim \int_{\mathbf{k}_T} \left\{ \overbrace{\Phi^2_{A_1}(y_p,\mathbf{k}_T)\Phi_{A_2}(y_p,\mathbf{p}_T-\mathbf{k}_T)}^{3 \text{ at } y_p} \overbrace{\Phi_{A_2}(y_q,\mathbf{q}_T+\mathbf{k}_T)}^{1 \text{ at } y_q} + (\mathbf{k}_T \leftrightarrow -\mathbf{k}_T) + (A_1 \leftrightarrow A_2) \right\}$$

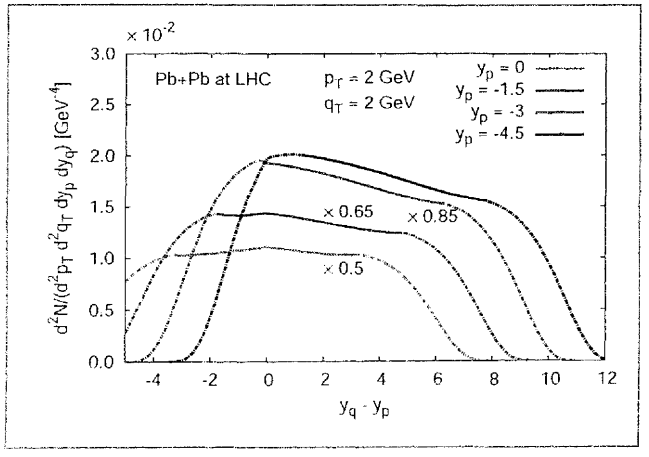

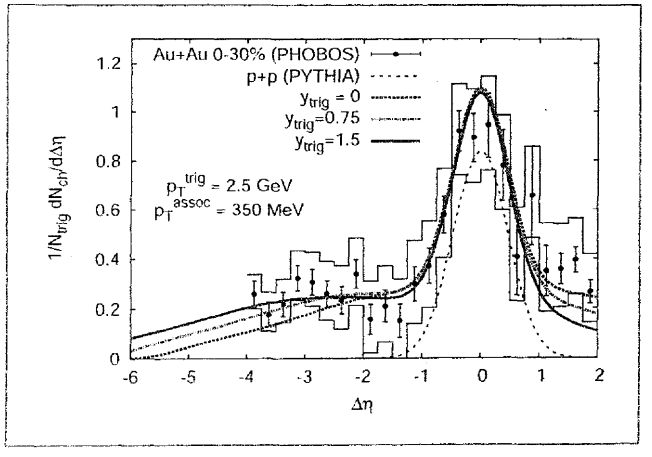

STAR Forward-Backward correlation data

at fixed N_R

$$b = \frac{\langle N_F N_B \rangle_{N_R} - \langle N_F \rangle_{N_R} \langle N_B \rangle_{N_R}}{\langle N_F{}^2 \rangle_{N_R} - \langle N_F \rangle^2{}_{N_R}}$$

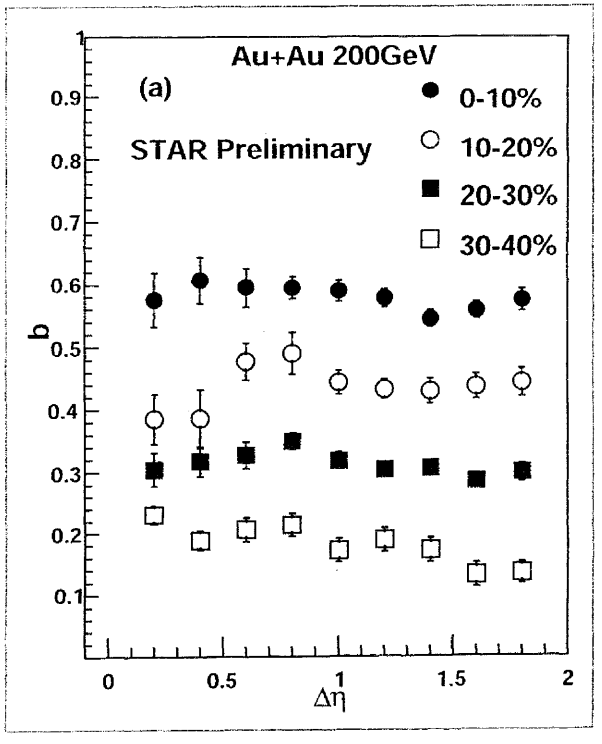

Huge increase in correlation, but what is actually measured?

STAR, B. I. Abelev *et al.*, Phys. Rev. Lett **103**, 172301 (2009):

3-particle correlation:

N_F, N_B and N_R

"... (N_F, N_B, $N_F{}^2$, $N_F N_B$) was obtained on an event-by-event basis as a function of the event multiplicity [N_R] ..."

Long range correlations;event simulation and parton percolation

C.Pajares
Dept Particle Physics,University Santiago de Compostela and IGFAE ,Santiago de Compostela,Spain

Abstract:We discuss different string models in relation to long range rapidity correlations data Special attention is paid to parton percolation.

We show similaties between parton percolation and color glass condensate in the behaviour of many observables due to a similar physical picture

(N. Armesto et al., PRL77 (96); J.Dias de Deus et al., PLB491 (00); M. Nardi and H. Satz(98).

• How?: Strings fuse forming clusters. At a certain critical density η_c (central PbPb at SPS, central AgAg at RHIC, central pp at LHC) a macroscopic cluster appears which marks the percolation phase transition (second order, non thermal).

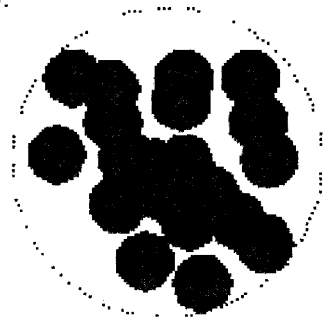

$\eta = N_s \frac{S_1}{S_A}$. $S_1 = \pi r_0^2$. $r_0 = 0.2$ fm. $\eta_c = 1.1 \div 1.2$.

• Hypothesis: clusters of overlapping strings are the sources of particle production, and central multiplicities and transverse momentum distributions are little affected by rescattering.

$$\mu_n = \sqrt{\frac{nS_n}{S_1}}\mu_1 \; ; \; < p_T^2 >_n = \sqrt{\frac{nS_1}{S_n}} < p_T^2 >_1$$

Energy-momentum of the cluster is the sum of the energy-momemtum of each string. As the individual color field of the individual string may be oriented in an arbitrary manner respective to one another, $\vec{Q}_n = n\vec{Q}$

- At high densities
  - $< \mu >_n = nF(\eta) < \mu >_1 \;\; < p_T^2 >_n = \frac{< p_T^2 >_1}{F(\eta)}$
  - $F(\eta) = \sqrt{\frac{1-e^{-\eta}}{\eta}}$, $\eta = N_S \frac{\pi r_0^2}{S_A}$
  - r_0 is the transverse size of a single string $\simeq$ 0.2 fm.

Transverse size $r_0^2 F(\eta)$

CGC $1/Q_s^2$

Effective number of clusters

$$< N >= \frac{(1-exp(-\eta))R_A^2}{F(\eta)\, r_0^2} = (1-exp(-\eta))^{1/2} \sqrt{\eta}\left(\frac{R_A}{r_0}\right)^2$$

low density $\eta\left(\frac{R_A}{r_0}\right)^2 , N_A^{4/3}, exp(2\lambda y)$

high density $\sqrt{\eta}\left(\frac{R_A}{r_0}\right)^2 , N_A, exp(\lambda y)$

$$CGC \quad \frac{1}{\alpha_s} R_A^2 Q_s^2 \ , \ N_A \ , \ exp(\lambda y)$$

rapidity extension

$$\Delta y_M = \Delta y_1 + 2 \ln N_A \quad , \qquad \ln N_A \ , \ \ln s$$

$$CGC \quad \frac{1}{\alpha_s} \qquad \ln N_A \ , \ \ln s$$

$$\kappa = \frac{< N >^2}{< N^2 > - < N >^2}$$

low density $k \to \infty$

high density $k \to \infty$

$$k = \frac{< N >}{(1 - exp(-\eta))^{3/2}}$$

high density $\sqrt{\eta}\left(\frac{R_A}{r_0}\right)^2, N_A, exp(\lambda\gamma)$

low density $\frac{1}{\sqrt{\eta}}\left(\frac{R_A}{r_0}\right)^2$

$CGC \quad k = R_S^2 Q_s^2, N_A, exp(\lambda\gamma)$

MULTIPLICITY DISTRIBUTIONS

NEGATIVE BINOMIAL

(k_0, single effective string)

low density $k = \langle N \rangle k_0$ Poisson

high density Bose-Einstein

$C\ G\ C^{k \to \infty,\ k_0 \to \infty} = 1$ $B : E$, $k = \langle N \rangle$

k first decreases with density (energy)

Above an energy(density) k increases $k \to \infty,\ k_0 \to 1$

$\Rightarrow$ Multiplicity distributions (normalized,

i.e. $\langle n \rangle P_n$ as a function of $n / \langle n \rangle$

will be narrower (Quantum Optical prediction)

$$b = \frac{1}{1 + \frac{d}{(1 - e^{-\eta})^{3/2}}}$$

low density $b \to 0$

high density (energy) $b \to 1/(1+d)$

CGC $b = \frac{1}{1 + \alpha_s^2 c}$

high density (energy) $b \to 1$

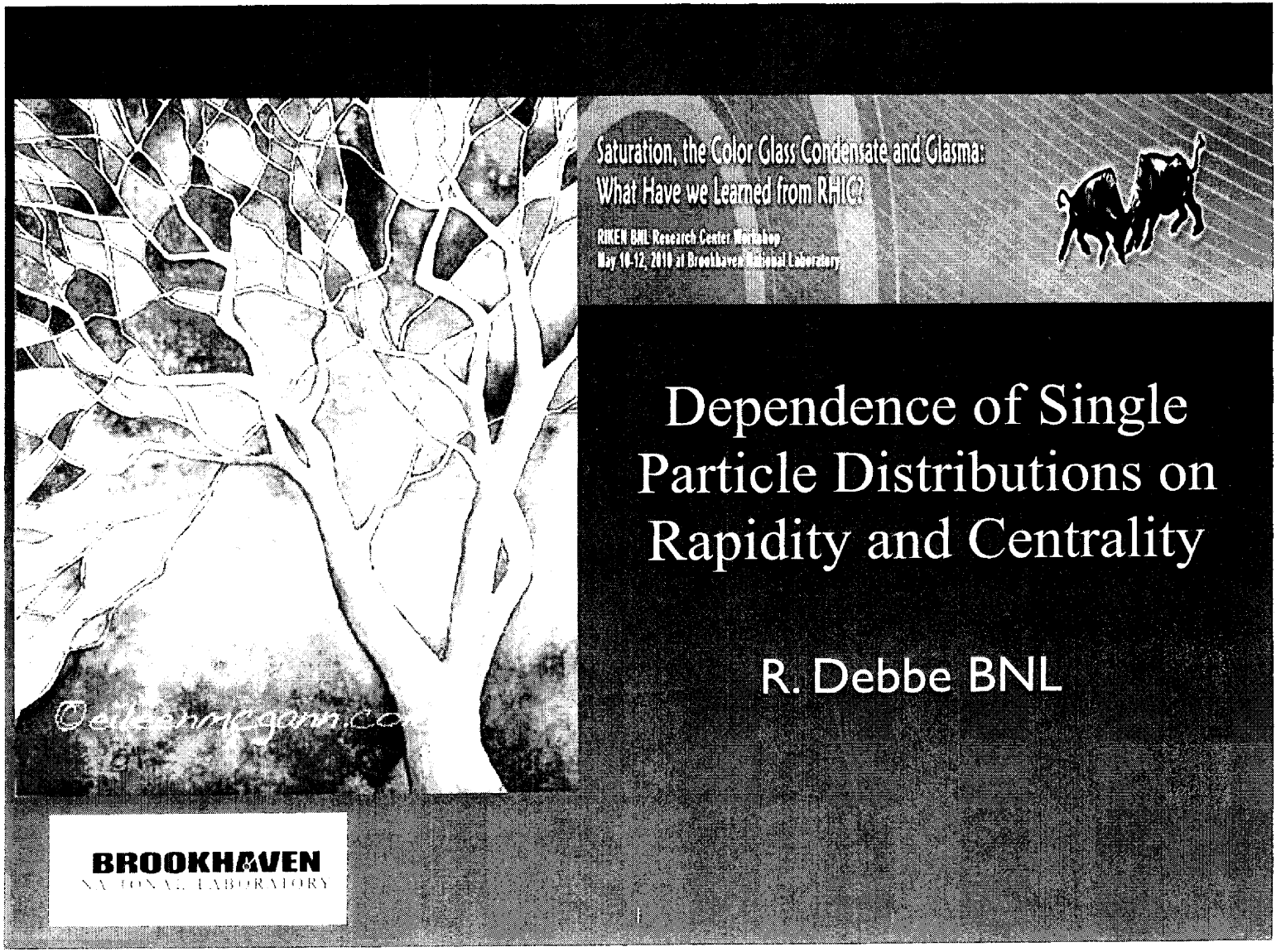
Saturation, the Color Glass Condensate and Glasma:
What Have we Learned from RHIC?
RIKEN BNL Research Center Workshop
May 10-12, 2010 at Brookhaven National Laboratory
Dependence of Single Particle Distributions on Rapidity and Centrality
R. Debbe BNL
BROOKHAVEN
NATIONAL LABORATORY

Summary

- d+Au collisions at RHIC have been studied thoroughly specially near y=0.
- Cronin enhancement seen at mid-rapidity.
- Enhancement depends on centrality of collisions.
- Protons show stronger enhancement.
- All mesons behave similarly as pions.
- NMFs of pions and kaons show similar suppression at high rapidity.
- NMF of protons and anti-protons shows suppressions as function of rapidity but also a competing Cronin type enhancement.

PHENIX Cronin at y=0 as function of centrality

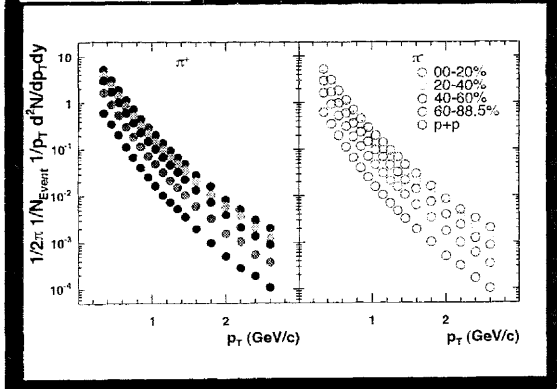

Calculations using a pQCD model of multiple semi-hard collisions and taking geometrical shadowing into account describe well the pion R_{dAu}

A. Accardi and M. Gyulassy, Phys. Lett. B586, 244 (2004).

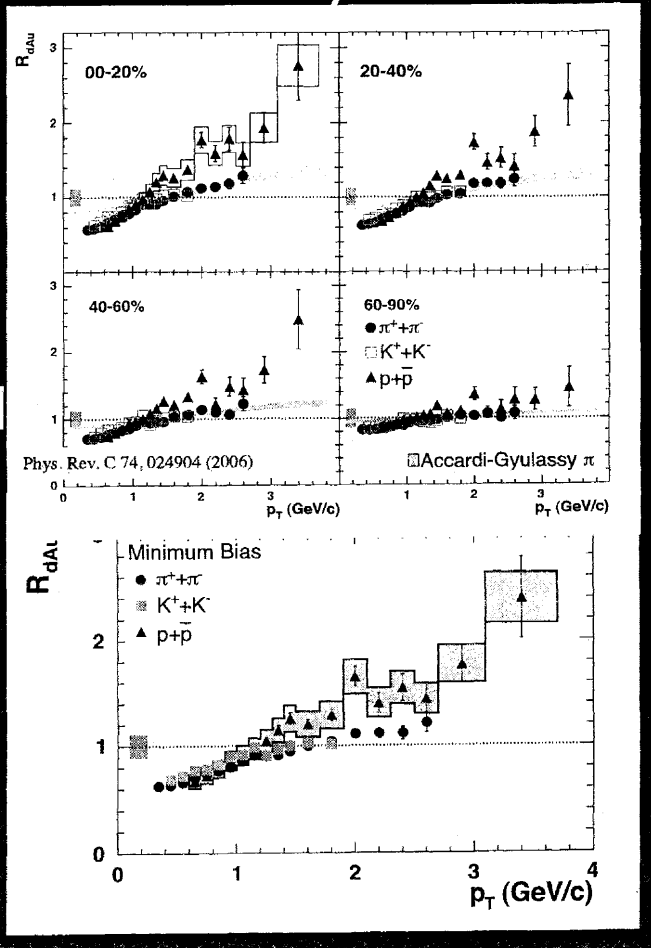

PID done with high resolution TOF, which covers $-0.35 \leq \eta \leq 0.35$ and $\Delta\varphi = \pi/8$

The proton and antiproton spectra are corrected for feed-down from weak decays via a Monte Carlo simulation using as input experimental data on Λ production.

The enhancement for protons is stronger, by approximately 30%-50% in the most central collisions

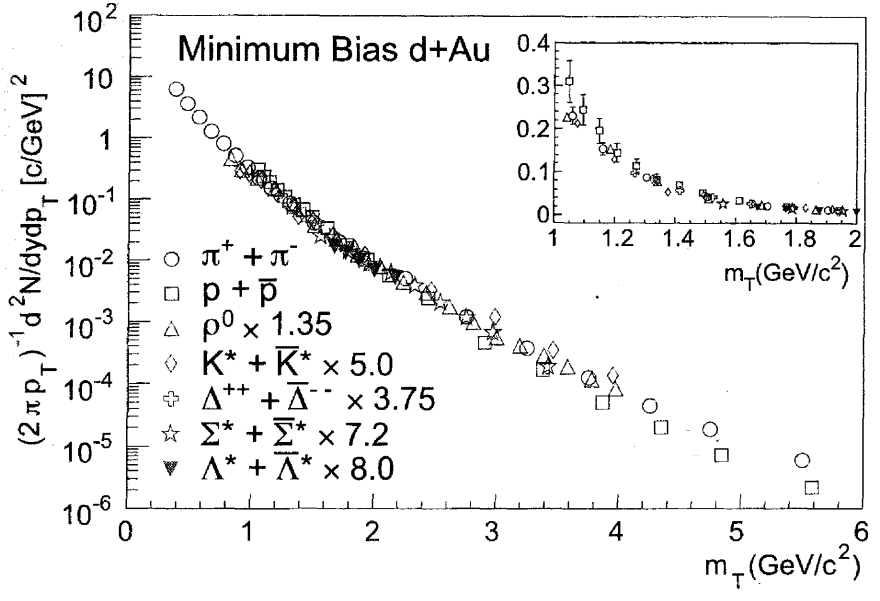

All resonances display m_T scaling and have similar R_{dAu} (consistent with pion's)

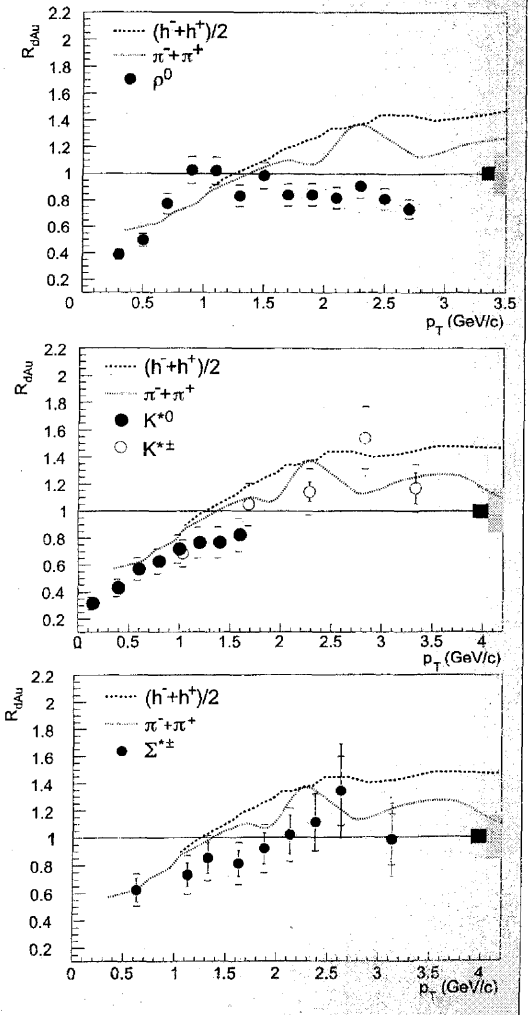

BRAHMS

R_{dAu} for pions in central collisions (0-30%)

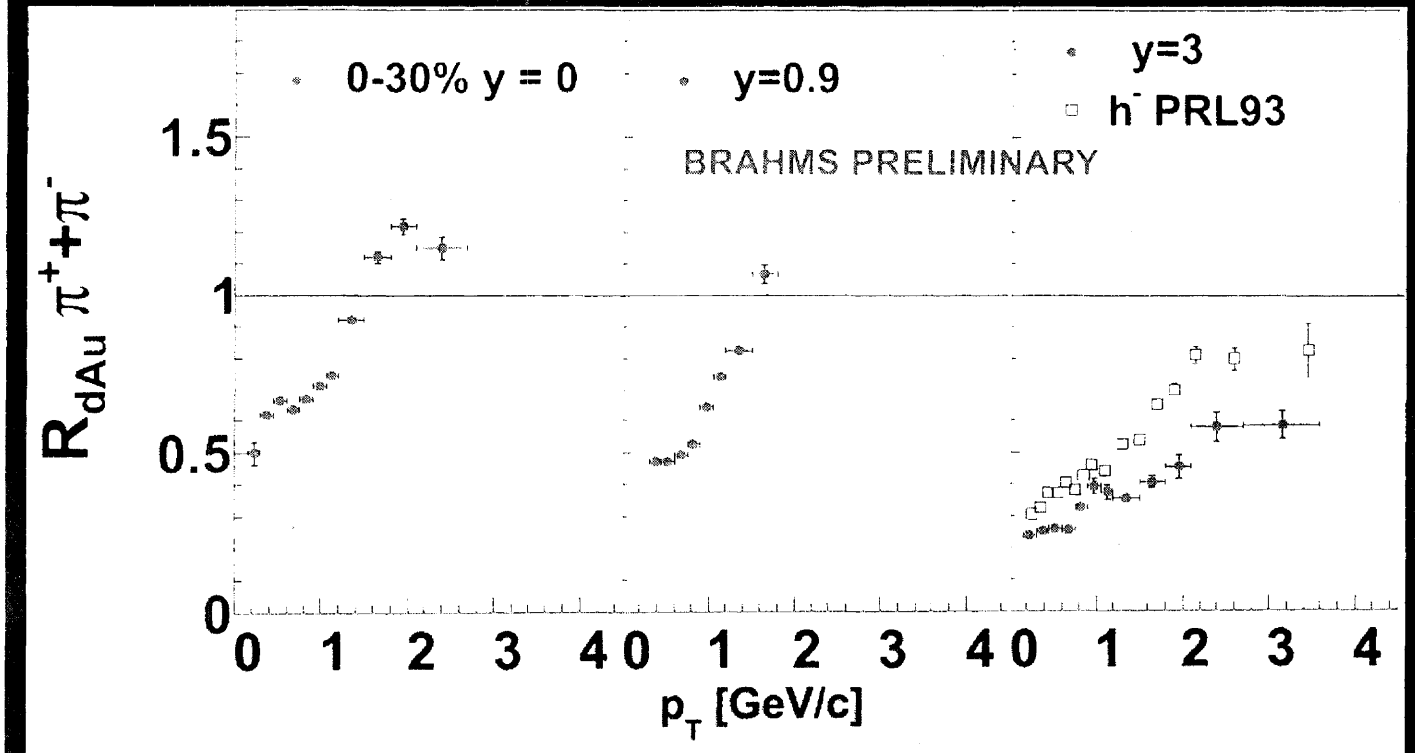

As the rapidity of the measurements increases, the growth of the cross section in the numerator slows down because of its proximity to the saturated regime (non-linear effects in quantum-evolution). Meanwhile, the cross section of the denominator (dilute p+p system) continues to increase.

5

Wednesday, May 12, 2010

BRAHMS

RdAu for Kaons in central collisions (0-30%)

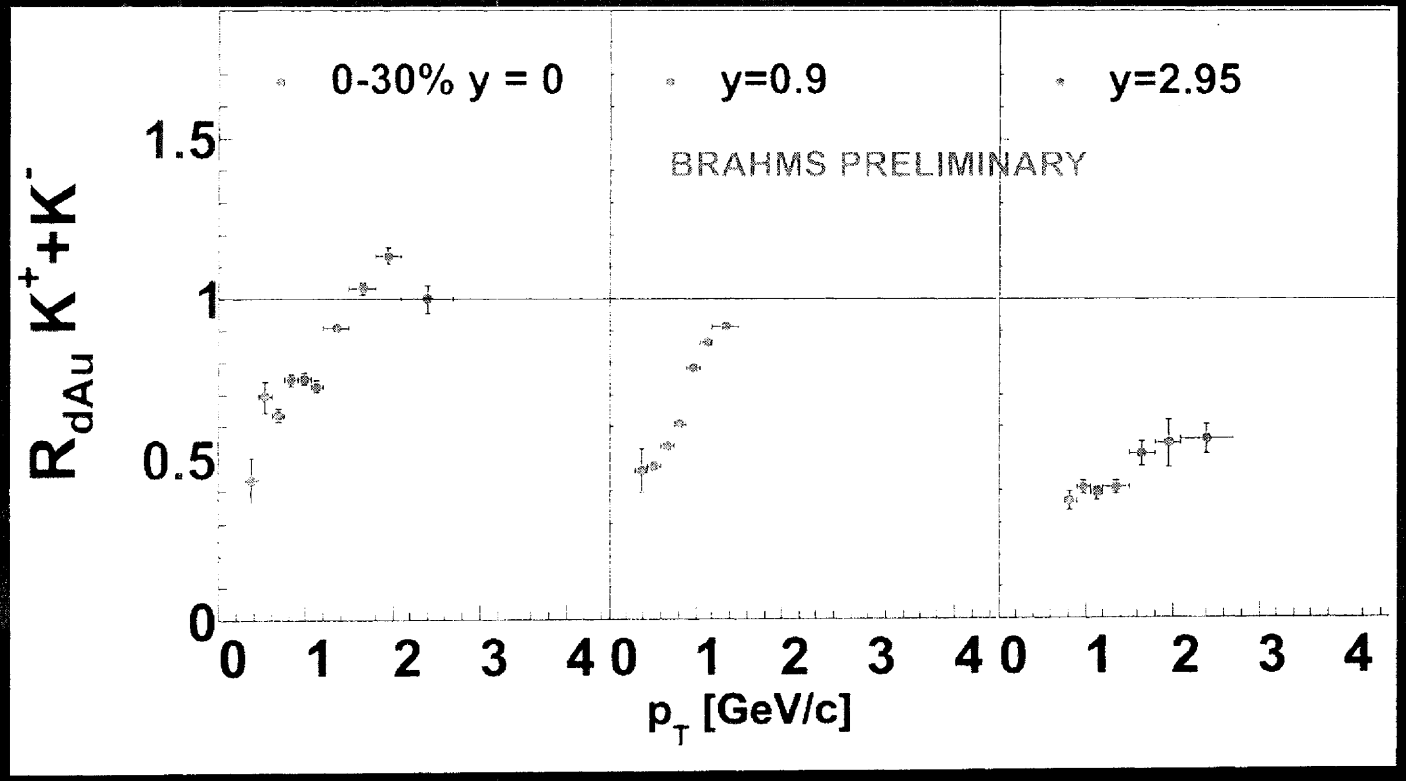

The kaons have a rapidity and centrality dependence that is very similar to the one found in pions.

BRAHMS

RdAu for protons in central collisions (0-30%)

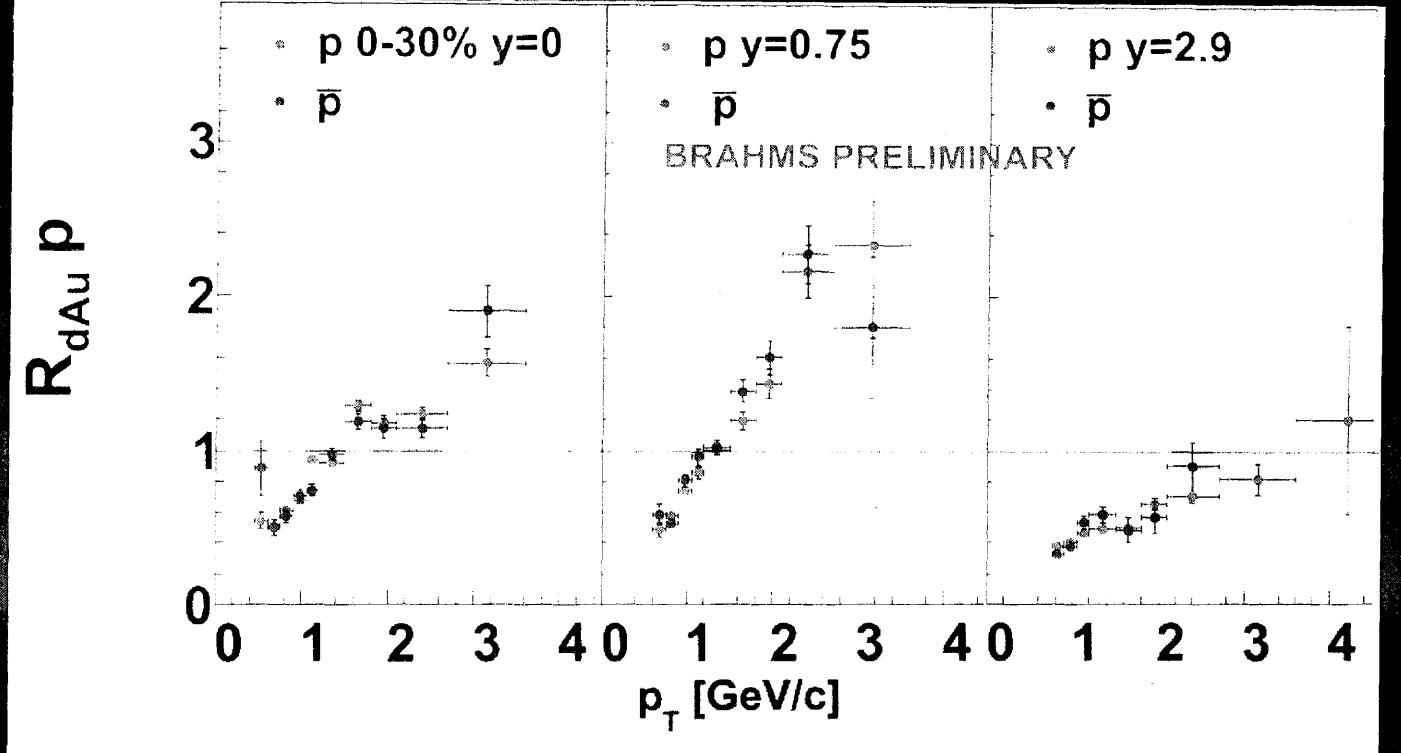

Protons have a more pronounced Cronin "peak" near mid-rapidity and they show similar behavior at high rapidity. There appears to be a shift of the peak towards higher values of transverse momentum.

Leading twist nuclear shadowing, onset of black disk regime and post selection effect for the leading hadron production

Mark Strikman, PSU

Summary

* QCD factorization theorems and use of unitarity allows to calculated nuclear shadowing for gluon and quark pdfs at $x < 0.01$ with a small theoretical uncertainty as a function of the impact parameter

* Post-selection leads to fractional energy losses in the black disk regime. It leads to explanation of the suppression of the forward pion production in D-Au collisions as due ~ 10% energy losses. It leads to dominance of peripheral collisions in the forward pion production without suppression correlation with pion production at y ~0. These predictions are consistent with the STAR data and qualitatively different from CGC inspired models where production is central and no correlation with central jet production is expected.

* Consistent evidence from analysis of HERA data and leading pion production in d- Au presence of the BDR up to transverse momenta 1 -- 1.5 GeV/c at $x \sim 10^{-4}$

* Critical test - strong suppression of the leading baryon and meson spectra at $x_F > 0.3$ in d-Au. In particular we predict that pions should dominate over nucleons at $x>0.2$ with the pion (nucleon) cross section proportional to $(1-x_F)^n$ with $n(\pi) \sim 4, n(N) \sim 6$.

Combining Gribov theory of shadowing and pQCD factorization theorem for diffraction in DIS allows to calculate LT shadowing for all parton densities (instead of calculating F_{2A} only)

Theorem: In the low thickness limit the leading twist nuclear shadowing is unambiguously expressed through the nucleon diffractive pdf's $f_j^D(\frac{x}{x_{I\!P}}, Q^2, x_{I\!P}, t)$:

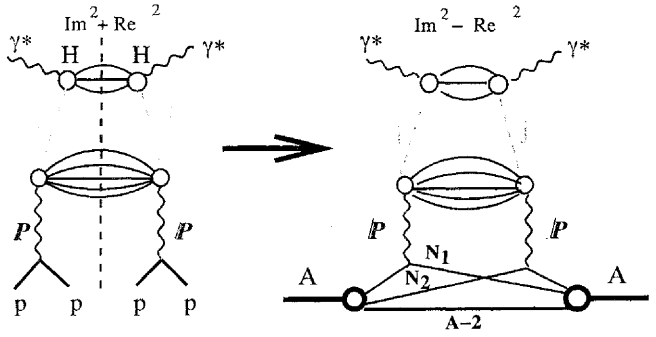

Hard diffraction off parton "j"

Leading twist contribution to the nuclear shadowing for structure function $f_j(x,Q^2)$

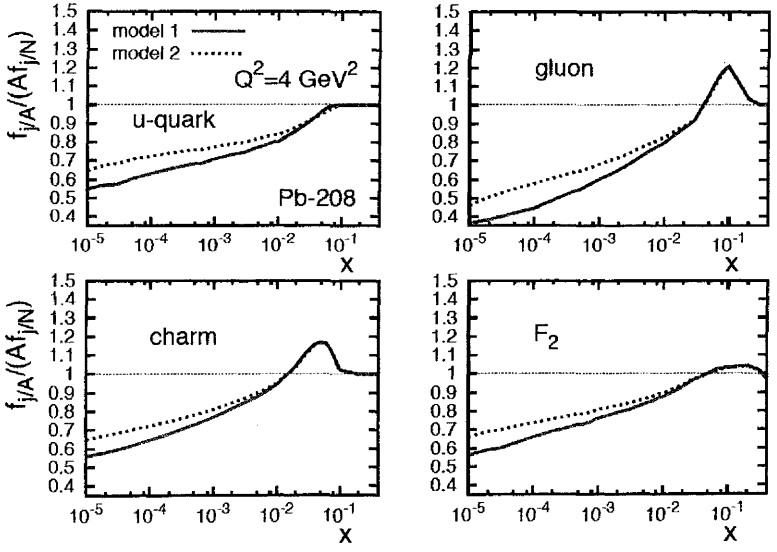

Predictions of the LT theory of nuclear shadowing for pdfs of Pb at Q^2= 4 GeV^2

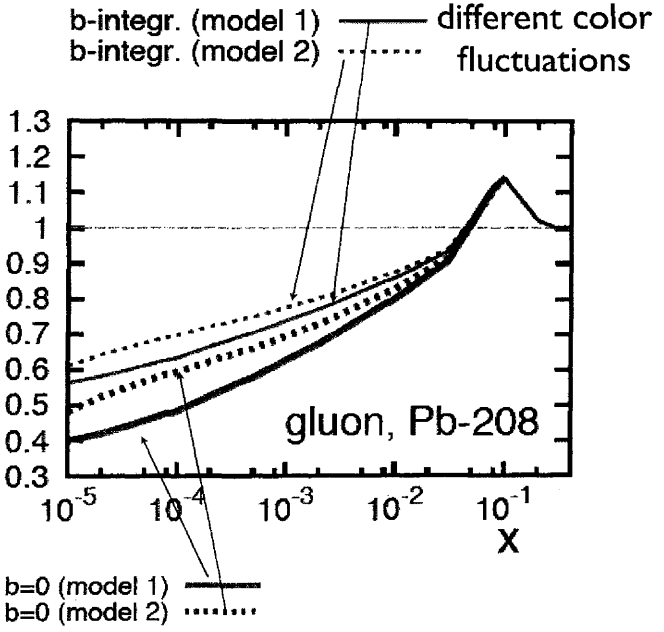

Impact factor Γ(b) for quark - antiquark dipole p/Pb scattering

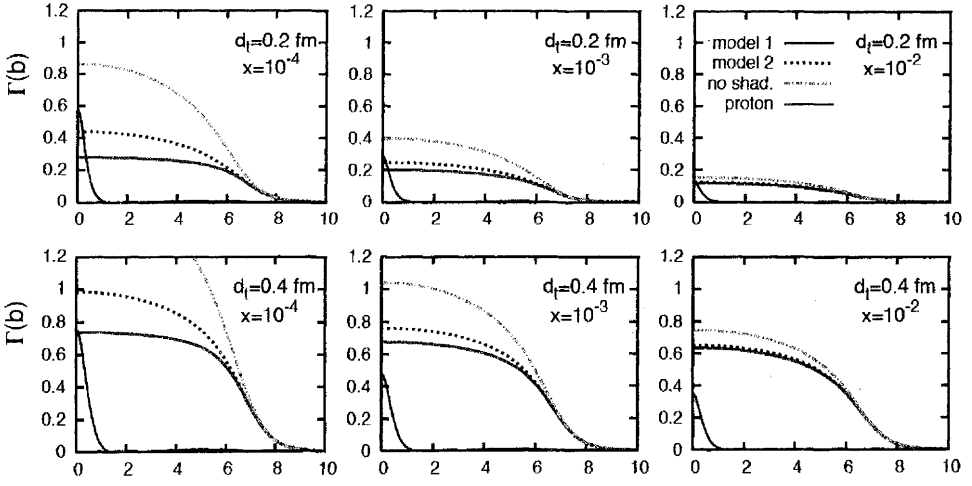

Update of Rogers et al 03

$$p_t \approx \frac{\pi}{d}$$

$$p_t \approx 1.5\,GeV/c$$

$$p_t \approx 0.75\,GeV/c$$

Probability of inelastic interaction is

$P_{in} = |1-\Gamma(b)|^2 \rightarrow P_{in}=3/4$ for $\Gamma(b)=1/2$

Gluon densities in nuclei and proton at b=0 are rather similar. However very few processes with proton are sensitive to b=0 not <b> while in nuclei it is trivial to select range of b with practically the same Γ(b).

Two possible explanations both based on presence of high gluon field effects

Color Glass Condensate inspired model

Assumes that the process is dominated both for a nucleus and nucleon target by the scattering of partons with minimal x allowed by the kinematics: $x \sim 10^{-4}$ in a $2 \rightarrow 1$ process.

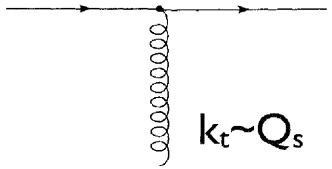

Two effects - (i) density is smaller than for the incoherent sum of participant nucleons by a factor N_{part}, (ii) enhancement due to increase of k_t of the small x parton: $k_t \sim Q_s$. → Overall dependence on N_{part} is $(N_{part})^{0.5}$, collisions with high p_t trigger are more central than the minimal bias events, no recoil jets in the kinematics expected in pQCD.

$\Rightarrow$ dominant yield from central impact parameters

Postselection (effective energy losses) in BDR regime - usually only finite energy losses discussed (BDMPS) - hence a rather small effect for partons with energies 10^4 GeV in the second nucleus rest frame. Not true in BDR - post selection - energy splits before the collision - effectively 10- 15 % energy losses decreasing with increase of k_t

$\Rightarrow$ dominant yield from peripheral impact parameters

To use information about central rapidities in a detailed way we used the relevant information from dAu BRAHMS analysis. Results are not sensitive to details.

We confirm that pion production is strongly dominated by peripheral collisions, and that there is no significant suppression of dijet mechanism for forward -central correlation.

For central impact parameters suppression is by a factor> 5, which requires energy losses of >10% (1TeV in gold rest frame)

Since the second jet has much smaller longitudinal momentum than the jet leading to the forward pion production it propagates in a much more pQCD like regime with much smaller energy losses, and hence does not affect the rate of correlation. If the energy losses were fractional but energy independent this would not be the case.

Test of our interpretation- ratio, R, of soft pion multiplicity at y ~0 with π^0 trigger and in minimal bias events.

In CGC scenario R ~ 1.3

In BDR energy loss scenario we calculated R ~ 0.5

STAR - R ~0.5 Gregory Rakness - private communication

Further confirmation - forward -central correlation data reported by STAR and PHENIX at QM 09

Single particle distributions, leading twist and beyond

Javier L. Albacete

IPhT CEA/Saclay

BNL, May 2010

Saturation, the Color Glass Condensate and Glasma: What have we learned from RHIC?

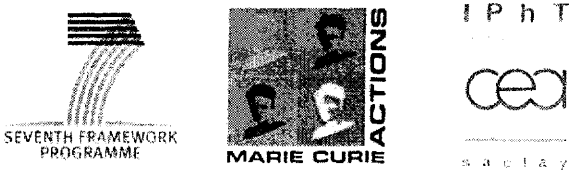

CGC evolution at NLO

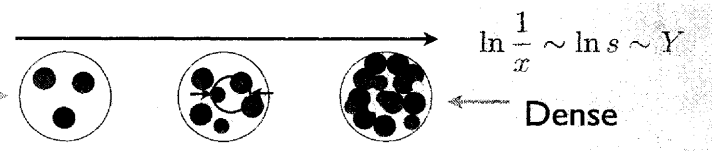

✓ NLO corrections to BK-JIMWLK equations have been calculated recently. Balitsky-Chirilli; Kovchegov-Weigert, Gardi et al.

✓ Phenomenological tool: The BK equation including only running coupling corrections in Balitsky's scheme grasps most of the NLO corrections (JLA-Kovchegov)

BK eqn: $$\frac{\partial \mathcal{N}(r,x)}{\partial \ln(x_0/x)} = \int d^2 r_1 \, K(r,r_1,r_2) \left[\mathcal{N}(r_1,x) + \mathcal{N}(r_2,x) - \mathcal{N}(r,x) - \mathcal{N}(r_1,x)\mathcal{N}(r_2,x)\right]$$

Running coupling kernel: $$K^{\rm run}(\mathbf{r},\mathbf{r_1},\mathbf{r_2}) = \frac{N_c\,\alpha_s(r^2)}{2\pi^2}\left[\frac{r^2}{r_1^2\,r_2^2} + \frac{1}{r_1^2}\left(\frac{\alpha_s(r_1^2)}{\alpha_s(r_2^2)} - 1\right) + \frac{1}{r_2^2}\left(\frac{\alpha_s(r_2^2)}{\alpha_s(r_1^2)} - 1\right)\right]$$

NLO corrections are large:

$$\lambda(Y) = \frac{d \ln Q_s(Y)}{dY}$$

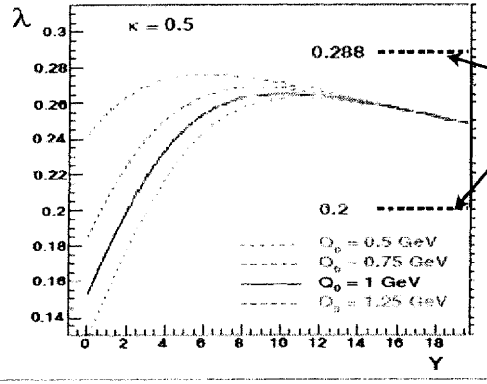

values compatible with data

$$\lambda^{LO} \approx 4.8\,\alpha_s$$

⇒ Forward hadron production in the CGC

(Dumitru, Jalilian-Marian)

large-x parton from proj. (pdf) — small-x glue from target (CGC)

$$\frac{dN_h}{dy_h\, d^2p_t} = \frac{K}{(2\pi)^2} \sum_q \int_{x_F}^1 \frac{dz}{z^2} \left[x_1 f_{q/p}(x_1, p_t^2)\, \tilde{N}_F\left(x_2, \frac{p_t}{z}\right) D_{h/q}(z, p_t^2) \right. \quad \rightarrow \text{fragmentation}$$

$$\left. + x_1 f_{g/p}(x_1, p_t^2)\, \tilde{N}_A\left(x_2, \frac{p_t}{z}\right) D_{h/g}(z, p_t^2) \right]$$

Unintegrated gluon from running coupling BK

$$\tilde{N}_{F(A)}(x,k) = \int d^2\mathbf{r}\, e^{-i\mathbf{k}\cdot\mathbf{r}} \left[1 - \mathcal{N}_{F(A)}(r, Y = \ln(x_0/x))\right]$$

MV Initial conditions:

$$\mathcal{N}(r, x = x_0) = 1 - \exp\left[-\frac{r^2 Q_0^2}{4} \ln\left(\frac{1}{r\,\Lambda} + e\right)\right]$$

JLA & C. Marquet 10

Two free parameters: (x_0, Q_0)

We use CTEQ6 pdf's and de Florian-Sassot ff's

Alternative approaches: Modelization of quantum corrections

(Dumitru-JalilianMarian-Hayashigaki; De Boer-Utermann-Wessels; Goncalves et al; Kharzeev-Kovchegov-Tuchin)

- Very good description of forward yields in d+Au collisions

- K=1 for h^-. K=0.4 for neutral pions (?)

$$0.01 \leq x_0 \leq 0.025 \qquad Q^2_{s0} = 0.4\,\mathrm{GeV}^2 \longrightarrow Q^2_{s0\,gluon} = 0.9\,\mathrm{GeV}^2$$

$$0.005 \leq x_0 \leq 0.01 \qquad Q^2_{s0} = 0.5\,\mathrm{GeV}^2 \longrightarrow Q^2_{s0,\,gluon} = 1.125\,\mathrm{GeV}^2$$

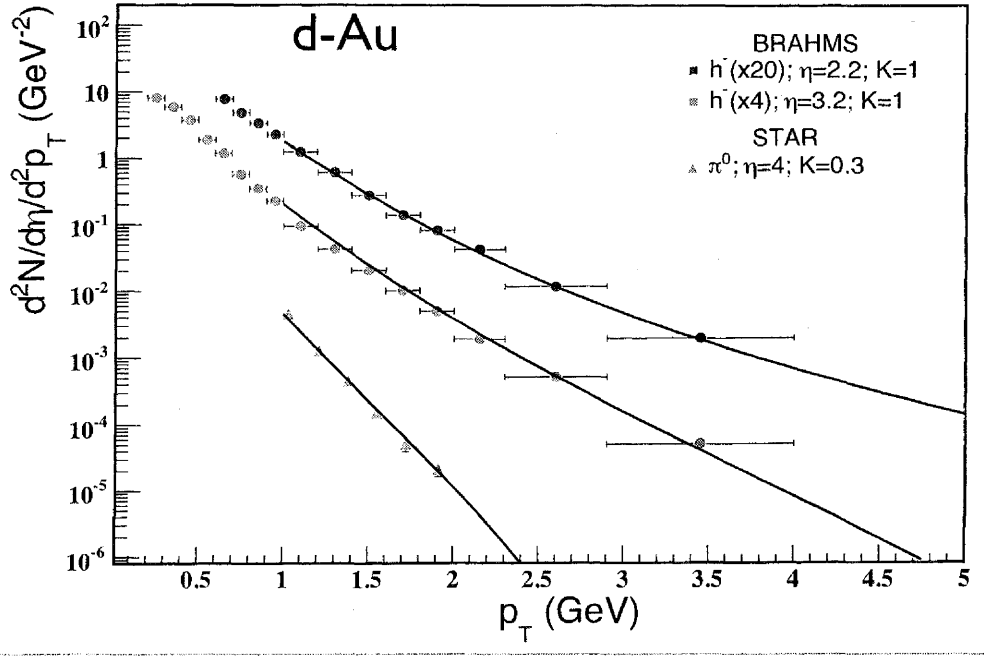

- ...by simply taking the ratio of d+Au and p+p spectra we get a good description of the nuclear modification factor (not a trivial statement!!)

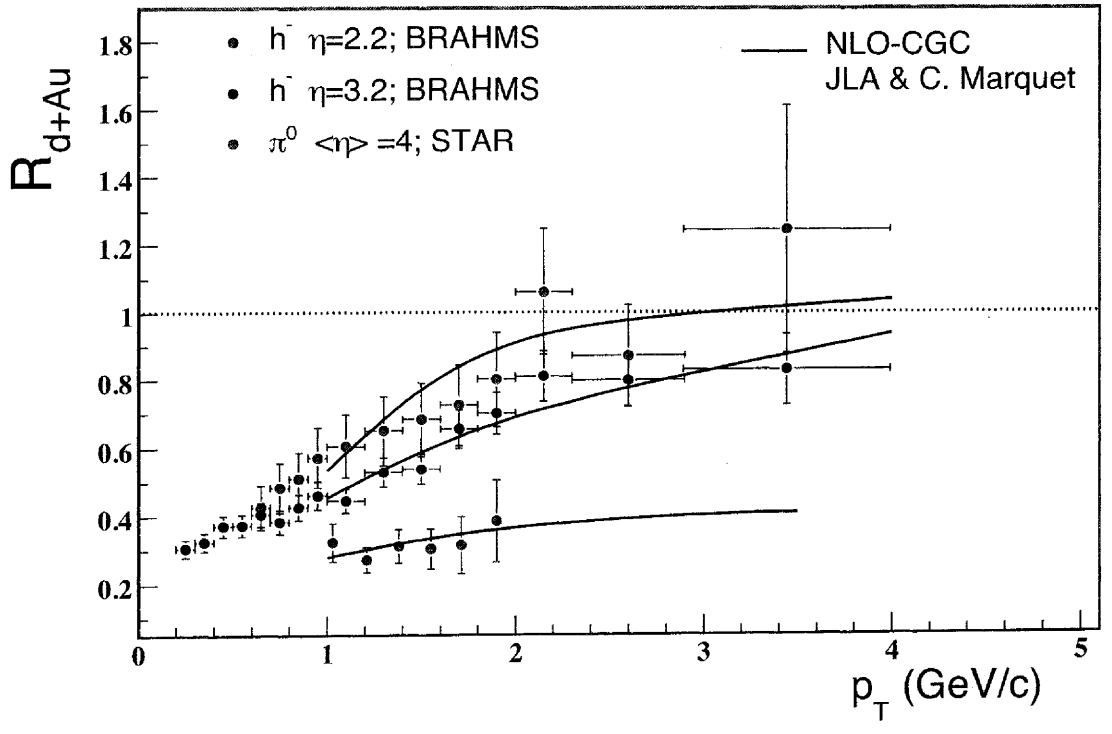

- So, is RHIC forward suppression a small-x_2 (CGC) or a large-xF (energy conservation) effect??
- p-Pb collisions at the LHC probe both the target and the projectile at small-x
- CGC calculations agree to predict a sizable suppression (~0.5) at y=0 in pPb at the LHC

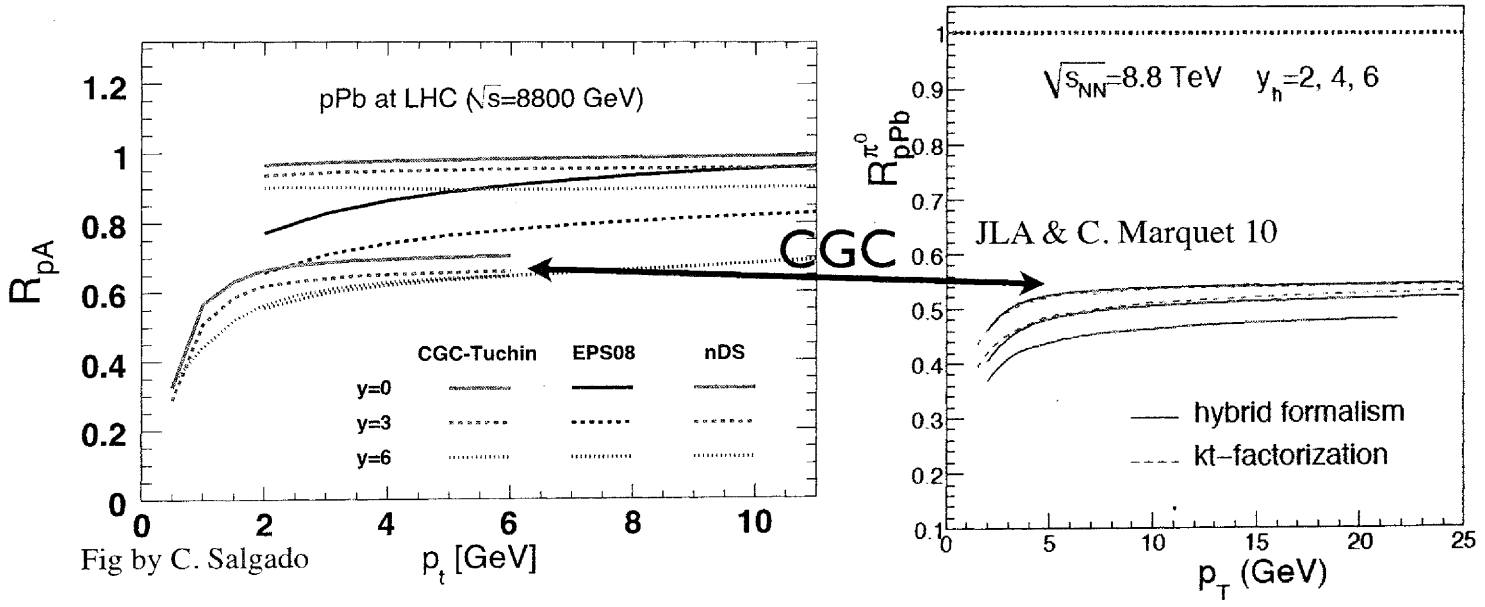

Fig by C. Salgado

Two Particle Correlations at Forward Rapidity in STAR

Ermes Braidot

for the STAR Collaboration

Utrecht University & Nikhef

During the 2008 run RHIC provided high luminosity in both p+p and d+Au collisions at $\sqrt{s_{NN}}$=200GeV. Electromagnetic calorimeter acceptance in STAR was enhanced by the new Forward Meson Spectrometer (FMS), and is now almost contiguous from $-1<\eta<4$ over the full azimuth. This large acceptance provides sensitivity to the gluon density in the nucleus down to $x\approx10^{-3}$, as expected for $2\rightarrow2$ parton scattering. Measurements of the azimuthal correlation between a forward π^0 and an associated particle at large rapidity are sensitive to the low-x gluon density. Data exhibit the qualitative features expected from gluon saturation. A comparison to calculations using the Color Glass Condensate (CGC) model is presented.

RBRC workshop 2010

Probing the medium:
azimuthal correlations

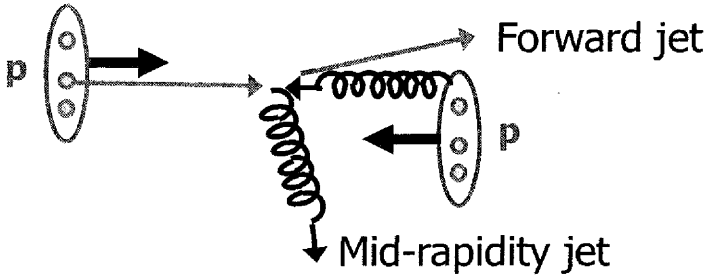

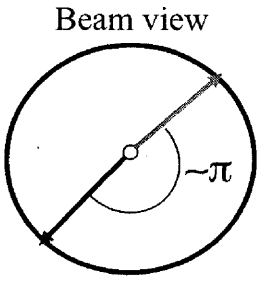

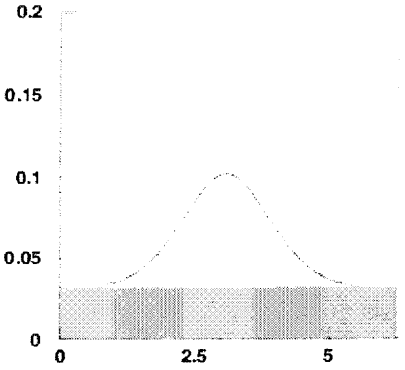

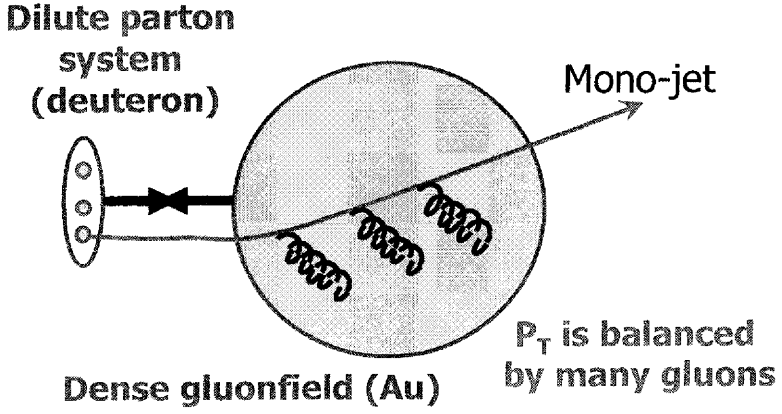

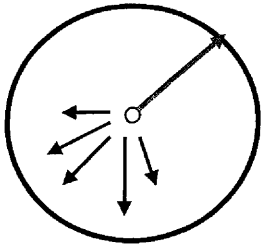

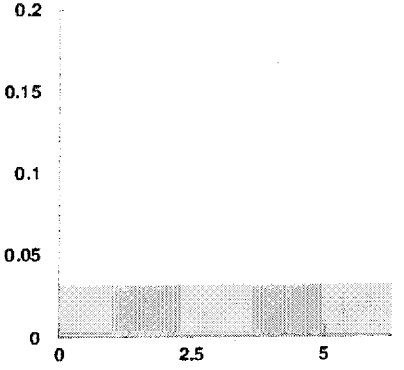

Ermes Braidot

FMS-FMS (π^0+π^0) correlations

- Forward (FMS) π^0 as trigger particle
- Forward (FMS) π^0 as associated

- Centrality averaged
- Near-side peak visible ($\Delta\eta$~0)
- Near-side peak similar p+p vs. d-Au
- Away-side signal suppression from p+p to d+Au
- Strong azimuthal broadening
- Azimuthal broadening p_T dependent:
  - above: σ_{dAu}-σ_{pp}= 0.11±0.06
  - below: σ_{dAu}-σ_{pp}= 0.52±0.05

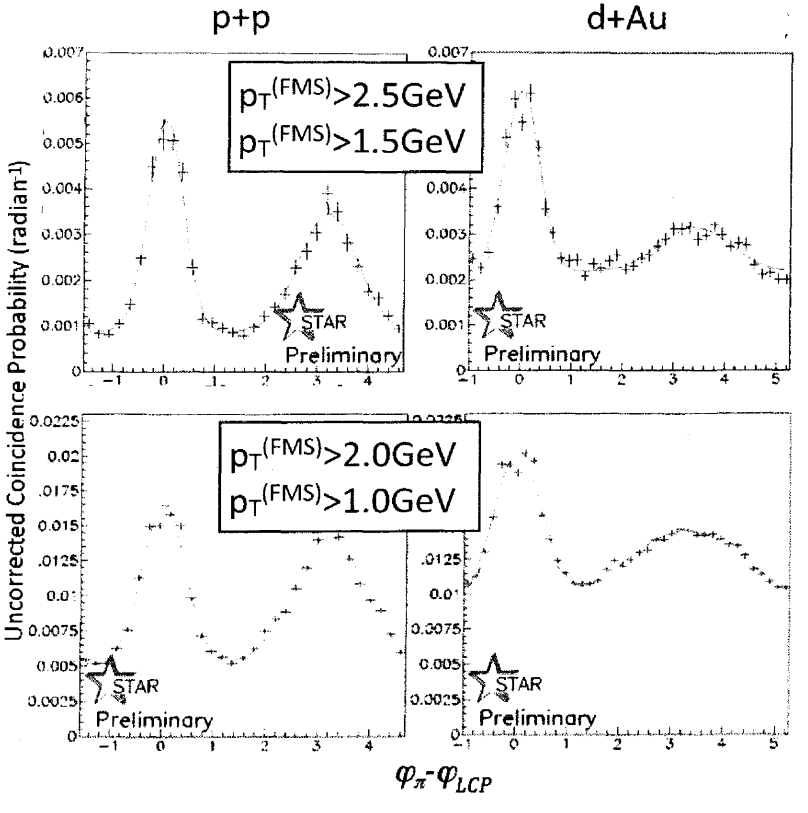

Ermes Braidot

Centrality dependence

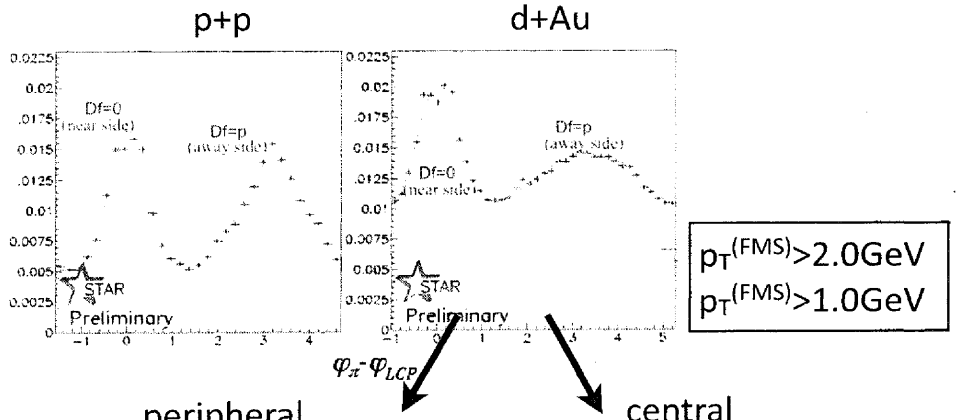

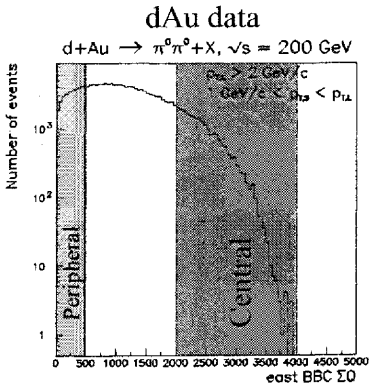

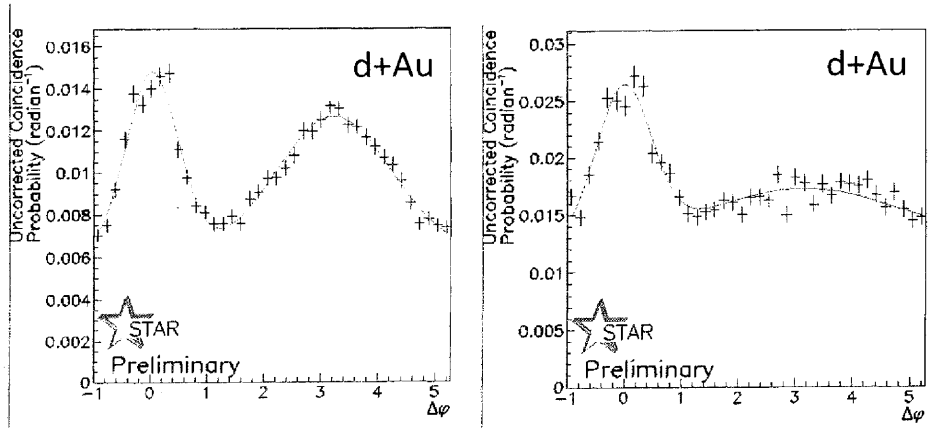

- Near-side peak similar p+p vs. d-Au
- Away-side signal changing with centrality:
- Peripheral d+Au collisions similar to p+p
- Central d+Au collision show strong suppression

Ermes Braidot

Theory comparison: CGC

- Cyrille Marquet: **arXiv:0708.0231**
  - calculation: central collisions b=0
  - data: central collision <b>=2.7fm
  - $\eta_{trg} = 3.0$; $\eta_{asso} = 3.0$
  - $x_g \sim 0.002$
  - uncorrelated background offset
  - normalization fixed from inclusive

- More CGC calculations show:
  - away-side peak disappearance for central d+Au collisions
  - de-correlations are p_T dependent
  - de-correlations are centrality dependent
  - near-side peak unchanged in d+Au

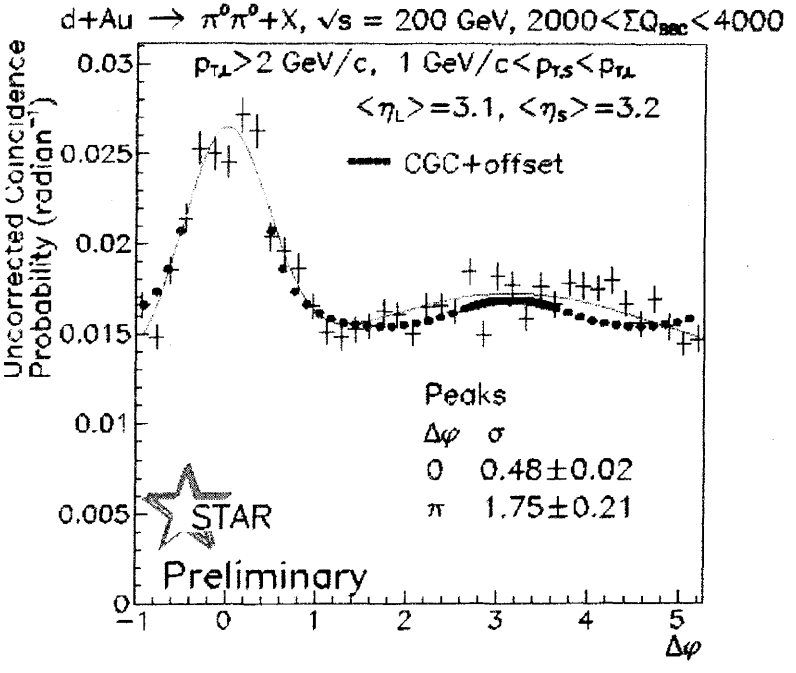

Ermes Braidot

Conclusions

- RHIC run-8 provided large d+Au data set
- **Strong suppression of away-side peak in central d+Au collisions compared to p+p (FMS-FMS)**
- CGC expectations of away-side peak suppression for central d+Au collisions are qualitatively consistent with data
- Is the CGC a unique explanation?

Signatures of Color Glass Condensate: Forward Azimuthal Angle Di-Hadron Correlations in PHENIX

Beau Meredith
University of Illinois at Urbana-Champaign
For the *PHENIX* Collaboration

Di-hadron azimuthal angle correlation functions using the PHENIX forward rapidity ($3.1 < \eta < 3.9$) EMCal (Muon Piston Calorimeter or MPC) are shown for the 2008 RHIC d+Au, p+p $\sqrt{s_{NN}} = 200\ GeV$ datasets. At forward rapidities, the correlation functions are expected to be sensitive to gluon saturation effects because one can probe very low momentum fraction, x, of the partons and thus enhance the saturation scale, Q_s. Signatures of gluon saturation are the broadening or disappearance of the away-side (di-jet) peak in the correlation functions.

Rapidity separated correlation functions with $\Delta\eta = 3.4$ where one particle is a forward π^0 in the MPC are shown for p+p and d+Au. Within systematic and statistical uncertainties, no broadening is seen; however, a large suppression is seen in central d+Au collisions relative to p+p in the conditional yield of the away-side peak (as seen by $I_{dA} = 0.5$), indicating a di-jet suppression.

Additionally, correlation functions where both particles are π^0 detected in the forward MPC are shown. The away-side peak in these correlation functions probes extremely small x ($\sim 10^{-3}$) and is predicted to be the most sensitive to saturation effects. The comparison of correlation functions in d+Au to p+p seem to show both a broadening and disappearance of the away-side peak, which could indicate that we are seeing strong effects from the color glass condensate.

$\Delta\eta$ = 3.4 Correlations: Widths

- No significant broadening between p+p and d+Au within large experimental uncertainties

Trigger π^0: $|\eta| < 0.35$, $2.0 < p_T < 3.0$ GeV/c

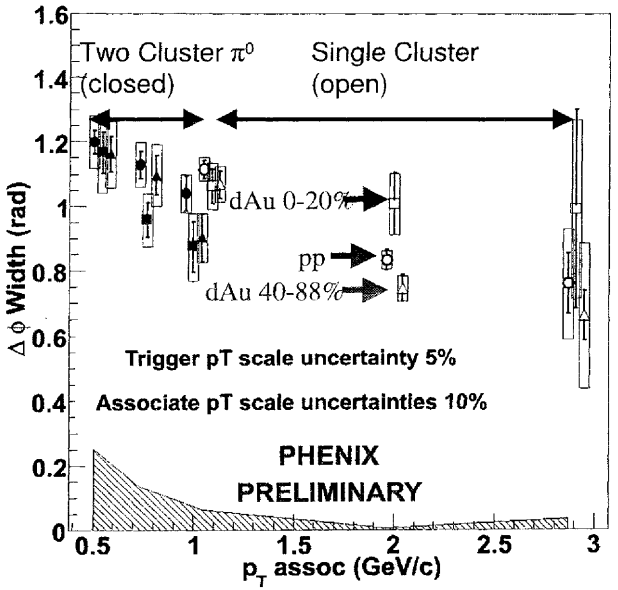

Trigger π^0: $|\eta| < 0.35$, $3.0 < p_T < 5.0$ GeV/c

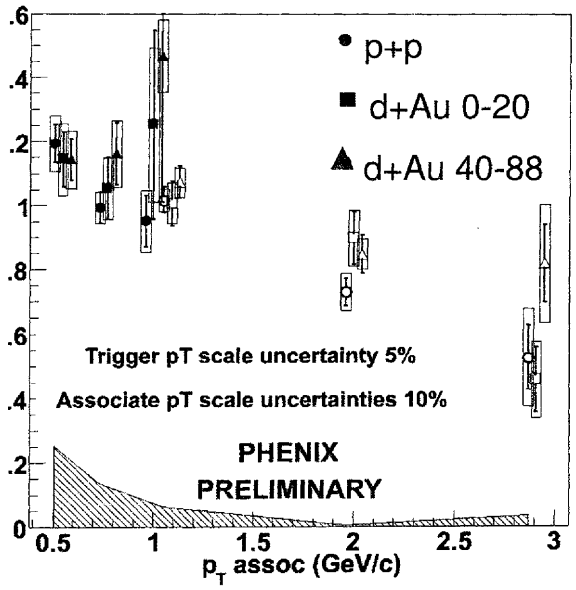

B. Meredith, Quark Matter 2009, arXiv:0907.4832

$\Delta\eta = 3.4$ Correlations: I_{dA}

- I_{dA} for central triggered events for reconstructed π^0
- Increasing suppression of I_{dA} reaches a factor 2 for central events
- Indicates di-jet suppression

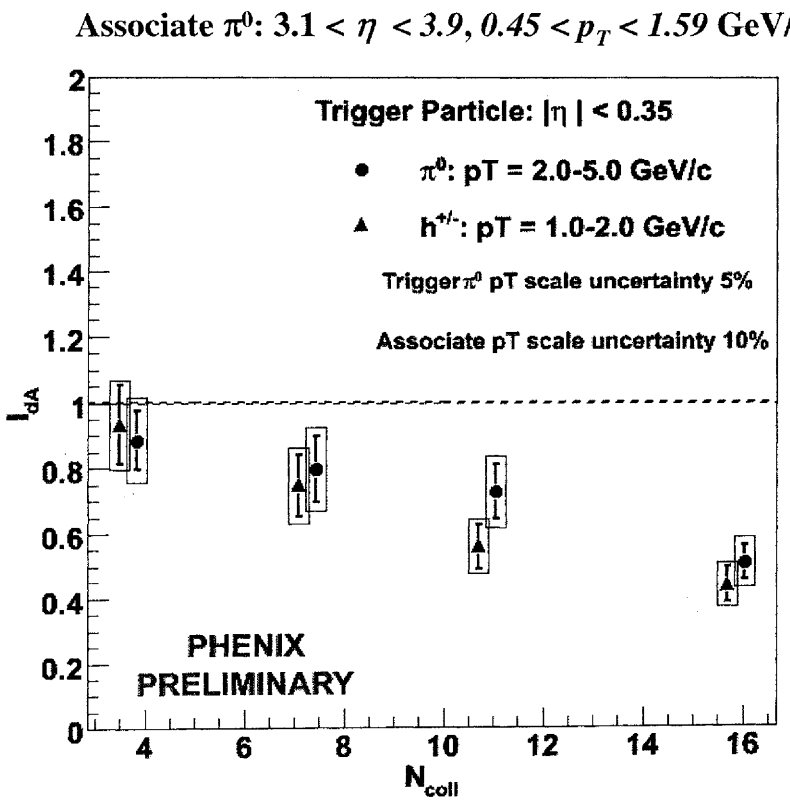

B. Meredith, Quark Matter 2009, arXiv:0907.4832

η_{trig}, η_{assoc} = 3.1-3.8; p+p vs d+Au MinBias

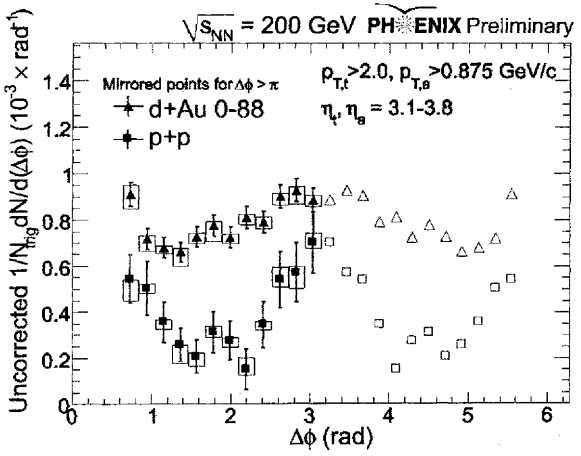

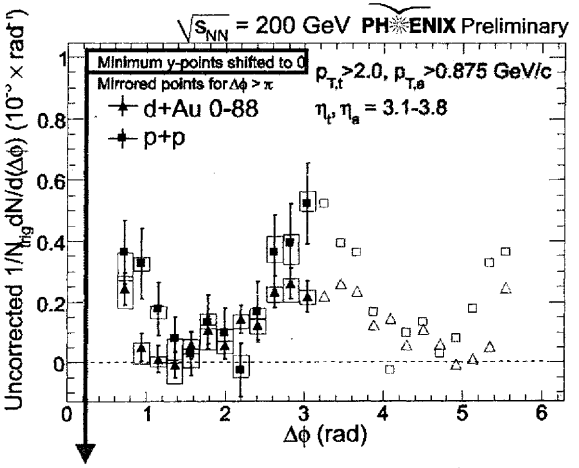

Shift minimum y-values to 0 (for comparison only)

Data qualitatively indicates angular decorrelation of d+Au compared to p+p

It also appears that there is a suppressed conditional yield in d+Au vs. p+p

η_{trig}, η_{assoc} = 3.1-3.8; d+Au Peripheral, p+p

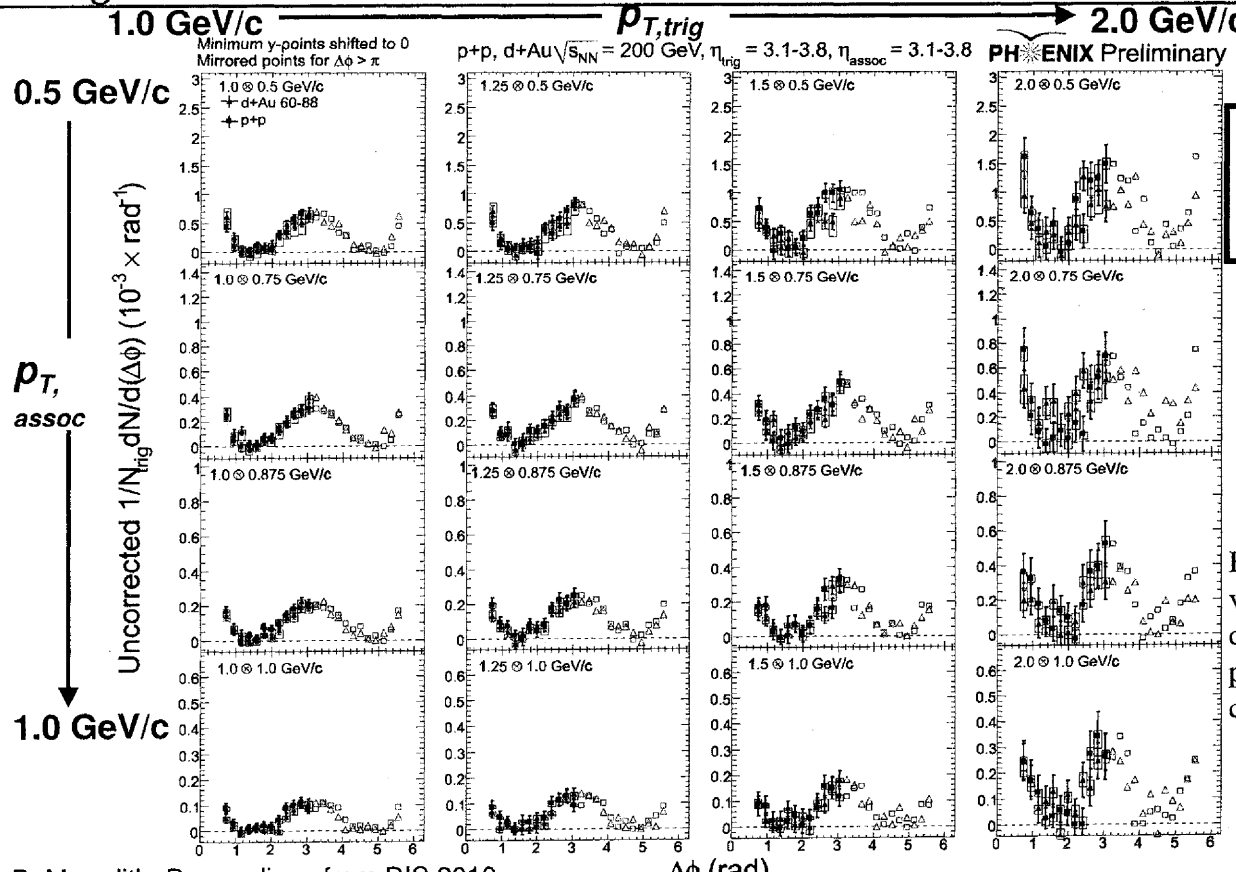

p+p and d+Au periph. are very similar

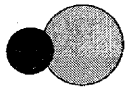

Beam view of d+Au periph. collision

η_{trig}, η_{assoc} = 3.1-3.8; d+Au Central, p+p

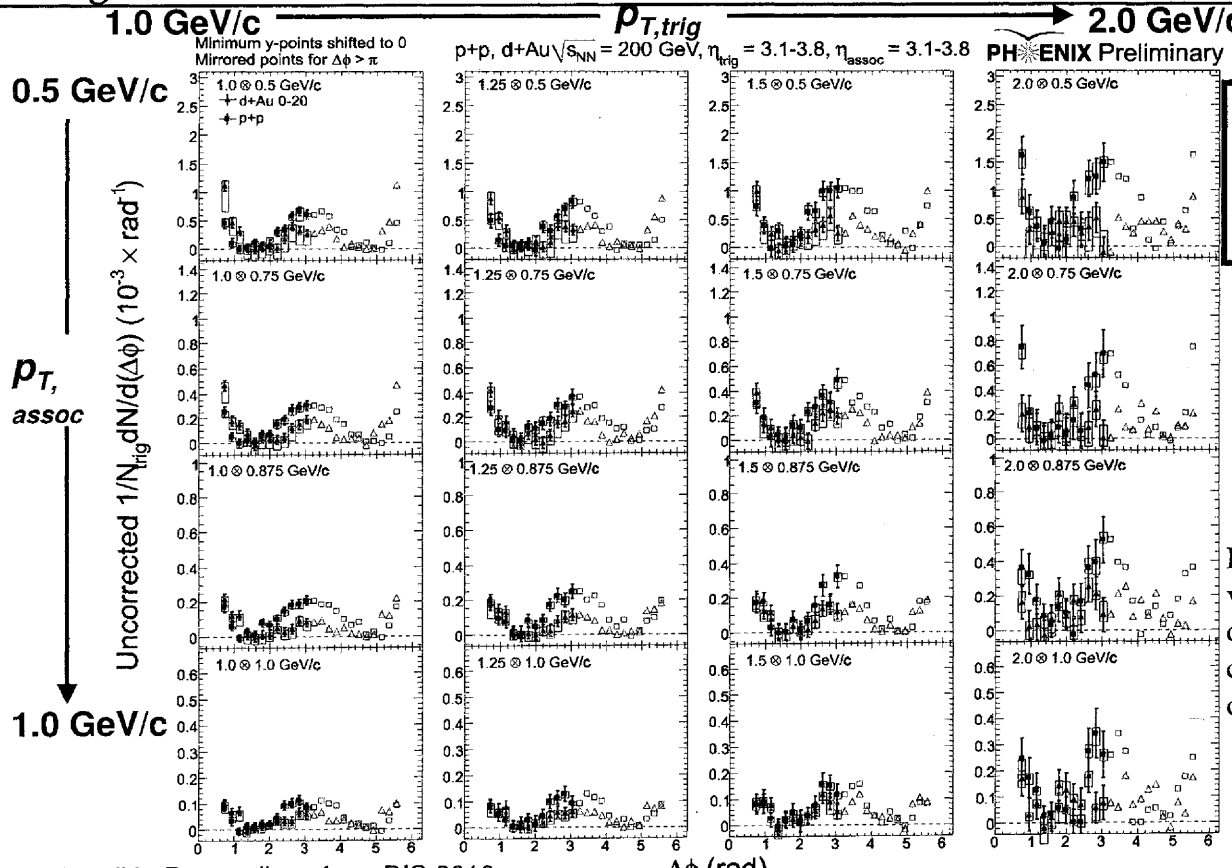

d+Au central away-side peak seems to disappear

Beam view of d+Au central collision

Forward di-hadron correlations in d+Au collisions

The STAR collaboration has recently measured the azimuthal correlation function of forward di-pions. The data show a disapearance of the away-side peak in central d+Au collisions, compared to p+p collisions. We argue that this effect, absent at mid-rapidity, is a consequence of the small-x evolution into the saturation regime of the Gold nucleus wave function, and we show that the data can be quantitavely described in the Color Glass Condensate framework. This confirmation that forward monojets are produced in central d+Au collision is a concrete evidence for parton saturation.

Cyrille Marquet

Institut de Physique Théorique, CEA/Saclay

Parton saturation

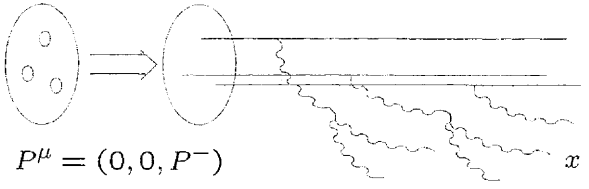

x : parton longitudinal momentum fraction

k_T: parton transverse momentum

the distribution of partons as a function of x and k_T :

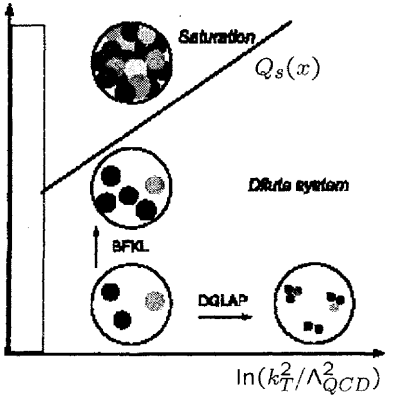

QCD linear evolutions: $k_T \gg Q_s$

DGLAP evolution to larger k_T (and a more dilute hadron)
BFKL evolution to smaller x (and denser hadron)

dilute/dense separation characterized by the saturation scale $Q_s(x)$

QCD non-linear evolution: $k_T \sim Q_s$ meaning $x \ll 1$

$\rho \sim \frac{xf(x,k_\perp^2)}{\pi R^2}$ gluon density per unit area
it grows with decreasing x

$\sigma_{rec} \sim \alpha_s/k^2$ recombination cross-section

recombinations important when $\rho\ \sigma_{rec} > 1$

the saturation regime: for $k^2 < Q_s^2$ with $Q_s^2 = \frac{\alpha_s x f(x,Q_s^2)}{\pi R^2}$

this regime is non-linear
yet weakly coupled
$\alpha_s(Q_s^2) \ll 1$

Di-hadron final-state kinematics

final state : $k_1, y_1 \quad k_2, y_2$ $\quad x_p = \frac{k_1 e^{y_1} + k_2 e^{y_2}}{\sqrt{s}} \quad x_A = \frac{k_1 e^{-y_1} + k_2 e^{-y_2}}{\sqrt{s}}$

- scanning the wave-functions

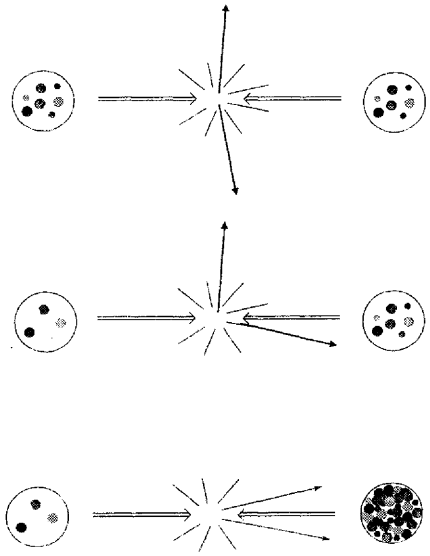

$x_p \sim x_A < 1$

central rapidities probe moderate x

x_p increases | x_A ~ unchanged

$x_p \sim 1, x_A < 1$

forward/central doesn't probe much smaller x

x_p ~ unchanged | x_A decreases

$x_p \sim 1, x_A << 1$

forward rapidities probe small x

Evidence of monojets

p+p

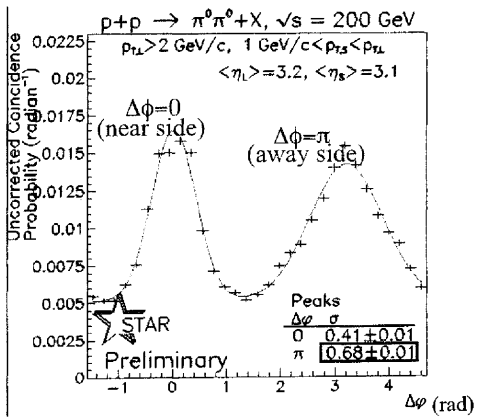

d+Au central

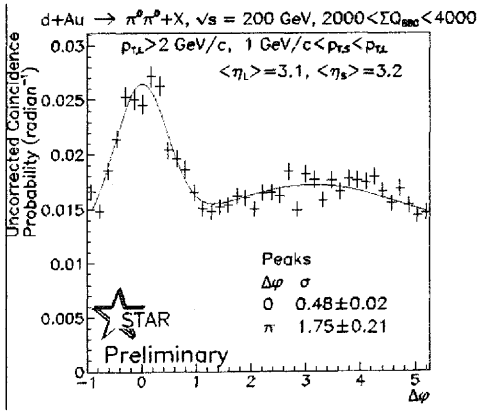

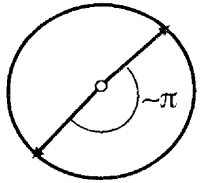

transverse view

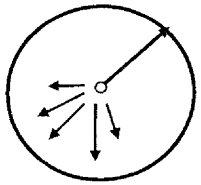

Forward di-jet production

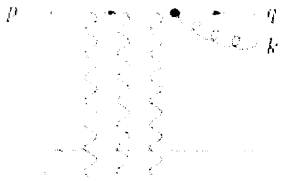

b: quark in the amplitude
x: gluon in the amplitude
b': quark in the conj. amplitude
x': gluon in the conj. amplitude

collinear factorization of quark density in deuteron

Fourier transform $k_\perp$ and $q_\perp$ into transverse coordinates

$$\frac{d\sigma^{dAu\to qgX}}{d^2k_\perp dy_k d^2q_\perp dy_q} = \alpha_S C_F N_c\, x_d q(x_d,\mu^2) \int \frac{d^2x}{(2\pi)^2}\frac{d^2x'}{(2\pi)^2}\frac{d^2b}{(2\pi)^2}\frac{d^2b'}{(2\pi)^2}\, e^{ik_\perp\cdot(\mathbf{x}'-\mathbf{x})} e^{iq_\perp\cdot(\mathbf{b}'-\mathbf{b})}$$

$$\left|\Phi^{q\to qg}(z,\mathbf{x}-\mathbf{b},\mathbf{x}'-\mathbf{b}')\right|^2 \Big\{ S^{(4)}_{qg\bar{q}g}[\mathbf{b},\mathbf{x},\mathbf{b}',\mathbf{x}';x_A] - S^{(3)}_{qg\bar{q}}[\mathbf{b},\mathbf{x},\mathbf{b}'+z(\mathbf{x}'-\mathbf{b}');x_A]$$

$$\underbrace{-S^{(3)}_{\bar{q}gq}[\mathbf{b}+z(\mathbf{x}-\mathbf{b}),\mathbf{x}',\mathbf{b}';x_A] + S^{(2)}_{q\bar{q}}[\mathbf{b}+z(\mathbf{x}-\mathbf{b}),\mathbf{b}'+z(\mathbf{x}'-\mathbf{b}');x_A]\Big\}}_{\text{interaction with hadron 2 / CGC}}$$

pQCD $q \to qg$ wavefunction

$$z = \frac{|k_\perp|e^{y_k}}{|k_\perp|e^{y_k}+|q_\perp|e^{y_q}}$$

n-point functions that resums the powers of $g_S A$ and the powers of $\alpha_S \ln(1/x_A)$

computed with JIMWLK evolution at NLO (in the large-Nc limit), and MV initial conditions no parameters

Monojets in central d+Au

- in central collisions where Q_S is the biggest

there is a very good agreement of the saturation predictions with STAR data

Albacete and C.M., to appear

an offset is needed to account for the background

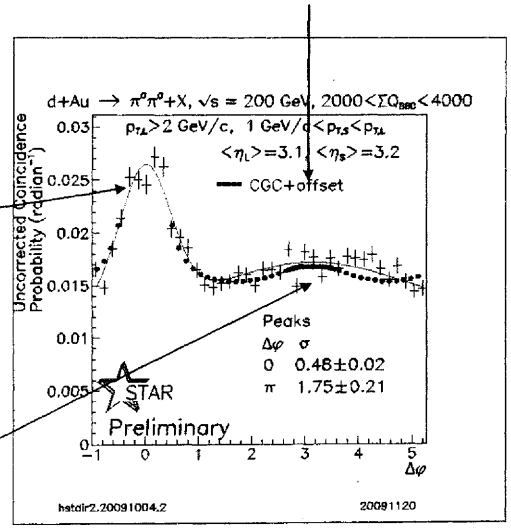

to calculate the near-side peak, one needs di-pion fragmentation functions

- the focus is on the away-side peak

where non-linearities have the biggest effect

suppressed away-side peak

standard (DGLAP-like) QCD calculations cannot reproduce this

Two Particle Correlations: Saturation and Issues with Universality

Bo-Wen Xiao

Lawrence Berkeley National Laboratory

BX and F. Yuan, arXiv:1003.0482 [hep-ph].

- We study the universality issue of the transverse momentum dependent parton distributions at small-x, by comparing the initial/final state interaction effects in dijet-correlation in pA collisions with those in deep inelastic lepton nucleus scattering. We demonstrate the non-universality by performing an explicit calculation in a particular model where the multiple gauge boson exchange contributions are summed up to all orders.
- In addition, we generalize the model calculation to the CGC formalism, and find the non-universality for quark distributions in CGC.

BNL workshop, May, 2010

Breaking down of the k_t factorization in di-jet production

- *[Bacchetta, Bomhof, Mulders and Pijlman; 04-06]* Wilson lines approach
  Studies of Wilson-line operators show that the TMD parton distributions are not generally process-independent due to the complicated combinantion of initial and final state interactions. TMD PDFs admit process dependent Wilson lines.
- *[Collins, Qiu; 07], [Collins; 07], [Vogelsang, Yuan; 07] and [Rogers, Mulders; 10]*
  Scalar QED models and its generalization to QCD (Counterexample to Factorization)

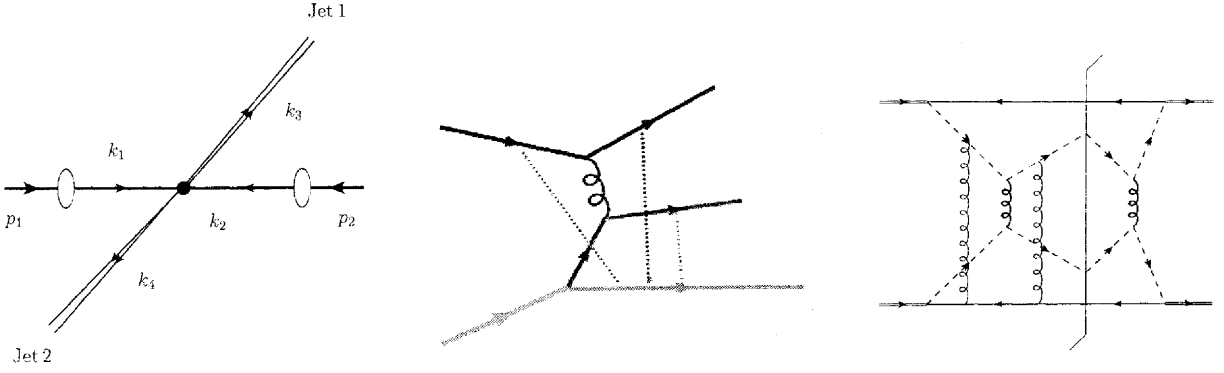

- Remarks: TMD parton distributions are non-universal.
- $\mathcal{O}(g^2)$ calculation shows non-vanishing anomalous terms with respect to standard factorization.
- Trouble? or Opportunity?
- Resummation up to all order of g including the anomalous terms*[BX, Yuan; 10]*.
- The effect of k_t factorization violation is resummable and calculable. Opportunity!

Comparison of the TMD pdfs among di-jet production, DIS and Drell-Yan

- The total amplitude $\Rightarrow$ the TMD pdf for the di-jet process *[Xiao, Yuan, 10]*

$$\begin{aligned}\tilde{q}_{\text{di-jet}}(x,q_\perp) &= \frac{xP^{+2}}{8\pi^4}\int dp^- p^- \int d^2R_\perp d^2R'_\perp d^2r_\perp e^{iq_\perp\cdot(R_\perp-R'_\perp)} \\ &\times V(r_\perp)\,V(r'_\perp)\,e^{-igg_2\left(G(R_\perp)-G(R'_\perp)\right)} \\ &\times\left\{1-e^{igg_1\left[G(R_\perp+r_\perp)-G(R_\perp)\right]}\right\}\left\{1-e^{-igg_1\left[G(R'_\perp+r'_\perp)-G(R'_\perp)\right]}\right\}.\end{aligned}$$

- TMD pdf in DIS and DY *[Brodsky, et al; 02], [Belitsky, Ji, Yuan; 03], [Peigne; 02]*

$$\begin{aligned}\tilde{q}_{\text{DIS, DY}}(x,q_\perp) &= \frac{xP^{+2}}{8\pi^4}\int dp^- p^- \int d^2R_\perp d^2R'_\perp d^2r_\perp e^{iq_\perp\cdot(R_\perp-R'_\perp)}V(r_\perp)\,V(r'_\perp) \\ &\times\left\{1-e^{igg_1\left[G(R_\perp+r_\perp)-G(R_\perp)\right]}\right\}\left\{1-e^{-igg_1\left[G(R'_\perp+r'_\perp)-G(R'_\perp)\right]}\right\}.\end{aligned}$$

  with $r'_\perp = R_\perp + r_\perp - R'_\perp$.

- Non-Universality and k_t factorization violation! However, calculable!

The Quark Distribution for a large nucleus in DIS

- TMD pdf in DIS *[Brodsky, et al; 02], [Belitsky, Ji, Yuan; 03]*

$$\begin{aligned}
\tilde{q}_{\mathrm{DIS}}\left(x,q_\perp\right) &= \frac{xP^{+2}}{8\pi^4}\int dp^- p^- \int d^2R_\perp d^2R'_\perp d^2r_\perp e^{iq_\perp\cdot\left(R_\perp-R'_\perp\right)} V\left(r_\perp\right) V\left(r'_\perp\right) \\
&\quad \times\left\{1-e^{igg_1\left[G\left(R_\perp+r_\perp\right)-G\left(R_\perp\right)\right]}\right\}\left\{1-e^{-igg_1\left[G\left(R'_\perp+r'_\perp\right)-G\left(R'_\perp\right)\right]}\right\} . \\
&\Downarrow \\
\frac{\mathrm{d}x\tilde{q}\left(x,q_\perp\right)}{d^2R_\perp} &= \frac{N_c}{16\pi^6}\int \mathrm{d}y d^2r_\perp d^2r'_\perp e^{-iq_\perp\cdot\left(r_\perp-r'_\perp\right)} \bigtriangledown_{r_\perp} K_0\left(\sqrt{y}r_\perp\right)\cdot\bigtriangledown_{r'_\perp} K_0\left(\sqrt{y}r'_\perp\right) \\
&\quad \times \left\{1+\exp\left[-Q_s^2\left(r_\perp-r'_\perp\right)^2/4\right]-\exp\left[-Q_s^2 r_\perp^2/4\right]-\exp\left[-Q_s^2 r'^2_\perp/4\right]\right\} ,
\end{aligned}$$

- Use fermionic quark.
- Perform a replacement as follows:

$$e^{-igg_1[G(x_\perp)]} \Longrightarrow U\left(x_\perp\right)=\mathrm{T}\exp\left[-igg_1\int \mathrm{d}z^-\mathrm{d}^2z_\perp G\left(x_\perp-z_\perp\right)\rho_a\left(z^-,z_\perp\right)t^a\right] .$$

Note that $U\left(x_\perp\right) \underbrace{\Longrightarrow}_{\rho_a\left(z^-,z_\perp\right)t^a=\delta\left(z_\perp\right)\delta\left(z^-\right)} e^{-igg_1[G(x_\perp)]}$

- Average the distribution over the gaussian distribution $W\left[\rho\right]$.
- Agrees with *[Mueller, 99]*. Drell-Yan also agree with *[Gelis, Jalilian-Marian, 02]*

The Quark Distribution for a large nucleus in di-jet production

- TMD pdf in di-jet production *[Work in progress]*

$$\begin{aligned}\tilde{q}_{\text{di-jet}}\left(x,q_\perp\right) &= \frac{xP^{+2}}{8\pi^4}\int dp^- p^- \int d^2R_\perp d^2R'_\perp d^2r_\perp e^{iq_\perp\cdot\left(R_\perp-R'_\perp\right)} \\ &\times V\left(r_\perp\right)V\left(r'_\perp\right)e^{-igg_2\left(G(R_\perp)-G(R'_\perp)\right)} \\ &\times\left\{1-e^{igg_1\left[G\left(R_\perp+r_\perp\right)-G(R_\perp)\right]}\right\}\left\{1-e^{-igg_1\left[G\left(R'_\perp+r'_\perp\right)-G\left(R'_\perp\right)\right]}\right\}\end{aligned}$$

$$\Downarrow$$

$$\begin{aligned}&\frac{\mathrm{d}x\tilde{q}\left(x,q_\perp\right)}{d^2R_\perp} \\ &= \frac{N_c}{16\pi^6}\int \mathrm{d}y d^2r_\perp d^2r'_\perp e^{-iq_\perp\cdot\left(r_\perp-r'_\perp\right)}\,\nabla_{r_\perp}K_0\left(\sqrt{y}r_\perp\right)\cdot\nabla_{r'_\perp}K_0\left(\sqrt{y}r'_\perp\right) \\ &\times \left\{\begin{array}{c}\exp\left[-Q_s^2\left(r_\perp-r'_\perp\right)^2/4\right]+\exp\left[-Q_s^2\left(r_\perp-r'_\perp\right)^2/2\right] \\ -\exp\left[-Q_s^2\left(\left(r_\perp-r'_\perp\right)^2+r_\perp^2\right)/4\right]-\exp\left[-Q_s^2\left(\left(r_\perp-r'_\perp\right)^2+r'^2_\perp\right)/4\right]\end{array}\right\},\end{aligned}$$

- Large N_c approximation.
- Two point functions $\left\langle U\left(x_\perp\right)U^\dagger\left(x'_\perp\right)\right\rangle$(DIS)
  and Four point functions $\left\langle U\left(x_\perp\right)U^\dagger\left(x'_\perp\right)U\left(y_\perp\right)U^\dagger\left(y'_\perp\right)\right\rangle$.

Non-Universality

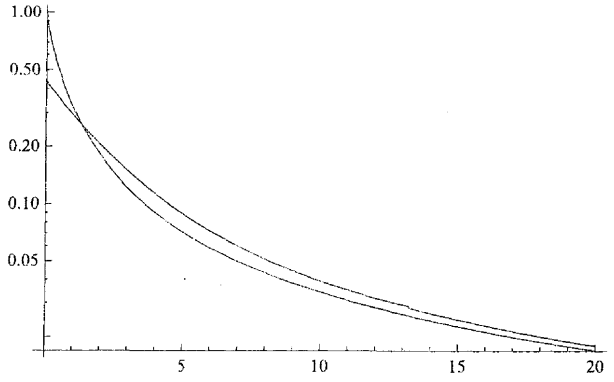

Figure: Comparison of quark distributions in DIS and di-hadron production as functions of $q_\perp^2$. The blue curve stands for the quark distribution in DIS and the red curve represents the distribution involved in di-hadron production.

- Non-Universality (as a result of initial and final state interactions) and k_t factorization violation in CGC. However, they are calculable.
- Integrated quark distributions are universal.
- Similar conclusions with respect to the k_t factorization violation have been reached in sea quark productions *[Blaizot, Gelis, Venugopalan, 04]*, two-gluon production *[Jalilian-Marian, Kovchegov, 04]* and quark-gluon production *[Marquet, 07]*.

Puzzles and Solutions
Boris Kapeliovich
Valparaiso, Chile
Brookhaven
May 10-12, 2010

Resolving the puzzle

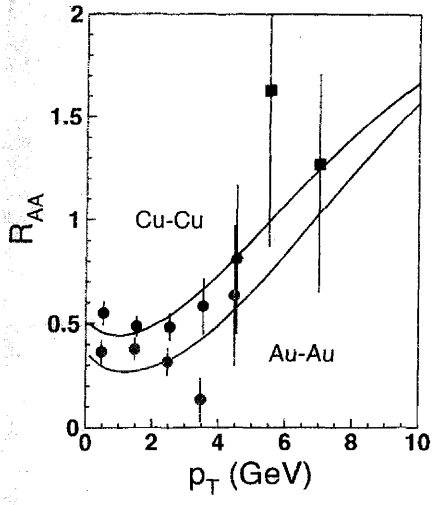

Three effects, which can be well calculated explain the puzzling behavior of $\mathrm{R_{AA}^{J/\Psi}(p_T)}$

- **Final state in-medium attenuation of $\mathrm{J/\Psi}$ controlled by the transport coefficient $\hat{\mathrm{q}}$**
- **Initial state shadowing/attenuation of the $\bar{\mathrm{c}}\mathrm{c}$ dipole (not $\mathrm{J/\Psi}$) passing through both nuclei**
- **Gluon saturation leads to broadening of $\langle \mathrm{p_T^2} \rangle$ of $\mathrm{J/\Psi}$ and to a strong Cronin enhancement.**

The only fitted parameter is the transport coefficient, which is found to be $\hat{\mathrm{q}}_0 = 0.3\,\mathrm{GeV}^2/\mathrm{fm}$, smaller than what comes out of jet quenching analyses.

$\mathrm{J/\Psi}$ suppression offers a novel way to measure $\hat{\mathrm{q}}$

BK, I.Potashnikova, I.Schmidt

Nuclear effects

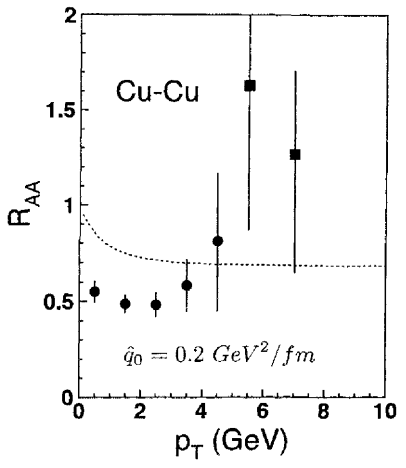

1 Final state attenuation

The absorption cross section for a dipole born in a central *AA* collision at impact parameter s is directly related to the parton broadening in the medium, i.e. to the transport coefficient $\hat{q}$

$$\mathbf{R(s,p_T) = \frac{1}{\pi}\int_0^{\pi} d\phi\ \exp\left[-\frac{1}{2}\langle r^2_{J/\Psi}\rangle \int_{l_0}^{\infty} dl\ \hat{q}(\vec{s}+\vec{l})\right]}$$

The breakup of J/Ψ in the medium is controlled by the same transport coefficient $\hat{q}$ as the energy loss.

We relied on the popular model $\hat{q}(b,s,t) = \frac{\hat{q}_0\, t_0}{t}\frac{n_{part}(b,s)}{n_{part}(0,0)}$, fixed $t_0 = 0.5$ fm

and adjusted the transport coefficient $\hat{q}_0$ to reproduce the data

Nuclear effects

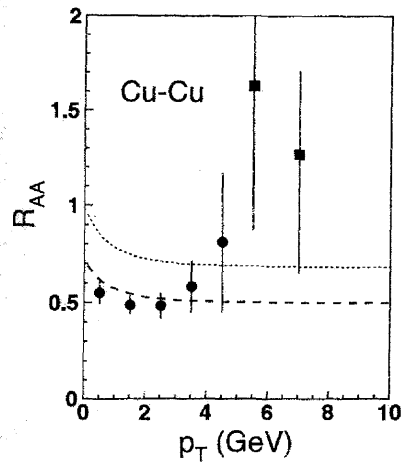

2 Initial state shadowing of charm

The $\bar{c}c$ production time in the nuclear rest frame

$$t_p^c = \frac{\sqrt{s}}{m_N\sqrt{4m_c^2 + p_T^2}} = \frac{1}{m_N x_2}$$

is sufficient ($5 < t_p < 13$ fm) for quark shadowing.

However, $x_2 > 0.015$ is too large (l_p^g is too short) for gluon shadowing, which sets up only at $x_2 < 0.01$!

Charm shadowing comes together with the breakup cross section, they are not separable. The result, $S_{NA} \approx 0.8$, is known from data. However, the impact parameter dependence is important and can be only calculated.

We assume $S_{AB}(s) = S_{NA}(s)\, S_{NB}(s)$

Nuclear effects

3 Initial state saturation of gluons

Due to saturation gluons experience broadening with the coefficient $C(s)$ known from DIS data.

$$\Delta p_T^2 = 2C(s)\, T_A(b)$$

The p_T distribution of J/Ψ has the form:

$$\frac{d\sigma}{dp_T^2} \propto \left(1 + \frac{p_T^2}{6\langle p_T^2\rangle}\right)^{-6}$$

Broadening results in $\langle p_T^2\rangle \Rightarrow \langle p_T^2\rangle + \Delta p_T^2$

$$R_T(p_T) = \frac{\frac{d\sigma}{dp_T^2}\Big|_{\langle p_T^2\rangle + \Delta p_T^2}}{\frac{d\sigma}{dp_T^2}\Big|_{\langle p_T^2\rangle}}$$

★ This can be tested with the E866 data for J/Ψ production in pA at 800 GeV:

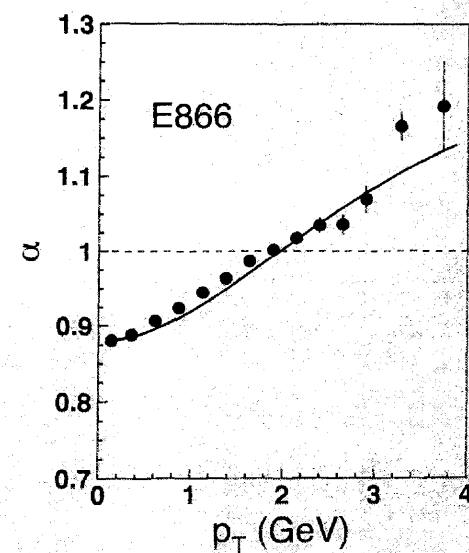

Works amazingly well with no adjustment!

Nuclear effects

Eventually, combining all three mechanisms we arrive at the final result

$$R_{AA}^{J/\Psi}(p_T) = \frac{\int_0^\infty ds^2\, T_A^2(s)\, R(s,p_T)\, S_{AA}(s) R_T(s,p_T)}{\int_0^\infty ds^2\, T_A^2(s)}$$

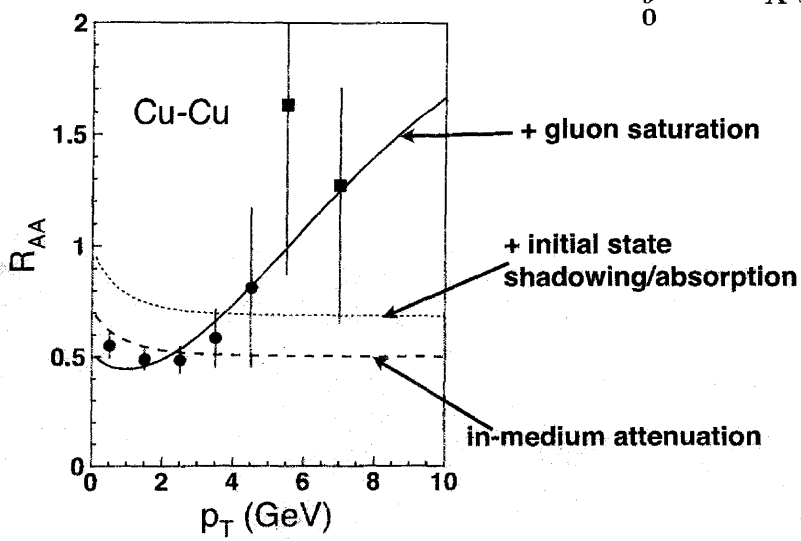

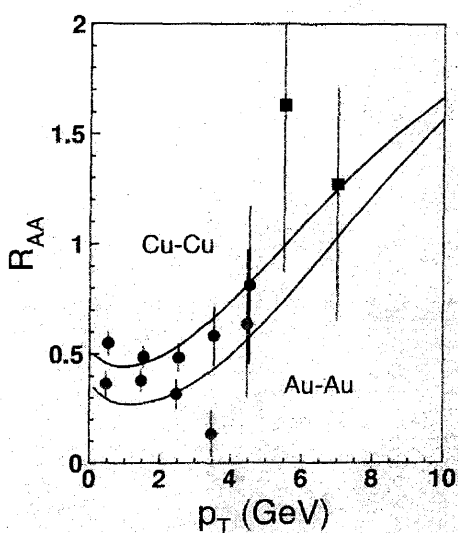

J/ψ and Charm at RHIC

Alexandre Lebedev, Iowa State University
for the PHENIX Collaboration

Comprehensive overview of charm-related measurements by the PHENIX collaboration at RHIC is presented in this talk.

It is shown that Cold Nuclear Matter effects can not be understood in terms of just shadowing and constand breakup cross-section.

There are Indication of J/ψ suppression in most central Au+Au collisions beyond CNM effects.

Open charm suppression and flow in Au+Au is similar to that of light quarks.

Expect more exciting new results with PHENIX detector upgrades.

RIKEN BNL Research Center Workshop
BNL, May 10-12, 2010

J/ψ and Cold Nuclear Matter Effects

Before attempting to understand what happens in Au+Au we must understand "cold nuclear matter" effects, including:

- *Pdf modification in nuclei*
- *Breakup by surrounding hadrons*
- *Gluon saturation at low x / CGC*
- *Initial state energy loss*
- *Cronin effect*

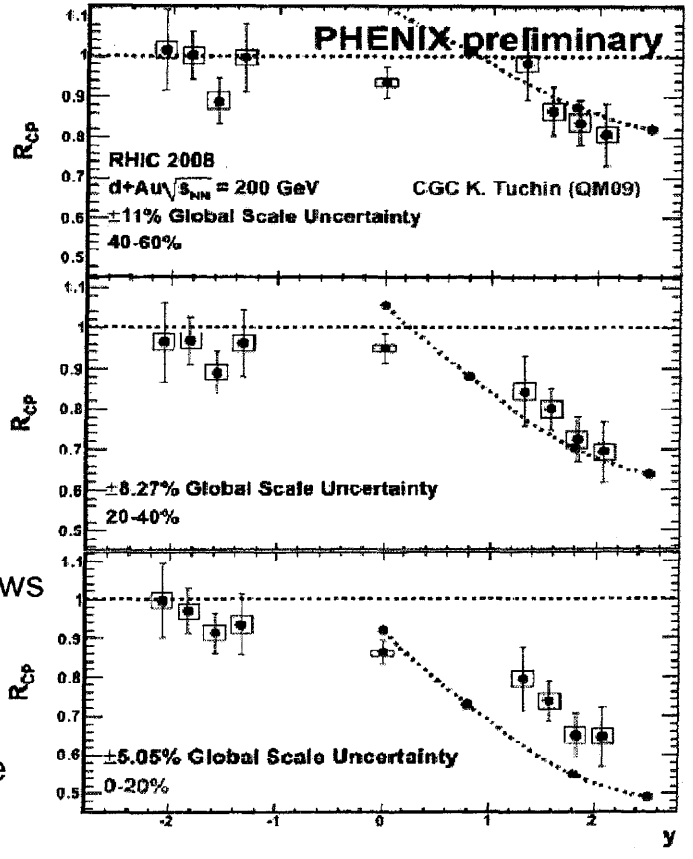

2008 d+Au data sample has ~40 times more statistics than 2003 published results and allows finer rapidity binning.

R_{CP} ~1 at negative rapidity (Au direction)

R_{CP} < 1 and decreases with rapidity at positive rapidity (deutron direction)

J/ψ in Au+Au

J/y suppression is similar to open charm suppression

Suppression at RHIC similar to one observed at SPS at mid-rapidity, but stronger at forward rapidity.

Many different interpretations exist ("cold nuclear matter" effects, re-generation, etc.) Exact picture is still unclear.

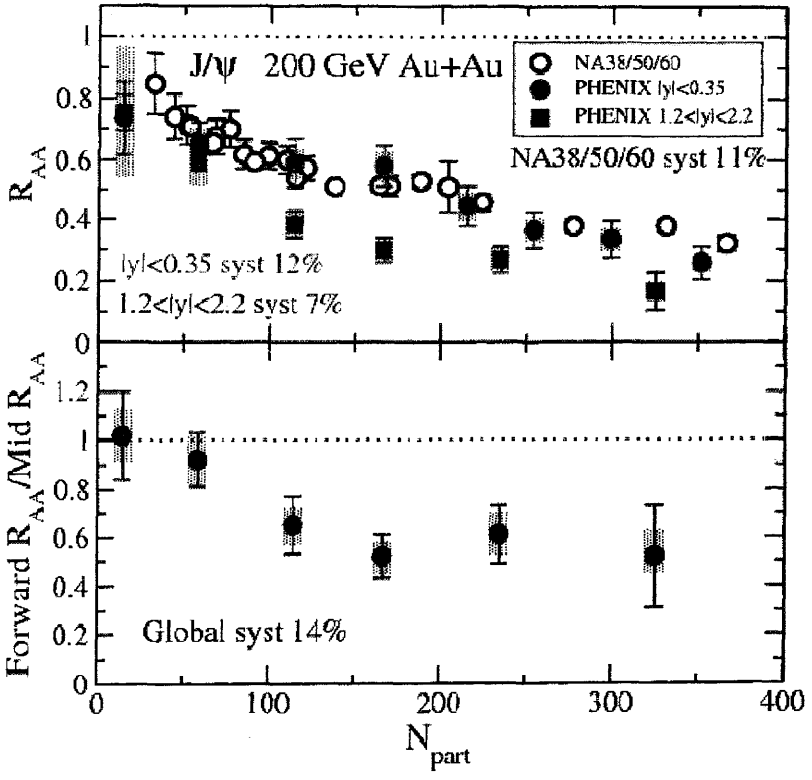

Can CNM Explain Observed Suppression?

Not a Phenix result, uses Phenix preliminary (QM09)
Calculation by Tony Frawley
CNM with rapidity dependent effective breakup cross-section.

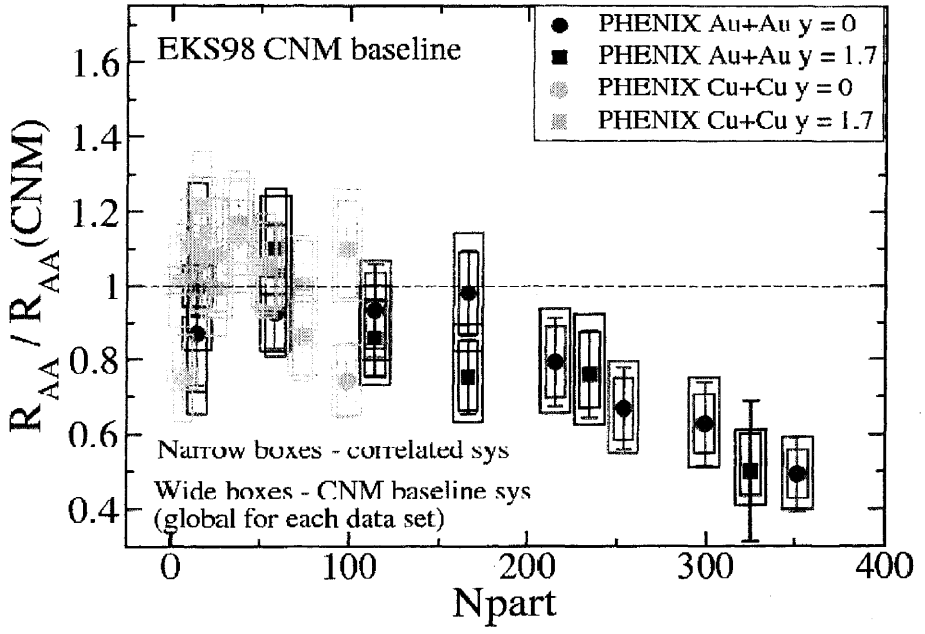

- Forward and central rapidity results become similar.
- Suppression beyond CNM in most central collisions.

Open Heavy Flavor in Au+Au

Heavy flavor electrons from Au+Au compared to N_{COLL} scaled p+p (FONLL x 1.71)

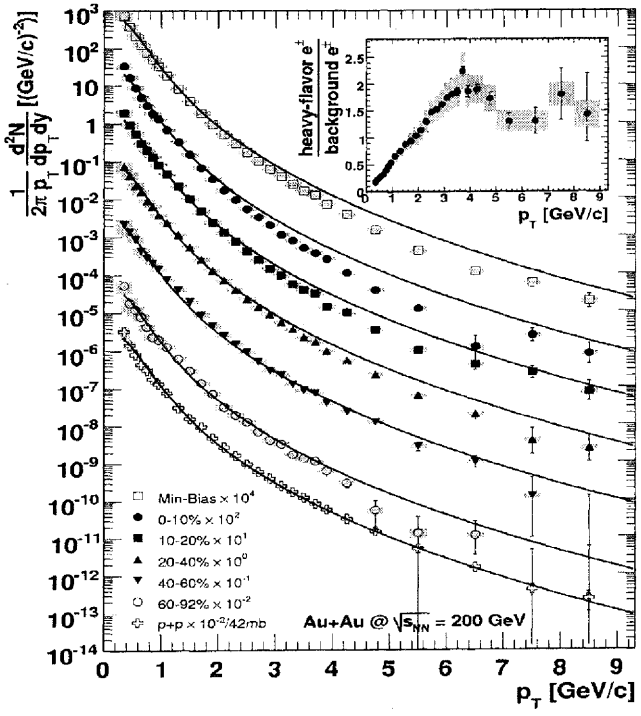

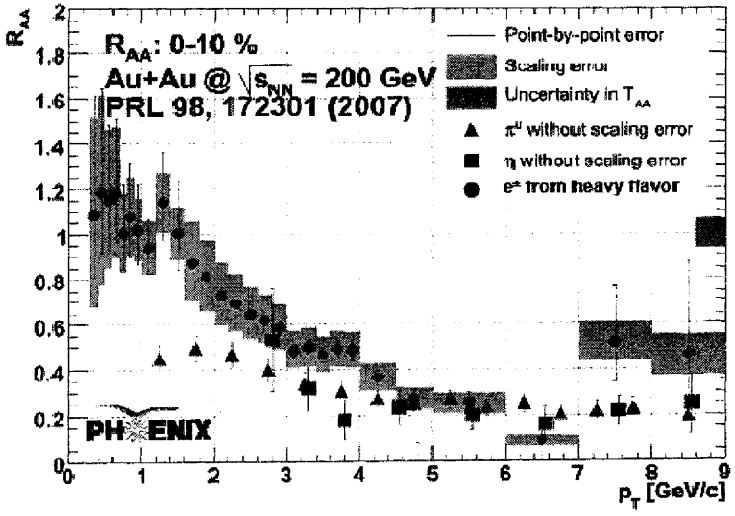

Charm suppression is almost the same as for light quarks at high P_T!

Open Heavy Flavor Flow

HF electrons flow

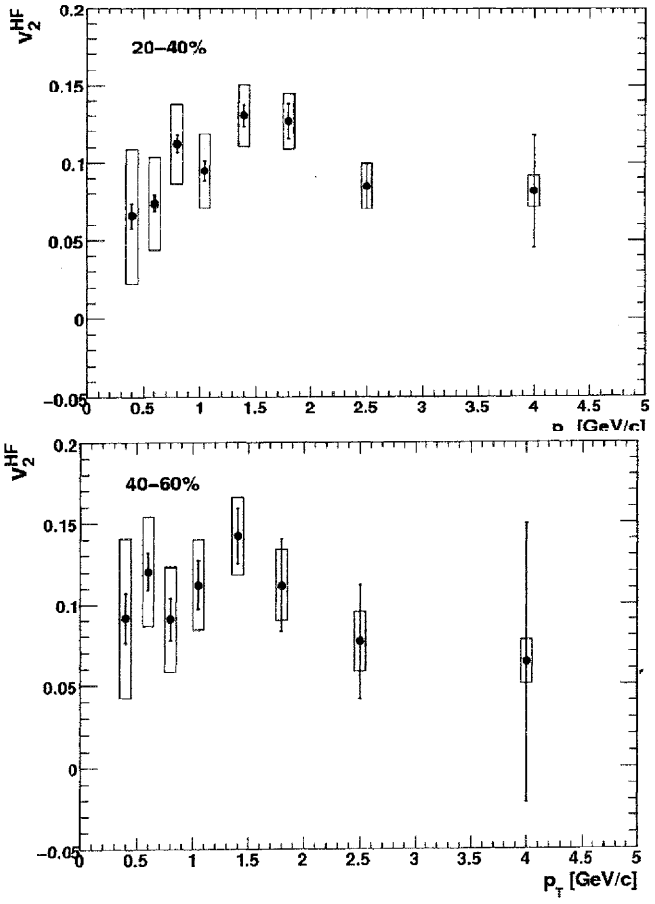

Photonic electrons flow

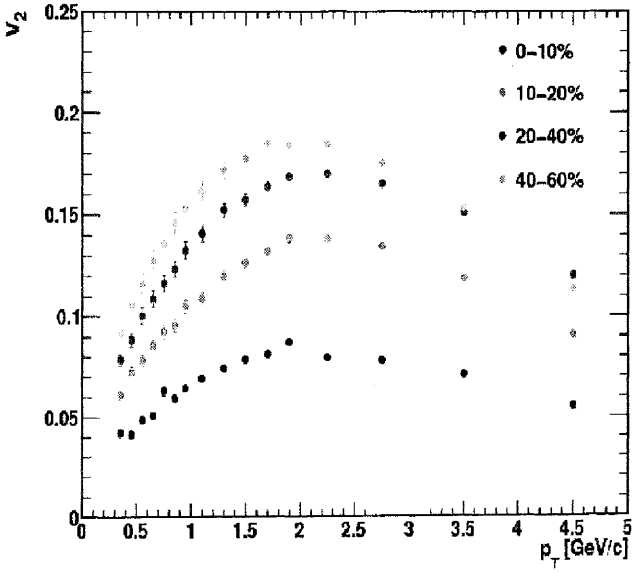

arXiv:1005.1627
Submitted today to PRC

Heavy flavor (charm) flow is comparable to that of light quarks!

Chris Perkins
UC Berkeley/Space Sciences Laboratory
Stony Brook University
For the STAR Collaboration

J/Ψ and Charm at STAR

Gluon saturation effects and Color Glass Condensate models become important at a scale $Q_S^2(x)$ which is proportional to $A^{1/3}e^{\lambda y}$. Hence, this scale can be reached by going to lower-x, larger sqrt(s), forward rapidities (y), or nuclear "targets" (large A). In regards to charm production, what becomes important is the relation between the saturation scale, Q_S, and the mass of the charm quark. When the saturation scale $Q_s < m_C$, as is the case at mid-rapidities at RHIC, charm production is not affected by gluon saturation/CGC models. If the saturation scale can be raised to above the charm quark mass, however, saturation effects can influence charm production and it is expected, based on CGC models, that charm particle production will follow similar patterns to those found in light quarks. This scale can potentially be reached in the charm sector by going to forward rapidities at RHIC and using nuclear "targets". CGC models expect that in this regime, forward production will be suppressed in d+Au collisions relative to p+p collisions, the p_T spectrum will be harder, and the scaling with the number of binary collisions will be suppressed in d+Au collisions as compared to mid-rapidity.

While STAR has a rich set of mid-rapidity J/Psi and charm particle measurements, we also have the possibility to measure charm production in the saturation regime using the Forward Meson Spectrometer (FMS). The FMS is an electromagnetic calorimeter at STAR with full azimuthal coverage over a pseudorapidity range of 2.5 to 4. Its large acceptance provides excellent geometric efficiency to measure high-x_F J/Psi production in p+p and d+Au collisions. A significant observation of high-x_F J/Psi has already been reported at QM09 with work ongoing to report forward cross sections and potentially x_F dependence. The FMS also has the possibility to measure forward open charm production by reconstructing D^0 through the decay channel $D \rightarrow K^0_S + \pi^0 \rightarrow 3\,\pi^0 \rightarrow 6$ photons.

By comparing d+Au measurements to p+p measurements in both quarkonia and open charm production, the FMS at STAR has the potential to test several predictions of CGC/Saturation models in the charm sector.

Saturation and Heavy Flavor Production

J/ψ Production in the CGC Framework

Also Open Charm Production

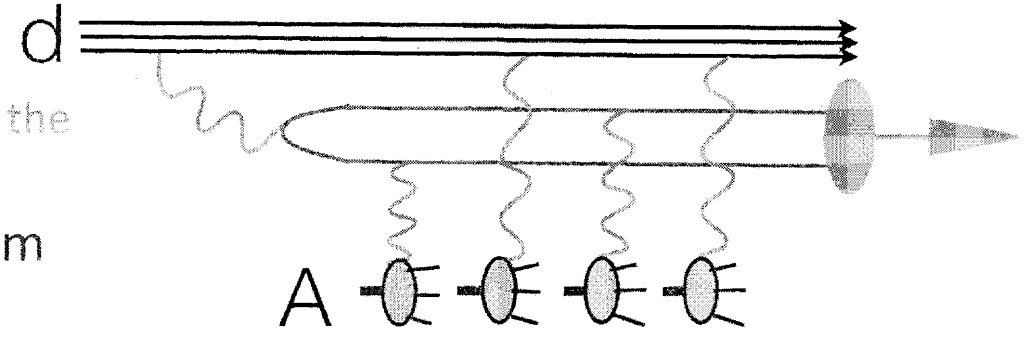

Kharzeev, Tuchin **Nucl.Phys.A770:40-56,2006.**

$c\bar{c}$ pair scatters coherently off all nucleons along its trajectory

- Traditional scale: $m_q > \Lambda_{QCD}$ → perturbative production
- But in CGC/Saturation picture, more relevant scale is Q_s
  - $Q_s > m_q$ → saturation affects heavy flavor production
  - Heavy quarks should follow similar pattern to light quarks
- At RHIC: Forward Rapidity + Nuclear Target → $Q_s > m_C$
- Charm quark production subject to CGC/Saturation

Expectations for Charm in CGC

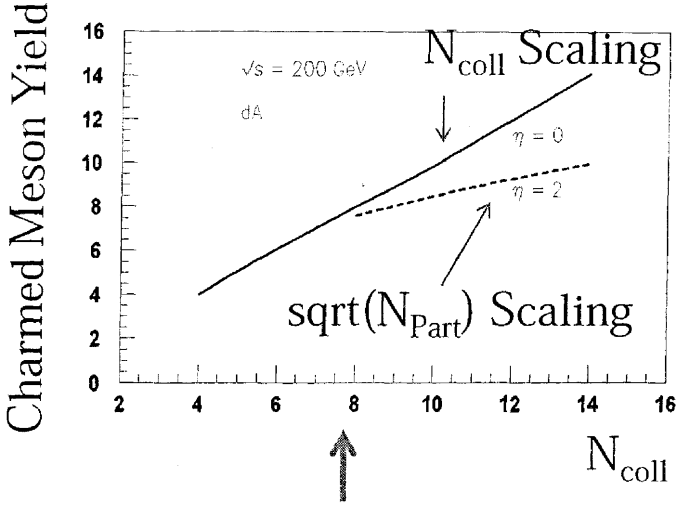

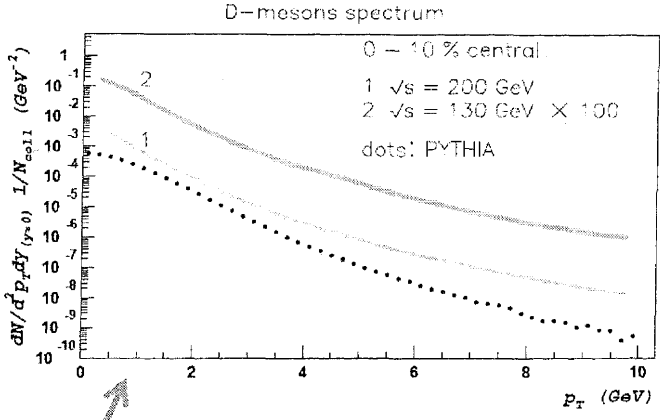

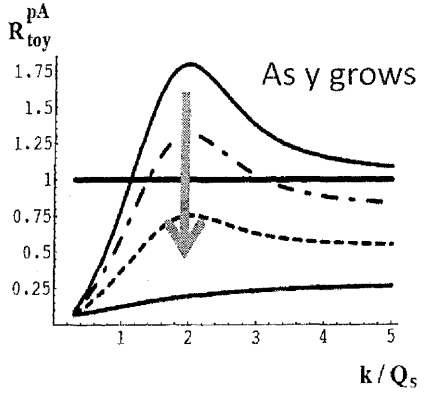

- AA: N_{part} scaling, p(d)A: sqrt(N_{part}) scaling
- Harder spectrum because of harder gluon spectrum
- Total Transverse Momentum doesn't vanish
  - ($\langle P_T^2 \rangle \approx Q_{smax}^2$ for forward rapidities at RHIC)
- Suppression of R_{pA} and disappearance of Cronin enhancement
- Supression is stronger with centrality because of scaling (sqrt(N_{part}))

Kharzeev, Tuchin **Nucl.Phys.A735:1-2,2004**.

Forward p+p J/ψ – 2-Cluster Analysis

Reconstructed 2-cluster invariant mass

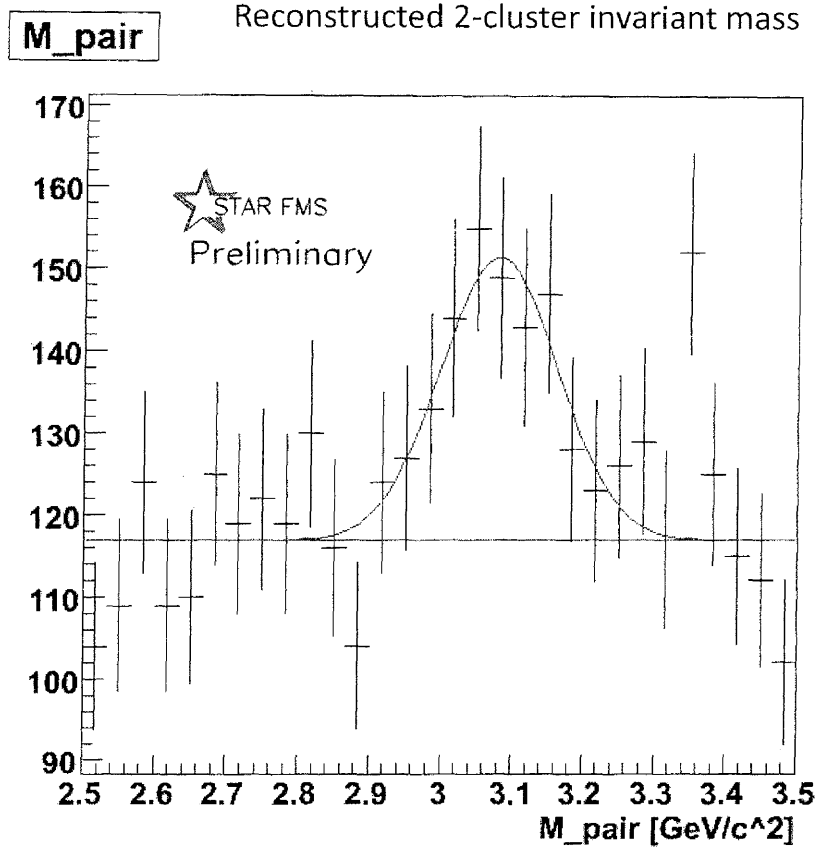

Fit with Gaussian + Offset

Gaussian Fit Parameters:

- $\mu = 3.080 \pm 0.020$ GeV/c^2
- $\sigma = 0.082 \pm 0.026$ GeV/c^2
- χ^2/d.o.f. = 20.83/26
- Significance from fit
  - 4.5 σ

Cuts Applied:

- E_pair > 60.0 GeV
- $Z_{\gamma\gamma} < 0.7$
- Isolation Radius:
  - 0.4 Eta-Phi
- p_T_cluster > 1.0 GeV/c

Presented at QuarkMatter 2009

First measurement of high-x_F J/ψ at sqrt(s) > 62 GeV at a collider.

C. Perkins [STAR Collaboration], Nucl. Phys. A **830**, 231c (2009)

Forward Open Heavy Flavor: $\overline{D}^0/D^0$

- Look for forward D^0 through decay channel:

$D \rightarrow K^0_S + \pi^0 \rightarrow 6$ photons

$(K^0_S \rightarrow \pi^0 + \pi^0)$

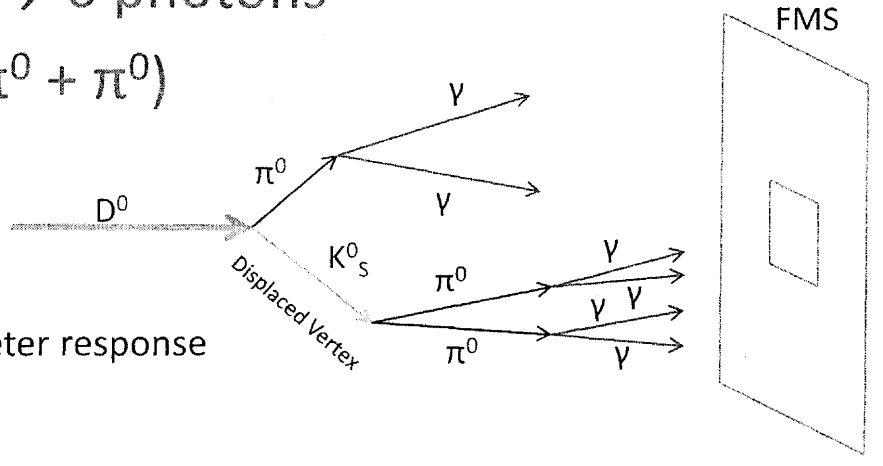

Using bare FMS calorimeter response

- Total Branching Ratio (from PDG) for

$D \rightarrow K^0_S + \pi^0 \rightarrow 3\pi^0 \rightarrow 6\gamma = 0.00361$

Conclusions and Outlook

- CGC/Saturation regime should be accessible to charm sector at forward rapidities in d+Au collisions at STAR
  - Expect qualitatively similar trends to lighter quarks based on current theories
  - Other theories may also contribute to suppression/enhancement at this rapidity
- Measurements of both Quarkonia and Open Heavy Flavor probing low-x gluons are possible at forward rapidities at STAR
- Significant signal of forward J/ψ in p+p has already been reported
  - Further work is needed to finish analysis
- Analysis of J/ψ in d+Au data should begin soon to look for hints of saturation in charm sector
- Feasibility for measuring open charm through the D^0 meson looks promising

Understanding J/ψ production in pp, dA, and AA collisions

Jian-Wei Qiu

Physics Department, Brookhaven National Laboratory, Upton, NY 11973, USA

In this talk, we present a new perturbative QCD factorization formalism for inclusive production of heavy quarkonia at large transverse momentum p_T at collider energies [1]. This factorization formula for calculating quarkonium cross section includes both the leading power (LP) and heavy quark mass m_Q enhanced next-to-leading power (NLP) contributions from the m_Q^2/p_T^2 expansion. Both the LP and NLP contributions are factorized in terms of perturbatively calculable short-distance partonic coefficient functions and universal non-perturbative fragmentation functions. We calculate at the leading order (LO) in α_s the partonic coefficients for both LP and NLP, as well as the evolution kernels of the fragmentation functions. We estimate the non-perturbative fragmentation functions at a scale $\mu_0 \sim 2m_Q$ in terms of NRQCD factorization formalism.

By including the mass-enhanced power corrections, our factorization formalism provides a consistent and perturbatively stable way to calculate the cross section of heavy quarkonium production for a wide range kinematics. Unlike the color singlet or NRQCD model calculations, which expresses the perturbative partonic scattering in a power series of α_s without asking any ordering in m_Q and p_T, we organize all partonic contributions in a power series of m_Q/p_T whose coefficients in a power series of $\alpha_s(p_T)$, and resum all logarithms from the huge phase space between p_T and $\mu_0 \sim 2m_Q$ into the fragmentation functions. For producing a color singlet heavy quark pair that turns into a heavy quarkonium, we get different sizes of contributions depending on where the pair was produced and the pair's quantum number. To produce a color singlet spin-1 heavy quark pair at the collision point of a distance scale $1/p_T$, QCD power counting told us that the production rate for producing such a pair is of the order of $(1/p_T^4)(m_Q^4/p_T^4)$ which is suppressed by m_Q^4/p_T^4 in comparison to the typical leading power $2 \to 2$ subprocesses. If the color singlet heavy quark pair was produced at a much later time $1/m_Q$ from a single parton fragmentation, the production of the single fragmenting parton is of the $1/p_T^4$-type leading power behavior. But, such contribution suffers in rate to convert the single parton, say gluon, to a color singlet heavy quark pair. In between these two sources, the spin-1 color singlet heavy quark pair could be formed at the $1/m_Q$ while a color octet heavy quark pair with the vector or axial vector charge was produced at the time scale of $1/p_T$. This contribution has a characteristic of $(1/p_T^4)(m_Q^2/p_T^2)$ with powers of $\log(p_T^2/\mu_0)$ enhancement. Although this contribution is power suppressed at the partonic level in comparison with the leading power single parton production, the pair has a much large probability to become a color singlet pair. In addition, we find that the production process prefers to have a large final-state phase space to keep the pair in an octet state until the last minute before the pair hadronize.

We also find that the leading power single parton fragmentation likes to produce a transversely polarized heavy quarkonium, and the subleading power heavy quark pair fragmentation produces mainly longitudinally polarized heavy quarkonium. The measured polarization is a competition between the leading and subleading power contributions. At the "ultra" high $p_T \gg m_Q$, it seems more likely to produce transversely polarized heavy quarkonia.

References

[1] Z. B. Kang, J. W. Qiu,and G. Sterman, in preparation.

[2] G. T. Bodwin, E. Braaten and G. P. Lepage, Phys. Rev. D **51**, 1125 (1995) [Erratum-ibid. D **55**, 5853 (1997)]

Quark mass

❑ Quark masses:

Flavor	Mass
u	1.5 – 4.5 MeV
d	5.0 – 8.5 MeV
s	80 – 155 MeV
c	1.0 – 1.4 GeV
b	4.0 – 4.5 GeV
t	171.3 ± 5.1 GeV

Quark masses span a wide kinematical range:

$$\frac{m_t}{m_u} \sim 10^4$$

Light quarks

$\longleftarrow \Lambda_{\rm QCD}$

$\longleftarrow Q_s(x \sim 1/\sqrt{s})$

Heavy quarks $\alpha_s(m_Q) \ll 1$

❑ Heavy quark is heavy if $Q_s(x \sim 1/\sqrt{s}) \ll m_Q$

❑ Heavy quark is "light" if $Q_s(x \sim 1/\sqrt{s}) \gtrsim m_Q$

The basic production mechanism

❑ Production of an **off-shell** heavy quark pair:

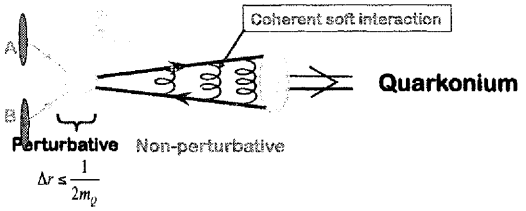

❑ Approximation: **on-shell** heavy quark pair + hadronization

$$\sigma_{AB\to J/\psi} = \sum_{\rm states} \int d\Gamma_{Q\bar{Q}} \left[\frac{d\hat{\sigma}(Q^2)}{d\Gamma_{Q\bar{Q}}}\right] F_{{\rm states}(Q\bar{Q})\to J/\psi}(p_Q, p_{\bar{Q}}, P_{J/\psi})$$

Different models ⇔ Different assumptions/treatments on how the heavy quark pair becomes a quarkonium?

$(1/P_T)^n$ vs $(\alpha_s)^n$ expansion

Kang, Qiu and Sterman, 2010

❑ The s=1 NR projection operator:

$$\mathcal{P}(P,q\to 0,s=1)=\frac{1}{\sqrt{2m_Q}}\gamma_\mu\epsilon^\mu_\lambda(P)\left[\gamma\cdot\frac{P}{2}+m_Q\right]$$

Picks up contributions that vanish as $m_Q \longrightarrow 0$

❑ $(\alpha_s)^n$ expansion does not pick up leading power in $(1/P_T)^n$

LO is $(1/P_T)^8$ vs NLO gives $(1/P_T)^6$

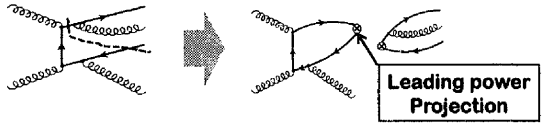

$\Longrightarrow$ $(1/P_T)^n$ – power expansion before $(\alpha_s)^n$ – expansion

PQCD factorization formalism

❑ Expansion in m_Q/P_T:

Kang, Qiu and Sterman, 2010

$$E\frac{d\sigma_{J/\psi}}{d^3P}:\quad \left|\ +\ +\ldots\ \right|^2$$

$$\Longrightarrow\quad \log^n\left(\frac{P_T^2}{\mu_0^2}\right)\quad \mu_0^2\log^n\left(\frac{P_T^2}{\mu_0^2}\right)\qquad \mu_0\sim 2m_Q$$

$$\mathcal{O}\left(\frac{1}{P_T^4}\right)\quad +\quad \mathcal{O}\left(\frac{1}{P_T^6}\right)$$

❖ **Leading power in 1/P:** $\Longrightarrow$ **much smaller FFs**

– color, symmetry, high orders

❖ **Subleading power in $1/P_T$:** $\Longrightarrow$ **much larger FFs**

PQCD evolution

❑ Single parton: Kang, Qiu and Sterman, 2010

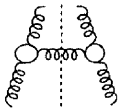

Same as normal DGLAP
Difference from input distribution

$$D_{g\to J/\psi}(z,\mu_0,m_Q)$$

❑ Heavy quark pair:

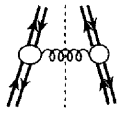

Differ from DGLAP – still logarithmic
Spin-color sensitive
Infrared safe evolution
Nonperturbative input distribution

$$\mu^2\frac{\partial}{\partial\mu^2}D_{[Q\bar{Q}(8)]\to H}(z,m_Q,\mu) = \int_z^1\frac{dz'}{z'}D_{[Q\bar{Q}(8)]\to H}(z',m_Q,\mu)\,\mathcal{K}^{(1)}_{[Q\bar{Q}(8)]\to[Q\bar{Q}(8)]}(z/z',\alpha_s)$$

$$\mathcal{K}^{(1)}_{[Q\bar{Q}(8)]\to[Q\bar{Q}(8)]}(z,\alpha_s) = \frac{\alpha_s}{2\pi}[2C_A]\left(\left[\frac{2z}{1-z}\right]_+ + \frac{1}{4}\delta(1-z)\right)$$

Evolution dominated by octet channels

NRQCD to input distributions

❑ Single parton:

Nayak, Qiu and Sterman, 2005

$$D_{g\to J/\psi}(z,\mu_0,m_Q)\to\sum_{[Q\bar{Q}(c)]}\hat{d}_{g\to[Q\bar{Q}(c)]}(z,\mu_0,m_Q)\langle\mathcal{O}_{[Q\bar{Q}(c)]}(0)\rangle|_{\rm NRQCD}$$

Dominated by transverse polarization

❑ Heavy quark pair:

Kang, Qiu and Sterman, 2010

$$D_{[Q\bar{Q}(8)]\to J/\psi}(z,\mu_0,m_Q)\to\sum_{[Q\bar{Q}(c)]}\hat{d}_{[Q\bar{Q}(8)]\to[QQ(c)]}(z,\mu_0,m_Q)\langle\mathcal{O}_{[QQ(c)]}(0)\rangle|_{\rm NRQCD}$$

Dominated by longitudinal polarization

This NRQCD factorization has not been proved!

So far, it works to 2-loop level for single parton case

Nayak, Qiu and Sterman, 2005

J/ψ polarization

❑ Competition between LP and NLP: Kang, Qiu and Sterman, 2010

$$E\frac{d\sigma_{J/\psi}}{d^3P}:$$ 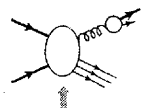 + 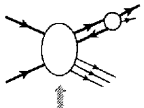 +...

Transverse polarization

Longitudinal polarization

Both dominated By octet channels!

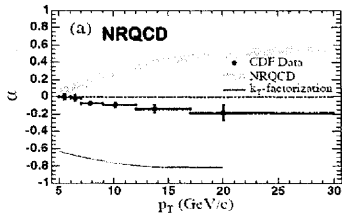

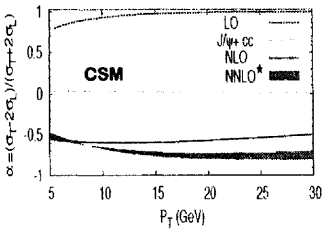

Broadening of heavy quarkonia in d+A

Kang, Qiu, PRD77(2008)

❑ Final-state effect is important:

$$\Delta\langle q_T^2\rangle^{J/\psi}_{\rm Abs} / \Delta\langle q_T^2\rangle_{\rm DY\ Abs} \approx 2C_A/C_F = 4.5$$

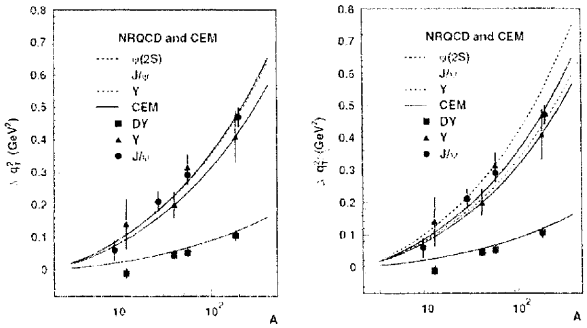

❑ Mass – independence, not very sensitive to the feeddown

Broadening of quarkonia in A+A

- If no hot medium was formed:

$$\Delta\langle q_T^2\rangle_{AB} \approx C_I \left(\frac{8\pi^2\alpha_s}{N_c^2-1}\right) A^{\frac{1}{3}} \langle Q|\mathcal{O}|Q\rangle \left(A^{\frac{1}{3}}+B^{\frac{1}{3}}\right)$$

Superposition of pA

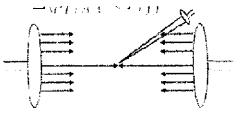

- If hot medium is formed:

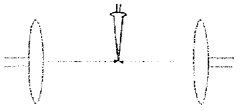

- $\Delta\langle q_T^2\rangle_{AB}$ [illegible]
- $\Delta\langle q_T^2\rangle_{AB}$ [illegible] superposition of $\Delta\langle q_T^2\rangle_{pA}$

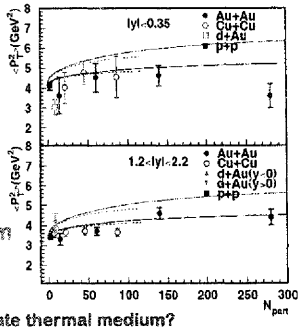

Some kind of slow moving medium was produced at RHIC!

$\Delta\langle q_T^2\rangle_{AA}$ could be as small as 0!

final-state energy loss, initial-state thermal medium?

Summary and outlook

- None of the existing factorized production models, including NRQCD model, were proved theoretically
- New pQCD factorization formula: LP + NLP
- Both LP and NLP hard production dominated by octet channels
- Polarization is a result of competition between LP and NLP
- Heavy quarkonium has two intrinsic scales, and could be a good probe to study the formation of bound states in QCD
- Harder to form J/ψ if $m_c \sim Q_s$ ⟶ suppression of J/ψ Tuchin's talk
- Experimental measurements, in particular, the upsilon polarization at LHC, are needed to test the production mechanism!

Charmonium and open charm production and saturation

Kirill Tuchin

IOWA STATE UNIVERSITY
OF SCIENCE AND TECHNOLOGY

RIKEN BNL Research Center

BNL, MAY 12, 2010

Inclusive gluons

Kovchegov, KT, 2001

There is an approximate k_T - factorization (LO). Though no pdf's...

$$\frac{d\sigma^{pA}}{d^2k\,dy} = \frac{C_F}{\alpha_s\,\pi\,(2\pi)^3}\,\frac{1}{\underline{k}^2}\int d^2B\,d^2b\,d^2z\,\left(\nabla_z^2\,n_G(\underline{z},\underline{b}-\underline{B},0)\right)e^{-i\underline{k}\cdot\underline{z}}\left(\nabla_z^2\,N_G(\underline{z},\underline{b},0)\right).$$

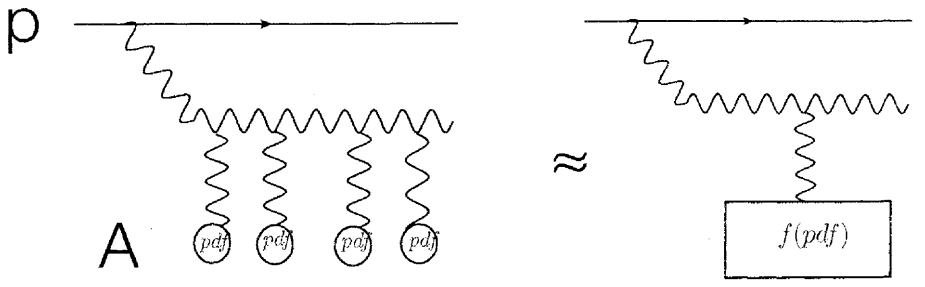

One can trace the origin of the (approximate) factorization in that there is no restriction on the quantum numbers of the product (Spin, Color etc.)

Phenomenology: light hadrons

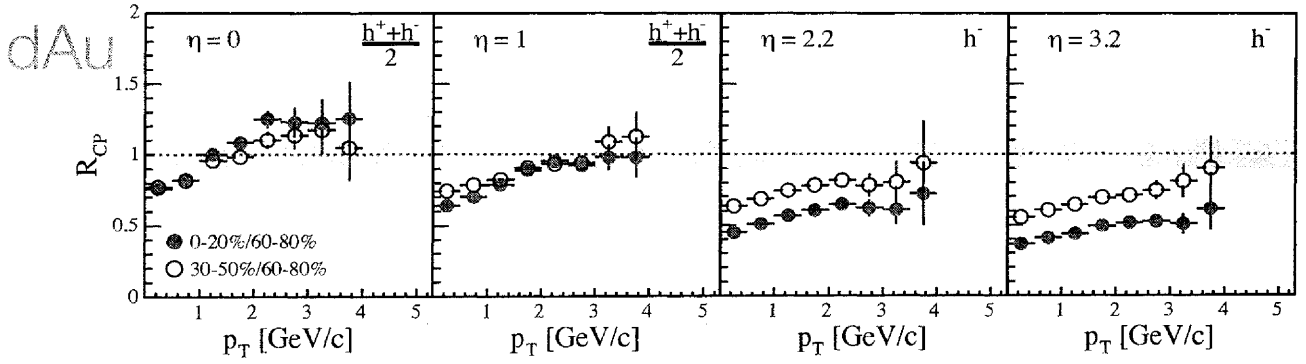

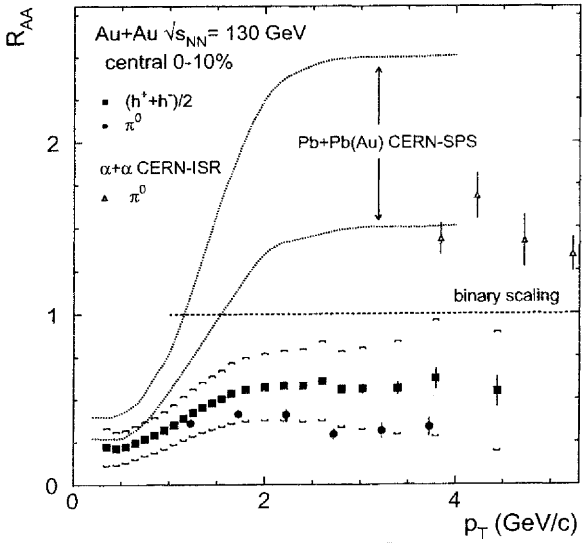

Due to factorization we can infer the size of the cold nuclear matter effect in AA from that in DA

This is true only if there is a factorization between the nuclei!

Factorization for J/ψ ?

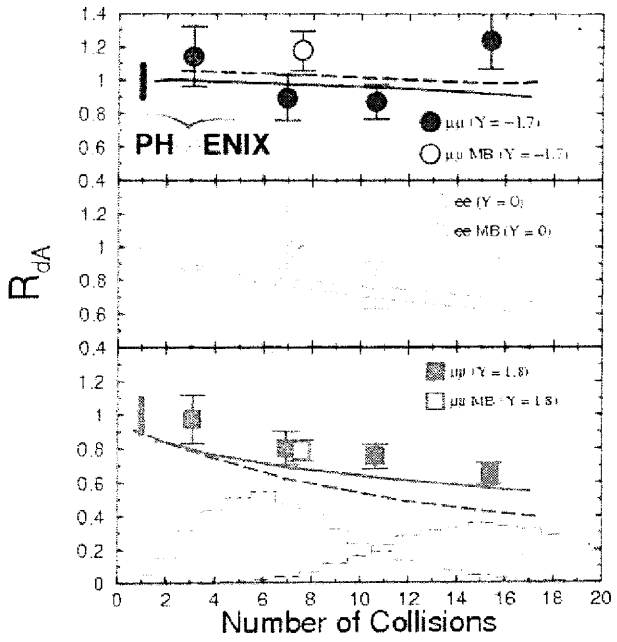

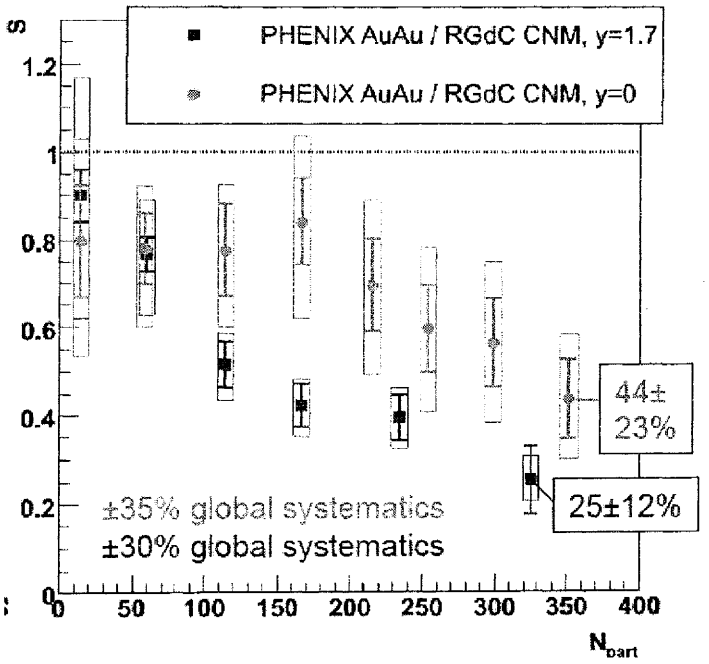

Can we infer the the cold nuclear matter effect in AA from DA?

NO! Because factorization is badly broken!

Production of J/ψ: pp vs pA

Kharzeev, KT,2005
Kharzeev, Levin, Nardi, KT,2009

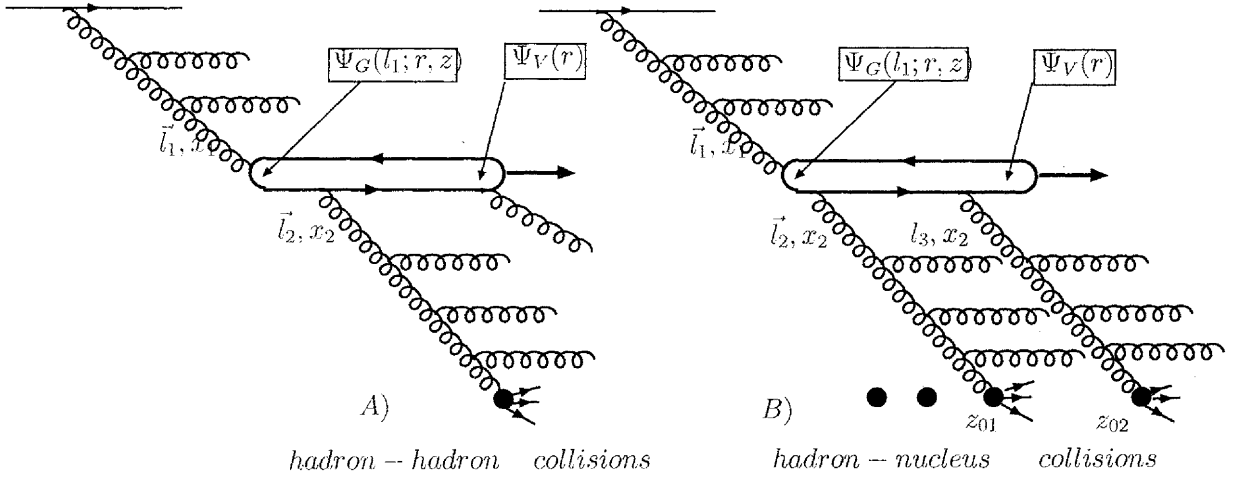

hadron – hadron collisions

hadron – nucleus collisions

$$\alpha_s^3 A^{1/3} = \alpha_s(\alpha_s^2 A^{1/3}) \sim \alpha_s \qquad \alpha_s^4 A^{2/3} = (\alpha_s^2 A^{1/3})^2 \sim 1$$

This mechanism is dominant only for central enough collisions

$$\Psi_G(m_c, r, z) \otimes \Psi_V(r, z) = \sqrt{\frac{3\,\Gamma_{J/\Psi \to e^+e^-}\, M_{J/\Psi}}{48\,\pi\,\alpha_{em}}}\,\frac{m_c^3\, r^2}{4}\,K_2(m_c r)$$

Cold J/ψ suppression

Kharzeev, Levin, Nardi, KT,2009

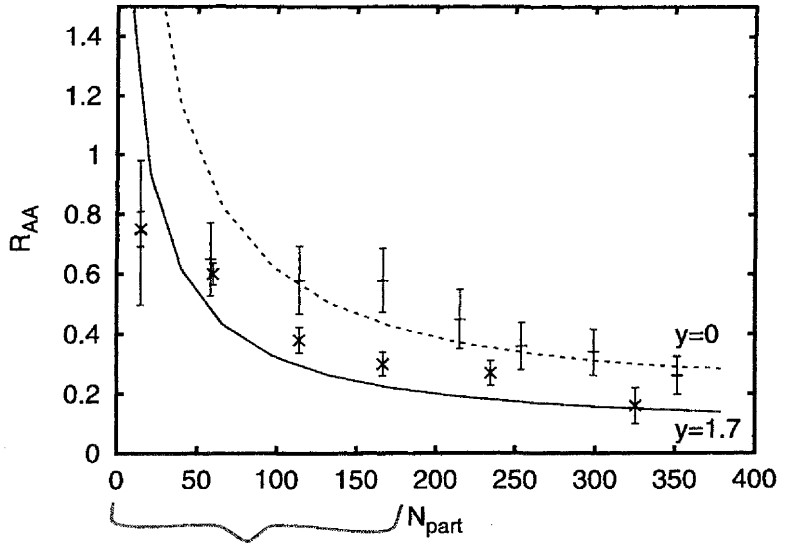

A+A→J/ψ+g
must be included

- Our results agree reasonably well with the data.
- Important corrections must be taken into account:
  - ✓ Finite coherence length effects $l_c \sim R_A$
  - ✓ Contribution of a conventional process: A+A→J/ψ+g
- Overall suppression must also include a certain plasma effect.

Photons and Dileptons

What have we learned at RHIC?

Well established p+p reference
- baseline for Au+Au, Cu+Cu, d+Au
- charm, bottom cross section measurements

Discovered low mass enhancement in central Au+Au
- strongly correlated to centrality
- mostly at low mass, low p_T

First measurement of thermal photons
- extrapolation of quasi-real virtual photons to m=0
- indicate initial temperature > 220 MeV

Future work
- Ongoing Run10
  - HBD is installed to improve dielectron S/B
  - energy scan ($\sqrt{s}$ = 200 / 62.5 / 39 GeV)
- 2008 d+Au dielectron spectra coming soon…

PHENIX

Jason Kamin, Stony Brook University
PHENIX Collaboration
RIKEN BNL Research Center Workshop
May 12, 2010

Lepton Pair Continuum

diverse physics

Modifications due to QCD phase transition

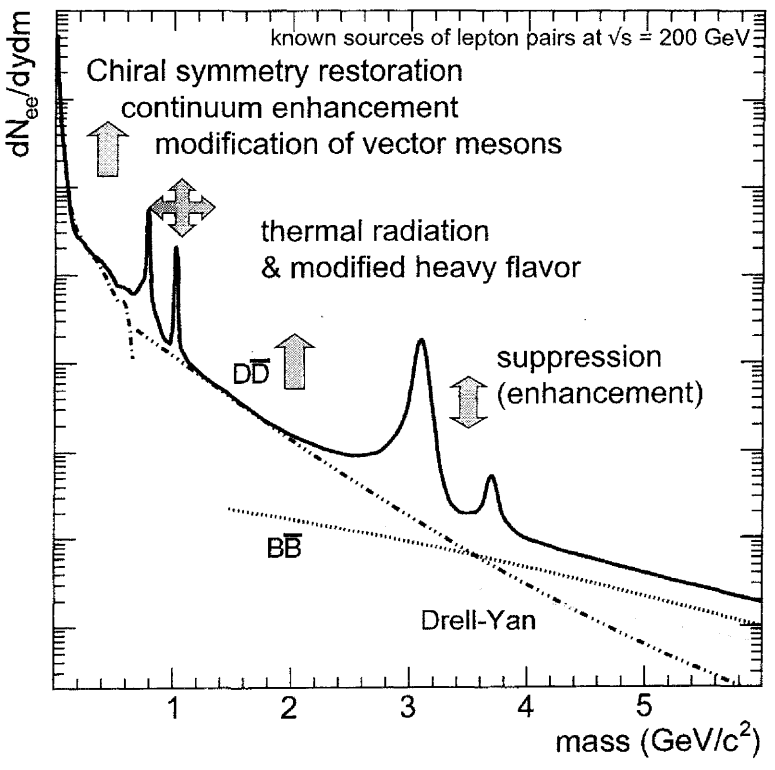

Sources "long" after collision:
- π^0, η, ω Dalitz decays
- (ρ), ω, ϕ, J/ψ, ψ' decays

Early in collision:
- Heavy flavor production
- Drell Yan, direct radiation

Baseline from p+p

Thermal (blackbody radiation):
- in dileptons and photons
- temperature evolution

Medium modifications of mesons:
- $\pi\pi \rightarrow \rho \rightarrow \ell^+\ell^-$
- chiral symmetry restoration

Medium effects on hard probes
- Heavy flavor energy loss

Large discovery potential at RHIC

p+p Dielectrons

agreement with cocktail

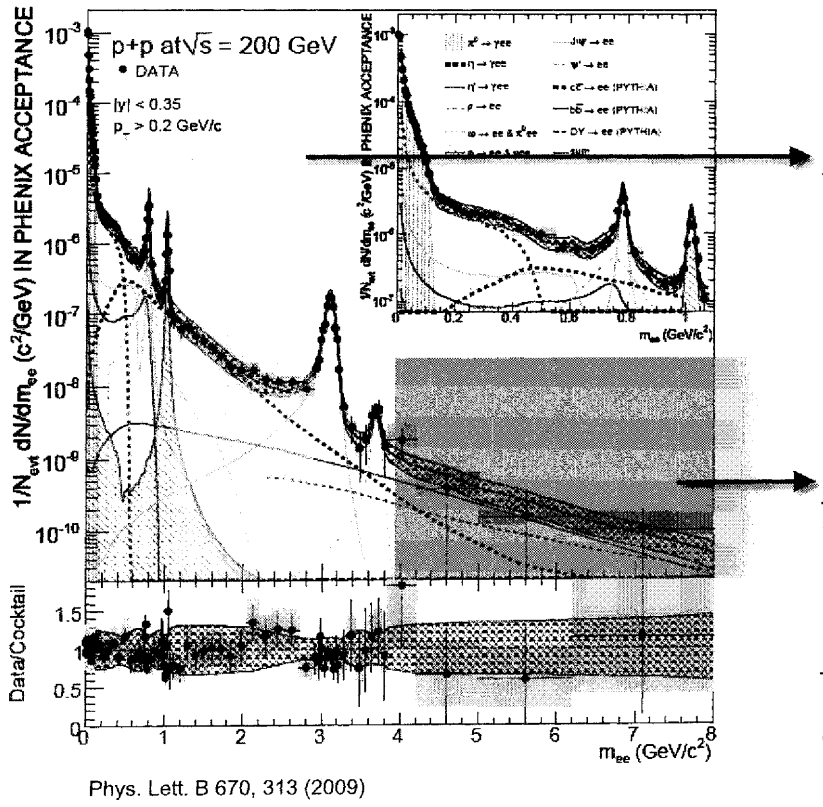

Phys. Lett. B 670, 313 (2009)

Low Mass Region:

- Excellent agreement with hadronic decay cocktail.

Intermediate Mass Region:

- Open Charm Continuum
- integrating the yield:

$\sigma_{c\bar{c}} = 544 \pm 39(\text{stat}) \pm 142(\text{syst}) \pm 200\ (\text{model})\ \mu b$

- agrees with single electron x-sec:

$\sigma_{c\bar{c}} = 567 \pm 57(\text{stat}) \pm 193\ (\text{syst})\ \mu b$

High Mass Region:

- Dominated by bottom

$\sigma_{b\bar{b}} = 3.9 \pm 2.4(\text{stat})\ ^{+3}_{-2}(\text{syst})\ \mu b$

Purpose of p+p:

- Provides a baseline for Au+Au
- New channel to measure x-sect for charm and bottom

Au+Au Dielectrons

regions of enhancement

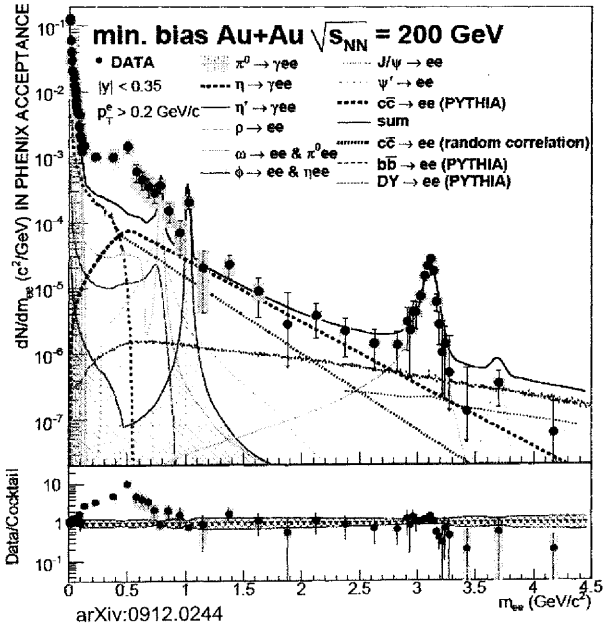

- data and cocktail of known sources.
- striking enhancement below the ω mass (LMR)
- Au+Au matches cocktail in IMR – surprise?

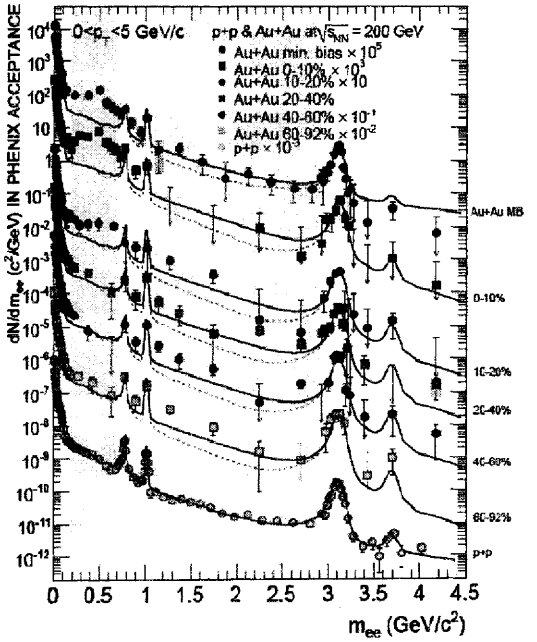

Centrality Dependence

- LMR excess in more central
- *slight* IMR excess in more peripheral
- dashed line is result of max smearing of charm pairs

LMR Enhancement

Centrality Dependance

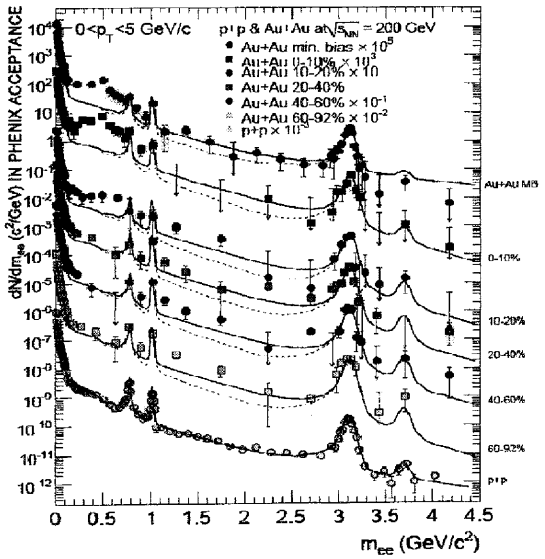

- Enhancement in low mass region is a strong function of centrality.
- Statistics are also sufficient to analyze p_T dependence.
- Need methodical approach to the spectra.

- Yield/(N_{part}/2) in 2 mass windows (a & b)
- π^0 region scales apprx with N_{part}
- Excess region:
  expect contribution from hot matter
  - in-medium production from $\pi\pi$ or qq annihilation
  - yield should scale faster than N_{part} (and it does!)

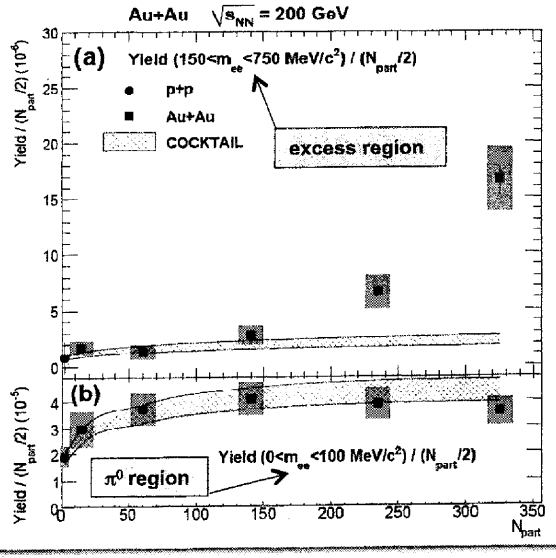

Excess mostly in central AuAu yield increase faster than N_{part}

Thermal Radiation at RHIC

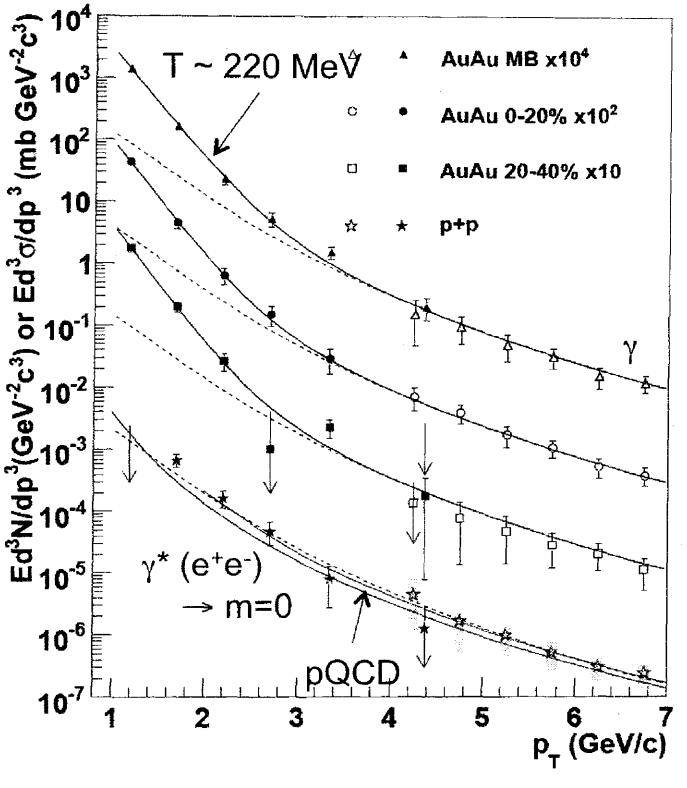

Direct photons from real photons
- measure inclusive photons
- subtract π^0 and η decay photons at S/B <1:10 for p_T<3 GeV
- blue points

Direct photons from virtual photons
- measure e^+e^- pairs at $m_\pi < m << p_T$
- subtract η decays at S/B ~ 1:1
- extrapolate to mass = 0
- red points

First thermal photon measurement:
$T_{ini} > 220$ MeV $> T_c$

Future Directions in CGC Studies at RHIC

L.C. Bland, BNL

RBRC Workshop on *Saturation*...

12 May 2010

We have learned from earlier forward particle production experiments at RHIC that (1) neutral pion production cross sections for p+p collisions at $\sqrt{s}$=200 GeV are consistent with next-to-leading order pQCD calculations for pions produced with large Feynman-x and p_T>2 GeV/c: (2) jet-like structures are observed in p+p collisions for azimuthal correlations between a forward pion and a second hadron, with clear "near-side" and "away-side" peaks with the latter sensitive to the rapid rise of the gluon density near x~0.001; (3) large analyzing powers, that increase with x_F, are observed for forward neutral pion production; (4) forward neutral pion production cross sections are suppressed in d+Au collisions at $\sqrt{s_{NN}}$=200 GeV; and (5) "near-side" azimuthal correlations are present for forward neutral pion pairs in d+Au collisions at $\sqrt{s_{NN}}$=200 GeV, nearly unchanged from those observed in p+p collisions, but "away-side" correlations are suppressed, especially for collisions with small impact parameter. For transversely polarized proton collisions, models that extend beyond the collinear picture to include spin-correlated transverse momentum in distribution and fragmentation functions are found consistent with our measurements. For d+Au collisions, both the suppression of the inclusive yield and the suppression of "away-side" azimuthal correlations are consistent with theoretical expectations for parton saturation in the Au nucleus at low x. The origin of large transverse spin effects and the question of parton saturation are primary motivations for a future electron-ion collider. Present theoretical understanding questions whether there is universality for the spin effects and sensitivity to parton saturation when looking at produced hadrons in p+p and d+Au collisions. Drell-Yan production of virtual photons at large rapidity is expected to be the most robust test of theoretical understanding for p+p and p/d+Au collisions, and then should provide universal quantities that would be probed in a future electron-ion collider. This contribution discusses the basic requirements for production of virtual photons at large rapidity in p+p collisions. Requirements for p+Au or d+Au collisions are similar to those for p+p for virtual photons produced in the deuteron beam direction. Major upgrades at STAR and/or PHENIX would be required for future Drell-Yan (DY) production experiments. We are developing a proposal for a colliding-beam experiment that would demonstrate the feasibility and fully establish the requirements for future upgrades targeted at measuring forward DY production. A key question is whether the charge of each lepton from virtual photon decay must be measured, to allow background subtaction of like-sign pairs. This contribution discusses the status of the DY feasibility experiment proposal.

Motivations for DY Feasibility at IP2

2015	HP13 (new)	Test unique QCD predictions for relations between single-transverse spin phenomena in p-p scattering and those observed in deep-inelastic lepton scattering

Report to NSAC from the Subcommittee on Performance Measures (August, 2008)
http://www.sc.doe.gov/np/nsac/docs/PerfMeasEvalFinal.pdf

- **Timeliness** – HP13 milestone completion by 2015. This could be accomplished during W program if 3IR impact is acceptable.
- **Acceptance/background rejection** – severe space constraints at STAR and PHENIX require major changes in the forward direction. Space constraints are not present at IP2.
- **Is charge sign a requirement?**

Objective of DY feasibility test is to establish the **requirements for future major forward upgrades at STAR and PHENIX** that would be used in a future p+Au or d+Au run that would emphasize Drell Yan production to probe low-x through scaling violations or virtual photon p_T dependence.

Schematic of detector considered

Run-13 configuration
(Uses PHOBOS Split Dipole for charge sign)

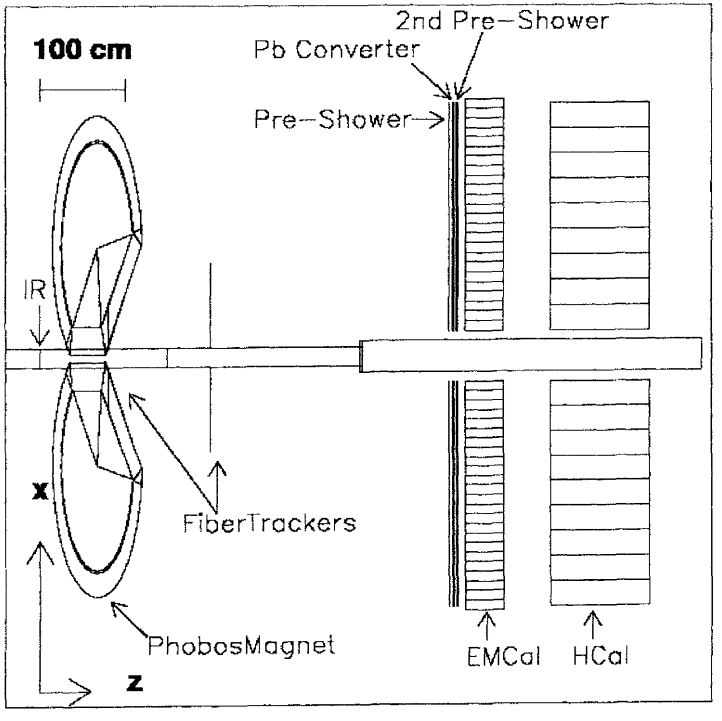

- Hcal is existing 9x12 modules from E864 (NIM406,227)
- EMcal is modeled as only $(3.8cm)^2x(45cm)$ lead glass
- Preshower would require construction
- PHOBOS split-dipole magnetic field in GEANT model
- Fiber tracker stations require specifications and construction

http://www.star.bnl.gov/~akio/ip2/topview3.jpeg

Strategy for estimates

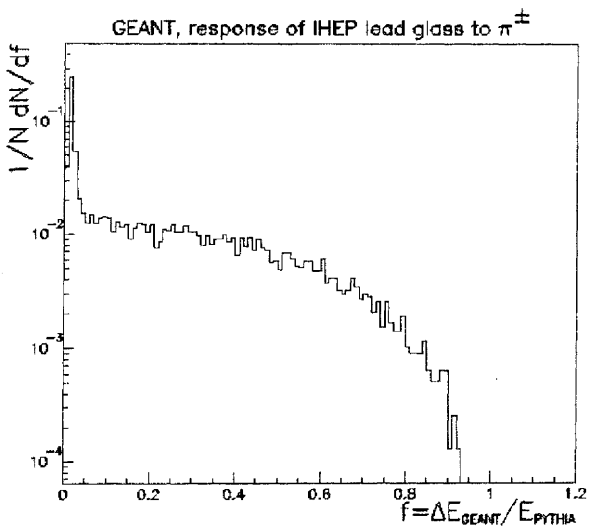

GEANT simulation of EMcal response to E>15 GeV $\pi^{\pm}$ from PYTHIA 6.222 incident on $(3.8cm)^2$x45cm lead glass calorimeter

- ~10^{12} p+p interactions in 50 / pb at $\sqrt{s}$=500 GeV ⇒ full PYTHIA/GEANT not practical
- Parameterize GEANT response of EMcal and use parameterized response in fast simulator applied to full PYTHIA events
- Estimate rejection factors from GEANT for hadron calorimeter and preshower detector (both critical to $h^{\pm}/e^{\pm}$ discrimination)
- Explicit treatment in fast simulator to estimate pathlengths through key elements (beam pipe and preshower), to simulate photon conversion to e+e- pair
- Estimate effects from cluster merging in EMcal ($d < \varepsilon d_{cell}$ / recommended is $\varepsilon \approx 1$)
- Estimate/simulate EMcal cluster energy and position resolutions. $\sigma_E = 15\%/\sqrt{E}$ and $\sigma_{x(y)} = 0.1 d_{cell}$, used to date for $\pi^0 \rightarrow \gamma\gamma$ rejection.

Estimate 3

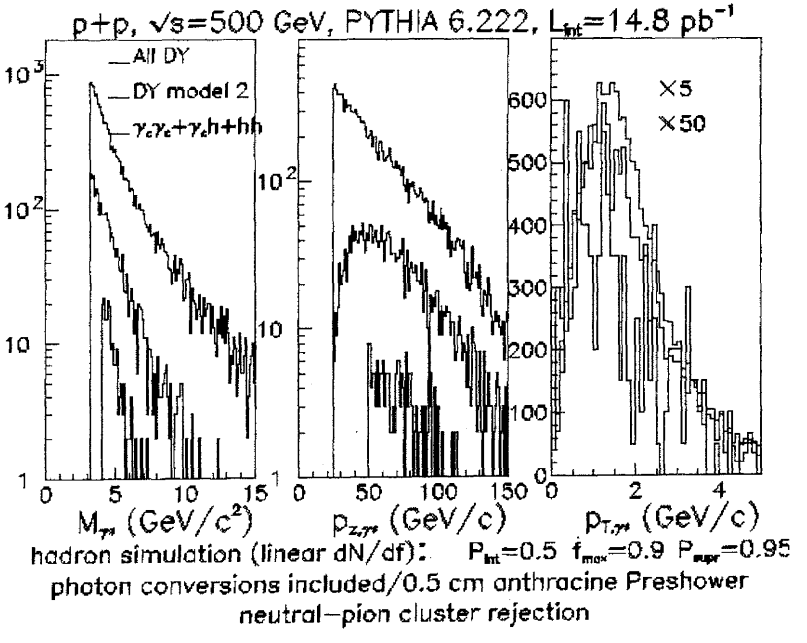

Comments:

- Conversion photons significantly reduced by $\pi^0 \rightarrow \gamma\gamma$ veto
- Preshower thickness tuned, although perhaps is not so critical given photon veto
- Linearly decreasing dN/df estimates smaller hadronic background $\Rightarrow$ increased sophistication needed for reliable estimates, although other model uncertainties could easily dominate.

Staging

Assumptions:

1) ~4 week polarized proton test run at $\sqrt{s}$=500 GeV in RHIC run 11
2) 12 week polarized proton W production run at $\sqrt{s}$=500 GeV in RHIC run 12
3) 12 week polarized proton W production run at $\sqrt{s}$=500 GeV in RHIC run 13

Planned Staging:

1) Hcal + newly constructed BBC at IP2 for RHIC run 11 with goals of establishing impact of 3IR operation and demonstrate calibration of Hcal to get first data constraints on charged hadron backgrounds
2) Hcal + EMcal + neutral/charged veto + BBC for RHIC run 12 with goals of zero-field data sample with L_{int}>50 / pb and P_{beam}=50% to observe dileptons from J/ψ, Υ and intervening continuum. Split-dipole tests envisioned.
3) Hcal + EMcal + neutral/charged veto + BBC + split-dipole for RHIC run 13 with goals data sample with Lint>50 / pb and Pbeam=50% to observe dileptons from J/ψ, Υ and intervening continuum to address whether charge sign discrimination is required

Decadal Planning in PHENIX

Jamie Nagle
University of Colorado, Boulder

for the PHENIX Collaboration

What You Might Know (0-5 Years)

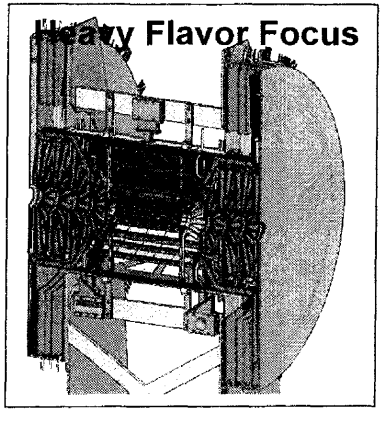

What You Don't Know (6-10 Years)

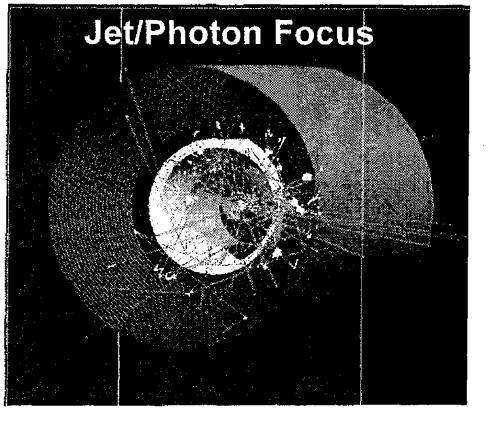

Next 5 Years

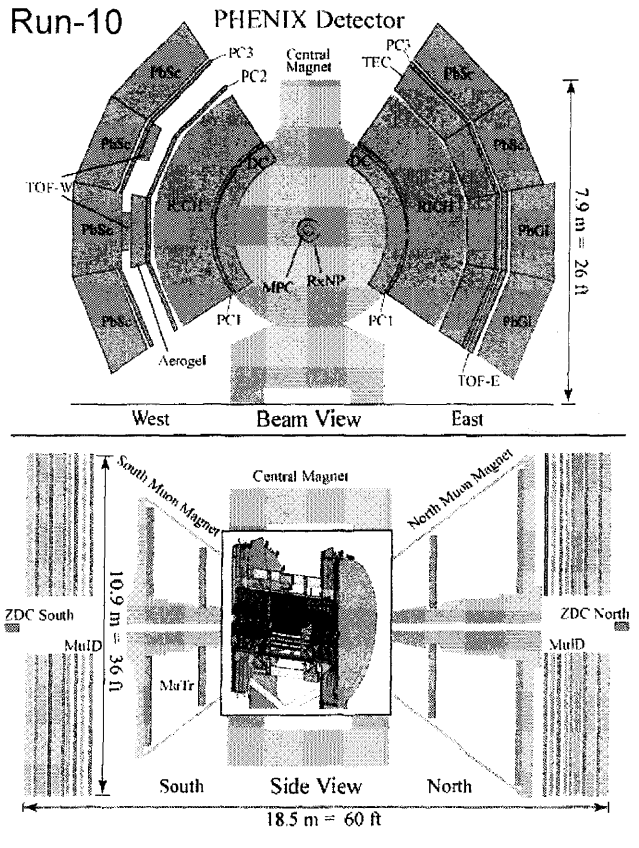

Run-11:

Silicon VTX on schedule.
Precision heavy flavor era!

Muon Trigger Upgrade on schedule! Forward $W \rightarrow \mu$

DAQ Upgrade on schedule!

Run-12:

Forward silicon VTX available.

Run-14:

Forward Calorimetry
(FOCAL proposal – see R. Seto's talk)

Critical to exploit the detectors to do the physics they were designed for.

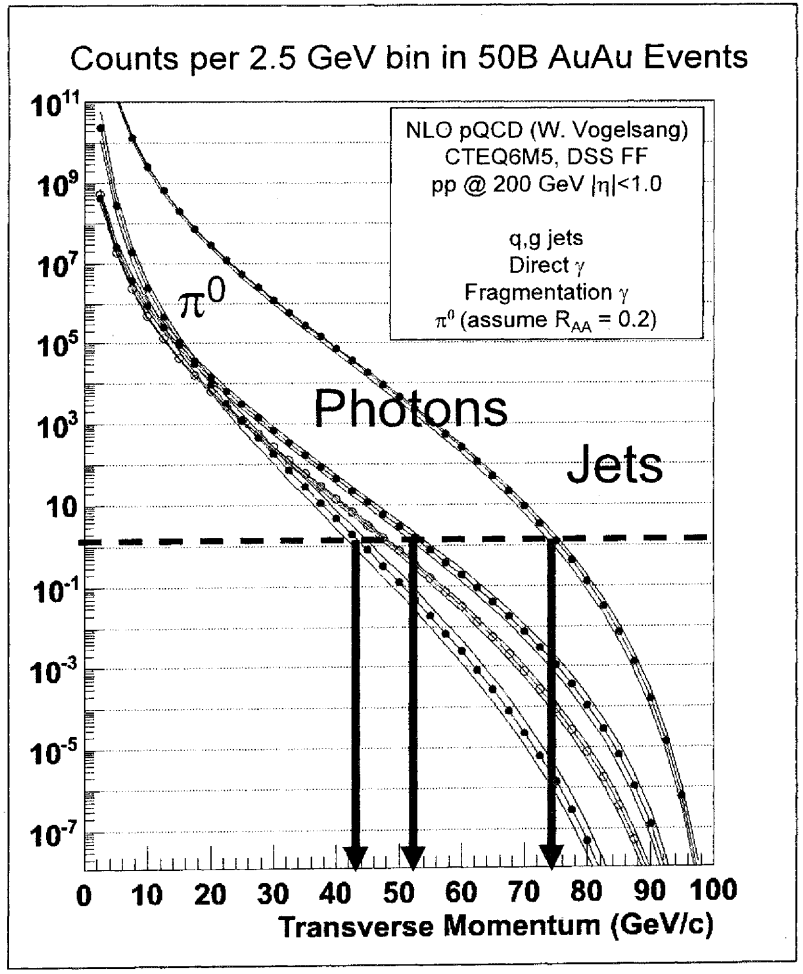
Counts per 2.5 GeV bin in 50B AuAu Events
NLO pQCD (W. Vogelsang)
CTEQ6M5, DSS FF
pp @ 200 GeV |η|<1.0
q,g jets
Direct γ
Fragmentation γ
π0 (assume RAA = 0.2)
π0
Photons
Jets
10^11
10^9
10^7
10^5
10^3
10
10^-1
10^-3
10^-5
10^-7
0 10 20 30 40 50 60 70 80 90 100
Transverse Momentum (GeV/c)

PHENIX New Detector Concept for 2016-2017 frame

Step #1: Remove the outer PHENIX Central Arms

Step #2: Replace Axial Field Magnet with Solenoid
(2 Tesla with inner radius = 70 cm).

Step #3: New silicon tracking layers at 40 and 60 cm

Step #4: Compact EmCal (Silicon/Tungsten) $|\eta|<1.0$
8 cm total depth and preshower layer

Step #5: Hadronic Calorimeter Outside Magnet

Step #6: Maintain high DAQ bandwidth and triggers

Result → PHENIX Reborn

Some steps can be done incrementally, and some would require a longer shutdown (~ 1 – 1 ½ years).

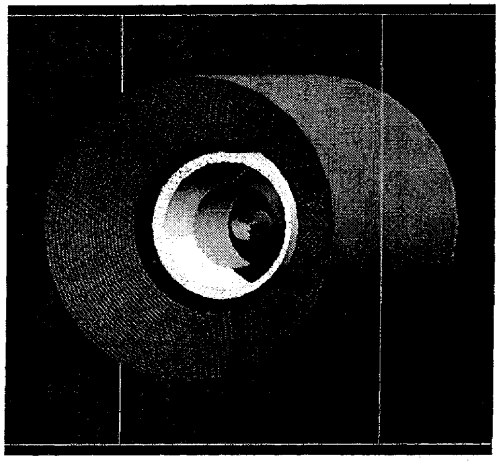

Jet Fragmentation Functions

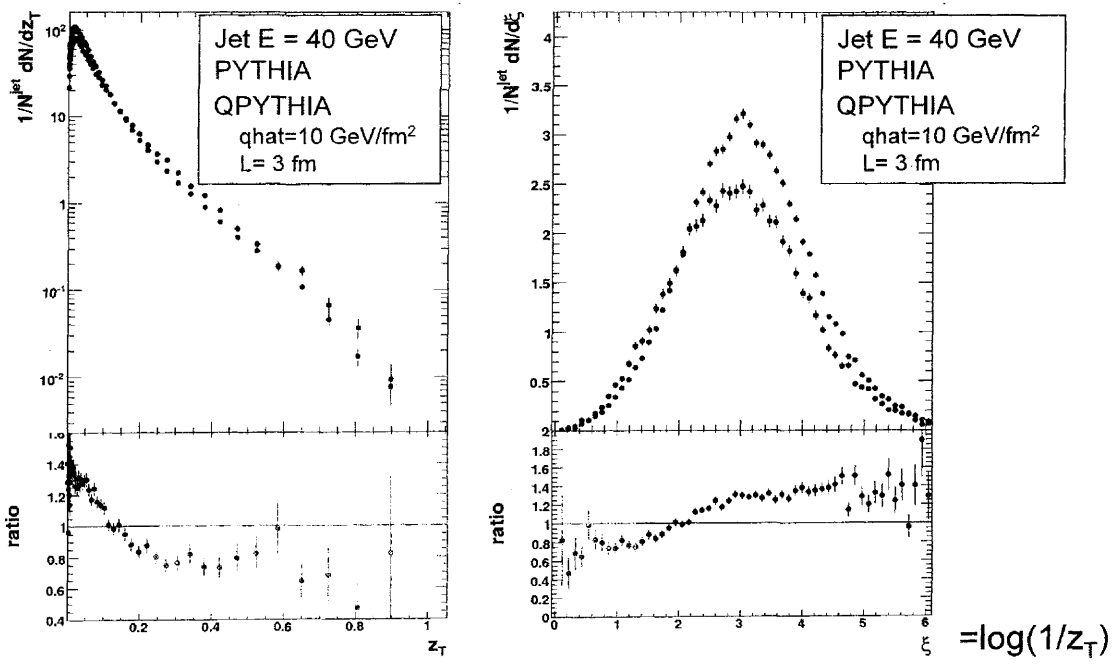

Without HCAL, if fakes dominate above p_T > 10 GeV, then yellow region is not possible without HCAL.
Key for understanding full evolution of high energy parton (far out of equilibrium) rapidly interacting in medium.

Forward Direction Ideas

Discussing in 5++ years to remove the south muon spectrometer and build an electron/photon endcap spectrometer.

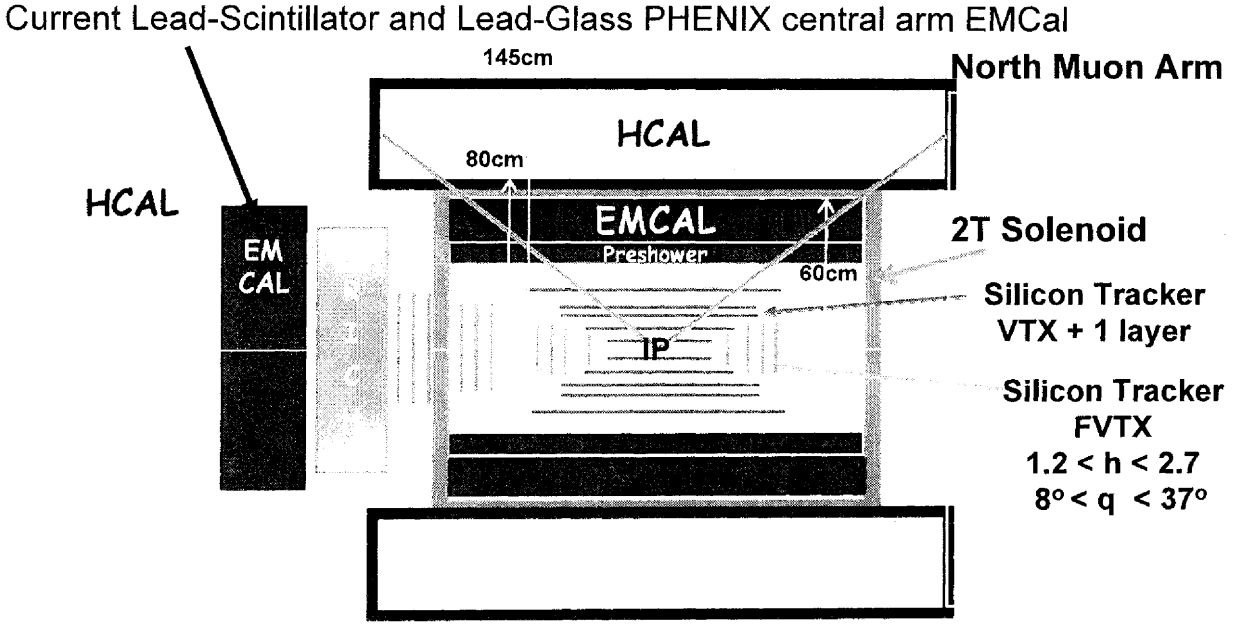

Transverse Drell-Yan measurement under study!
Collins/Sivers measurements beyond FOCAL under study
ePHENIX capabilities under study (led by Elke Aschenauer)

FOCAL a Forward Calorimeter for PHENIX

Richard Seto, University of California, Riverside

The FOCAL is proposed new detector subsystem for PHENIX. Its purpose is to study cold nuclear at low x by measuring direct photons. This topic is of particular interest because the state is expected to be described as a Color Glass Condensate, which in turn is a description of the initial state of the sQGP. The FOCAL is a uniquely new device in that it is a hybrid of a tracking detector and a calorimeter.

What is the FOCAL?

- Si-W calorimeter
  - 44cm from the interaction point
  - Replaces existing Cu nosecone
  - Modular Brick construction
- Prototype performance consistent with expectations
  - Detector is well understood

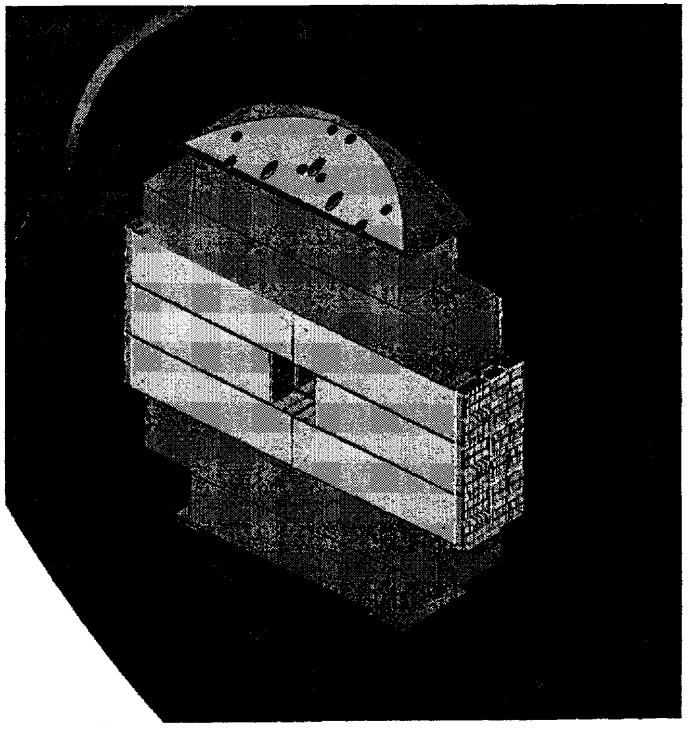

This is a very new type of detector!
A hybrid between a calorimeter and a tracking detector

FOCAL Design

FOCAL Supertower

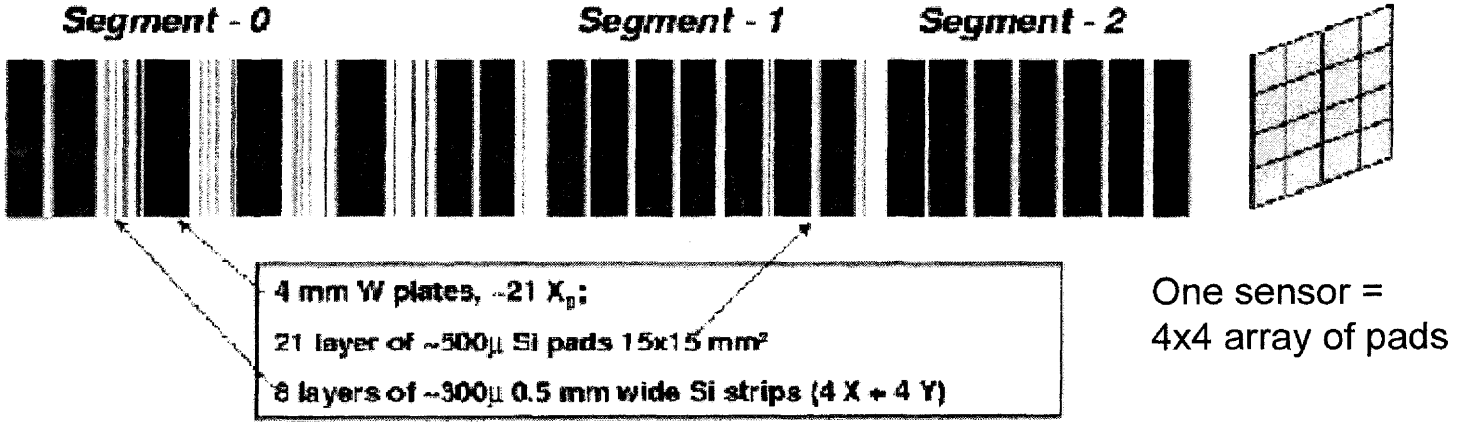

- 4mm tungsten plates in three longitudinal segments
  - Detector is $24X_0$, $0.9L_{abs}$
- 15.5 mm^2 pads (matched to EM showers) for energy measurement
- 8 layers of 500μm Si strips in Segment 0 (4X layers, 4Y layers)
  - Positioned at $2X_0$, $3X_0$, $4X_0$, $5X_0$
  - π^0/γ separation for E<50GeV

Key to measuring γ_{direct} ⇨Measuring the π^0

- A high energy π^0 shower as seen by the pads:
- Reconstruct "Track"
  - Find Center of gravity in each segment
  - NOTE: It's a tracking calorimeter with several planes
  - Found Center of Gravity but
  - Individual photon tracks not distinguishable

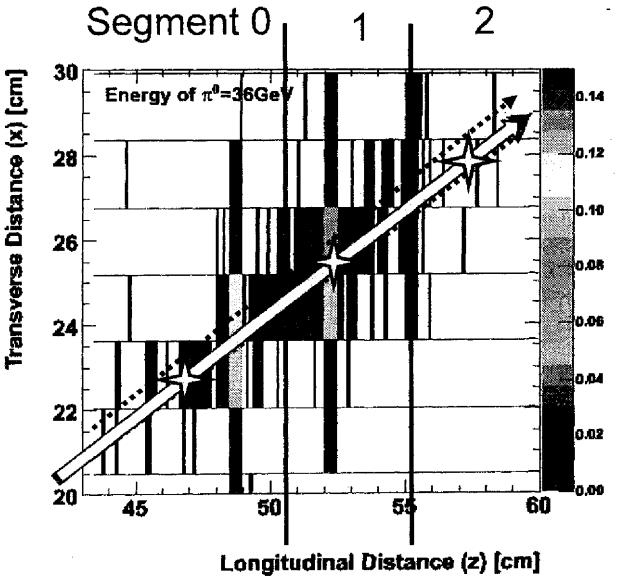

Look at GEANT Hits

Invariant Mass Distribution
"Single track" π^0

- Calculate invariant mass
  - Opening angle: derived only by strips
  - Photon energy: derived only by pads

    Energy is assumed to be shared equally between each γ
  - photons reconstruct to small invariant mass
- Double-peak feature of the reconstruction:
  - Due to correctly reconstructed mass
  - 2nd photon is low energy or overlap too complete
  - Ratio can be gotten from test beam

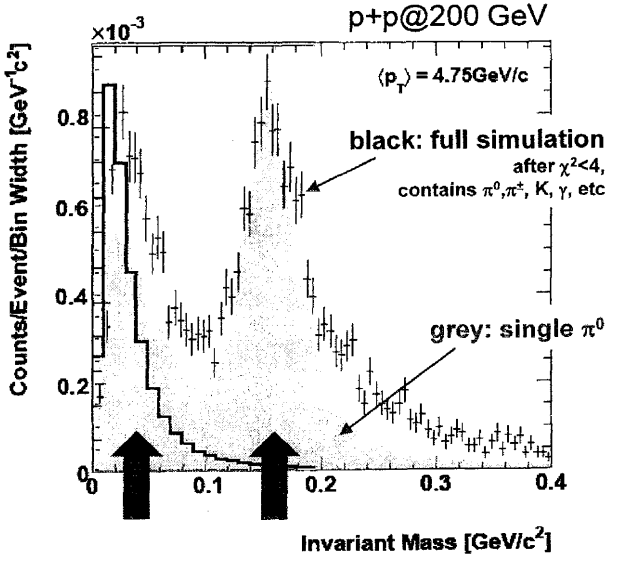

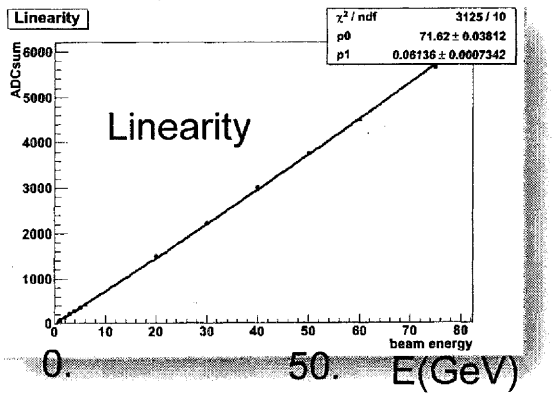

0. 50. E(GeV)

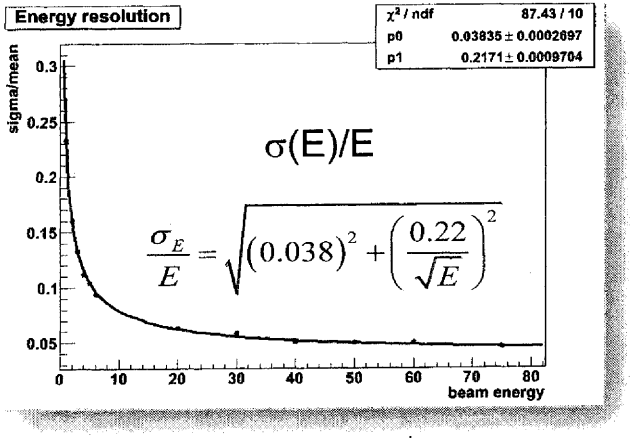

Simulation: 0.23/√E

(test beam- cable problem, HV?)

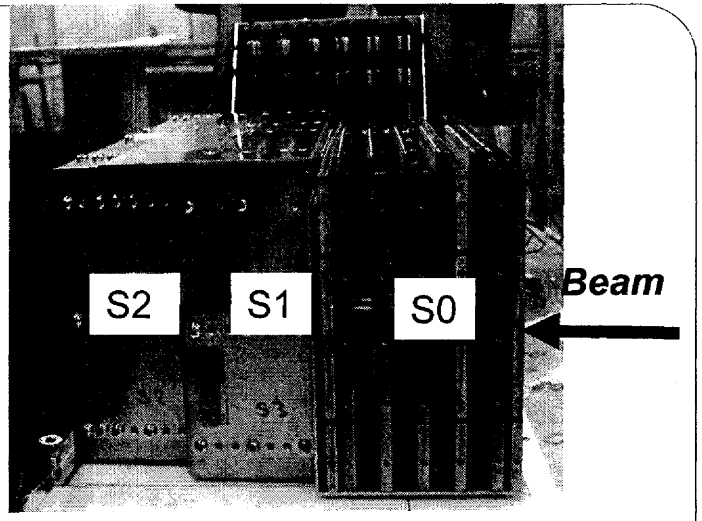

DATA

SIM

longitudinal

transverse

S0

E(GeV)

x-x_{CG}

longitudinal and transverse profiles

S1

S2

Timescale and Summary

- **Timescale**
  - FOCAL could be on the floor for first data taking in Run-13 (2012-2013)
  - A reasonable timescale for the next d+Au run is probably Run-14

    Runs 11-12 dominated by pp (*W* physics), AuAu
- **Summary**
  - **The FOCAL will make possible exciting new measurements of the gluon PDF at low-x**

    Addresses saturation and CGC physics & the initial state of Heavy Ion Collisions

    Main channel: Direct photon
    - direct probe of the gluon distribution making it simpler theoretically
    - complementary to existing efforts

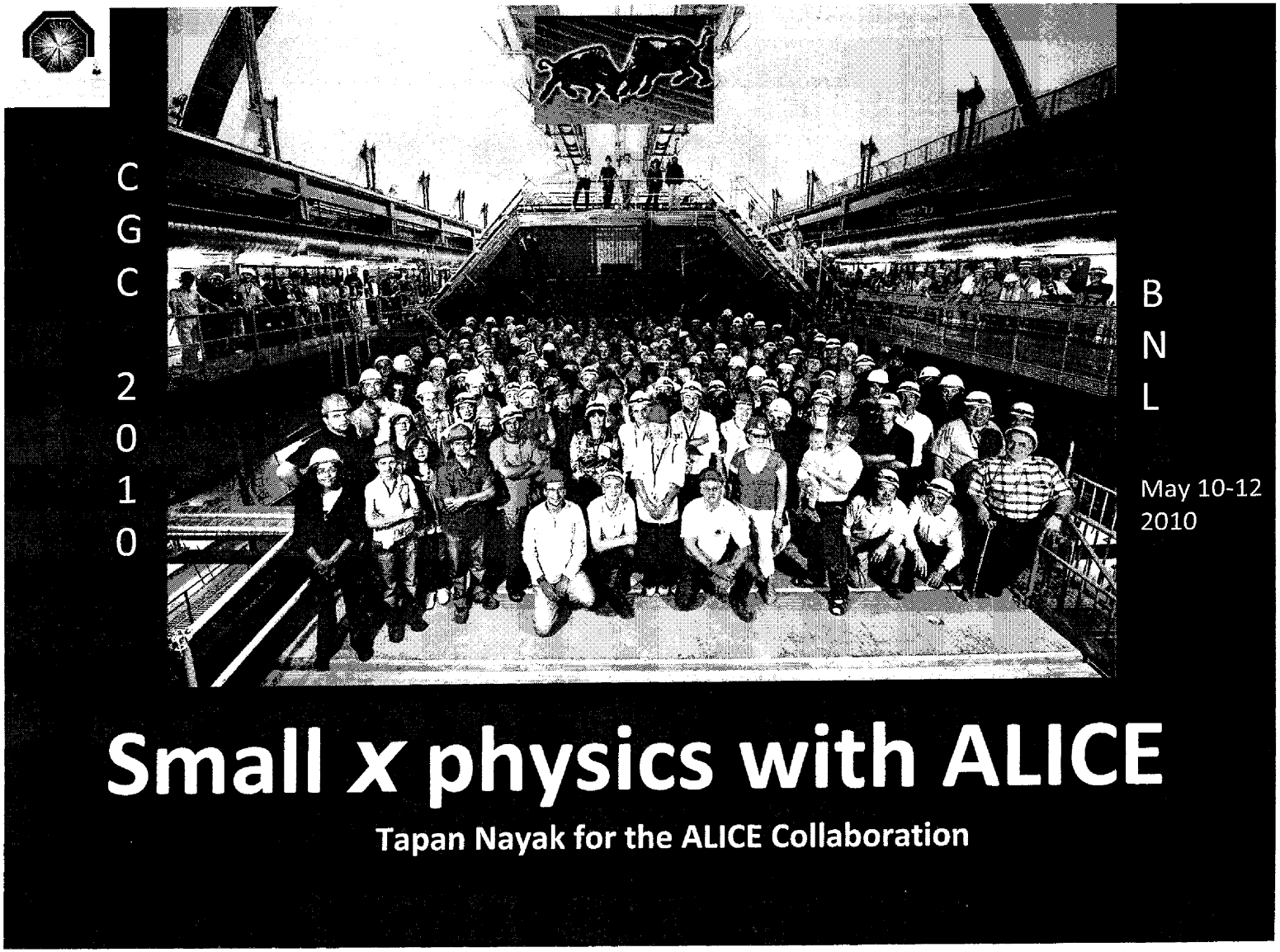
CGC 2010
BNL
May 10-12 2010
Small x physics with ALICE
Tapan Nayak for the ALICE Collaboration

Small *x* physics with ALICE

OUTLINE:

1. Introduction
2. ALICE: present Capabilities
3. ALICE Future plans: Forward EM Calorimeter
4. Sample of Results from ALICE p-p runs so far

Study of Small-*x* Parton Distributions

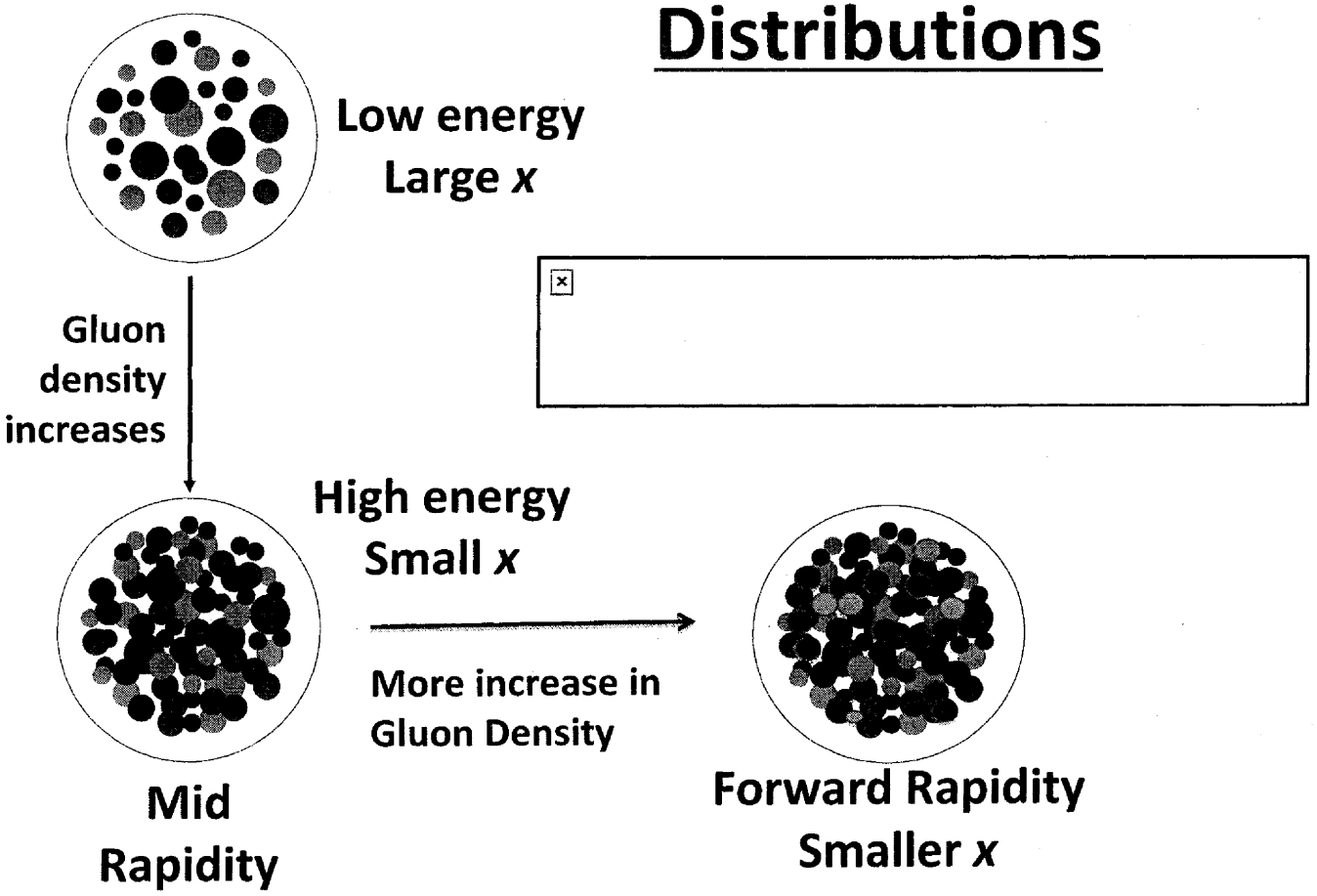

Collisions at the LHC

p-p: $\sqrt{s}$ = 14 TeV
p-Pb: $\sqrt{s}$ = 8.8 TeV
Pb-Pb: $\sqrt{s_{NN}}$ = 5.5 TeV

- **p-p collisions**
  - Test of pQCD and saturation models in a new $\sqrt{s}$ and *x* regime
  - Baseline for Pb-Pb
- **p-Pb collisions**
  - Probe nuclear PDFs
  - Disentangle initial and final state effects
- **Pb-Pb collisions**
  - Probe the hot and dense medium

• Unexplored small-*x* region
• Window on the rich phenomenology of high-density PDFs:
Shadowing, Gluon saturation, Color Glass Condensate

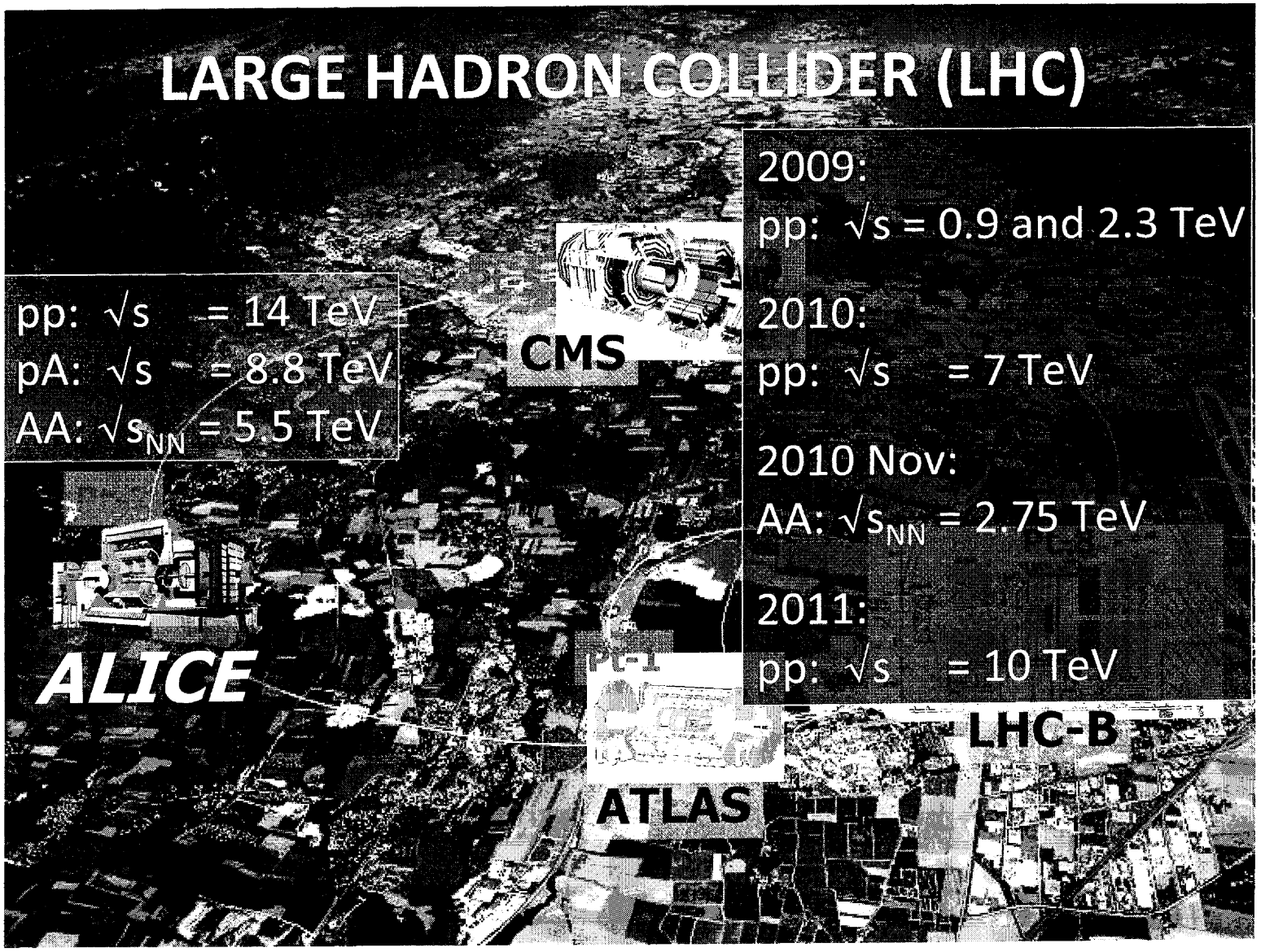
LARGE HADRON COLLIDER (LHC)
pp: √s = 14 TeV
pA: √s = 8.8 TeV
AA: √s_NN = 5.5 TeV
CMS
2009:
pp: √s = 0.9 and 2.3 TeV
2010:
pp: √s = 7 TeV
2010 Nov:
AA: √s_NN = 2.75 TeV
2011:
pp: √s = 10 TeV
ALICE
ATLAS
LHC-B

Summary

• p-p, p-Pb and Pb-Pb collisions at LHC offer unprecedented opportunities for studying wide variety of physics related to small Bjorken-*x*

• Because of the low p_T acceptance of measured particles, ALICE is well suited for small-*x* study

• Most of the global observables measure by ALICE will be interesting from the small-*x* physics (CGC) point of view
Heavy flavours provide good tool for gluon saturation study

• Future instrumentation of Forward EM Calorimeter will be crucial to small-*x* physics of LHC

Small-x physics with CMS at LHC

We present the capabilities of the **CMS** experiment at the LHC to study **small-x physics**. The LHC is designed to provide p+p, p+A and A+A collisions at maximal $\sqrt{s_{NN}}$ = 14, 8.8 and 5.5 TeV respectively with peak luminosities of 10^{34}, 10^{29} and $5 \cdot 10^{26}$ $cm^{-2}s^{-1}$. Such large energies and luminosities will allow **detailed QCD studies** at unexplored low-x values using different probes like jets, quarkonia, heavy quarks, etc.

CMS is a general-purpose experiment **designed** for the exploration of the physics at the TeV energy scale. CMS is the **largest acceptance detector** at the LHC. This detector is a 22 m (length)× 15 m (diameter) apparatus featuring a 3.8 T solenoid surrounding **central tracking** detectors (silicon pixel and microstrip detectors) and **electromagnetic** ($|\eta|<3$) and **hadronic** ($|\eta|<5$) **calorimeters**. **Muon detectors** ($|\eta|<2.4$) are embedded in the flux return iron yoke of magnet. CMS has unique detection capabilities in the forward region thanks to **CASTOR** ($-6.6<\eta<-5.2$) and the **ZDC** ($|\eta|>8.3$) calorimeters.

We present a selection of **five observables** which are sensitive to parton saturation effects and measurable in CMS in both **p+p** (forward jets, Mueller-Navelet dijets, energy flow) and **Pb+Pb** (charged hadron rapidity density, ultra-peripheral photoproduction of Υ) collisions. Also **first experimental results** from 0.9, 2.36 and 7 TeV p+p collisions at LHC are presented.

Magdalena Malek

University of Illinois at Chicago

on behalf of the CMS collaboration

p+p collisions: FORWARD JETS

- **very low-x** gluon density in the proton is poorly known: forward jet cross sections $d\sigma(p+p\rightarrow jet) = \mathbf{PDF}(x_1,Q^2)\otimes\mathbf{PDF}(x_2,Q^2)\otimes d\sigma(qg\rightarrow jet)$ constrain low-x gluon PDF
- forward jet production in CMS calorimeters: for **HF x~10^{-4}**, for **CASTOR x~10^{-5}**
- the minimum x probed decreases by a factor of ~10 every 2 units of rapidity

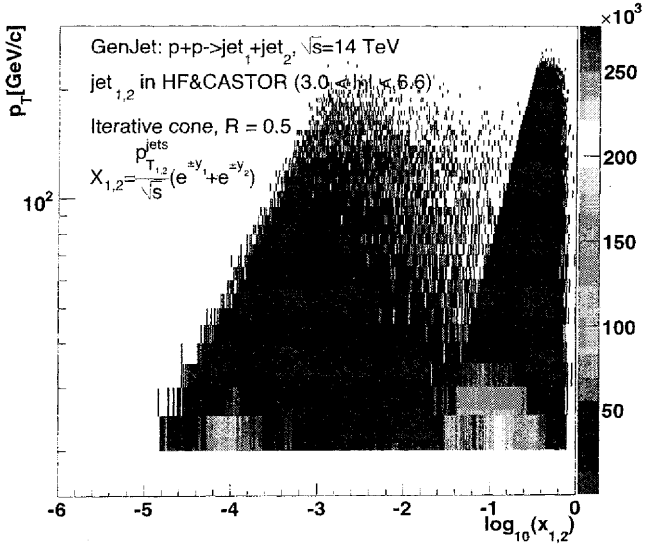

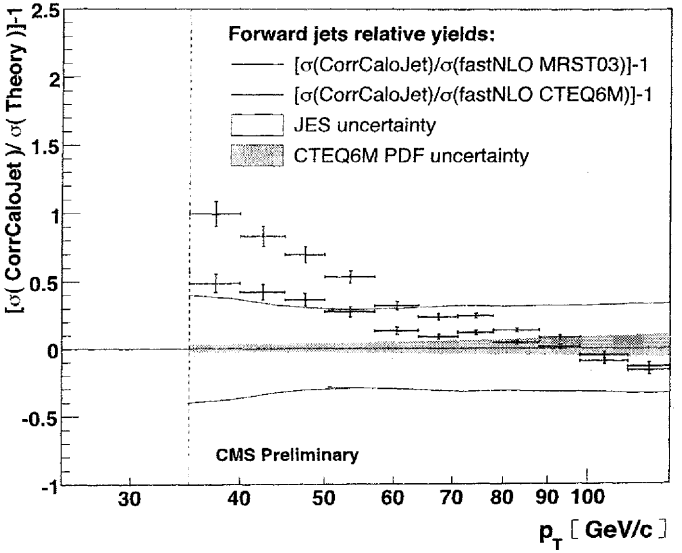

unprecedented calorimetric coverage in pseudo-rapidity !

p+p collisions: MUELLER-NAVELET DIJETS

- Mueller-Navelet dijets with **large Δη separation** very sensitive to low-x QCD evolution allow testing ground for **BFKL evolution**
  - ✦ BFKL **extra radiation** between the 2 jets will **smear out** back-to-back topology
  - ✦ enhanced radiation partially compensated by gluon saturation?
- **increased azimuthal decorrelation** with increasing Δη

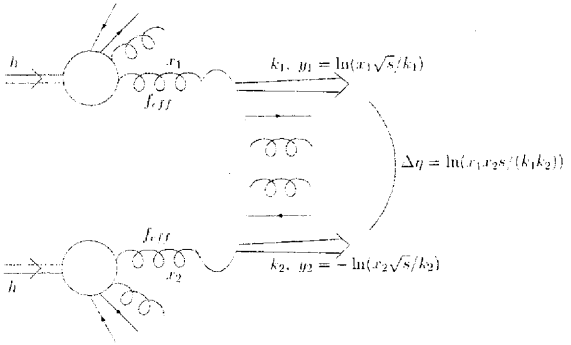

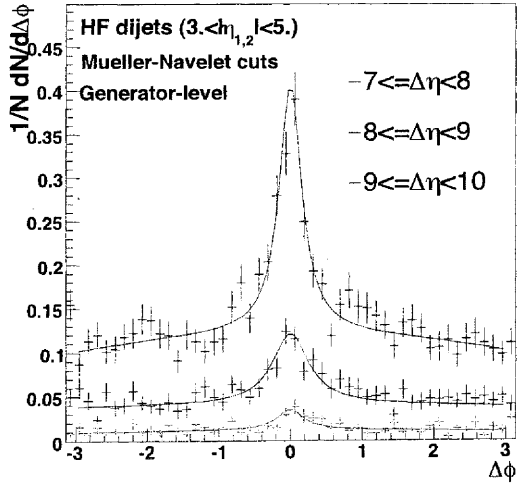

dedicated trigger !

p+p collisions: FORWARD ENERGY FLOW

- improve the understanding of the **parton radiation** in the initial state
- Monte Carlo based predictions: energy flow in central region at low energy does not change much with tunes but **significant difference** observed in the **large pseudo-rapidity region** ($|\eta|>2$)
- energy flow ratio definition:
  Ratio = Energy deposited for 2.36 (7) TeV / Energy deposited for 0.9 GeV
- results on the **detector level**, no systematics uncertainties included

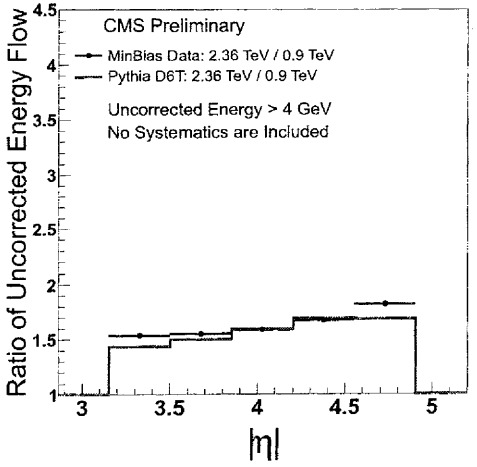

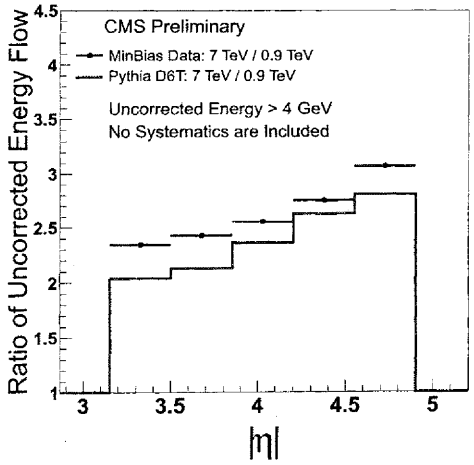

- more energy deposited when increasing energy; more energy deposited in the large η

first results very encouraging !

Pb+Pb collisions: TOTAL HADRON MULTIPLICITY

- final hadron **rapidity density** ∝ number of **initially release partons** at given $\eta \propto Q_s^2$
- **reduced multiplicity** predicted by saturation models: **gluon recombination** reduces incoming parton flux
- saturation driven predictions for LHC: $dN/d\eta$ (η=0)~2000 (8000 before RHIC results)
- method: hit counting in the pixel tracker for $|\eta|<2.5$

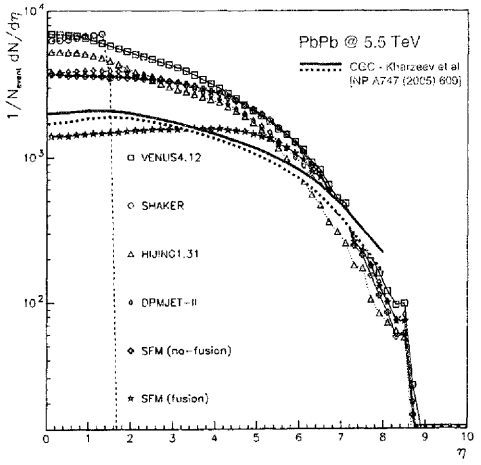

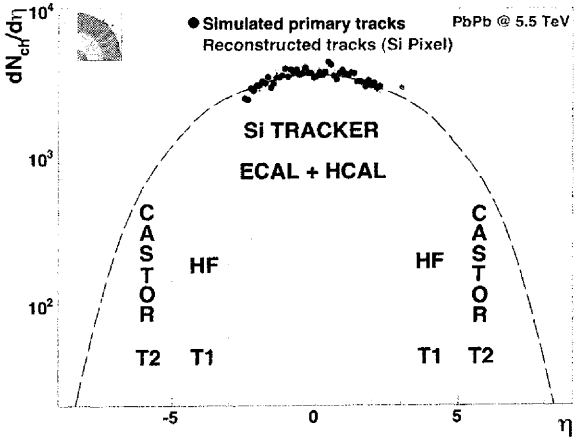

day-1 measurement !

Pb+Pb collisions: QQbar PHOTOPRODUCTION

- in **Ultra-Peripheral Collisions**: electromagnetic field (coherent action of Z=82 proton charges) generates an equivalent flux of **photons**. γ-flux ~ Z^2: **enhancement factor** of 7000 is expected for **Pb beam** (if compared to proton beam)

- **sensitive to the square of the gluon density** in the nucleus; x probed in $\gamma + A \rightarrow \Upsilon + A$ process at LHC: for **y=0 $x \sim 2 \cdot 10^{-3}$**, for **y=2.5 $x \sim 10^{-4}$** ; unexplored (x,Q2) range can be studied !

- **background** from coherent production of lepton pairs in two-photon processes

- full **CMS** simulation (background subtracted)

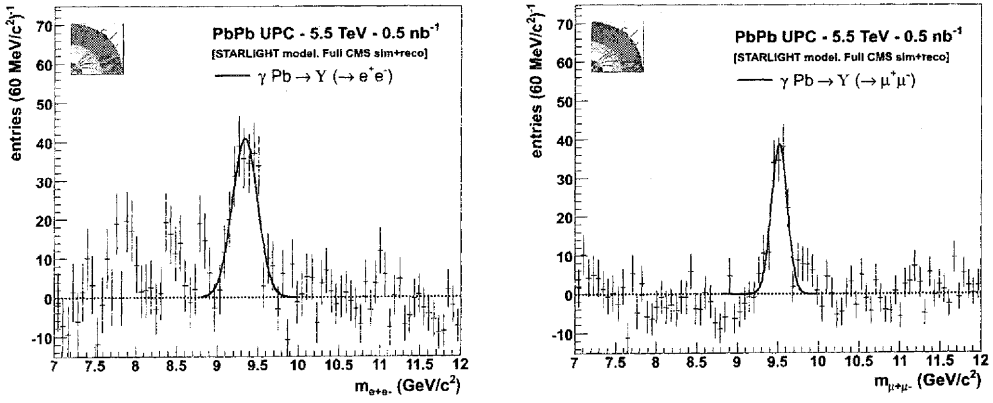

large statistics for detailed studies of PDF !

Low-x Measurements with ATLAS

Brian A. Cole, Columbia University

May 12, 2010

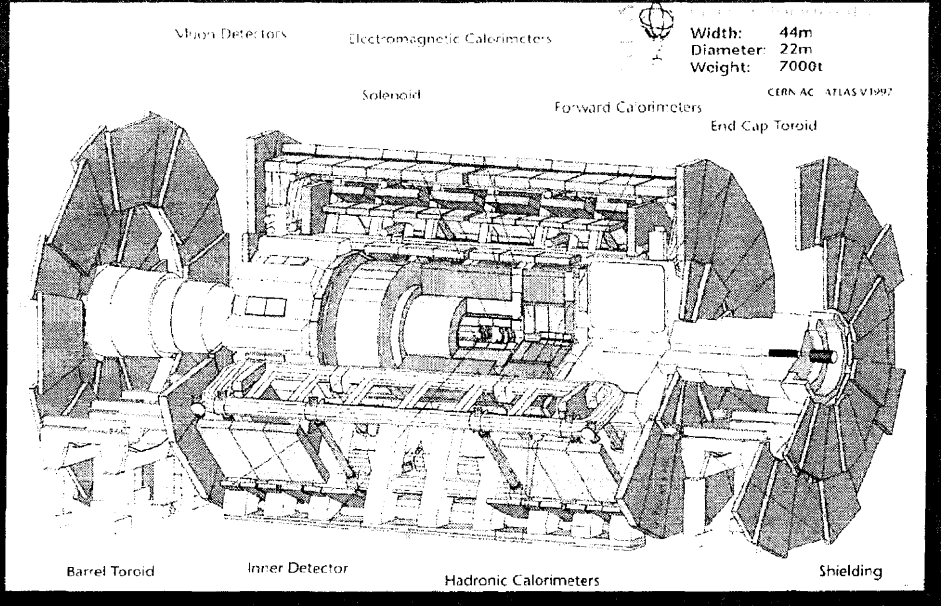

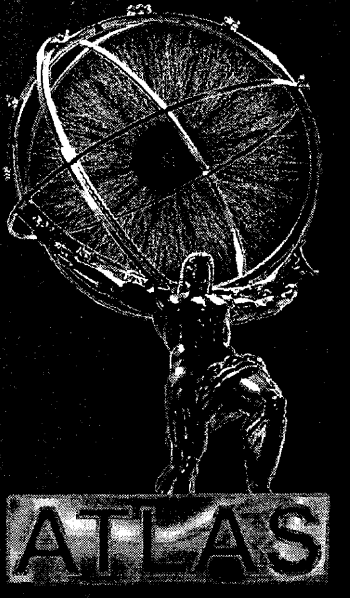

Some ancient history

p-A Physics in ATLAS - Overview

- Study of p-A collisions is essential @ LHC
  - To provide baseline for heavy ion measurements.
  - Physics intrinsically compelling
    - Mini-jet production, multiple semi-hard scattering.
    - Shadowing – test of "Eikonal" QCD.
    - Gluon saturation – probe QCD @ high gluon density.
    - Test factorization.
    - Multiple hard scattering – Measure parton correlations in nucleon (and nucleus ?)
- ATLAS is ideal detector for p-A studies
  - η coverage, calorimeter performance, b tagging, lepton identification, inner tracking.

April 2. 2002 **B.A. Cole – p-A physics w/ ATLAS** 1

- **Low-x physics was the reason I became interested in ATLAS in the first place ...**

"Low-x" Measurements in ATLAS

- p+p
  - Inclusive particle production
  - Rapidity-separated jets (BFKL)
  - Diffractive hard processes (BFKL)
- Pb+Pb
  - Inclusive particle production
  - Direct photon, Z production (shadowing)
    ⇒Measure b dependence of shadowing?
  - Ultra-peripheral (γ^*+A)
- p+Pb
  - ~ all hard processes especially γ+jet (shadowing)
  - Moderate p_T hadrons, jets, direct γ vs η
  - Very forward π^0 production with ZDC with fully implemented high-resolution EM module

The ATLAS Detector: Schematic

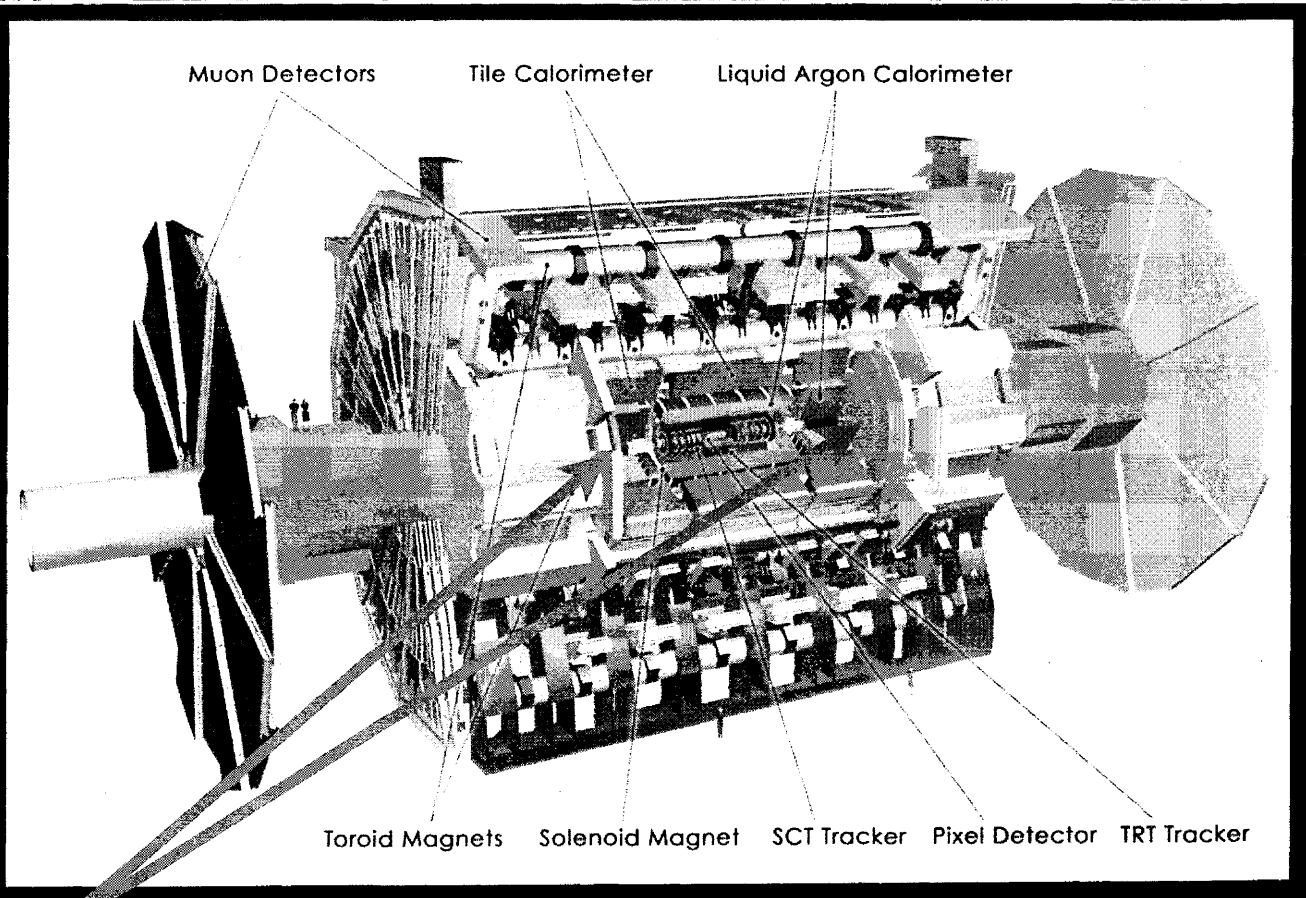

MBTS
trigger scintillators

ATLAS Acceptance

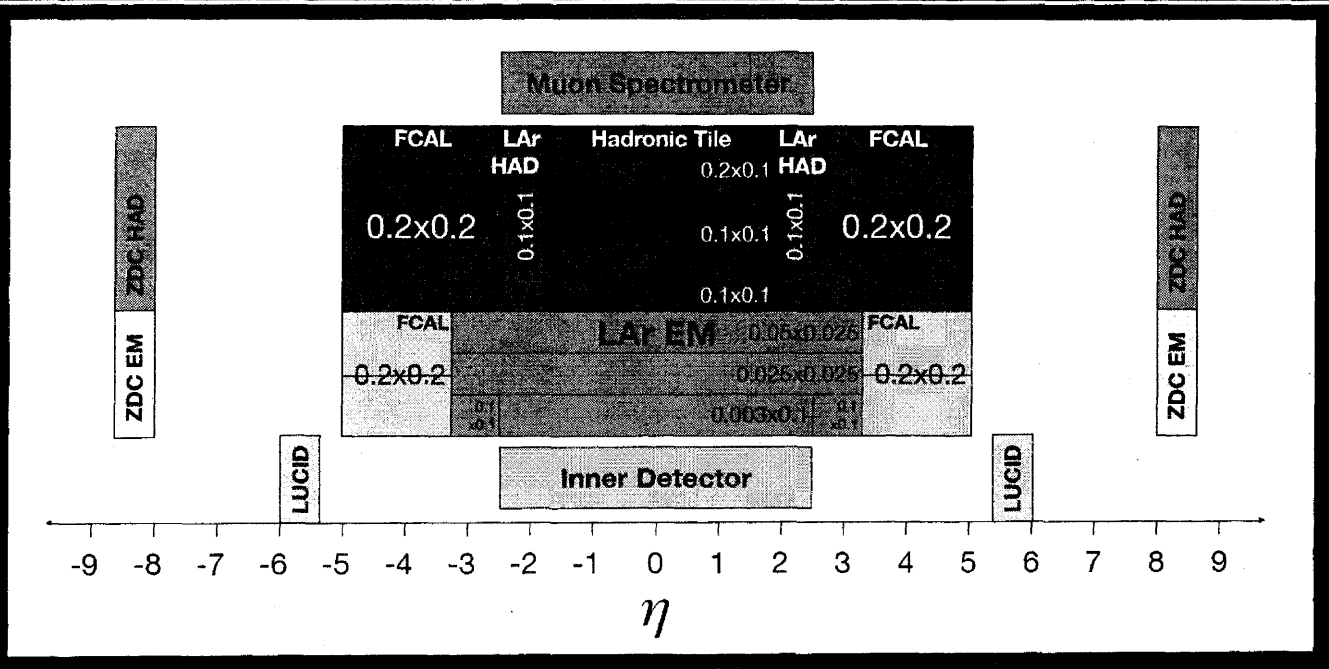

Bulk observables

γ, π^0, isolated γ

Y, Y'

Jets

ATLAS Event Display

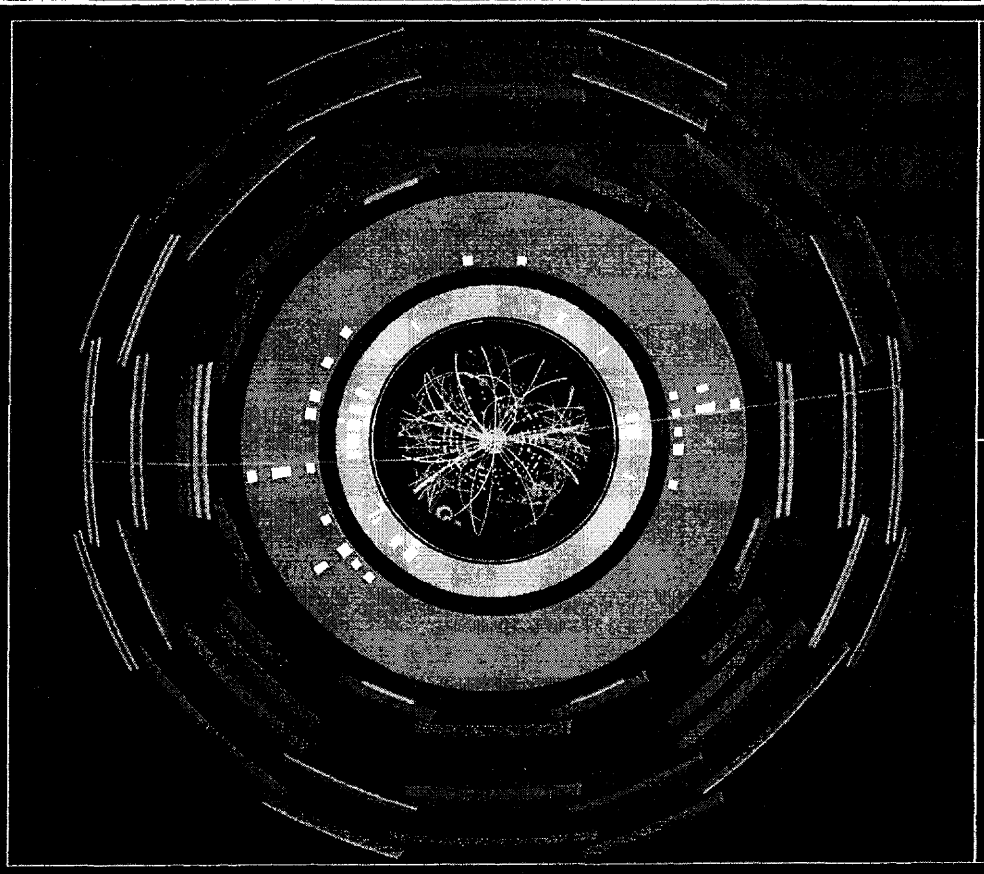

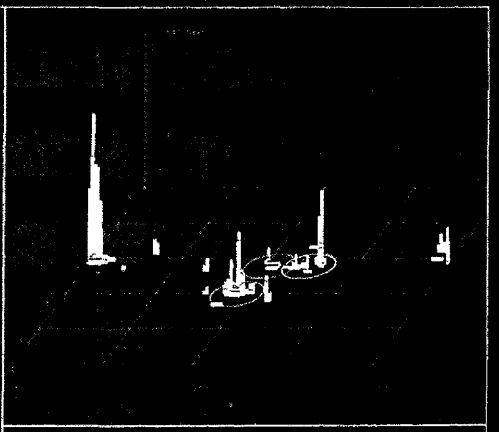

ATLAS EXPERIMENT

Run Number: 152166, Event Number: 890572

Date: 2010-03-30 15:19:40 CEST

7 TeV Event with Jets and 2 Muons

- Di-jet + two muons (heavy quark di-jet?)

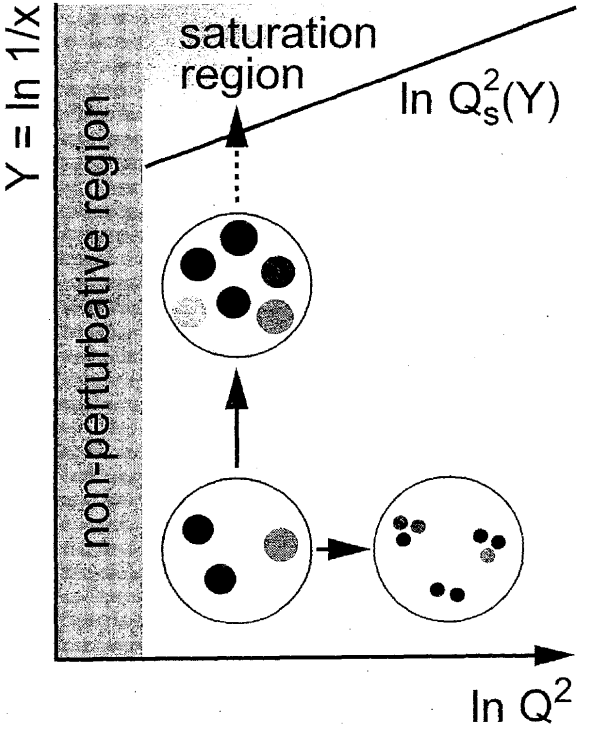

The EIC, Saturation, and the CGC

Thomas Ullrich (BNL)

RIKEN Glasma Workshop, BNL

Wednesday, May 12, 2010

BROOKHAVEN
NATIONAL LABORATORY

EIC Science Case

How do we understand the visible matter in our universe in terms of the fundamental quarks and gluons of QCD?

- What is the nature and role of gluons and their self-interactions (eA, ep)
  - Study the Physics of Strong Color Fields
    - Establish (or not) the existence of the saturation regime
    - Explore non-linear QCD
    - Measure momentum & space-time distributions of glue
  - Study the nature of color singlet excitations (Pomerons)
  - Test and study the limits of universality (eA vs. pA)

EIC Science Case

How do we understand the visible matter in our universe in terms of the fundamental quarks and gluons of QCD?

- What is the nature and role of gluons and their self-interactions (eA, ep)
- What is the internal landscape of the nucleons
  - What is the nature of the spin of the proton?
    - $\Delta G(Q^2, x)$, polarization of the sea quarks
    - Transverse spin and momentum measurements and correlations
  - What is the Three-Dimensional Spatial Landscape of Nucleons?
    - Transverse imaging of quarks and gluons in nucleons
    - Transverse momentum dependent measurements and correlations

EIC Science Case

How do we understand the visible matter in our universe in terms of the fundamental quarks and gluons of QCD?

- What is the nature and role of gluons and their self-interactions (eA, ep)
- What is the internal landscape of the nucleons
- What governs the transition of quarks and gluons into pions and nucleons?
  - How do fast probes interact with the gluonic medium?
    - Energy loss of quarks and gluons
  - Mechanism of fragmentation?

EIC Science Case

How do we understand the visible matter in our universe in terms of the fundamental quarks and gluons of QCD?

- What is the nature and role of gluons and their self-interactions (eA, ep)
- What is the internal landscape of the nucleons
- What governs the transition of quarks and gluons into pions and nucleons?
- Electroweak Physics (studies underway)
  - Parity Violating deep inelastic scattering (PVDIS)
    - Quark helicity distributions
    - Isovector EMC effect
    - Potential ultraprecise weak mixing angle measurements
  - Lepton Flavor and Number Violation
    - Electron-tau lepton conversion

EIC Science Case

How do we understand the visible matter in our universe in terms of the fundamental quarks and gluons of QCD?

The machine presents a unique opportunity for fundamental physics:

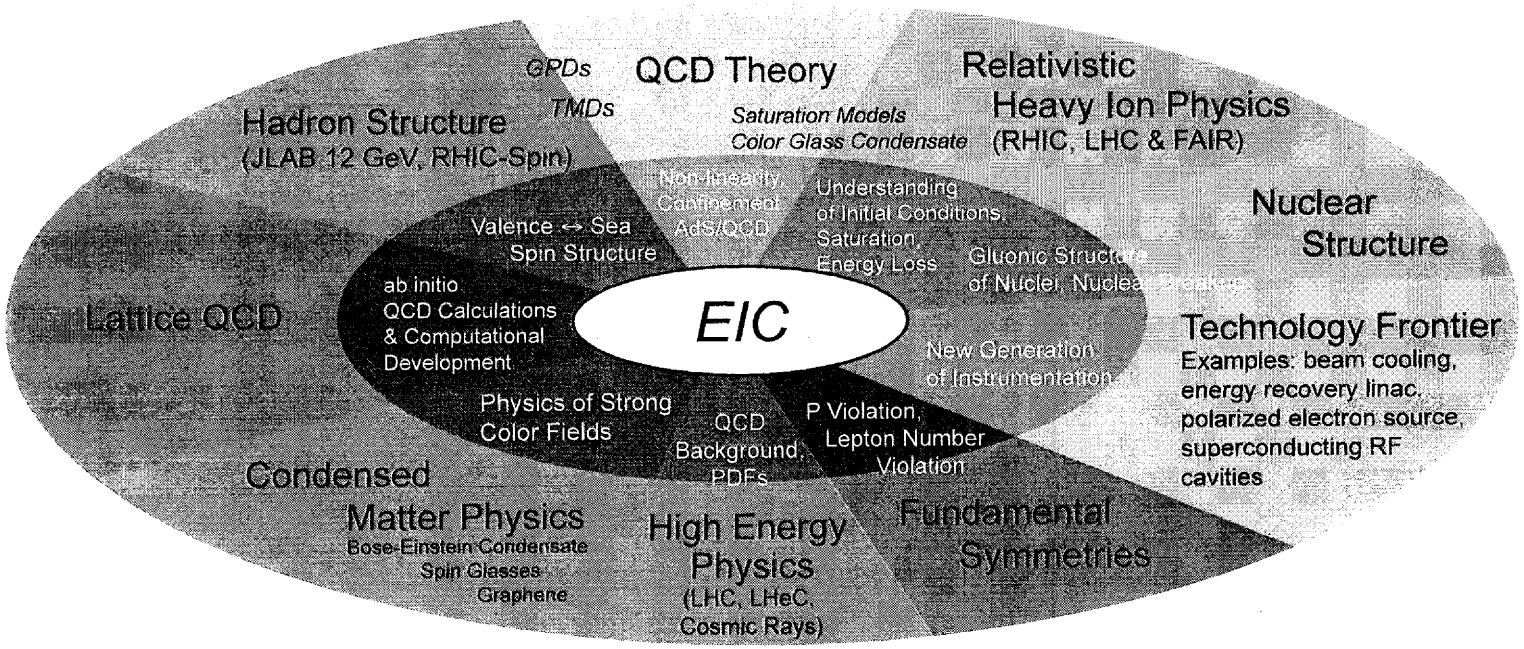

Using Heavy Ions (Pb+Pb) to Search for New forms of QCD matter at LHC

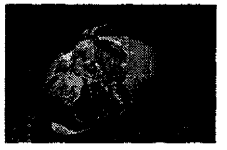

Can the sQGP shed light on its Glasma embryo?

Miklos Gyulassy, Columbia University 5/12/2010

Abstract: In this talk I discuss how the sQGP discovered at RHIC be used as a sensitive detector at LHC to illuminate the theoretical Glasma phase of CGC matter

Part 1: Why are LHC initial conditions so hard to predict?
Part 2: Will Perfect Fluidity evolve into "Divine" Flow at LHC?
Part 3: Will the Glasma solve the (possible) breakdown of sQGP hydro at LHC?
Part 4: Will we be able to deconvolute the Glasma quenching from final state Plasma quenching via pA at LHC?

The challenge to CGCers:
We only have six months to *Predict* new physics and put new ideas on the LHC butcher block

Unshadowed modern LO pdf => much higher entropy dN^{tot}/dy ~ 5000 than popular CGC models (M.Gyulassy 2010)

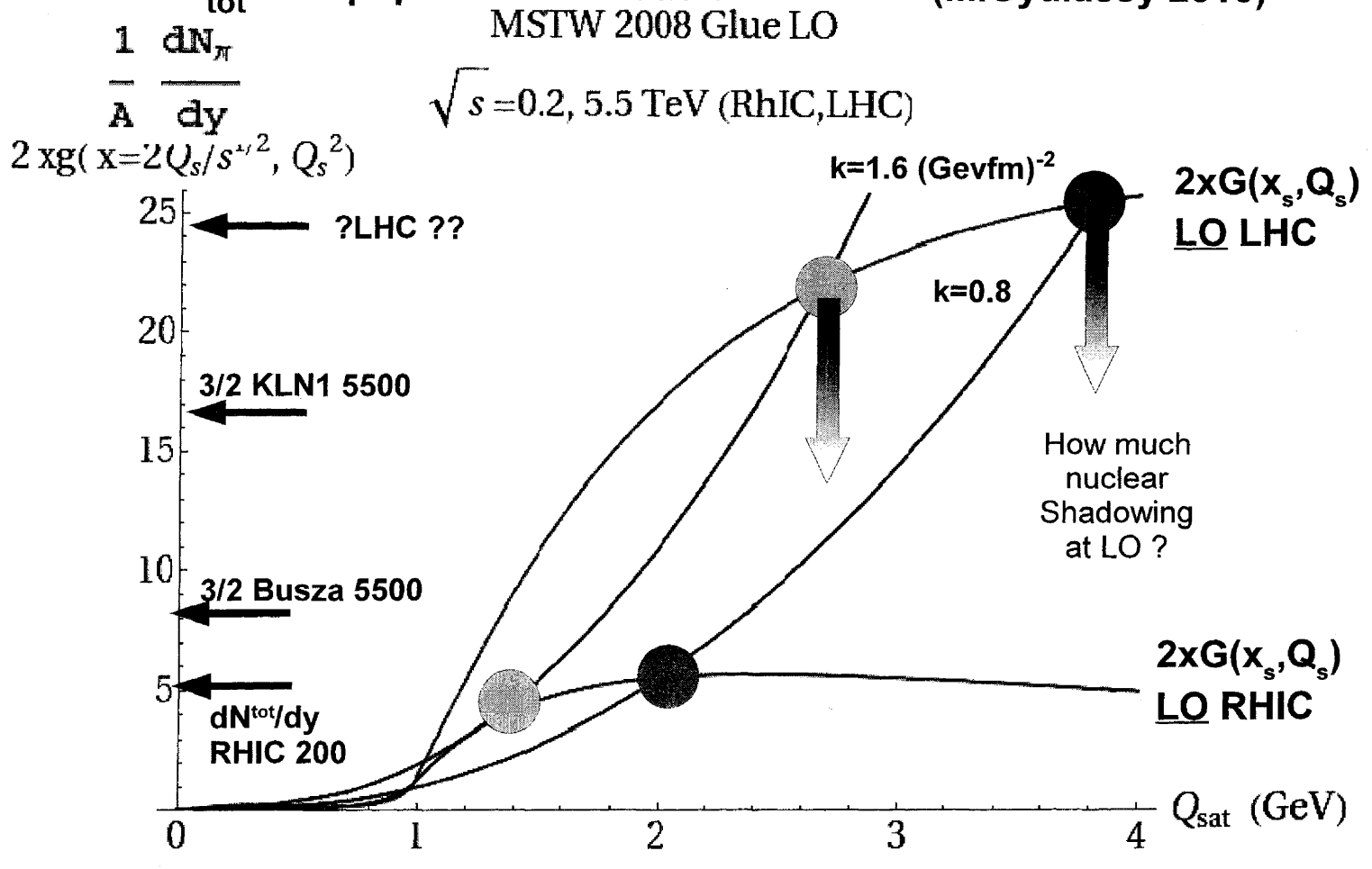

$dN_g/dy/(N_{part}/2) = 2\,xG(x_s=2Q_s/s^{1/2}, Q_s^2) = k\,Q_s^2R^2/(\alpha(Q_s)A)$

RHIC v2 systematics suggests that v2(LHC) maybe > v2 (ideal, η/s=0)

fluidity

"Divine"

ideal

Perfect

Lousy Hadron gas

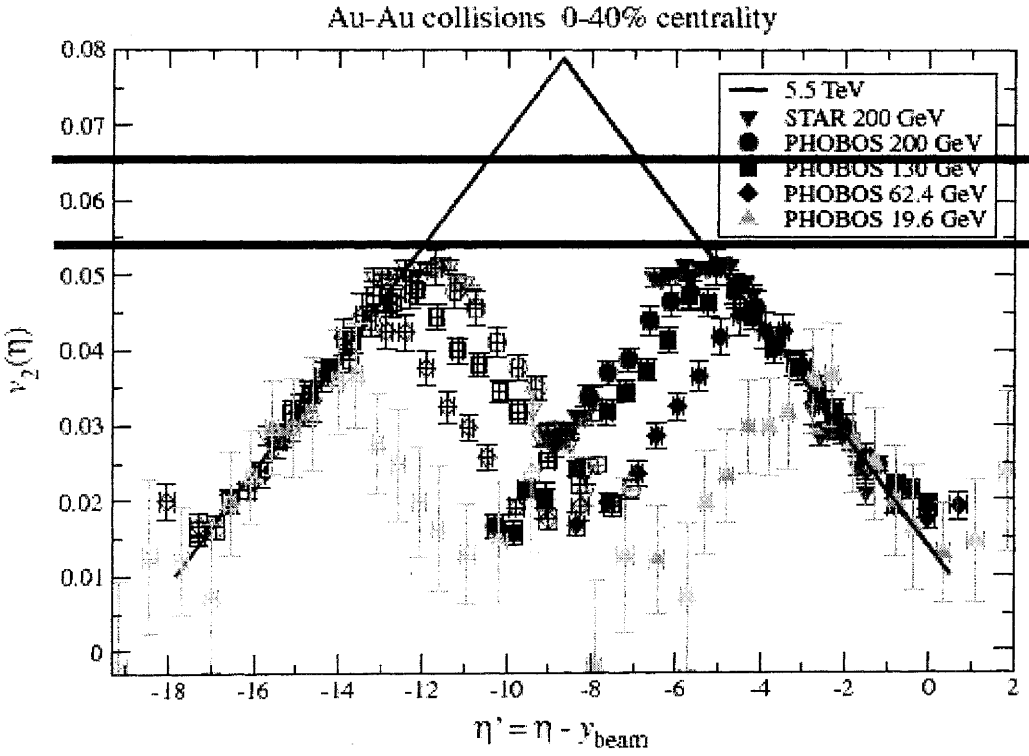

η/s < 0

η/s=0

η/s=1/4π

W.Busza 2006

Figure 4. The elliptic flow v_2, averaged over centrality (0–40%), at various collision energies. Data (full symbols) from PHOBOS [41] and STAR [42] are plotted as a function of $\eta - y_{beam}$ and reflected (open symbols) across the LHC $-y_{beam}$ value.

Gyulassy 05/12/10 BNL

Fuji,Itakara: arXiv:0806.1840

The ideal Glasma flux tube YM Solutions expand radially

equilibrate on fast $1/Q_s < 1$ fm time scales

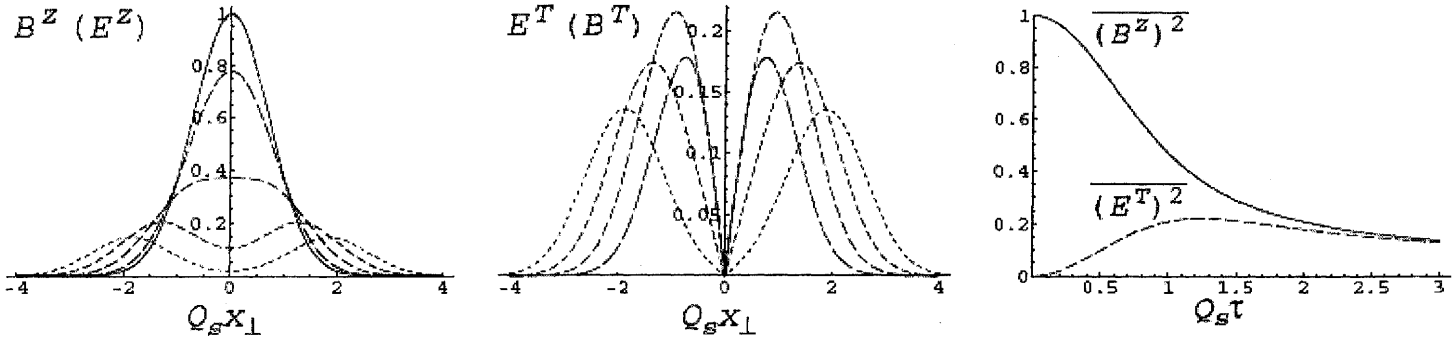

The Glasma transverse expansion could give the sQGP fluid an ***initial radial boost*** to seed "apparent elliptic flow" beyond the zero viscosity limit at LHC. The bulk sQGP could then serve as a detector of the Glasma

(Work in progress by R. Venugopalan et al)

Getting to the bottom of the heavy quark jet puzzle *Physics* **2**, 107 (2009)

Bottom Quark Jet Quenching

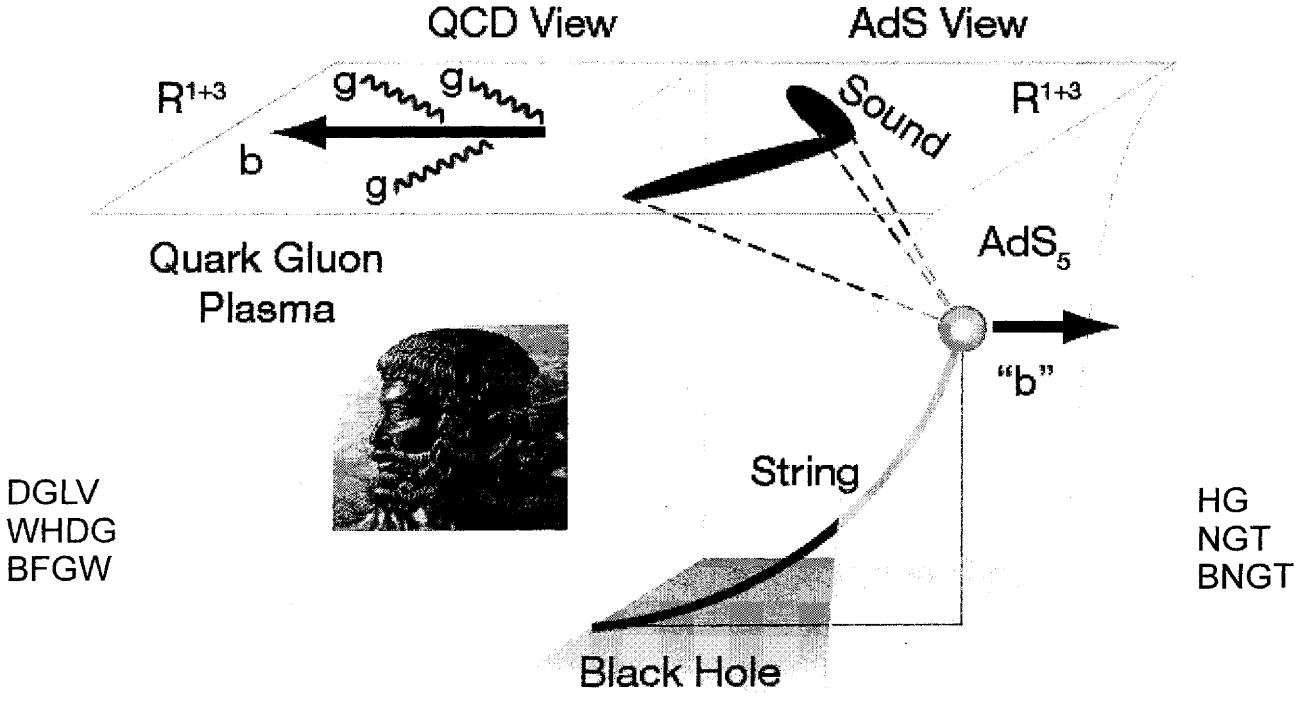

Will Janus require a third face toward CGC to help unravel anomalous heavy quark quenching at LHC ?

Open LHC QCD Matter Challenges

Part 1: LHC initial conditions are hard to predict because quantal CGC is nonlinear physics, sensitive to boundary conditions. But without accurate IC bulk sQGP flow, Jet Quenching etc cannot be inverted.

Part 2: Perfect Fluidity at RHIC may become "Divine Fluidity" with apparent eta/s < 0 on day 1 at LHC

Part 3: Divine flow could be *the* signature of Glasma prequilib transverse flow. Urgent need for numerical predictions for both RHIC and LHC

Part 4: Jet tomography will require extensive p+A studies to enable deconvolution of CGC, Glasma, and final state quenching physics in AA at LHC

the LHC butcher block awaits our predictions!

The Status of Saturation, CGC and Glasma

« What have we learned from RHIC? »

BNL, May 12, 2010

J.-P. Blaizot, IPhT, CEA Saclay and CNRS

OUTLINE

What is the wave function of a nucleus at high energy ?

What is saturation, CGC, Glasma ?

Can one probe the CGC?

Where do we stand?

Looking forward

Conclusions

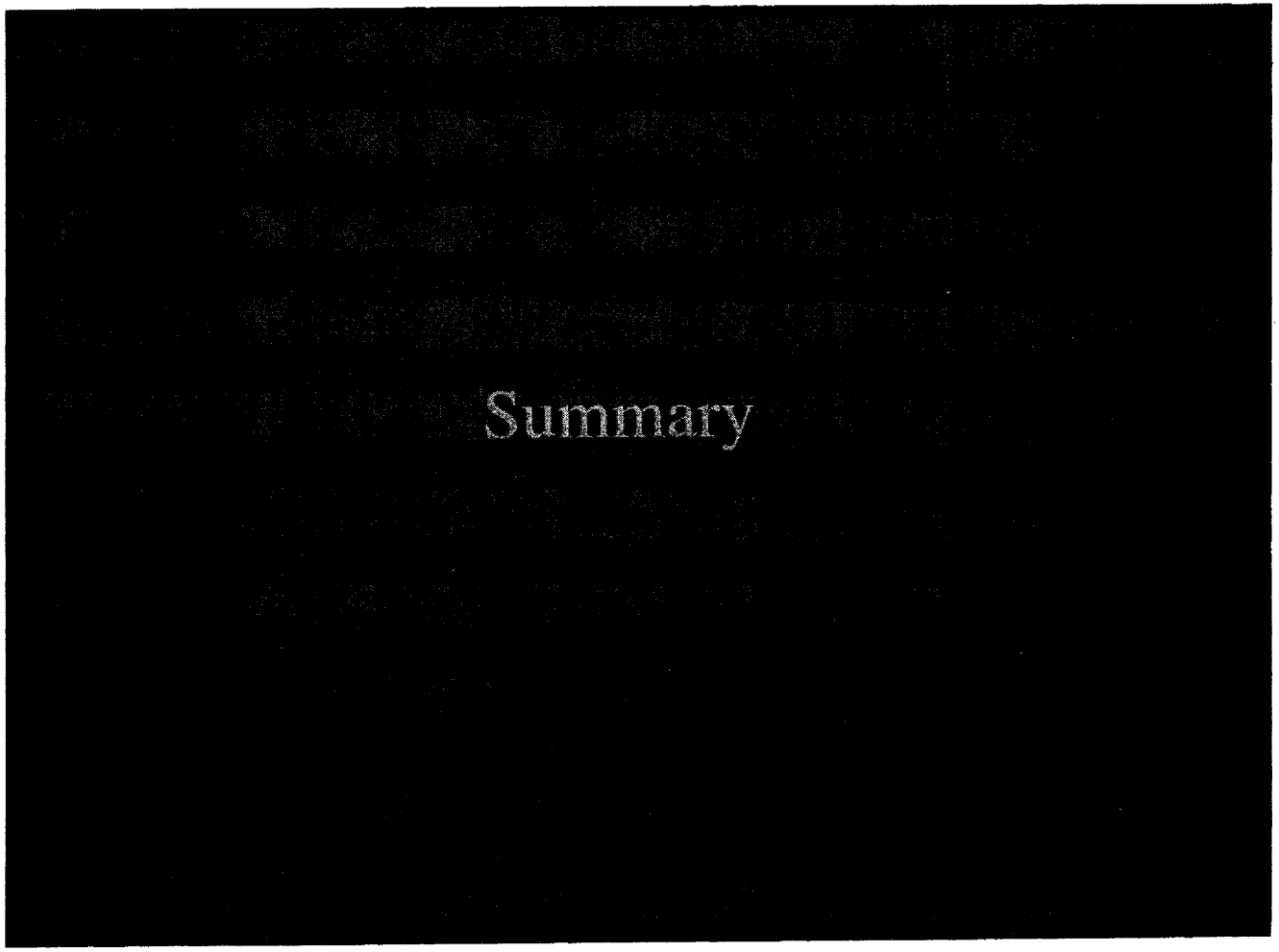
Summary

Saturation is a generic feature of the non linear evolution equations. It is a non perturbative phenomenon produced by the large densities of gluons (in special kinematical regimes).

The CGC formalism is well established theoretically (evolution equations are derived from controlled weak coupling techniques).

The CGC can be **improved**, by calculting evolution equations beyond leading order. When this has been done carefully, this led to a better description of the data.

The CGC (or CGC inspired models) have produced a systematic and sucessful phenomenology, based on a few basic ingredients: the saturation momentum and its variation with energy, size of the systems, and simple (but not always accurate) approximations, such as the kT-factorization. Some features are common to other models (and hence not discriminant), but one may argue in most cases that the CGC provides a better connection to QCD, and the overall picture it provides is more systematic.

The CGC has established itself as an extremely useful reference, organizing principle, suggesting new ways to look at the data and new experiments.

CGC has become an essential step in the building of a space-time picture of nucleus-nucleus collisions ('CGC initial conditions', or 'Glasma initial conditions' are now used in many analysis).

New theoretical results have been obtained (factorization theorems) that allow for controlled calculations of initial stages of heavy ion collisions.

The transition between the glasma and the thermalized quark-gluon plasma remains an outstanding issue.

Recent progress have been truly impressive: the CGC is becoming a **reliable, predictive** tool (and not only a phenomenological guide).

Saturation, The Color Glass Condensate and the Glasma: What Have We Learned from RHIC?

May 10-12, 2010

Organizers: James Dunlop, Larry McLerran, Dave Morrison, and Raju Venugopalan

Workshop Participants

Name	Affiliation	E-Mail Address
Zubayer Ahammed	LBNL	za@veccal.ernet.in
Javier Lopez Albacete	IPhT-CEA-Saclay	javier.lopez-albacete@cea.fr
Tolga Altinoluk	Univ of CT	altinoluk@phys.uconn.edu
Burak Alver	MIT	alver@mit.edu
Anthony Baltz	BNL	baltz@bnl.gov
Ian Bearden	Niels Bohr Institute	bearden@nbi.dk
Dana Beavis	BNL	beavis@bnl.gov
Barbara Betz	Columbia Univ	betz@phys.columbia.edu
Guillaume Beuf	BNL	gbeuf@quark.phy.bnl.gov
Leslie Bland	BNL	bland@bnl.gov
Jean Paul Blaizot	CNRS	jean-paul.blaizot@cea.fr
Ermes Braidot	Utrecht Univ-Nikhef	braidot@rcf.rhic.bnl.gov
Wit Busza	MIT	busza@mit.edu
Alessandro Buzzatti	Columbia Univ	buzzatti@phys.columbia.edu
Chin-Hao Chen	Stony Brook Univ	chinchen@ic.sunysb.edu
Brian Cole	Columbia University	cole@nevis.columbia.edu
Ramiro Debbe	BNL	debbe@bnl.gov
Abhay Deshpande	Stony Brook Univ	abhay.deshpande@stonybrook.edu
Fabio Dominguez Gonzalez	Columbia Univ	fabio@phys.columbia.edu
Adrian Dumitru	Baruch College, CUNY & RBRC	Adrian.Dumitru@Baruch.cuny.edu
James Dunlop	BNL	dunlop@bnl.gov
Kevin Dusling	BNL	kdusling@quark.phy.bnl.gov
Andrej Ficnar	Columbia Univ	aficnar@phys.columbia.edu
Stefano Forte	Milan University	forte@mi.infn.it
Kenji Fukushima	Yukawa Inst for Theoretical Phys	fuku@yukawa.kyoto-u.ac.jp
Sean Gavin	Wayne State Univ	sean@physics.wayne.edu
Francois Gelis	IPhT, CEA/Saclay	francois.gelis@cea.fr
Frederique Grassi	Universidade de Sao Paulo (Brazil)	grassi@if.usp.br
Wlodek Guryn	BNL	guryn@bnl.gov
Miklos Gyulassy	Columbia Univ	gyulassy@phys.columbia.edu
Prasad Hegde	Stony Brook Univ	phegde@quark.phy.bnl.gov
Edmond Iancu	Inst de Physique Thorique de Saclay	edmond.iancu@cea.fr
Jason Kamin	Stony Brook Univ	jkamin@skipper.physics.sunysb.edu
Zhongbo Kang	RBRC	zkang@bnl.gov
Frithjof Karsch	BNL	karsch@bnl.gov
Dmitri Kharzeev	BNL	kharzeev@bnl.gov
Toru Kojo	RBRC	torujj@quark.phy.bnl.gov
Boris Kopeliovich	Technical U Federico Santa Maria	boris.kopeliovich@usm.cl
Yuri Kovchegov	The Ohio State Univ	yuri@mps.ohio-state.edu
Alex Kovner	Univ of CT	kovner@phys.uconn.edu
Henri Kowalski	DESY	henri.kowalski@desy.de
Tuomas Lappi	Univ of Jyvaskyla	tuomas.lappi@jyu.fi
Alexandre Lebedev	Iowa State University	lebedev@iastate.edu
J.H. Lee	BNL	jhlee@bnl.gov

Saturation, The Color Glass Condensate and the Glasma: What Have We Learned from RHIC?

May 10-12, 2010

Organizers: James Dunlop, Larry McLerran, Dave Morrison, and Raju Venugopalan

Workshop Participants

Name	Affiliation	E-Mail Address
Eugene Levin	Tel Aviv University	leving@post.tau.ac.il
Wei Li	MIT	davidlw@mit.edu
Ronald Longacre	BNL	Longacre@bnl.gov
Magdalena Malek	U of Illinois, Chicago / CERN	magdalena.malek@cern.ch
Cyrille Marquet	IPhT - CEA/Saclay	cyrille.marquet@cea.fr
Larry McLerran	RBRC/BNL	mclerran@bnl.gov
Beau Meredith	U of IL at Urbana-Champaign	beau.meredith@gmail.com
Chuan Miao	BNL	chuan@quark.phy.bnl.gov
Jose Guilherme Milhano	CENTRA-IST(Lisbon) & CERN-PH-TH	guilherme.milhano@ist.utl.pt
David Morrison	BNL	morrison@bnl.gov
Berndt Mueller	Duke Univ	mueller@phy.duke.edu
James Nagle	Univ of CO	jamie.nagle@colorado.edu
Tomoaki Nakamura	RIKEN	nakamura@ribf.riken.jp
Tapan Nayak	Variable Energy Cyclotron Cntr	nayak@veccal.ernet.in
Pawan Kumar Netrakanti	Purdue University	pawan@purdue.edu
Jorge Noronha	Columbia Univ	noronha@phys.columbia.edu
Carlos Pajares	Univ Santiago de Compostela	pajares@fpaxp1.usc.es
Peter Paul	Stony Brook Univ	peter.paul@stonybrook.edu
Chris Perkins	UC Berkeley / Stony Brook U	cwperkins@lbl.gov
Rob Pisarski	BNL	pisarski@quark.phy.bnl.gov
Jianwei Qiu	BNL	jqiu@bnl.gov
Robert Ray	Univ of TX at Austin	ray@physics.utexas.edu
Nicholas Samios	BNL / RBRC	samios@bnl.gov
Rolf Scharenberg	Purdue Univ	schrnbrg@purdue.edu
Bjoern Schenke	McGill Univ	schenke@physics.mcgill.ca
Richard Seto	Univ of CA, Riverside	richard.seto@ucr.edu
Edward Shuryak	Stony Brook Univ	shuryak@tonic.physics.sunysb.edu
Michael Skoby	Purdue University	skoby@purdue.edu
Paul Sorensen	BNL	prsorensen@bnl.gov
Brijesh Srivastava	Purdue university	brijesh@purdue.edu
Anna Stasto	RBRC	astasto@phys.psu.edu
Mark Strikman	Penn State Univ	strikman@phys.psu.edu
Michael Tannenbaum	BNL	mjt@bnl.gov
Terence Tarnowsky	Michigan State Univ	tarnowsk@nscl.msu.edu
Giorgio Torrieri	JW Goethe Universitat	lunogled@gmail.com
Kirill Tuchin	Iowa State Univ / RBRC	tuchin@iastate.edu
Thomas Ullrich	BNL	thomas.ullrich@bnl.gov
Raju Venugopalan	BNL	raju@bnl.gov
Flemming Videbaek	BNL	videbaek@bnl.gov
Harmen Warringa	Goethe Univ	warringa@th.physik.uni-frankfurt.de
Bowen Xiao	LBNL / RBRC	bxiao@lbl.gov
Nu Xu	LBNL	nxu@lbl.gov
Feng Yuan	LBNL / RBRC	fyuan@lbl.gov

Saturation, the Color Glass Condensate and Glasma: What have we learned from RHIC?

May 10-12 2010, Physics Department, Large Seminar Room

Monday, May 10, 2010

Registration and Coffee -- 8:30 - 9:00

Session I: Introduction and Overview: 9:00 - 12:30
(Chair: Peter Paul)

Welcome and Perspective Talk (Nick Samios) (10 min)

Introduction to the Physics of Saturation (Yuri Kovchegov) (30 min)

The Glasma and Color Glass Condensate (Francois Gelis) (30 min)

The Color Glass Condensate at Strong Coupling (Edmond Iancu) (30 min)

Coffee Break

HERA Results and DGLAP Evolution (Stefano Forte) (30 min)

Review of HERA Data (Henri Kowalski) (30 min)

Summary of RBRC Workshop on Event by Event P and CP Violation (Harmen Warringa) (20 min)

Lunch – 12:30 - 2:00

Session II: Global Event Structure at RHIC: 2:00 - 5:30
(Chair: Dmitri Kharzeev)

Extended Longitudinal Scaling: Direct Evidence of Saturation (Wit Busza) (30 min)

Multiplicity, Multiplicity Fluctuations and Negative Binomial Distributions (Tomoaki Nakamura for PHENIX) (30 min)

Eccentricity Fluctuations (Paul Sorenson for STAR) (30 min)

Coffee Break

Limiting Fragmentation (Anna Stasto) (20 min)

Initial Conditions and Global Event Properties (Adrian Dumitru) (20 min)

Transport Processes in the Turbulent Glasma (Berndt Mueller) (20 min)

Hydrodynamics for Fluctuating Initial Conditions (Frederique Grassi) (20 min)

Tuesday, May 11, 2010

Session III: Long Range Rapidity Correlations and the Ridge: 8:30 - 12:00
(Chair: Eugene Levin)

The Ridge in STAR (Lanny Ray for STAR) (30 min)

Long Range Correlations in Phenix (John Chen for PHENIX) (30 min)

Long Range Correlations in Phobos (Wei Li for PHOBOS) (30 min)

Collision Geometry Fluctuations and Triangular Flow (Burak Alver for PHOBOS) (15 min)

Coffee Break

Three Particle Correlations in STAR (Pawan Netrakanti for STAR) (15 min)

The Ridge and Colored Flux (Edward Shuryak) (20 min)

Long Range Correlations and Hydrodynamic Expansion (Sean Gavin) (20 min)

Lunch – 12:00 - 1:00

Session IV: Long Range Rapidity Correlations I : Forward Backward Correlations: 1:00 - 2:00
(Chair: Nu Xu)

STAR Results on Forward Backward Correlations (Mike Skoby for STAR) (20 min)

Theoretical Treatment of Forward Backward Correlations and Negative Binomial Distributions (Tuomas Lappi) (20 min)

Long Range Correlations, Event Simulations and Parton Percolation (Carlos Pajares) (20 min)

Session V: Single Particle Distributions in the Forward Region: 2:00 - 3:45

Dependence of Single Particle Distributions on Rapidity and Centrality (Ramiro Debbe from BRAHMS Summarizing Results from all RHIC experiments) (45 min)

Single Particle Distributions in Perturbative QCD and Shadowing (Mark Strikman) (30 min)

Single Particle Distributions, Leading Twist and Beyond (Javier Albacete) (30 min)

Coffee Break

Session VI: The Forward Region Two Particle Correlations: 4:00 - 5:45
(Chair: Raju Venugopalan)

Two Particle Correlations at Forward Rapidity in STAR (Ermes Braidot for STAR) (30 min)

Two Particle Correlations with Forward Rapidity Particle in PHENIX(Beau Meredith for PHENIX) (30 min)

Two Particle Forward Correlations: Leading Twist, Next to Leading Twist and Saturation (Cyrille Marquet) (30 min)

Two Particle Correlations: Saturation and Issues with Universality (Bowen Xiao) (15 min)

Dinner for Registered Participants, Center South Room -- 6:30 – 8:30

Wednesday, May 12, 2010

Session VII: J/Psi and Charm at RHIC: 8:30 - 12:00
(Chair: David Morrison)

The J/Psi in pA and AA Collisions at CERN-SPS and FNAL (Boris Kopeliovich) (30 min)

The J/Psi and Charm at RHIC (Alexandre Lebedev for PHENIX) (45 min)

The J/Psi and Charm at RHIC (Chris Perkins for STAR) (45 min)

Coffee Break

Understanding J/Psi Production in pp, dA and AA Collisions (Jian Wei Qiu) (30 min)

Charmonium and Open Charm Production and Saturation (Kirill Tuchin) (15 min)

Leptons and Dileptons (Jason Kamin for Phenix) (20 min)

Lunch – 12:00 - 1:00

Session VIII Future Directions: 1:00 - 4:00
(Chair: James Dunlop)

Future Directions in CGC Studies at RHIC (Les Bland for STAR) (30 min)

Decadal Upgrade in Phenix (Jamie Nagle for PHENIX) (20 min)

Forward Calorimetry for Phenix (Rich Seto for Phenix) (20 min)

Small x Physics with ALICE (Tapan Nayak for ALICE) (20 min)

Small x Physics with CMS (Magdalena Malek for CMS) (20 min)

Small x Physics with ATLAS (Brian Cole for ATLAS) (20 min)

The EIC, Saturation and the CGC (Thomas Ullrich) (20min)

Coffee Break

Can the Near Perfect Fluid Shed Light on Its Pre-Equilibrium Glasma? (Miklos Gyulassy)(30 min)

Session IX Summary Talk: 4:30 - 5:30
(Chair: Larry McLerran)

The Status of Saturation, the CGC and Glasma (Jean Paul Blaizot) (1 hr)

Additional RIKEN BNL Research Center Proceedings:

Volume 97 - RBRC Scientific Review Committee Meeting, October 21-22, 2009 - BNL-90674-2009
Volume 96 - P- and CP-Odd Effects in Hot and Dense Matter, April 26-30, 2010 - BNL-94237-2010
Volume 95 - Progress in High-pT Physics at RHIC, March 17-19, 2010 - BNL-94214-2010
Volume 94 - Summer Program on Nucleon Spin Physics at LBL, June 1-12, 2009 - BNL-
Volume 93 - PHENIX Spinfest School 2009 at BNL - July 1-31, 2009. BNL-90343-2009
Link: PHENIXSpinfestSchool2009@BNL
Volume 92 - PKU-RBRC Workshop on Transverse Spin Physics, June 30-July 4, 2008, Beijing, China, BNL-81685-2008
Volume 91 - RBRC Scientific Review Committee Meeting, November 17-18, 2008 - BNL-81556-2008
Volume 90 - PHENIX Spinfest School 2008 at BNL, August 4-8, 2008 - BNL-81478-2008
Volume 89 - Understanding QGP through Spectral Functions and Euclidean Correlators, April 23-25, 2008 - BNL-81318-2008
Volume 88 - Hydrodynamics in Heavy Ion Collisions and QCD Equation of State, April 21-22, 2008 - BNL-81307-2008
Volume 87 - RBRC Scientific Review Committee Meeting, November 5-6, 2007 - BNL-79570-2007
Volume 86 - Global Analysis of Polarized Parton Distributions in the RHIC Era, October 8, 2007 - BNL-79457-2007
Volume 85 - Parity-Violating Spin Asymmetries at RHIC-BNL, April 26-27, 2007 - BNL-79146-2007
Volume 84 - Domain Wall Fermions at Ten Years, March 15-17, 2007 - BNL 77857-2007
Volume 83 - QCD in Extreme Conditions, July 31-August 2, 2006 - BNL-76933-2006
Volume 82 - RHIC Physics in the Context of the Standard Model, June 18-23, 2006 - BNL-76863-2006
Volume 81 - Parton Orbital Angular Momentum (Joint RBRC/University of New Mexico Workshop) February 24-26, 2006 - BNL-75937-2006
Volume 80 - Can We Discover the QCD Critical Point at RHIC?, March 9-10, 2006 - BNL-75692-2006
Volume 79 - Strangeness in Collisions, February 16-17, 2006 - BNL-79763-2008
Volume 78 - Heavy Flavor Productions and Hot/Dense Quark Matter, Dec 12-14, 2005 - BNL-76915-2006
Volume 77 - RBRC Scientific Review Committee Meeting - BNL-52649-2005
Volume 76 - Odderon Searches at RHIC, September 27-29, 2005 - BNL-75092-2005
Volume 75 - Single Spin Asymmetries, June 1-3, 2005 - BNL-74717-2005
Volume 74 - RBRC QCDOC Computer Dedication and Symposium on RBRC QCDOC, May 26, 2005 - BNL-74813-2005
Volume 73 - Jet Correlations at RHIC, March 10-11, 2005 - BNL-73910-2005
Volume 72 - RHIC Spin Collaboration Meetings XXXI(January 14, 2005), XXXII (February 10, 2005), XXXIII (March 11, 2005) - BNL-73866-2005
Volume 71 - Classical and Quantum Aspects of the Color Glass Condensate - BNL-73793-2005
Volume 70 - Strongly Coupled Plasmas: Electromagnetic, Nuclear & Atomic - BNL-73867-2005
Volume 69 - RBRC Scientific Review Committee - BNL-73546-2004
Volume 68 - Workshop on the Physics Programme of the RBRC and UKQCD QCDOC Machines - BNL-73604-2004
Volume 67 - High Performance Computing with BlueGene/L and QCDOC Architectures
Volume 66 - RHIC Spin Collaboration Meeting XXIX, October 8-9, 2004, Torino Italy - BNL-73534-2004
Volume 65 - RHIC Spin Collaboration Meetings XXVII (July 22, 2004), XXVIII (September 2, 2004), XXX (December 6, 2004) - BNL-73506-2004
Volume 64 - Theory Summer Program on RHIC Physics - BNL-73263-2004
Volume 63 - RHIC Spin Collaboration Meetings XXIV (May 21, 2004), XXV (May 27, 2004), XXVI (June 1, 2004) - BNL-72397-2004
Volume 62 - New Discoveries at RHIC, May 14-15, 2004 - BNL- 72391-2004
Volume 61 - RIKEN-TODAI Mini Workshop on "Topics in Hadron Physics at RHIC", March 23-24, 2004 - BNL-72336-2004
Volume 60 - Lattice QCD at Finite Temperature and Density - BNL-72083-2004
Volume 59 - RHIC Spin Collaboration Meeting XXI (January 22, 2004), XXII (February 27, 2004), XXIII (March 19, 2004)-BNL-72382-2004
Volume 58 - RHIC Spin Collaboration Meeting XX - BNL-71900-2004
Volume 57 - High pt Physics at RHIC, December 2-6, 2003 - BNL-72069-2004
Volume 56 - RBRC Scientific Review Committee Meeting - BNL-71899-2003
Volume 55 - Collective Flow and QGP Properties - BNL-71898-2003
Volume 54 - RHIC Spin Collaboration Meetings XVII, XVIII, XIX - BNL-71751-2003

Additional RIKEN BNL Research Center Proceedings:

Volume 53 – Theory Studies for Polarized pp Scattering – BNL-71747-2003
Volume 52 – RIKEN School on QCD "Topics on the Proton" – BNL-71694-2003
Volume 51 – RHIC Spin Collaboration Meetings XV, XVI – BNL-71539-2003
Volume 50 – High Performance Computing with QCDOC and BlueGene – BNL-71147-2003
Volume 49 – RBRC Scientific Review Committee Meeting – BNL-52679
Volume 48 – RHIC Spin Collaboration Meeting XIV – BNL-71300-2003
Volume 47 – RHIC Spin Collaboration Meetings XII, XIII – BNL-71118-2003
Volume 46 – Large-Scale Computations in Nuclear Physics using the QCDOC – BNL-52678
Volume 45 – Summer Program: Current and Future Directions at RHIC – BNL-71035
Volume 44 – RHIC Spin Collaboration Meetings VIII, IX, X, XI – BNL-71117-2003
Volume 43 – RIKEN Winter School – Quark-Gluon Structure of the Nucleon and QCD – BNL-52672
Volume 42 – Baryon Dynamics at RHIC – BNL-52669
Volume 41 – Hadron Structure from Lattice QCD – BNL-52674
Volume 40 – Theory Studies for RHIC-Spin – BNL-52662
Volume 39 – RHIC Spin Collaboration Meeting VII – BNL-52659
Volume 38 – RBRC Scientific Review Committee Meeting – BNL-52649
Volume 37 – RHIC Spin Collaboration Meeting VI (Part 2) – BNL-52660
Volume 36 – RHIC Spin Collaboration Meeting VI – BNL-52642
Volume 35 – RIKEN Winter School – Quarks, Hadrons and Nuclei – QCD Hard Processes and the Nucleon Spin – BNL-52643
Volume 34 – High Energy QCD: Beyond the Pomeron – BNL-52641
Volume 33 – Spin Physics at RHIC in Year-1 and Beyond – BNL-52635
Volume 32 – RHIC Spin Physics V – BNL-52628
Volume 31 – RHIC Spin Physics III & IV Polarized Partons at High Q^2 Region – BNL-52617
Volume 30 – RBRC Scientific Review Committee Meeting – BNL-52603
Volume 29 – Future Transversity Measurements – BNL-52612
Volume 28 – Equilibrium & Non-Equilibrium Aspects of Hot, Dense QCD – BNL-52613
Volume 27 – Predictions and Uncertainties for RHIC Spin Physics & Event Generator for RHIC Spin Physics III – Towards Precision Spin Physics at RHIC – BNL-52596
Volume 26 – Circum-Pan-Pacific RIKEN Symposium on High Energy Spin Physics – BNL-52588
Volume 25 – RHIC Spin – BNL-52581
Volume 24 – Physics Society of Japan Biannual Meeting Symposium on QCD Physics at RIKEN BNL Research Center – BNL-52578
Volume 23 – Coulomb and Pion-Asymmetry Polarimetry and Hadronic Spin Dependence at RHIC Energies – BNL-52589
Volume 22 – OSCAR II: Predictions for RHIC – BNL-52591
Volume 21 – RBRC Scientific Review Committee Meeting – BNL-52568
Volume 20 – Gauge-Invariant Variables in Gauge Theories – BNL-52590
Volume 19 – Numerical Algorithms at Non-Zero Chemical Potential – BNL-52573
Volume 18 – Event Generator for RHIC Spin Physics – BNL-52571
Volume 17 – Hard Parton Physics in High-Energy Nuclear Collisions – BNL-52574
Volume 16 – RIKEN Winter School - Structure of Hadrons - Introduction to QCD Hard Processes – BNL-52569
Volume 15 – QCD Phase Transitions – BNL-52561
Volume 14 – Quantum Fields In and Out of Equilibrium – BNL-52560
Volume 13 – Physics of the 1 Teraflop RIKEN-BNL-Columbia QCD Project First Anniversary Celebration – BNL-66299
Volume 12 – Quarkonium Production in Relativistic Nuclear Collisions – BNL-52559
Volume 11 – Event Generator for RHIC Spin Physics – BNL-66116
Volume 10 – Physics of Polarimetry at RHIC – BNL-65926
Volume 9 – High Density Matter in AGS, SPS and RHIC Collisions – BNL-65762
Volume 8 – Fermion Frontiers in Vector Lattice Gauge Theories – BNL-65634
Volume 7 – RHIC Spin Physics – BNL-65615
Volume 6 – Quarks and Gluons in the Nucleon – BNL-65234
Volume 5 – Color Superconductivity, Instantons and Parity (Non?)-Conservation at High Baryon Density – BNL-65105

Additional RIKEN BNL Research Center Proceedings:

Volume 4 – Inauguration Ceremony, September 22 and Non-Equilibrium Many Body Dynamics –BNL-64912
Volume 3 – Hadron Spin-Flip at RHIC Energies – BNL-64724
Volume 2 – Perturbative QCD as a Probe of Hadron Structure – BNL-64723
Volume 1 – Open Standards for Cascade Models for RHIC – BNL-64722

For information please contact:

Ms. Pamela Esposito
RIKEN BNL Research Center
Building 510A
Brookhaven National Laboratory
Upton, NY 11973-5000 USA

Phone: (631) 344-3097
Fax: (631) 344-4067
E-Mail: pesposit@bnl.gov

Ms. Susan Foster
RIKEN BNL Research Center
Building 510A
Brookhaven National Laboratory
Upton, NY 11973-5000 USA

(631) 344-5864
(631) 344-2562
sfoster@bnl.gov

Homepage: http://www.bnl.gov/riken